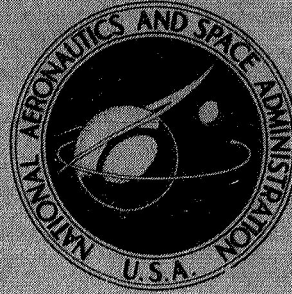


N 69 36413

**NASA CONTRACTOR
REPORT**



NASA CR-1425

NASA CR-1425

**CASE FILE
COPY**

**PROPERTIES OF
NONAQUEOUS ELECTROLYTES**

*by Rudolf Keller, James N. Foster, Douglas C. Hanson,
John F. Hon, and James S. Muirhead*

Prepared by
NORTH AMERICAN ROCKWELL CORPORATION
Canoga Park, Calif.
for Lewis Research Center

NATIONAL AERONAUTICS AND SPACE ADMINISTRATION • WASHINGTON, D. C. • AUGUST 1969

PROPERTIES OF NONAQUEOUS ELECTROLYTES

By Rudolf Keller, James N. Foster, Douglas C. Hanson,
John F. Hon, and James S. Muirhead

Distribution of this report is provided in the interest of
information exchange. Responsibility for the contents
resides in the author or organization that prepared it.

Prepared under Contract No. NAS 3-8521 by
ROCKETDYNE
A Division of North American Rockwell Corporation
Canoga Park, Calif.

for Lewis Research Center

NATIONAL AERONAUTICS AND SPACE ADMINISTRATION

ABSTRACT

Aprotic electrolytes with and without dissolved cupric fluoride and cupric chloride were studied. The electrolytes were based on four solvents: propylene carbonate, dimethyl formamide, acetonitrile, and methyl formate. Characterized components were used to prepare the solutions. Structural studies were performed utilizing nuclear magnetic resonance and electron paramagnetic resonance techniques. Various physical properties were determined including solubility, heat of solution, vapor pressure, viscosity, density, sonic velocity, conductance, diffusion coefficient, and dielectric constant.

FOREWORD

The research described in this report was conducted in the Chemical and Material Sciences Department of the Research Division of Rocketdyne. The work was done under NASA Contract NAS 3-8521, with Mr. Robert B. King, Direct Energy Conversion Division, Lewis Research Center, as the NASA Project Manager. This report was originally issued as Rocketdyne report R-7703.

CONTENTS

Summary	1
Introduction	3
Preparation of Electrolytes	5
Selection of Solvents	5
Analysis of Solvents	5
Purification of Solvents	25
Selection of Solutes	29
Analyses of Solutes	32
Preparation of Solutions	62
Handling of Chemicals and Glassware	64
Sensitivity Testing of Perchlorate Solutions	65
Structural Studies	66
Instrumentation	66
Electrolytes Containing Aluminum and Lithium Ions	67
Electrolytes Containing Cupric Species	98
Electrolytes Containing Quarternary Ammonium Ions	120
LiAsF ₆ /MF Electrolytes	124
Physical Property Determinations	126
Solubilities	126
Heats of Solution	134
Vapor Pressures	139
Viscosities and Densities	141
Sonic Velocities	143
Conductance Measurements	148
Conductometric Titrations	189
Hittorf Experiments	195
Diffusion Coefficients	207
Dielectric Constants	214

Discussion of Results	224
Electrolyte Solutions	224
Copper Halide Solutions	229
Activity Effects in Electrolyte Solutions	231
Dielectric Constants and Solubilities	232
Transport Properties	233
Impurity Effects	234
Conclusions	235
References	237

ILLUSTRATIONS

1. Initial Portion of Chromatogram of Purified Propylene Carbonate Containing 100-ppm Water	10
2. Initial Portion of Chromatograms of Spectroquality Dimethyl Formamide	13
3. Initial Portion of Chromatogram of Acetonitrile on Porapak Q Column	15
4. Initial Portion of Chromatogram of Methyl Formate	18
5. H^1 Spectrum of Methyl Formate with 1-Percent H_2O Added	23
6. H^1 Spectrum of $LiAsF_6$ #1/MF	23
7. H^1 Spectrum of $LiAsF_6$ #1/MF with 1-Percent H_2O Added	24
8. H^1 Spectrum of $LiAsF_6$ #1/MF with 1-Percent Methanol Added	24
9. Infrared Spectrum of Phosphorous Pentafluoride	53
10. Infrared Absorbance of Phosphorous Trifluoride and Phosphorous Oxychloride as a Function of Pressure	55
11. H^1 Spectrum for Pure DMF	68
12. H^1 Spectrum for 0.0528 M $AlCl_3$ /DMF	69
13. Broadline Cl^{35} Spectrum of 0.5 M $LiCl$ + 0.5 M $LiClO_4$ /DMF	73
14. High-Resolution H^1 Spectrum in Pure AN	75
15. High-Resolution H^1 Spectrum in 0.983 M $AlCl_3$ /AN	76
16. High-Resolution H^1 Spectrum in 0.983 M $AlCl_3$ /AN Saturated with $LiCl$	77
17. Al^{27} Nuclear Magnetic Resonance in 1 M $AlCl_3$ /AN Containing Various Concentrations of $LiCl$ (a) No $LiCl$, (b) 0.25 M $LiCl$, (c) 0.5 M $LiCl$, (d) 0.9 M $LiCl$	78
18. Approximate Relative Population of Coordinating Al Species in 1 M $AlCl_3$ /AN as a Function of Added $LiCl$	81

19.	High-Resolution Proton (H^1) Resonance in 1 M $AlCl_3/AN$	83
20.	Al^{27} Nuclear Magnetic Resonance in 1 M $AlCl_3/AN$ Containing Various Concentrations of $LiClO_4$, (b) 0.5 M $LiClO_4$, (c) 1 M $LiClO_4$	84
21.	Cl^{35} Magnetic Resonance in 1 M $LiClO_4$ + 1 M $AlCl_3/AN$	87
22.	High-Resolution H^1 Spectrum in Pure PC	90
23.	High-Resolution H^1 Spectrum in 1.00 M $AlCl_3/PC$	91
24.	High-Resolution H^1 Spectrum in 1.00 M $AlCl_3/PC$	92
25.	Al^{27} Nuclear Magnetic Resonance in 1 M $AlCl_3/PC$ Containing Various Concentrations of $LiCl$	94
26.	Approximate Relative Population of Coordinating Al Species in 1 M $AlCl_3/PC$ as a Function of Added $LiCl$	95
27.	Al^{27} Nuclear Magnetic Resonance in 0.1 M $AlCl_3/PC$	96
28.	Proton Spectrum in 1 M $CuCl_2/DMF$, Freshly Prepared Specimen	99
29.	Proton Spectrum in 0.5 M $LiCl$ + 1 M $CuCl_2/DMF$, Freshly Prepared Specimen	100
30.	Proton Spectrum in 1 M $LiCl$ + 1 M $CuCl_2/DMF$, Freshly Prepared Specimen	101
31.	Proton Spectrum in 2 M $LiCl$ + 1 M $CuCl_2/DMF$, Freshly Prepared Specimen	102
32.	Proton Spectrum in 1 M $CuCl_2/DMF$, 1 Month After Preparation	103
33.	Proton Spectrum in 0.5 M $LiCl$ + 1 M $CuCl_2/DMF$, 1 Month After Preparation	104
34.	Proton Spectrum in 1 M $LiCl$ + 1 M $CuCl_2/DMF$, 1 Month After Preparation	105
35.	Proton Spectrum in 2 M $LiCl$ + 1 M $CuCl_2/DMF$, 1 Month After Preparation	106
36.	Splitting of Large Proton Peaks as a Function of Time for $LiCl + CuCl_2/DMF$	108
37.	Position of Small Far-Downfield Resonance as a Function of Time for $LiCl + CuCl_2/DMF$	109

38.	Proton Spectrum (High Resolution) in 1 M CuCl_2/DMF , 4 Months After Preparation	110
39.	EPR Spectrum of 1 M CuCl_2/DMF	111
40.	EPR Spectrum of 0.5 M LiCl + 1 M CuCl_2/DMF	112
41.	EPR Spectrum of 1 M LiCl + 1 M CuCl_2/DMF	113
42.	EPR Spectrum of 2 M LiCl + 1 M CuCl_2/DMF	114
43.	EPR Spectrum of 1 M CuCl_2/DMF at High Gain	115
44.	EPR Spectrum of Freshly Prepared 0.1 M CuCl_2/DMF	117
45.	H^1 Spectrum of TMA^+ in Propylene Carbonate	122
46.	H^1 Spectrum of TMA^+ in Acetonitrile	123
47.	H^1 Spectrum of $\text{TEA}\cdot\text{F}$ in Propylene Carbonate	123
48.	As^{75} Magnetic Resonance in 1.1 M LiAsF_6/MF	125
49.	Heat of Solution Calorimeter	135
50.	Apparatus for Measuring Vapor Pressures by Gas Saturation Method	140
51.	Determination of Sonic Velocities	145
52.	Equivalent Conductance of LiClO_4 in Propylene Carbonate at 25 and 60 C	156
53.	Equivalent Conductance of LiClO_4 in Propylene Carbonate at 25 and 60 C	157
54.	Equivalent Conductance of LiCl in Propylene Carbonate at 25 and 60 C	158
55.	Equivalent Conductance of LiCl in Propylene Carbonate at 25 and 60 C	159
56.	Equivalent Conductance of $\text{TMA}\cdot\text{PF}_6$ in PC at 25 and 60 C	160
57.	Equivalent Conductance of $\text{TMA}\cdot\text{PF}_6$ in PC at 25 and 60 C	161
58.	Equivalent (Molar) Conductance of AlCl_3 in Propylene Carbonate at 25 and 60 C	162
59.	Comparison of Equivalent (Molar) Conductances of Electrolytes Containing LiCl and/or AlCl_3 in PC at 25 and 60 C	163
60.	Equivalent Conductance of LiClO_4 in DMF at 25 and 60 C	165

61.	Equivalent Conductance of LiCl in DMF at 25 and 60 C	166
62.	Equivalent Conductance of LiCl in DMF at 25 and 60 C	167
63.	Equivalent Conductance of TMA·PF ₆ in DMF at 25 and 60 C	168
64.	Equivalent Conductance of TMA·PF ₆ in DMF at 25 and 60 C	169
65.	Equivalent (Molar) Conductance of LiCl/DMF, AlCl ₃ /DMF, and LiCl+AlCl ₃ /DMF at 25 and 60 C	170
66.	Equivalent Conductance of LiClO ₄ in Acetonitrile at 25 and 60 C	171
67.	Equivalent Conductance of LiClO ₄ in Acetonitrile at 25 and 60 C	172
68.	Equivalent Conductance of TMA·PF ₆ in AN at 25 and 60 C	173
69.	Equivalent Conductance of TMA·PF ₆ in AN at 25 and 60 C	174
70.	Equivalent (Molar) Conductance of LiCl+AlCl ₃ in Acetonitrile at 25 and 60 C	175
71.	Equivalent Conductance of LiAsF ₆ and LiClO ₄ in Methyl Formate at 25 C	179
72.	Conductometric Titration of 1.0 M LiCl/DMF With CuCl ₂ at 25 C	190
73.	Conductometric Titration of 0.1 M LiCl/DMF With CuCl ₂ at 25 C	191
74.	Conductometric Titration of 1 M LiClO ₄ /DMF With CuF ₂ at 25 C	193
75.	Hittorf Cell Schematic	196
76.	Hittorf Cell	197
77.	Microwave Setup at 8.5 GHz, TE _{0,1} Mode	215
78.	Cole-Cole Plots for AN Solutions	218
79.	Cole-Cole Plots for DMF Solutions	220
80.	Cole-Cole Plots for PC Solutions	221
81.	Cole-Cole Plots for MF Solutions	222

TABLES

1. Physical Properties of Propylene Carbonate (PC), Dimethyl Formamide (DMF), Acetonitrile (AN), and Methyl Formate (MF) . . .	6
2. Experimental Parameters and Response for the Routine Determination of Water in Propylene Carbonate, Dimethyl Formamide, Acetonitrile, and Methyl Formate	7
3. Response of Cross-Section Detector to Various Amounts of Water in Propylene Carbonate	11
4. Experimental Parameters Used for the Determination of Methanol in Methyl Formate	19
5. Ratios of Methanol and Methyl Formate Responses for Thermoconductivity Detector	19
6. Solvents Purchased, Grades and Suppliers	26
7. Distillation Procedures for Purification of Solvents	27
8. Characterization of Distilled Solvent Batches	30
9. Source and Purities of Procured Solutes	33
10. Lower Limit for Detection of Various Metals in Lithium Carbonate Matrix by Emission Spectrography	37
11. Impurity Concentrations in LiClO_4 #2 Determined by Spark Source Mass Spectrometry and Emission Spectroscopy	39
12. Impurity Concentrations in LiClO_4 #3 Determined by Spark Source Mass Spectrometry and Emission Spectroscopy	40
13. Impurity Concentrations in LiCl #2 Determined by Spark Source Mass Spectrometry and Emission Spectroscopy	42
14. Impurity Concentrations in LiCl #3 Determined by Spark Source Mass Spectrometry and Emission Spectroscopy	43
15. Impurity Concentrations in LiF #2 Determined by Spark Source Mass Spectrometry and Emission Spectroscopy	44
16. Impurity Concentrations in $\text{TMA} \cdot \text{PF}_6$ #1 Determined by Spark Source Mass Spectrometry and Emission Spectroscopy	46
17. Impurity Concentrations in AlCl_3 #3 Determined by Spark Source Mass Spectrometry and Emission Spectroscopy	49
18. Impurity Concentrations in AlCl_3 #4 Determined by Spark Source Mass Spectrometry and Emission Spectroscopy	50

19.	Impurity Concentrations in CuF_2 #2 Determined by Spark Source Mass Spectrometry and Emission Spectroscopy	57
20.	Impurity Concentrations in CuF_2 #3 Determined by Spark Source Mass Spectrometry and Emission Spectroscopy	58
21.	Impurity Concentrations in CuCl_2 #2 Determined by Spark Source Mass Spectrometry and Emission Spectroscopy	60
22.	Solubilities of Electrolytes	128
23.	Solubilities of Copper Halides	129
24.	Solubility of CuF_2 and CuCl_2 in LiCl #3 + AlCl_3 #4/PC #5-5	132
25.	Heats of Solution at 25 C	138
26.	Vapor Pressures	142
27.	Viscosities and Densities	144
28.	Sonic Velocities at 25 C	147
29.	Solvation Numbers Calculated from Sonic Velocity Data	149
30.	Specific Conductance of Pure Solvents	151
31.	Specific Conductance of 1-Molar and Saturated Solutions	152
32.	Specific Conductance (λ) and Equivalent Conductance (Λ) of LiClO_4 #2/PC #2-6 at 25 and 60 C	155
33.	Specific Conductance (λ) and Equivalent Conductance (Λ) of LiClO_4 #3/MF #2-6 at 25 C	177
34.	Specific Conductance (λ) and Equivalent Conductance (Λ) of LiAsF_6 #1/MF #2-5 at 25 C	178
35.	Equivalent Conductances at Infinite Dilution (Λ_0) for Special Solutions Used to Determine Individual Ion Mobilities	181
36.	Equivalent Conductance at Infinite Dilution (Λ_0) for Several Solutes and Individual Ions in Propylene Carbonate.	182
37.	Equivalent Conductance at Infinite Dilution (Λ_0) for Several Solute and Individual Ions in Dimethyl Formamide	183
38.	Equivalent Conductance at Infinite Dilution (Λ_0) for Several Solute and Individual Ions in Acetonitrile	184

39.	Ionic Radii Calculated From Ion Mobilities	186
40.	Ions Involved in the Conductometric Titration of LiCl/DMF with CuCl_2	192
41.	Determination of Transference Numbers, t , for LiClO_4 Electrolytes by the Hittorf Method	199
42.	Determination of Transference Numbers, t , in LiCl/DMF by the Hittorf Method	200
43.	Hittorf Experiments with Electrolytes Containing LiCl and AlCl_3	202
44.	Hittorf Experiments with Electrolytes Containing Copper Halides	205
45.	Diffusion Coefficients at 25 C	208
46.	Comparison of Diffusion Coefficient, D , with Solution Conductance, λ and Viscosity, η_{solution} , and Solvent Viscosity, η_{solvent} , at 25 C	210
47.	Dielectric Constants	217
48.	Summary of Complexing Property of Solvents	226

SUMMARY

Physical property measurements and structural studies were conducted in the aprotic solvents propylene carbonate (PC), dimethyl formamide (DMF), acetonitrile (AN), and methyl formate (MF). Among the solutes studied were lithium perchlorate, lithium chloride with and without AlCl_3 added, tetramethylammonium hexafluorophosphate, and lithium hexafluoroarsenate. Copper fluoride and copper chloride in solution were investigated, representing electroactive battery materials.

Characterized components were used to prepare solutions. Karl Fischer titration, nuclear magnetic resonance, and vapor phase chromatography (VPC) were used to characterize the solvents; VPC was employed for routine analysis of distilled solvent batches. The water content of the solvents used was normally 40 ± 20 ppm. Emission spectrography and spark source mass spectrography were the main methods used to analyze solutes.

Nuclear magnetic resonance (NMR) and electron paramagnetic resonance (EPR) techniques were used to determine species in nonaqueous solutions. LiClO_4 , LiCl , and tetramethylammonium hexafluorophosphate ($\text{TMA} \cdot \text{PF}_6$) formed univalent electrolyte solutions analogous to aqueous systems. Solutions containing AlCl_3 , with or without LiCl added, were studied in detail; a tendency to form aluminum complexes was revealed, and an order of complexing strength was established: $\text{DMF} > \text{Cl}^- > (\text{AN}, \text{PC}, \text{ClO}_4^-)$.

Solutions of copper halides were examined using high resolution NMR, broadline NMR, and EPR techniques. Systems containing CuCl_2 and LiCl in DMF were studied in detail. Observations over a period of months revealed a redistribution of cupric species with time. Addition of LiCl resulted in the formation of CuCl_4^{2-} but a complete disproportionation into Cu^{+2} and CuCl_4^{2-} was not observed. Measurements on other cupric systems were limited because of the low solubilities of the cupric compounds.

These structural studies were complemented by Hittorf experiments and conductometric titrations. Confirmation of the NMR and EPR results was obtained.

Solute solubilities were measured in pure solvents and in selected electrolytes. A very low solubility was exhibited by LiF. The solubility of copper halides depended to a large extent on the anions present in solution.

Conductance measurements were made and the values extrapolated to infinite dilution to yield individual ion mobilities. A low mobility was found for the Li^+ ion, which was confirmed by transference measurements in concentrated solutions. Ion mobilities appeared to depend only on ion size and solvent viscosity. In concentrated solutions, activity effects seem to be more pronounced than in aqueous solutions because of relatively high solute to solvent mole ratios.

Other physical properties were determined. They included heat of solution which was measured using an LKB calorimeter, vapor pressure which was determined by a saturation method, viscosity, and density. Compressibilities were calculated from sonic velocity data, but an attempt to calculate solvation numbers from such data was not successful. Diffusion coefficients were determined with a porous disk method. A microwave method was used to determine dielectric constants of solutions.

INTRODUCTION

Lithium batteries have the potential to deliver the high-energy density beneficial in space and other applications. Use of nonaqueous, aprotic electrolytes should provide the necessary stability for such systems.

Investigations in the field of high-energy lithium batteries have been published by groups working at the American University, Battelle Memorial Institute, Electric Storage Battery Company, Electrochimica Corporation, Globe-Union, Inc., Honeywell's Livingston Electronic Laboratory, Lockheed Missiles and Space Company, P. R. Mallory and Company, Inc., Monsanto Research Corporation, Tyco Laboratories, Inc., NARMCO Research and Development Division of Whittaker Corporation, and elsewhere.

During the course of such investigations, excessive performance limitations for lithium cells were encountered. The factors contributing to such limitations are only sparingly known. A comprehensive understanding was hampered by the lack of knowledge of the properties or characteristics of nonaqueous electrolytes. Solubility, solvation effects, and transport properties were not well understood. Composition of the electrolyte, and relationships of the components of the electrolyte to each other should be known for an effective approach to further develop lithium batteries. The present effort to study the properties of nonaqueous, aprotic electrolytes was thus undertaken.

The first task was to extensively characterize the systems used in these studies, developing and applying new analytical techniques when necessary. Then, structural information on selected electrolytes was to be gained by NMR and EPR techniques as well as by electrochemical and other physical property measurements. The species formed by the electroactive materials, copper fluoride and copper chloride, in nonaqueous electrolytes were of particular concern. Physical property determinations were made to provide further background for the interpretation of data obtained with lithium cells.

Five quarterly reports and one summary report describing the progress of the work were previously issued (Ref. 1 through 6).

In addition to the authors of this report, Dr. Otto Kalman, Dr. James D. Ray, and Mr. Jack M. Sullivan contributed major portions of the experimental data described herein.

PREPARATION OF ELECTROLYTES

SELECTION OF SOLVENTS

Propylene carbonate (PC), dimethyl formamide (DMF), and acetonitrile (AN) are the three solvents which were selected at the beginning of the program. Methyl formate (MF) was added to the list at a later date. Table 1 gives the structure of these solvents and summarizes their physical properties.

ANALYSIS OF SOLVENTS

Several methods were used to analyze the solvents for trace impurities. Vapor phase chromatographic (VPC) methods were developed to analyze purified solvent batches. Very small solvent samples are required for this technique, and it was used for routine testing of the purified solvent batches. Karl Fischer titration was employed for verifying the VPC results, and for some determinations of the water content of solutions. Nuclear magnetic resonance (NMR) techniques were also used for cross-checking.

Vapor Phase Chromatography

Each batch of solvent was characterized by vapor phase chromatography (VPC) to ensure that it was of sufficient purity to be used on this program. A routine analysis procedure was developed to determine water, the most important impurity, as well as likely organic impurities on a Porapak Q column. The experimental parameters and responses for this routine determination are presented in Table 2. Porapak Q is an ethylvinylbenzene-divinylbenzene polymer and is similar to the material described by Hollis (Ref. 7) and Hollis and Hays (Ref. 8). Porapak Q separates water from most organic compounds. Hydrocarbons lighter than ethane and some inorganics are eluted prior to water; however, most other organic compounds are eluted after water. The water peak is usually sharp and well-defined.

TABLE 1

PHYSICAL PROPERTIES OF PROPYLENE CARBONATE (PC), DIMETHYL FORMAMIDE (DMF),
ACETONITRILE (AN), AND METHYL FORMATE (MF)

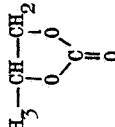
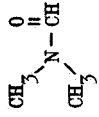

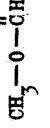
Structure	PC	DMF	AN	MF
				
Molecular Weight	102.09	73.10	41.05	60.05
Melting Point, C	-49.2 (Ref. 9)	-61 (Ref. 10)	-45.72 (Ref. 11)	-99 (Ref. 11)
Boiling Point at 760 mm Hg, C	241.7 (Ref. 9)	153 (Ref. 10)	80.06 (Ref. 11)	31.5 (Ref. 11)
Vapor Pressure at 25 C, mm Hg	0.069	3.95 (3.7; Ref. 10)	89.0	590
at 60 C, mm Hg	0.80	26.3		
Density at 25 C, gm/cm ³	1.203	0.944	-0.777	0.968
at 60 C, gm/cm ³	1.161	0.910	0.737	
Viscosity at 25 C, millipoises	24.8	7.93 (8.02; Ref. 10)	3.36	3.38
at 60 C, millipoises	13.3	5.55	2.63	
Sonic Velocity at 25 C, m/sec	1443	1451	1275	1148
Dielectric Constant at Room Temperature	65.1 (Ref. 12)	41.9 (37.2; Ref. 13; 56.71; Ref. 10)	39.3 (37.5; Ref. 14)	8.4 (8.5; Ref. 14)
Refractive Index at Room Temperature	1.421 (1.432; Ref. 11)	1.429 (1.427; Ref. 11)	1.343 (1.344; Ref. 11)	1.342 (1.343; Ref. 11)
Specific Conductance at 25 C, ohm ⁻¹ cm ⁻¹	1.2 to 8.6 x 10 ⁻⁷	3.3 to 13.8 x 10 ⁻⁷	1.6 to 16.5 x 10 ⁻⁷	
at 60 C, ohm ⁻¹ cm ⁻¹	1.5 to 10.0 x 10 ⁻⁷	4.5 to 18.8 x 10 ⁻⁷	5.5 to 18.4 x 10 ⁻⁷	

TABLE 2

EXPERIMENTAL PARAMETERS AND RESPONSE FOR THE ROUTINE DETERMINATION OF WATER IN
PROPYLENE CARBONATE, DIMETHYL FORMAMIDE, ACETONITRILE, AND METHYL FORMATE

Conditions ^a	Solvent			
	PC	DMF	AN	MF
Sample Size, microliters	100	100	100	25
Column Dimension	3/16 inch by 6 feet	3/16 inch by 6 feet	3/16 inch by 6 feet	3/16 inch by 6 feet
Column Packing	Porapak Q	Porapak Q	Porapak Q	Porapak Q
Column Temperature, C	165	165	150	150
Injector Temperature, C	175	175	175	175
Carrier Gas	Hydrogen	Hydrogen	Hydrogen	Hydrogen
Flowrate, cm ³ /min	25	25	25	25
Detector	Cross section	Cross section	Cross section	Cross section
Detector Temperature, C	165	165	165	165
Response, micrograms H ₂ O/cm ²	6.0	6.4	7.1 ^b	6.2 ^c

a. Chromatograph: Aerograph 660, Wilkens Instrument & Research, Inc.

Recorder: Leeds & Northrup Speedomax G; 670 microvolts full scale,
1/2-in./min chart speed.

b. Value used with second Porapak Q column

c. Value based upon average of values for PC and DMF

Because of its peak shape and rapid elution, water can be easily determined in organic solvents on Porapak Q.

Two Porapak Q columns were prepared on this program for the determination of water. There were two minor differences between the columns. Firstly, peaks eluted from the second column were sharper but their retention times were the same. Because of the better separations, the response for water in acetonitrile appeared different on the second column. No other changes in responses were found. Secondly, a single peak was found for water in propylene carbonate on the second column, whereas two peaks had been obtained on the first column which probably contained a catalyst that hydrolyzed part of the propylene carbonate. These differences will be discussed further in later sections.

Vapor phase chromatographic analysis utilizing a single column analysis is not definitive because an impurity could be eluted at the same time as the major component or an impurity could have a very long retention time. Relatively long retention times appear to be characteristic of Porapak columns; dimethyl formamide, for example, has a retention time of 8 minutes at 200 C on Porapak Q, but is not retained on Carbowax 20M or Apiezon L at this temperature. Changing the nature of a column, particularly the polarity of the liquid phase, results in a change of the retention times for each component. Thus, two components that have the same retention time on a nonpolar column (e.g., because of the similarity in their boiling points) may have different retention times on a polar column (e.g., because of the difference in their polarities).

One batch each of purified dimethyl formamide and one batch of acetonitrile were analyzed on polar and nonpolar columns, and no impurities having a concentration greater than 100 ppm were found. The polar column was 5-percent Carbowax 20M on Chromosorb W (DMCS-AW, 60/80 mesh) packed in 1/8-inch by 20-foot stainless-steel tubing. The nonpolar column was packed with 5-percent Apiezon L on Chromosorb W (DMCS-AW, 60/80 mesh) in

1/8-inch by 10-foot stainless-steel tubing. A flame-ionization detector was employed with these two columns. Several chromatograms were made at different temperatures to obtain sharp, easily delineated peaks. Peaks preceding the solvent generally show better resolution at lower temperatures; peaks which follow the solvent peak are generally sharper at higher temperatures. In determining impurities having concentrations of 100 ppm, several isothermal chromatograms obtained at different column temperatures appeared preferable to one gas chromatogram with programmed temperature control. Programmed-temperature gas chromatography usually results in good resolution and peak shape because the temperature increases during elution of the sample. However, better baseline stability and reproducibility are inherent in the isothermal technique.

Propylene Carbonate. The water content of each batch was determined using the conditions given in Table 2 . Propylene carbonate had a retention time of greater than 2 hours under these conditions. Replicate water determinations could be made by successively injecting aliquots of propylene carbonate before the elution of the first propylene carbonate peak. The initial portion of a chromatogram with two injections of propylene carbonate is shown in Fig. 1 ; this chromatogram was made on the first Porapak Q column. One characteristic of this column was that a third peak appeared between the air and water peaks, which had the same retention time as carbon dioxide. The area of this peak increased with subsequent injections and the area of the water peak decreased a corresponding amount. The sum of the area of the two peaks remained constant even though the individual areas varied. This unusual behavior is probably due to the presence of a catalyst that promoted hydrolysis of the propylene carbonate to produce carbon dioxide. The second Porapak Q column did not exhibit this behavior but gave successive water peaks identical with the first.

The detector response for water was determined by adding measured volumes of water to weighed amounts of propylene carbonate. The data are given in Table 3. The water peak area was graphed as a function of the amount of

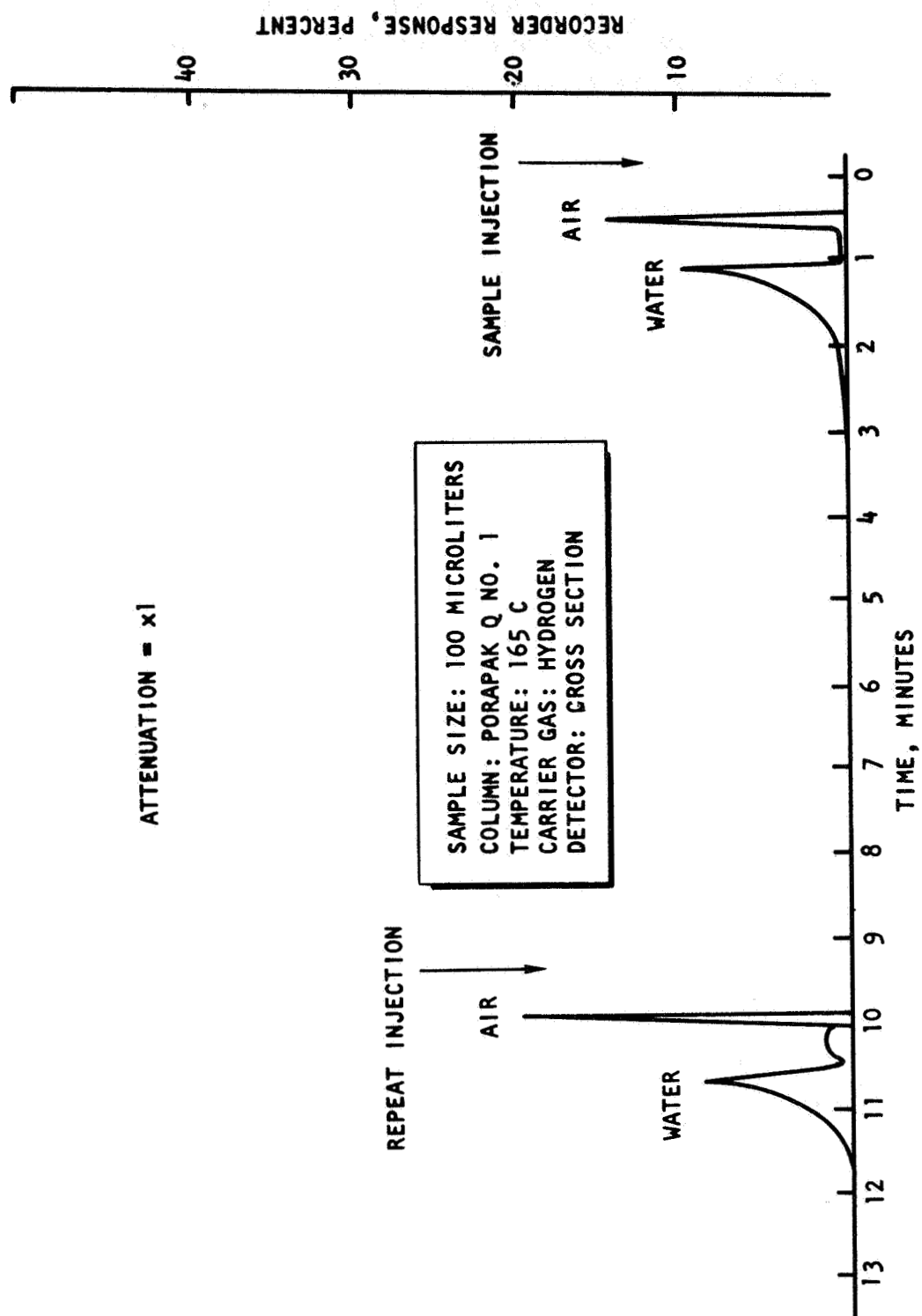


Figure 1. Initial Portion of Chromatogram of Purified Propylene Carbonate Containing 100-ppm Water

TABLE 3

RESPONSE OF CROSS-SECTION DETECTOR TO VARIOUS AMOUNTS OF
WATER IN PROPYLENE CARBONATE*

Sample	Amount of H ₂ O Added, ppm	H ₂ O Peak Area, cm ²
#1	0	2.4
#2	54	3.3
#3	1000	22.3

*The sample to which the water was added contained some water. Based upon a response to 50 cm²/ppm, 120 ppm water was present in the original sample.

water added; from the slope of the resulting line, the detector response was found to be 0.167 cm² per microgram of water, which is equivalent to 50 ppm/cm² (by weight) of water in propylene carbonate. The response was redetermined on the second Porapak Q column and was found to be the same. The lower limit for the detection of water in propylene carbonate was about 5 ppm.

The vapor phase chromatographic method was cross-checked with the Karl Fischer method using a second propylene carbonate sample. The water content determined by these two methods was 180 and 158 ppm, respectively. These values are in agreement within the experimental accuracy of the two methods.

Three additional peaks sometimes appeared on the chromatograms. One peak was propylene glycol, which has a retention time of about 50 minutes. The other two peaks were not identified; they had retention times of 3 and 6 minutes and were merely designated A and B, respectively. The corresponding compounds appear to be decomposition products of propylene carbonate. Usually the concentration of these materials was less than 20 ppm. The detection limit for compounds A and B was about 10 ppm, assuming that

these compounds had the same detector response as water. The propylene glycol peak was broader due to its long retention time and, consequently, its detection limit was greater, probably 50 ppm.

Propylene carbonate was not completely characterized by VPC but was characterized by NMR. No impurities were found with a concentration greater than 100 ppm.

Dimethyl Formamide. The water content of each batch of dimethyl formamide was determined using the parameters given in Table 2. The initial portion of a chromatogram of dimethyl formamide on the first Porapak Q column is shown in Fig. 2. The second Porapak Q column gave identical chromatograms for dimethyl formamide.

The detector response for water in dimethyl formamide was determined by adding measured volumes of water to weighed amounts of dimethyl formamide, according to the procedure as described previously for propylene carbonate. The detector response was found to be 0.156 cm^2 per microgram of water which is equivalent to 67 ppm/cm^2 (by weight) of water in dimethyl formamide. The detection limit for water in dimethyl formamide is about 5 ppm. The VPC method was cross-checked with the Karl Fischer method. The water content was found to be 93 and 83 ppm, respectively. These values agree within the expected accuracy of the two methods.

Formic acid, formaldehyde, dimethyl amine, and methanol are eluted from the Porapak Q column after water but before dimethyl formamide. If present, peaks for these compounds could be observed; but generally no peaks were found and, hence, their concentrations were less than 10 ppm, their approximate detection limits.

In addition to the routine analysis on the Porapak Q column using the cross-section detector, one batch of dimethyl formamide, DMF #4-1, was also analyzed with the Carbowax 20M column and the Apiezon L column, using

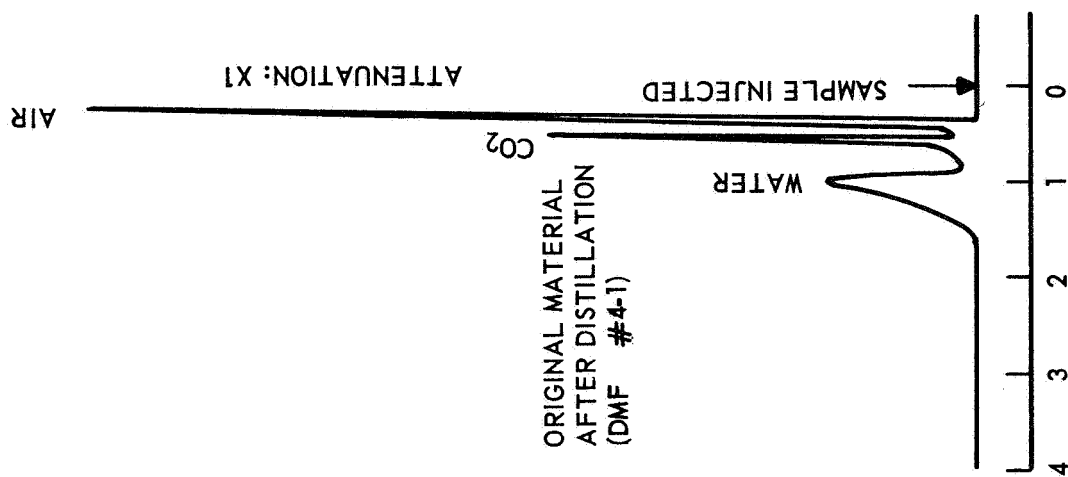
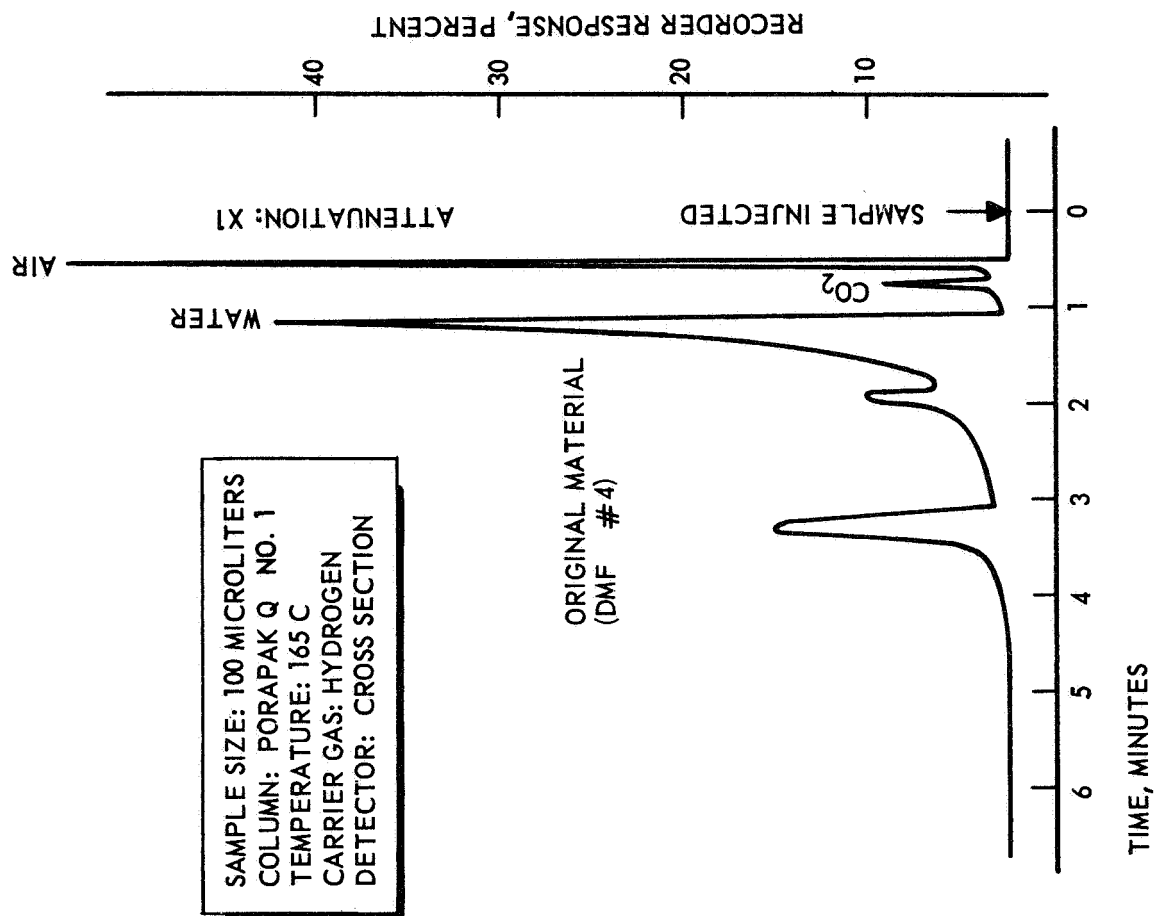


Figure 2. Initial Portion of Chromatograms of Spectroquality Dimethyl Formamide

a flame-ionization detector. Isothermal chromatograms were obtained at temperatures of 66, 96, and 165 C on the Carbowax 20M column. The three chromatograms were very similar: two peaks appeared at the beginning of the chromatogram followed by the solvent peak. No peaks were found after the dimethyl formamide peak, even though the chromatograms were continued for 40 minutes after the solvent peak. The dimethyl formamide retention time at 96 C is 5 minutes. Isothermal chromatograms were obtained on the Apiezon L column at 40, 102, and 165 C. The dimethyl formamide retention time at 102 C is 4 minutes. The chromatograms are similar to those obtained on the Carbowax 20M column.

The flame ionization detector response is approximately proportional to the weight concentration of the components found. The solvent peak area corresponded to 6000 cm^2 . If an organic impurity were present at a concentration of 100 ppm, a peak area of 0.6 cm^2 would be expected. This area would correspond to a triangular peak having a 1-cm base and a 12-cm height at the most sensitive range employed. No such peaks were found; the two peaks at the beginning of the chromatograms have areas of less than 0.05 cm^2 .

Based upon the chromatograms of dimethyl formamide on the Porapak Q, Carbowax 20M, and Apiezon L columns, DMF #4-1 contained no impurities having concentrations greater than 100 ppm.

Acetonitrile. Each batch of acetonitrile was analyzed using the parameters given in Table 2. The initial portion of a chromatogram of acetonitrile on Porapak Q (second column) is shown in Fig. 3. A good separation between water and acetonitrile was obtained. The detector response for water was determined by adding 470 ppm of water to an acetonitrile sample; the increase in the water peak area was 5.1 cm^2 . The detector response therefore was 0.141 cm^2 per microgram of water which is equivalent to 92 ppm/cm^2 (by weight) of water in acetonitrile. The lower limit for the detection of water in acetonitrile appeared to be about 10 ppm.

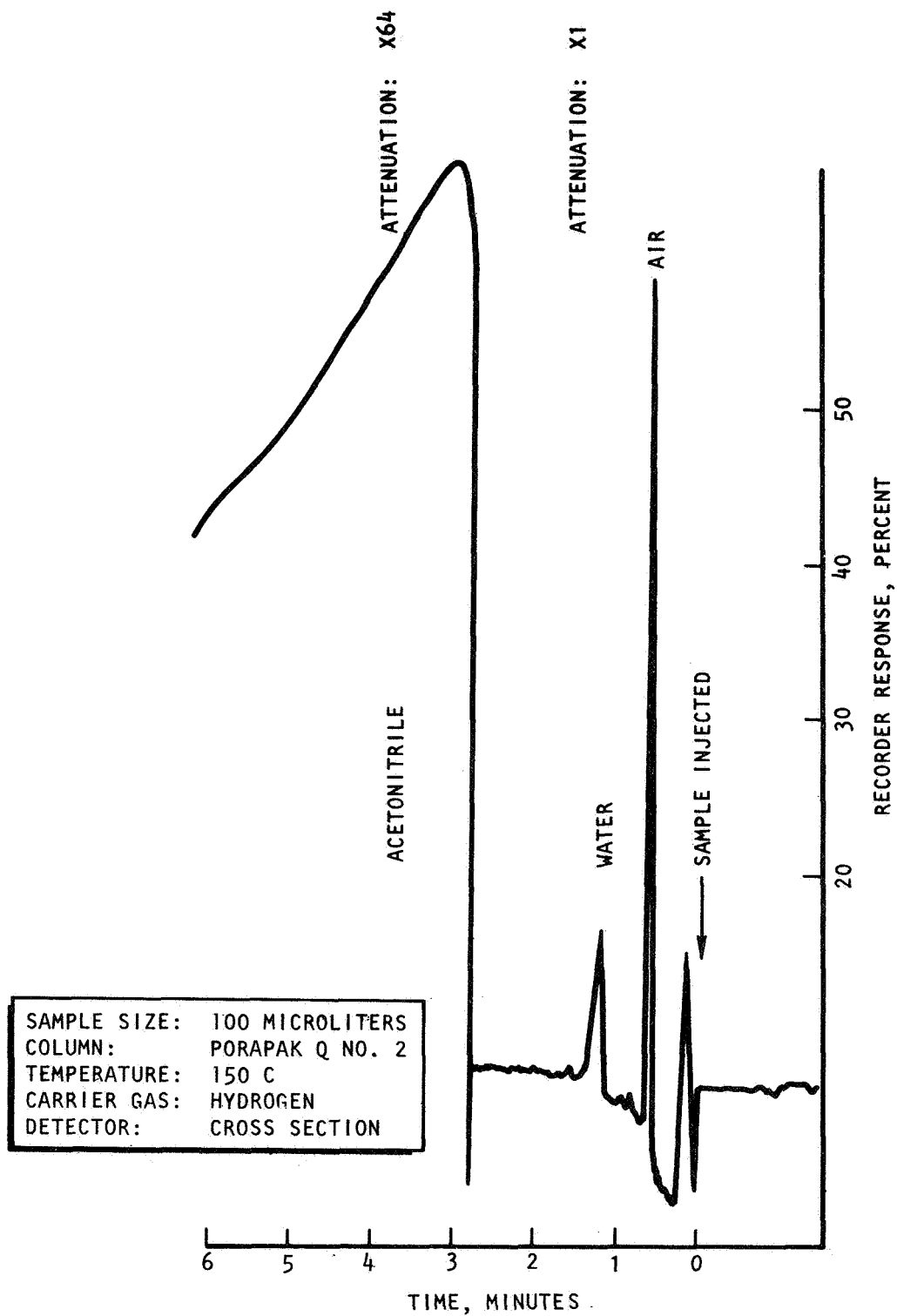


Figure 3. Initial Portion of Chromatogram of Acetonitrile on Porapak Q Column (AN #3-2)

The separation of acetonitrile and water was not as good on the first Porapak Q column prepared. It was necessary to extrapolate the water peak under the acetonitrile peak in this case. The detector response was found to be 0.115 cm^2 per microgram of water, which is equivalent to 112 ppm/ cm^2 (by weight) of water in acetonitrile. This response was lower due probably to inaccurate extrapolation of the water peak under the acetonitrile peak.

In addition to the routine analysis on the Porapak Q column using a cross-section detector, AN #1-2 was also analyzed on the Carbowax 20M, Apiezon L, and the first Porapak Q column using the flame ionization detector, and no impurities having concentrations greater than 100 ppm were found. Chromatograms were obtained on the Apiezon L column at 40 and 100 C. Only the solvent peak, with a retention time of 2 minutes at 40 C, appeared on the chromatograms even though they were recorded for 60 minutes. Acetonitrile was analyzed on the Carbowax 20M column at 35 and 100 C and only one peak for the solvent appeared on the 60-minute chromatogram. The acetonitrile retention time was 3 minutes on this column (at 35 C).

The analyses on the Apiezon L and Carbowax 20M columns show that no higher boiling materials were present in the acetonitrile. Because the solvent is eluted so rapidly, it is possible that more volatile material could have been eluted simultaneously with the solvent. It was not practical to cool these columns to give longer retention times, therefore another column material was used. The Porapak Q column was selected to analyze for any volatile impurities because long retention times were characteristic of this column. AN #1-2 was analyzed on the first Porapak Q column at 140 C. Again, only the solvent peak was found which had a retention time of 6.5 minutes.

Acrylonitrile is an impurity which may be present in acetonitrile and which may not be removed by distillation. A 1-percent solution of acrylonitrile in acetonitrile was analyzed on the Porapak Q column. The

acrylonitrile retention time was 10.5 minutes and the peak was sharp and well-separated from the acetonitrile. No acrylonitrile peak was found in AN #1-2.

Methyl Formate. Each batch of methyl formate was analyzed for water, methanol, and formic acid. The water analysis was performed on the second Porapak Q column using the conditions shown in Table 2. The separation of methyl formate and water was poor unless the sample size was reduced to 25 μ l. A chromatogram of MF #2-6 is shown in Fig. 4. The baseline disturbance before the air peak was due to a pressure surge caused by injecting the sample. The water peak must be extrapolated under the methyl formate peak as shown by the dotted line. The detector response for water was assumed to be an average of the two values found for propylene carbonate and dimethyl formamide. This value is 0.161 cm^2 per microgram of water which is equivalent to 256 ppm/cm^2 (by weight) for water in methyl formate. The lower detection limit for water was about 40 ppm.

The methanol content was determined on a third Porapak Q column using the conditions given in Table 4. The retention times of water, methanol, methyl formate, and formic acid were 0.7, 1.8, 3.4, and 5.6 minutes, respectively. Each peak was very sharp and well separated from the others. The detector response ratio for methanol and methyl formate was determined by adding measured volumes of methanol to a known volume of methyl formate. These data are given in Table 5. The ratio of the methanol and methyl formate peak areas was graphed as a function of the methanol added. The proportionality constant for the methanol content and the ratio of the methanol and solvent peak areas was found from the slope of the line. The methanol content (ppm, by weight) was calculated by multiplying the ratio of the peak areas by 6.65×10^5 .

Some further work was done to determine if water or formic acid caused any interference in the methanol determination. Addition of 0.5-percent water to MF #2-5 did not change the methanol concentration found in this sample.

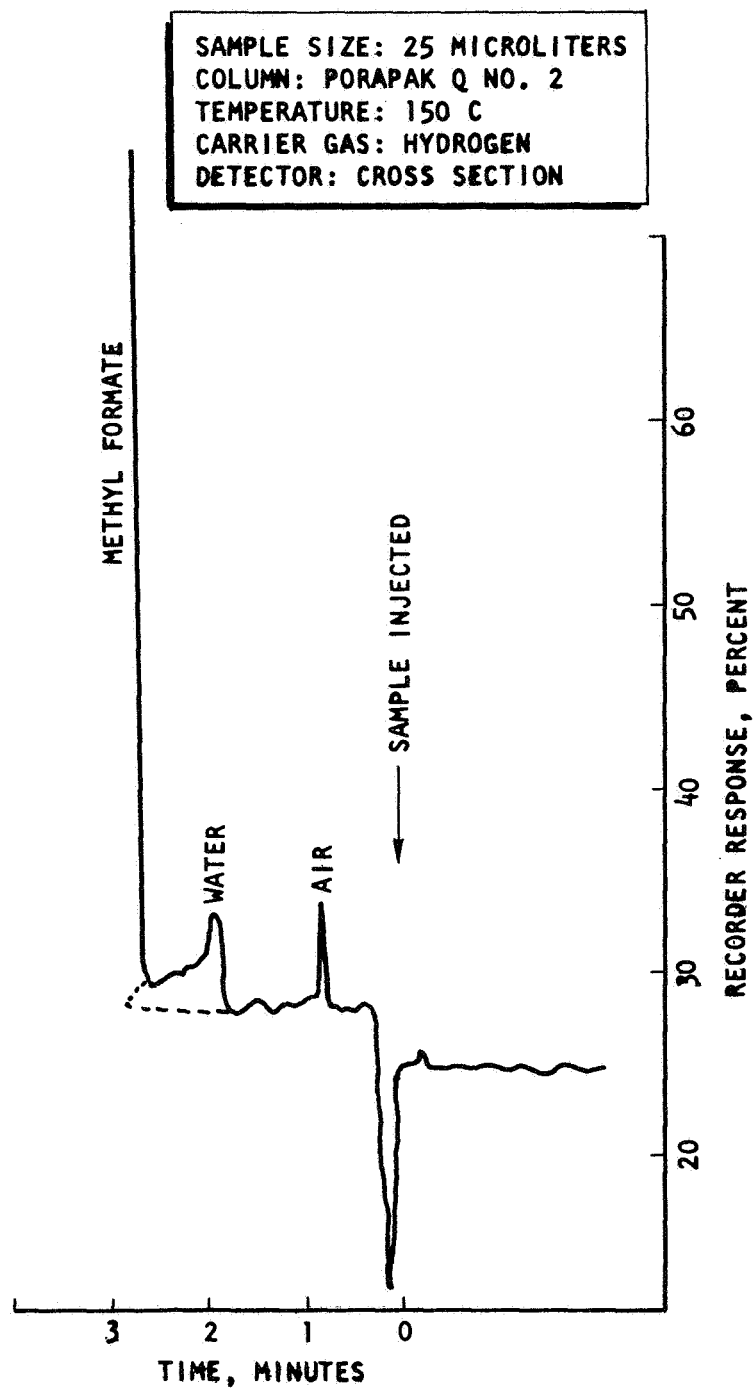


Figure 4. Initial Portion of Chromatogram of Methyl Formate (MF #2-6)

TABLE 4

EXPERIMENTAL PARAMETERS USED FOR THE DETERMINATION OF
METHANOL IN METHYL FORMATE

Sample Size, μ l	1
Column	3/16-inch x 3-feet packed with Porapak Q
Column Temperature, C	130
Carrier Gas	Helium
Flowrate, cm^3/min	50
Detector	Thermoconductivity
Detector Current, milliamperes	250
Gas Chromatograph	Beckman GC2A
Recorder	L & N Speedomax G, 1 millivolt full scale, 1/2 inch per minute chart speed

TABLE 5

RATIOS OF METHANOL AND METHYL FORMATE RESPONSES FOR
THERMOCONDUCTIVITY DETECTOR

Sample No.	Methanol Added, Volume Percent	Ratio of Methanol to Methyl Formate Peak Areas
1	0	$6.6 \times 10^{-4*}$ 6.6×10^{-4}
2	0.1	16.8×10^{-4} 16.5×10^{-4}
3	0.2	2.86×10^{-4} 2.88×10^{-4}
4	0.3	37.3×10^{-4} 37.6×10^{-4}
5	0.5	57.9×10^{-4} 59.9×10^{-4}
6	0.7	75.6×10^{-4} 80.2×10^{-4}

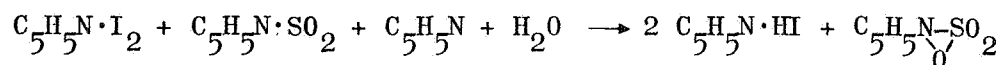
*MF #2-3 contained an unknown amount of methanol. Based upon
this data, 440-ppm methanol was present in the original MF #2-3.

Addition of 0.5-percent formic acid to the MF #2-5/water mixture also did not change the methanol concentration. These two experiments give considerable support to the accuracy for the determination of methanol. Apparently, little or no decomposition, hydrolysis, or esterification occurred during this analysis of the pure solvent.

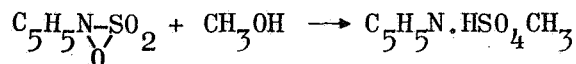
There was no complete characterization of methyl formate by VPC. However, no impurities other than methanol and water were observed on the Porapak Q column. Assuming that the thermal conductivities of any other impurities were the same as methanol and that no impurities were eluted simultaneously with the solvent, no impurities were found to be present having concentrations greater than 300 ppm. Methanol, of course, is an exception to this statement.

Karl Fischer Titration

As an independent check of the results obtained by VPC, Karl Fischer reagent (Ref. 15) was employed to determine water contents. Karl Fischer reagent is a well specified mixture of pyridine, iodine, methanol, and sulfur dioxide. The titration of H_2O in this CH_3OH solution involves a sequence of reactions that can be represented by the following equations:



and



The standard reagent titrates 5 milligrams of water per milliliter of titrant. To determine trace quantities of water in solvents, the titrant was diluted with methanol to an activity of ~ 1 mg H_2O /ml titrant. If 100 grams (~ 100 milliliters) of solvent are titrated, each milliliter of

titrant corresponds to 10 ppm of water, giving a 1 milliliter titration with a 5-milliliter micro-burette (0.01 ml/div). The lower limit for the determination of water is less than 10 ppm. The direct titration endpoint was determined potentiometrically and the titrations were performed in a closed system. The titrant was standardized against the water of hydration of weighed quantities of sodium tartrate.

Several substances interfere with Karl Fischer analyses including: alkaline materials, compounds containing active hydrogen, and strong oxidizing or reducing agents. One problem associated with large sample sizes is the disruption of the electrolytic nature of the titration system such that the standard endpoint cannot be employed. This problem was not found in the titration of propylene carbonate or acetonitrile.

The titration of dimethyl formamide containing small amounts of water was unusual because the endpoint was apparently passed when the first drop of Karl Fischer reagent was added. This was because the reagent slowly reacted with the sample; subsequent additions of reagent reacted rapidly so that the sample could be titrated in the usual fashion. This reaction appears to be autocatalytic, but the mechanism was not investigated. Karl Fischer titration yielded results in accordance with the VPC method for solutions with intermediate water content, but could not be applied in cases of very pure dimethyl formamide. Difficulties in titrating for water in dimethyl formamide have been indicated also by other investigators (Ref. 10).

Nuclear Magnetic Resonance (NMR) Techniques

Early in the program, NMR techniques were explored as a method for the independent analysis of water in solvents. This work included a preliminary investigation of a method, described in an earlier report (Ref. 2), which employed broadline techniques in recording high resolution spectra and held promise of achieving the same sensitivity as either VPC or Karl Fischer titration. Results consistent with the other analytical methods were obtained.

More recently, standard high resolution NMR was used to determine water and methanol contents in methyl formate, and in its solutions where ambiguous results had been obtained by VPC and Karl Fischer titration. The H^1 resonance due to H_2O and CH_3OH was compared to the resonance obtained in samples containing known additional amounts of these impurities. The sensitivity of this method may not be as great as the sensitivity of the NMR method mentioned above, but it allows the detection of impurities at a level of 200 to 500 ppm, the sensitivity depending to a certain extent on the solvent system. As an example, the spectrum of MF#2-5 is given in Fig. 5 with 1-percent water added.

Methyl formate was used for experimentation in $LiClO_4$ and $LiAsF_6$ solutions. The task to analyze methyl formate was twofold because not only pure, distilled methyl formate had to be analyzed, but also the methyl formate which was contained in the $LiAsF_6$ /MF stock solution supplied by Honeywell's Livingston Electronic Laboratories. A preliminary VPC analysis of this stock solution had indicated a water content of 0.25 percent but the solution was found stable in contact with a lithium dispersion, and the high water content could not be confirmed by Karl Fischer titration. NMR results then indicated decisively that the VPC results were erroneous probably because of decomposition of the solvent.

A sample of $LiAsF_6$ #1/MF (designation for the undiluted stock solution obtained from Livingston) gave the spectrum represented in Fig. 6. On addition of water, no water peak could be found, as shown in Fig. 7. Instead, the methanol peak had increased as compared to the spectrum obtained before the water addition. This can be verified by comparing with a spectrum obtained after addition of 1-percent methanol, Fig. 8. A formic acid peak, not shown, had also increased accordingly. This indicates that a fast hydrolysis occurred. Such a reaction was not observed in pure methyl formate, and it appears that the hydrolysis process was accelerated in the presence of $LiAsF_6$ or of certain impurities introduced with it.

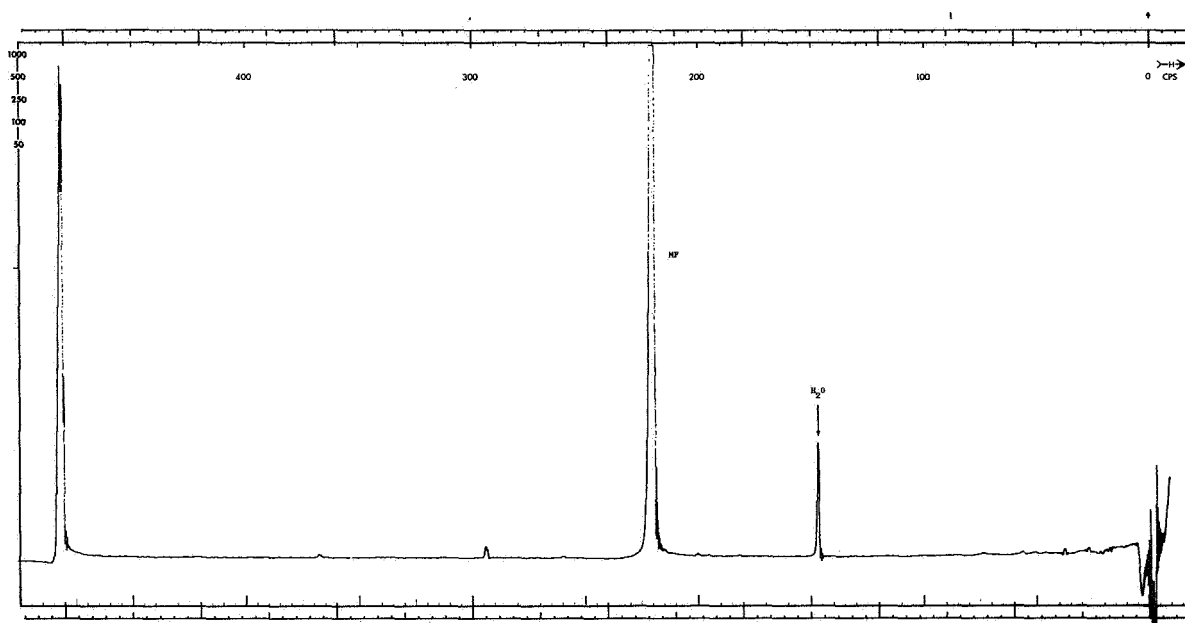


Figure 5. H^1 Spectrum of Methyl Formate with 1-Percent H_2O Added

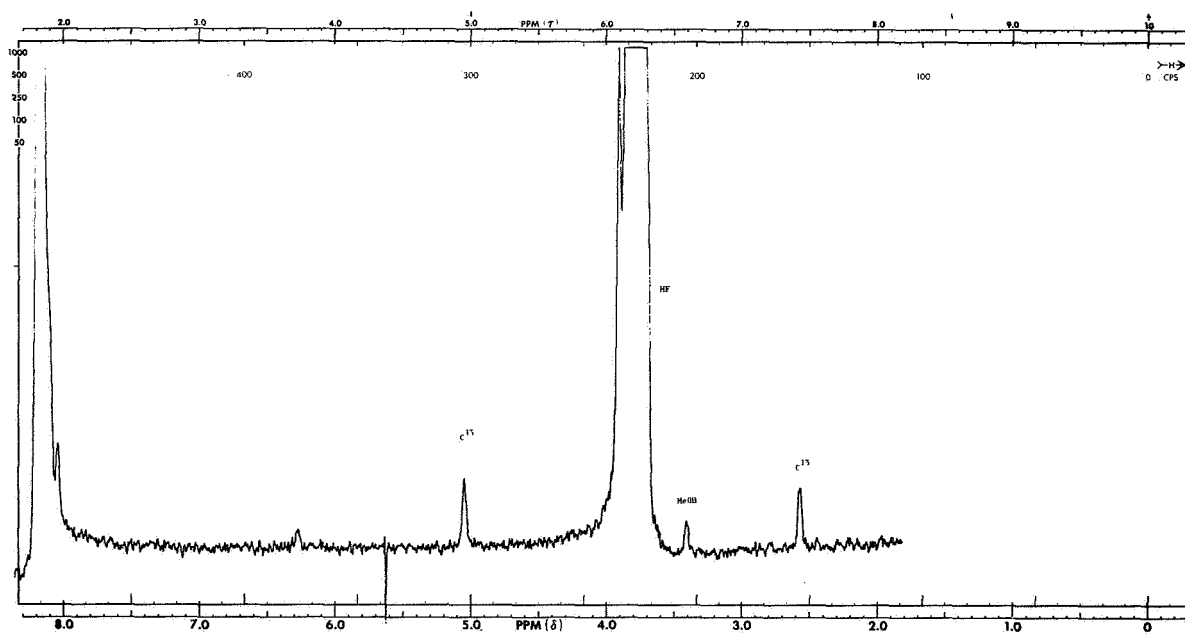


Figure 6. H^1 Spectrum of $LiAsF_6$ #1/MF

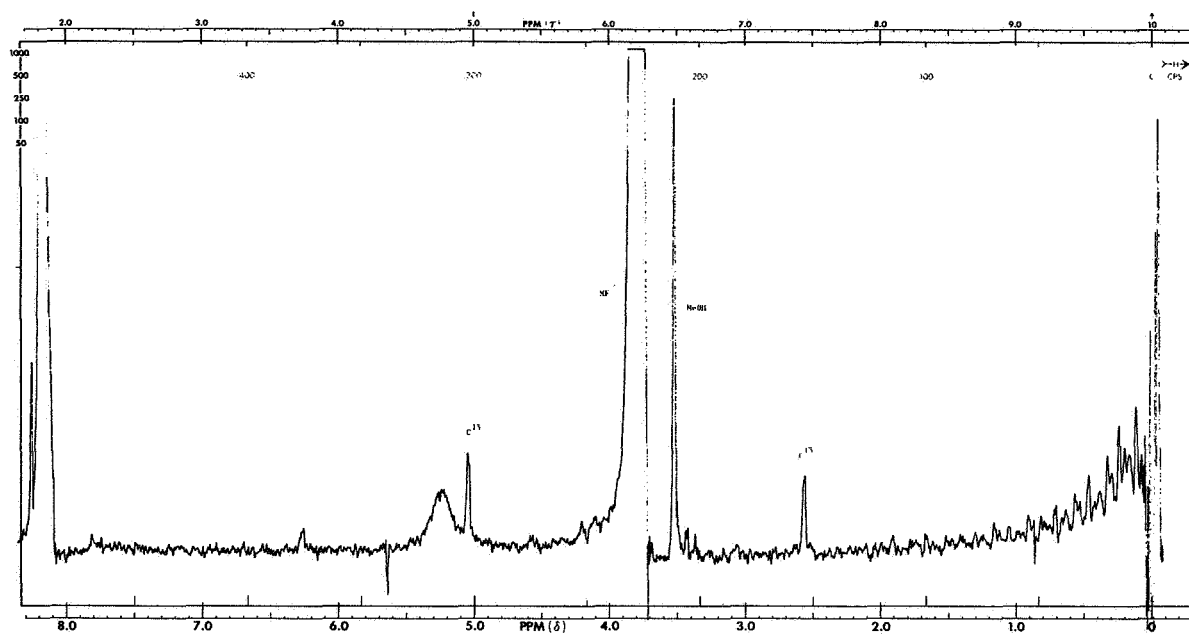


Figure 7. H^1 Spectrum of LiAsF_6 #1/MF with 1-Percent H_2O Added

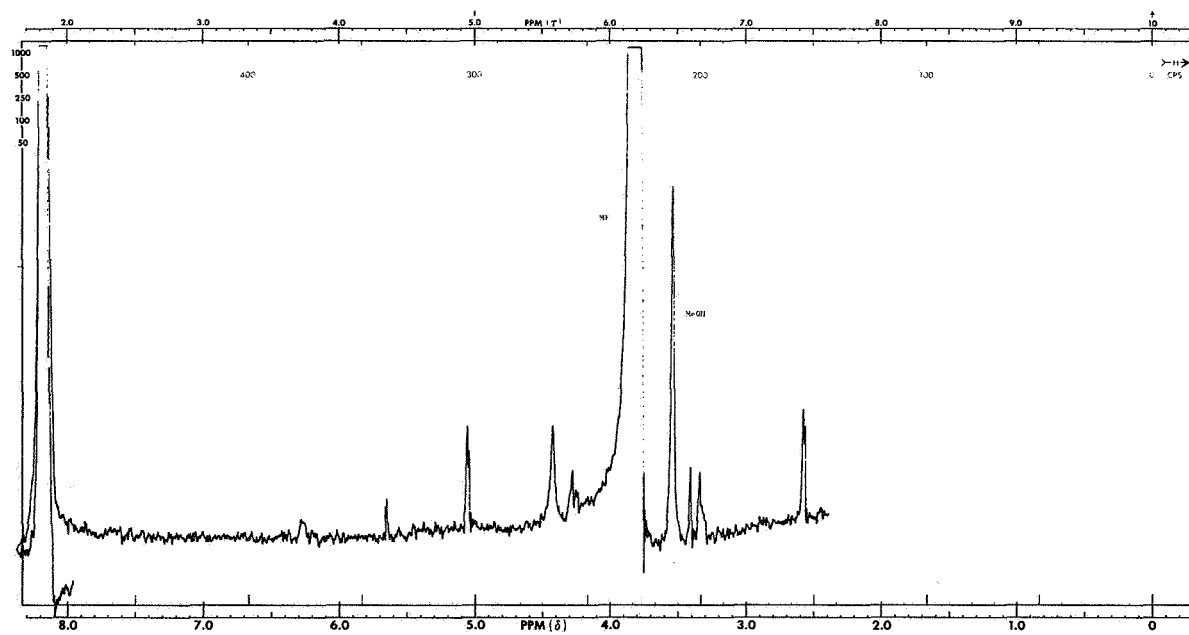


Figure 8. H^1 Spectrum of LiAsF_6 #1/MF with 1-Percent Methanol Added

PURIFICATION OF SOLVENTS

Starting Materials

Table 6 lists the solvents purchased. Solvents of different origin and frequently also with different lot numbers were given different code numbers (an additional number was added for the different purified and analyzed batches).

Distillation

Solvents were purified by distillation. Methods were established which furnished solvents with acceptable impurity levels fairly reliably; the procedures are summarized in Table 7. Two distillation procedures are given for PC, DMF, and AN. Each of the first procedures was used in early stages of the program and produced acceptable materials, as summarized in Ref. 3. Because of the breakdown of the spinning band column and also to improve the reliability, the distillation processes were modified, and the second set of distillation conditions represents the methods which eventually appeared optimal in regard to reliability and simplicity. These later procedures are discussed in more detail below.

Propylene Carbonate. Liter batches of PC were distilled from CaH_2 with a 1-foot Vigreux column (packed with Heli-pak) at 8 to 14 mm Hg and 100 to 115 C. The column was wrapped with heating tape and insulated with asbestos to prevent flooding. Dry nitrogen was used to bring the system to atmospheric pressure when cutting fractions. No predrying of the solvent was necessary, possibly because the starting material, at least in batches purchased toward the end of the program, had a low water content. However, several samples distilled from the very latest batches were found to contain approximately 100 ppm of an unidentified organic impurity with a VPC retention time of 6 minutes. The impurity level was reduced by simply distilling off 150 to 200 ml from the distilled batch, in the absence of CaH_2 , and retaining the rest of the batch as the purified solvent.

TABLE 6
SOLVENTS PURCHASED, GRADES AND SUPPLIERS

Solvent	Source	Quality	Lot No.	Analysis
PC #1	Eastman Organic Chemicals Matheson, Coleman and Bell Chemicals, Procurement Laboratories Matheson, Coleman and Bell Matheson, Coleman and Bell	Practical Chemical	14	38 ppm H ₂ O; 400 ppm propylene glycol
PC #2				
PC #3		Chemical	16	
PC #4		Chemical	18	
PC #5				
PC #6	Matheson, Coleman and Bell	Chemical	19	70 ppm H ₂ O; 150 ppm dimethylamine 230 ppm H ₂ O
DMF #1	Matheson, Coleman and Bell J. T. Baker	Reagent	24	
DMF #2		Reagent	32021	
DMF #3	Matheson, Coleman and Bell J. T. Baker J. T. Baker J. T. Baker J. T. Baker	Spectro	8; 96	
DMF #4		GC-Spectrophotometric	9-571	
DMF #5		GC-Spectrophotometric	Several	
DMF #6		GC-Spectrophotometric	1-1648	
DMF #7		GC-Spectrophotometric	1-3378	1700 ppm H ₂ O
AN #1	Matheson, Coleman and Bell J. T. Baker Matheson, Coleman and Bell J. T. Baker Matheson, Coleman and Bell Matheson, Coleman and Bell	Reagent		
AN #2		Analyzed Reagent		
AN #3		Spectro	97; 32	
AN #4		Analyzed Reagent	3772	
AN #5		Chromato	Several	
AN #6		Chromato	27	
MF #1	Matheson, Coleman and Bell Matheson, Coleman and Bell	Spectro	12	2 percent methanol 490 ppm methanol
MF #2		Spectro	27	

TABLE 7
DISTILLATION PROCEDURES FOR PURIFICATION OF SOLVENTS

Solvent	Quality	Drying Agent	Column	Condition
PC	Practical, chemical	CaH ₂	Spinning Band	5 to 10 mm Hg; reflux ratio: 30/1
DMF	Chemical	CaH ₂	Vigreux (Packed with Heli-pak)	8 to 14 mm Hg; 100 to 115 C
	Spectro	Multrathane M	Spinning Band or Vigreux	25mm Hg; reflux ratio: 10/1
	Spectro	Molecular Sieves	Vigreux (Packed with Heli-pak)	Atmospheric Pressure; 151 C
AN	Reagent	P ₂ O ₅	Spinning Band	Atmospheric Pressure; dry nitrogen; reflux ratio: 25/1
MF	Chromato	P ₂ O ₅	Oldershaw Bubble-Plate	Atmospheric Pressure; 81 C; reflux ratio: 5/1 (initial) to 2/1 (final)
	Spectro	Lithium Dispersion	Vigreux (Packed with Heli-pak)	Atmospheric Pressure; 31 C

In cases where water contents below 20 ppm were obtained in distilled PC batches, some H_2O (approximately 20 ppm) was added with a micro syringe to meet the contract specification requiring solvents to contain 40 ± 20 ppm H_2O .

Dimethyl Formamide. The purification of the spectrograde DMF involved the following steps:

1. DMF was shaken vigorously with activated, chromatographic grade molecular sieves (3\AA , 12-30 mesh) for 6 hours.
2. The molecular sieves were allowed to settle for 15 to 20 hours.
3. DMF was decanted off and centrifuged for 2 to 3 hours.
4. The predried DMF was distilled with a 1-foot Vigreux column, packed with Heli-pak, at atmospheric pressure and 151°C (no drying agent was needed during distillation).

Care was taken to remove molecular sieves used for predrying as completely as possible because they appeared to give off water during the distillation step. Total removal was difficult if the shaking period was too long because fine particles of molecular sieves which were hard to separate formed through a grinding action.

Acetonitrile. One-liter batches of AN were distilled from P_2O_5 with a 3-1/2-foot Oldershaw bubble-plate column at atmospheric pressure and 81°C . The reflux ratio was varied from an initial value of 5:1 to a final value of 2:1. Batches were predried by allowing them to contact P_2O_5 for 20 to 50 hours.

Methyl Formate. Liter batches of MF were distilled from a 50-percent lithium/50-percent heptane dispersion (1 percent added to the MF) with a 1-foot Vigreux column (packed with Heli-pak) at atmospheric pressure and 31°C . The MF was refluxed for about 1 hour before distillation. Some

batches were passed through a chromatographic column packed with molecular sieves before distillation. However, this procedure appeared to be unnecessary. The spectroquality MF used at first presented some difficulties because it had an excessive methanol content. A vigorous reaction occurred upon addition of the lithium dispersion. These difficulties were not encountered on newly supplied material which was low in methanol (<500 ppm), as had been requested from the supplier.

Characterization of Solvent Batches

The solvents were usually purified in batches of 500 to 1000 milliliters. A gas chromatographic test for water and major organic impurities with a Porapak Q column was employed for routine characterization of the solvents. Analysis results for solvent batches used for experimental work are presented in Table 8. Impurities listed as absent were not detected, the detection limits being 2 to 5 ppm for water and about 10 ppm for those organics which could be separated on the Porapak Q column.

Ordinarily, only batches showing water contents of 40 ± 20 ppm were used for experimentation. In some cases, some water was added to bring the water content within these limits. No single organic contaminant at a level above 60 ppm was tolerated. Unacceptable solvent batches were redistilled or discarded.

The above tolerances were relaxed in the case of MF to the impurity levels of solutions used in cell studies at the Livingston Electronic Laboratories.

SELECTION OF SOLUTES

Lithium perchlorate (LiClO_4), lithium chloride (LiCl), lithium fluoride (LiF), tetramethylammonium fluoride ($\text{TMA}\cdot\text{F}$), tetramethylammonium hexafluorophosphate ($\text{TMA}\cdot\text{PF}_6$), tetraethylammonium fluoride ($\text{TEA}\cdot\text{F}$), and lithium

TABLE 8

CHARACTERIZATION OF DISTILLED SOLVENT BATCHES

Solvent Code	H ₂ O Content, ppm per weight	Organics ppm per weight
PC #1-4	180	
PC #2-1	25	160
PC #2-2	55	20
PC #2-3	25	None
PC #2-4	20	15
PC #2-5	20	35
PC #2-6	35	None
PC #2-7	20	35
PC #2-8	40	65 + 35 (two impurities)
PC #2-9	20	20
PC #2-10	20	None
PC #2-11	32	None
PC #2-12	33	None
PC #4-1	None	None
PC #4-2	None	12
PC #4-3	None	14
PC #4-4	None	12
PC #4-5	None	17
PC #5-1	None	20 + 35
PC #5-2	None	20 + 35
PC #5-3	None	230 + 280
PC #5-4	None	22 + 40
PC #5-5	None	20 + 28
PC #6-1	None	100
PC #6-2	None	185
PC #6-3	None	None
DMF #1-2	20	140
DMF #3-2	40	None
DMF #3-3	45	35
DMF #3-4	70	None
DMF #3-5	65	None
DMF #4-1	50	None
DMF #4-2	100	None
DMF #5-1	52	26
DMF #5-2	65	9
DMF #5-3	38	None
DMF #5-4	56	None
DMF #5-5	57	None
DMF #5-6	52	None
DMF #6-1	59	None
DMF #6-2	30	None
DMF #6-3	114	None
DMF #6-4	109	None

TABLE 8
(Concluded)

Solvent Code	H ₂ O Content, ppm per weight	Organics ppm per weight
DMF #6-5	75	None
DMF #6-6	150	None
DMF #6-7	155	None
DMF #6-8	110	None
DMF #6-9	77	None
DMF #6-10	48	None
DMF #6-11	110	None
DMF #6-12	54	None
DMF #6-13	32	None
DMF #6-14	113	None
DMF #6-15	36	None
DMF #6-16	55	None
DMF #6-17	59	None
DMF #6-18	44	None
DMF #7-1	28	None
DMF #7-2	46	None
AN #1-1	23	None
AN #1-2	40	None
AN #3-1	50	None
AN #3-2	55	None
AN #4-1	48	None
AN #4-2	60	None
AN #4-3	49	None
AN #4-4	41	None
AN #4-5	49	None
AN #4-6	46	None
AN #5-1	40	None
AN #5-2	48	None
AN #5-3	63	None
AN #5-4	52	None
AN #5-5	54	None
AN #5-6	61	None
AN #5-7	60	None
MF #1-3	118	600 (MeOH)
MF #2-1	54	520 (MeOH)
MF #2-2	83	430 (MeOH)
MF #2-3	90	390 (MeOH)
MF #2-4	90	450 (MeOH)
MF #2-5	67	460 (MeOH)
MF #2-6	120	410 (MeOH)

hexafluoroarsenate (LiAsF_6) were selected as electrolyte solutes. Aluminum chloride (AlCl_3), boron trifluoride (BF_3), phosphorous pentafluoride (PF_5), and water were considered as complexing agents. Lithium tetrafluoroborate and lithium hexafluorophosphate solutions result from the addition of BF_3 or PF_5 , respectively, to a slurry of LiF . Anhydrous cupric fluoride (CuF_2) and cupric chloride (CuCl_2) were studied as electroactive materials. For the determination of individual ion mobilities, lithium bromide (LiBr) tetramethylammonium bromide ($\text{TMA}\cdot\text{Br}$), and tetrabutylammonium bromide ($\text{TBA}\cdot\text{Br}$) were used, also tetrabutylammonium tetraphenylboride ($\text{TBA}\cdot\text{TPB}$) which was synthesized from sodium tetraphenylboride ($\text{Na}\cdot\text{TPB}$) and tetrabutylammonium bromide.

Sources and purities of the materials procured to be used as solutes are given in Table 9 . Detailed analysis results are presented and discussed below.

ANALYSES OF SOLUTES

A comprehensive analysis of a solute is very difficult because a very large number of impurities may be present. The major portion of analyses of solids were performed by spark source mass spectrography (SSMS). The analysis of the metal ions was duplicated by emission spectroscopy, and some supplemental analyses were made to answer special questions. Mass spectrographic and gas chromatographic techniques were applied to analyze the gaseous solutes.

Analysis by Spark Source Mass Spectrography (SSMS)

Spark source mass spectrography is an instrumental method of analysis in which trace elements of a solid material may be determined by separating constituents according to their masses. The sample is broken up and ionized by a high-frequency RF high voltage source. The resulting ions are accelerated through a mass spectrometer and recorded on a photographic plate. This plate can be interpreted for both qualitative and quantitative analysis.

TABLE 9
SOURCE AND PURITIES OF PROCURED SOLUTES

Chemical	Source	Quality
LiClO ₄ #1	Foote Mineral Co.	99.75%
LiClO ₄ #2	Atomergic Chemetals Co. (Lot B5057)	99.9%
LiClO ₄ #3	Atomergic Chemetals Co. (Lot B7523)	99.9%
LiCl #1	Foote Mineral Co.	99.75%
LiCl #2	Atomergic Chemetals Co. (Lot B5095)	99.9% (optical)
LiCl #3	Atomergic Chemetals Co. (Lot B7948)	99.9 + % (optical)
LiF #1	Foote Mineral Co.	99.8%
LiF #2	Electronic Space Products, Inc.	99.9%
LiF #3	Research Inorganic Chemical Corp.	99.99%
TMA·F #1	Ozark-Mahoning Co. (Lot VM-4-125)	Special
TMA·F #2	Aldrich Chemical Company, Inc.	(20% Na)
TMA·F #3	Southwestern Analytical Chemicals	
TMA·F #4	Southwestern Analytical Chemicals	
TMA·PF ₆ #1	Ozark-Mahoning Co. (Lot KW-2-1-C)	99.85%
TEA·F #1	Southwestern Analytical Chemicals	Purified (25% H ₂ O)
LiAsF ₆ #1	Livingston Electronic Labs.	2.2M LiAsF ₆ /MF Solution
AlCl ₃ #1	Mallinkrodt Chemical Works	Analytical Reagent
AlCl ₃ #2	J. T. Baker Chemical Co.	Analyzed Reagent
AlCl ₃ #3	Rocky Mountain Research, Inc.	99.999%
AlCl ₃ #4	Rocky Mountain Research, Inc. (Lot LP03088)	99.999%
BF ₃ #1	Matheson Co., Inc.	99.5%
PF ₅ #1	Research Inorganic Chemical Co.	Chemically Pure
H ₂ O	In-House	Deionized
CuF ₂ #1	Research Inorganic Chemical Co.	Chemically Pure
CuF ₂ #2	Ozark-Mahoning Co.	Special
CuF ₂ #3	Ledoux & Co.	Special
CuCl ₂ #1	Matheson, Coleman and Bell	Reagent
CuCl ₂ #2	Fisher Scientific Co. (Lot 752944)	Certified Reagent

TABLE 9
(Concluded)

Chemical	Source	Quality
TBA·TPB #1	Synthesized from TBA·Br #1 and Na·TPB #1	Reagent
Na·TPB #1	Baker and Adamson Reagent, General Chemical Division, Allied Chemical Corporation	
TBA·Br #1	Columbia Organic Chemicals Co., Inc.	Polarographic
TMA·Br #1	Southwestern Analytical Chemicals	Polarographic
LiBr #1	Matheson, Coleman and Bell	Reagent
LiBr #2	Gallard-Schlesinger Chemical Mfg. Corp. (Lot B5111)	99.99% (optical)

The analyses were performed at the Bell and Howell Research Laboratories, Pasadena, on a semiautomatic Consolidated Electrodynamics Corporation X21-110 mass spectrometer. A SpectraDataMeter was utilized to measure line positions and identify spectral mass lines. Quantitative information was obtained from a plate reader-computer system.

The samples were prepared by pressing the solids into pellets at about 60,000 psi, and were enclosed in a rubber bag at this stage to avoid contamination by the atmosphere. Each pellet was then trimmed in a dry box on all sides to form electrodes and mounted on gold-capped sample holders just prior to sparking. The samples were exposed to the laboratory atmosphere briefly when they were transferred to the spark chamber of the mass spectrometer.

Because the samples were sparked against ultra-high-purity gold probes and tantalum slits were used in the instruments, no results for these two metals were obtained. All other elements at concentrations of 10 ppm or more were detected, unless there was some interference by background lines from major components in the solid.

Before the exposures were made, the samples were given a prespark; that is, the surface of the samples was sparked to reduce the possibility of surface contamination. For each sample, a set of exposures with variable exposure times was taken to allow quantitative determination of constituents present at various concentrations.

This analysis method provided elemental analyses covering all elements from hydrogen up to uranium, although an analysis for hydrogen was not always performed. Some erratic results were obtained occasionally such as varying contents indicated for a certain element on varying exposures of one set. Also, the spark source mass spectrographic results did not always agree perfectly with the results obtained by other methods. One has to consider that only a very small part representing the bulk solid

is actually sampled (this applies also to the emission spectrography). Heterogeneity of a sample is more likely to lead to erratic results than in a wet analytical technique. Nevertheless, SSMS has been a most useful analytical tool for examining impurity contents of the solids used on the program.

Analysis by Emission Spectrography

Emission spectrography is a common technique employed to determine metal contents at levels less than 100 ppm. Table 10 gives some lower limits as obtained by Pacific Spectrochemical Laboratory, Inc., Los Angeles, where the emission spectrographic analyses were made.

The results obtained by emission spectrography are considered semiquantitative, with an accuracy of ± 50 percent and reproducibility of ± 15 percent. Empirical corrections were made based on the major anion present, because individual calibrations for most of the matrices were not available.

Analysis Results and Purification of Solutes

Lithium Perchlorate. Two batches of 99.9-percent LiClO_4 supplied by the Atomergic Chemetals Company, LiClO_4 #2 and LiClO_4 #3, were analyzed, the results being given in Tables 11 and 12. The samples had been dried at elevated temperature (i.e., at 90 to 120 C) under vacuum; this purification procedure was applied to all LiClO_4 used on the program.

Because of interferences, Mg, P, S, V, Cr, and Nb could not be determined by SSMS. Only one impurity above 100 ppm was found in LiClO_4 #2, and it is not conceivable that 260 ppm Na affected any measurements significantly. The sodium content was also high in LiClO_4 #3. A high fluoride content was indicated by SSMS, but this result was not confirmed in a test described below where an Orion fluoride electrode was used. The hydrogen content probably was caused by contamination of the sample with water; because oxygen was a major constituent, a balance between H and O content cannot be made.

TABLE 10

LOWER LIMIT FOR DETECTION OF VARIOUS METALS
IN LITHIUM CARBONATE MATRIX
BY EMISSION SPECTROGRAPHY

<u>Element</u>	<u>Lower Limit, ppm</u>
Aluminium	2
Antimony	40
Arsenic	300
Barium	100*
Beryllium	0.3
Bismuth	1
Boron	30
Cadmium	30
Calcium	0.05
Chromium	1
Cobalt	3
Columbium	40
Copper	0.3
Gallium	2
Germanium	5
Gold	10
Indium	3
Iron	3
Lead	20*
Magnesium	0.1
Manganese	1
Mercury	200
Molybdenum	5
Nickel	3
Palladium	2
Phosphorus	1000
Platinum	5
Potassium	300
Rubidium	20
Silicon	5
Silver	0.3
Sodium	100
Strontium	3
Tantalum	200
Thallium	100

*Special spectrographic techniques are available which may determine smaller quantities of the metal.

TABLE 10

(Concluded)

<u>Element</u>	<u>Lower Limit,</u> <u>ppm</u>
Thorium	100
Tin	5
Titanium	4
Tungsten	100
Vanadium	5
Zinc	100
Zirconium	5

TABLE 11

IMPURITY CONCENTRATIONS IN LiClO_4 #2 DETERMINED BY SPARK
SOURCE MASS SPECTROMETRY AND EMISSION SPECTROSCOPY

Impurity	Spark Source Mass Spectrometry			Emission Spectroscopy
	Detection Limit, ppm atomic	Content, ppm atomic	Content, ppm per weight	Content, ppm per weight
H	3.0	500.0	28	
B	1.0	20.0	12	
C	1.0	20.0	14	
N	1.0	6.5	5.1	
F	2.0	23.0*	25*	
Na	0.3	200.0	260	
Al	0.5	1.0	1.5	
Si	1.0	23.0	36	10
K	0.3	16.0	35	
Ca	0.7	5.9	13	17
Cu	2.0	12.0*	43*	4
Zn	2.0	3.0	11	
As	1.0	21.0	89	
I	2.0	3.0	21	
Mg				3
Fe				2
Sn				4
Pb				16

*May be due to residuals in the mass spectrometer

TABLE 12

IMPURITY CONCENTRATIONS IN LiClO_4 #3 DETERMINED BY SPARK
SOURCE MASS SPECTROMETRY AND EMISSION SPECTROSCOPY

Impurity	Spark Source Mass Spectrometry			Emission Spectroscopy
	Detection Limit, ppm atomic	Content, ppm atomic	Content, ppm per weight	Content, ppm per weight
H	3.0	5000	280	1.5
B	1.0	2.7	1.6	
C	1.0	41-590	28-400	
N	1.0	28	22	
F	2.0	2800*	3000*	
Na	0.3	800	1000	
Mg	1.0	12	16	
Al	0.5	32	49	
Si	10	<10	<16	
K	0.3	110	240	
Ca	0.7	320	720	180
Fe	2.0	14	44	<0.3
Cu				
H ₂ **	-	39	4.4	
OH**	-	240	320	
HCl**	-	1000	2100	

*High F content not confirmed by test with fluoride ion activity electrode.

**Reported for comparison purposes only

For the test of LiClO_4 #3 for fluoride, a fluoride ion activity electrode (Orion Research Incorporated) was used. The electrode indicated a slightly irreproducible potential of -140 mv with an aqueous solution of 0.25 M LiClO_4 #3. An identical solution which contained additional 0.00042 M LiF gave a potential of +24 mv versus the same reference electrode. From these values, a fluoride concentration of 5 ppm or less can be calculated for LiClO_4 #3.

Lithium Chloride. Two batches of optical grade lithium chloride (99.9 percent) supplied by Atomergic Chemicals Company, LiCl #2 and LiCl #3, were analyzed, and the results are presented in Tables 13 and 14. The sodium and the potassium contents were slightly above 100 ppm in both products, but they are not considered representing significant impurities.

Both (samples submitted for analysis and materials used for experimentation on the program) were dried under vacuum at elevated temperatures of about 120 C. The high oxygen content in LiCl #3 appears to originate from some oxide rather than from water contamination, because the hydrogen found did not balance with the oxygen observed.

Lithium Fluoride. Two products were analyzed by emission spectrography: LiF #2, 99.9 percent, supplied by Electronic Space Products, Inc., and LiF #3, 99.9 percent, optical grade, supplied by Research Inorganic Chemical Corporation. Because the impurity content of the less expensive product, LiF #2, was not significantly greater according to this analysis, this product was further analyzed by SSMS. The results are given in Table 15. Several impurities were revealed at levels greater than 100 ppm. They are carbon, probably from carbonate, oxygen which may have been present in part in complex anions and also as oxide (the low hydrogen content indicates little H_2O was present), and sulfur, probably from sulfate. The metals sodium, potassium, and antimony which complete the list were also present; the figures for chlorine and copper are upper values only because of possible cross-sparking of a CuCl_2 sample also in the mass spectrometer.

TABLE 13

IMPURITY CONCENTRATIONS IN LiCl #2 DETERMINED BY SPARK
SOURCE MASS SPECTROMETRY AND EMISSION SPECTROSCOPY

Impurity	Spark Source Mass Spectrometry			Emission Spectroscopy
	Detection Limit, ppm atomic	Content, ppm atomic	Content, ppm per weight	Content, ppm per weight
Be	0.2	0.42	0.2	<0.3
C	1	120	68	
N	1	6.5	4.3	
O	1	3900	2900	
F	1	17	15	
S	5	8	12	
Na	0.3	180	195	<100
Mg	1	5.4	6.2	2.5
Al	0.5	0.8	1.0	<5
Si	1	2.8	3.8	<10
K	0.5	100	185	<300
Ca	1	6.0	11.5	36
Ti	10	Not detected	(<23)	<4
Cr	1	3.2	7.9	<1
Fe	1	3.3	8.7	<2
Ni	1	13	36	<5
Cu	1	4.4	13	0.6
Zn	1	4.0	12	<100
Ge	10	Not detected	(<34)	<5
Se	1	2.1	7.8	
Br	1	2.0	7.5	
Cd	1	5.3	28	<30
Hg	2	2.1	20	<200

TABLE 14

IMPURITY CONCENTRATIONS IN LiCl #3 DETERMINED BY SPARK
SOURCE MASS SPECTROMETRY AND EMISSION SPECTROSCOPY

Impurity	Spark Source Mass Spectrometry			Emission Spectroscopy
	Detection Limit, ppm atomic	Content, ppm atomic	Content, ppm per weight	Content, ppm per weight
H	2	760	36	0.8
C	1	33	19	
N	1	4.1	2.7	
O	1	6400	4800	
F	1	29	26	
Na	0.3	120	130	
Mg	1	7.3	8.4	
Al	0.5	2.6	3.3	
Si	1	2	3	
S	1	65	98	
K	0.5	56	103	96
Ca	1	50	95	
Ti	10	<10	<22	
Cu	1	1.9	5.7	
Ge	10	<10	<34	
Br	1	36	134	
H ₂ *	-	25	2.4	
OH*	-	260	210	
HCl*	-	440	760	

*Reported for comparison purposes only

TABLE 15

IMPURITY CONCENTRATIONS IN LiF #2 DETERMINED BY SPARK
SOURCE MASS SPECTROMETRY AND EMISSION SPECTROSCOPY

Impurity	Spark Source Mass Spectrometry			Emission Spectroscopy
	Detection Limit, ppm atomic	Content, ppm atomic	Content, ppm per weight	Content, ppm per weight
H	3	290	22	
B	1	2.7	2.3	
C	1	750	690	
N	1	40	43	
O	1	7000	8600	
Na	0.3	4800	8500	<100
Al	0.5	5.8	12.1	4.8
Si	1	28	60	96
P	5	10	24	
S	3	220	540	
Cl	1	1600*	4400*	
K	0.3	270	810	<300
Ca	0.7	14	43	44
V	1	2.0	7.9	<5
Cr	1	2.0	8.0	<1
Cu	1	38*	187*	10
Nb	3	7.0	50	
Sb	5	17	160	<40
Mg				2.2
Pb				16
Fe				4.0
Sn				Trace (<3)
Ni				4.4

*May be caused by cross sparking of a copper chloride sample also in the the mass spectrometer.

Before using lithium fluoride for experimentation, the material was dried at about 120 C under vacuum. The samples submitted for analysis were treated in the same manner.

Tetramethylammonium Fluoride. A special grade tetramethylammonium fluoride, TMA·F #1, was obtained from the Ozark-Mahoning Company, but a product supplied by the Aldrich Chemical Company, Inc., TMA·F #2, appeared to be a much drier product. Emission spectrography revealed a sodium content on the order of 20 percent for TMA·F #2, however. Two products supplied by Southwestern Analytical Chemicals, Inc., TMA·F #3 and TMA·F #4, had a somewhat cakey appearance and a relatively high water content of these products was suspected; but no significant impurities were found in TMA·F #3 by emission spectrography.

No results could be obtained by spark source mass spectrography because the sample lost its consistency upon exposure to vacuum and could not be sparked; TMA·F undergoes thermal decomposition to $(\text{CH}_3)_3\text{N}$, CH_4 , and CH_3F in a vacuum of 0.5 to 1 mm Hg according to Ref. 16, and decomposition could be expected to occur at room temperature at a vacuum of 10^{-7} to 10^{-8} mm Hg, which are the conditions in the mass spectrometer.

A completely satisfactory tetramethylammonium fluoride product was therefore not available for testing, and only limited, preliminary studies were performed with this compound.

Tetramethylammonium Hexafluorophosphate. A product supplied by the Ozark-Mahoning Company, TMA·PF₆ #1, was used for experimental work without further purification. Analysis results are given in Table 16.

A complete determination of organic impurities would have been very difficult and was not attempted. During the course of the NMR investigations, no other organic constituents than tetramethylammonium were detected. It was expected, however, that only organic impurities present at concentrations of 1 percent or higher would have been noticed.

TABLE 16

IMPURITY CONCENTRATIONS IN TMA.PF₆ #1
 DETERMINED BY SPARK SOURCE MASS SPECTROMETRY
 AND EMISSION SPECTROSCOPY

Impurity	Spark Source Mass Spectrometry			Emission Spectroscopy
	Detection Limit, ppm atomic	Content, ppm atomic	Content, ppm per weight	Content, ppm per weight
Li	1	27	20	
B	3	5.7	6.8	<30
O	3	290	510	
Na	1	8.3	20.9	<100
S	20	Not detected	<70	
Cl	3	960*	3720*	
K	1	2.3	9.9	<300
Cu	3	2400*	16700*	5.2
Zn	5	27	194	<100
Mg				8
Si				50
Fe				Trace(<30)
Ca				25

*May be caused by residuals in the mass spectrometer

Tetraethylammonium Fluoride. The tetraethylammonium fluoride, TEA·F #1, was supplied by Southwestern Analytical Chemicals, Inc. Some TEA·F was dissolved in PC which contained less than 5-ppm water. Gassing of this solution was observed which was accelerated upon exposure to 60 C; the nature of the decomposition reaction was not determined. The water content of this solution was 3.1 percent according to Karl Fischer titration, which corresponds to approximately 25-percent H₂O content of TEA·F #1.

Direct drying of TEA·F was not possible because of decomposition. A purification procedure used at the Livingston Electronic Laboratory (Ref. 17) was therefore employed. The TEA·F was first recrystallized from acetonitrile, and needles with a neat appearance were obtained. A solution was made up in propylene carbonate, and the analysis by Karl Fischer indicated a water content of 13 percent of the recrystallized product. This solution was also tested in a vapor phase chromatographic procedure involving a Porapak Q column and a precolumn to retain the solid part of the sample; this test indicated a water content of 8 percent based on the TEA·F.

A further step of the purification procedure involved the removal of water by distilling off a benzene-water azeotrope. The water content, based on TEA·F, was found to be 6 percent according to a Karl Fischer titration and 2 percent as indicated by the VPC technique. A benzene content of 300 ppm (based on the total approximately 1 molar solution) remained even after prolonged exposure to vacuum. NMR investigations indicated that the lower value (i.e., the one obtained by VPC) is more realistic. There may be decomposition products of TEA·F interfering in the Karl Fischer titration, causing that value to appear too high.

The final TEA·F/PC solution was discolored yellowish. The presence of tetraethylammonium in this solution was verified by NMR, but an equivalent fluoride content could not be found. The F¹⁹ resonance could not be observed in NMR investigations, and a direct analysis indicated a fluoride content of only about 0.005 molar. No extensive studies were made in this system.

Lithium Hexafluoroarsenate. A solution of lithium hexafluoroarsenate in methyl formate was obtained from Livingston Electronic Laboratory where it was made by metathesis from LiBF_4 and KAsF_6 . The code LiAsF_6 #1 in this report will designate the use of this solution.

The solution was analyzed by atomic absorption for lithium (2.27 moles/liter), potassium (0.035 M), and boron (0.010 M). The potassium and the boron contents are due to the solubility of KBF_4 . The potassium to boron ratio is not stoichiometric for KBF_4 because the metathesis was not performed entirely stoichiometrically.

Analysis of the solution for water and methanol will be discussed later.

Aluminum Chloride. Two batches of aluminum chloride supplied by Rocky Mountain Research, Inc., AlCl_3 #3 and AlCl_3 #4, were used without purification. Analysis results are presented in Table 17 and 18.

The purity of 99.999 percent claimed by the supplier refers to the metal aluminum only. The metallic impurities were low indeed, although there was a considerably higher content than 10 ppm. The high value of titanium in AlCl_3 #3 is probably due to an inhomogeneity in the sample because it was found only in some of the exposures. The fluorine content in AlCl_3 #4 is probably also not a bulk figure.

A high oxygen content was obtained for both products. This was most likely caused by contamination from the laboratory atmosphere to which the samples were very briefly exposed, whereby the visible appearance of the sample surface slightly changed. The fact that higher values were found at the surface of the AlCl_3 #4 sample supports the above assumption.

TABLE 17

IMPURITY CONCENTRATIONS IN AlCl_3 #3 DETERMINED BY SPARK
SOURCE MASS SPECTROMETRY AND EMISSION SPECTROSCOPY

Impurity	Spark Source Mass Spectrometry			Emission Spectroscopy	
				Content (Sample 1), ppm per weight	Content (Sample 2), ppm per weight
	Detection Limit	Content, ppm atomic	Content, ppm per weight		
Li		Not determined		<50	<50
Be	0.2	1.4	0.4	<0.3	<0.3
B	0.3	0.64	0.21	<30	<30
C	1	91	33		
N	1	58	24		
O	1	2700	1300		
Si				28	54
F	1	24	14		
Na	0.3	57	40	<100	<100
Mg	1	130	95	9.2	12
P	1	51	47		
K	0.5	7.6	8.9	<300	<300
Ca	1	4.9	5.9	9.8	22
Ti	1	(540)	(780)	<4	<4
Cr	1	2.2	3.4	<1	<1
Fe	1	56	94	12	<10
Co	1	20	35	<3	<3
Ni	1	4.4	7.8	<3	<3
Cu	1	8.3	16	21	59
Zn	5	5.8	11.3	<100	<100
Nb	1	6.3	18		
Sb	2	52	190	<40	<40
Hg	2	15	90	<200	<200
Pb				30	<20

TABLE 18
 IMPURITY CONCENTRATIONS IN AlCl_3 #4 DETERMINED BY SPARK
 SOURCE MASS SPECTROMETRY AND EMISSION SPECTROSCOPY

	Spark Source Mass Spectrometry			Emission Spectroscopy
Impurity	Detection Limit, ppm atomic	Content, ppm atomic	Content, ppm per weight	Content, ppm per weight
H	1	150	4.5	
B	0.3	5.3	1.7	
C	1	42	15	
N	1	67	28	
O*	1	200-16,000	100-7700	
F*	1	3-1800	2-1000	
Na	0.3	130	90	
Mg	1	34	25	3.8
Si	3	35	30	
P	1	1600	1500	
S	2	140	130	
K	0.5	7.9	9.3	
Ca	1	60	72	7.2
Cr	1	12	19	
Fe	1	5.0	8.4	<5
Cu				0.4
Co	1	1	2	
Zn	5	<5	<10	
Ga	2	36	75	
As	2	14	31	
Br	2	7.6	18	
In	2	20	69	
Sb	2	93	340	
H ₂ **	-	38	2.3	
OH**	-	12	6	
HCl**	-	4500	5000	
AlO**	-	50	65	

*Higher values on surface exposures only

**Reported for comparison purposes only

Boron Trifluoride. A cylinder of chemically pure grade boron trifluoride, BF_3 #1, was procured from the Matheson Company, Inc., for use on the program (without purification). It was analyzed using a CEC 21-103C mass spectrometer. Trifluoroboroxime was the only impurity found. Its concentration was determined to be greater than 1 mole percent. Although the mass spectrometer was extensively passivated, the $(\text{BOF})_3$ found may not be present in the sample, but may instead be generated inside the mass spectrometer. Fisher, Lehmann, and Shapiro (Ref. 18) report that $(\text{BOF})_3$ is not stable at temperatures below 250 C, and that a sample of $(\text{BOF})_3$ is essentially decomposed (>99 percent) after 1 hour at 25 C. Thus, the $(\text{BOF})_3$ found in this analysis must have been generated in the mass spectrometer and is not actually present in the BF_3 sample. Permanent gases, such as SiF_4 , CF_4 , N_2 , O_2 , and SF_6 , were not detected and, consequently, were present at concentrations less than 0.1 mole percent, which is the detection limit for these species (fluorine cannot be detected mass spectrometrically in the presence of large amounts of boron trifluoride).

The BF_3 was also analyzed by gas chromatography using a Halocarbon Oil 13-21 on a Chromasorb W column but the results were inconclusive; peaks were found but they were not reproducible, indicating that the sample was incompatible with the packing or the column had not been completely passivated.

The infrared spectrum of BF_3 in a 5-centimeter cell with silver chloride windows containing 80 millimeters of BF_3 was recorded from 670 to 3500 cm^{-1} on a Perkin Elmer Infracord, Model 137. No peaks were found other than those expected for BF_3 (Ref. 19). Hydrogen fluoride was determined by measuring the absorbance at 3878 cm^{-1} on a Cary 14 recording spectrometer (a calibration curve was prepared by measuring the absorbance of hydrogen fluoride at various pressures).

In a first determination, using a 10-centimeter cell with calcium fluoride windows at a sample pressure of 653 millimeters, a peak was found for hydrogen fluoride, but the peak height was approximately the same as the baseline noise and was at the limit of detection. The determination was repeated using a 10-centimeter cell with sapphire windows and a sample pressure of 1495 millimeters. The peak height again was on the order of the baseline noise. The actual HF content was therefore at the limit of detection, 200 ppm, or less.

Phosphorous Pentafluoride. Chemically pure grade phosphorous pentafluoride, PF₅ #1 was obtained from the Research Organic Chemical Company and used without purification.

The only impurity found in PF₅ #1 by mass spectrometry was POF₃, its concentration being greater than 1 percent. As in the case of BF₃, the oxygen-containing impurity found may not be present in the PF₅ sample but may be generated inside the mass spectrometer. Permanent gases, such as SiF₄, CF₄, N₂, O₂, and SF₆ were not detected, and hence were not present at concentrations greater than 0.1 mole percent. PF₃ cannot be determined mass spectrometrically in the presence of a large excess of PF₅ because the major species generated by ionization of PF₃, i.e., PF₂⁺, is also generated by the ionization of PF₅. In addition, fluorine cannot be detected because fluoride ions are also produced by the ionization of PF₅.

The analyses of PF₅ by gas chromatography using a column of Halocarbon Oil 13-21 on Kel F was inconclusive. Peaks were obtained but they were not reproducible, indicating incompatibility with column packing or that the column had not been completely passivated.

The phosphorous pentafluoride was analyzed by infrared spectrometry to supplement the mass spectrometric results. The spectrum of phosphorous pentafluoride at 720 millimeters is shown in Fig. 9 ; it was recorded on a Perkin Elmer Infracord, Model 137, using a 10-centimeter cell with

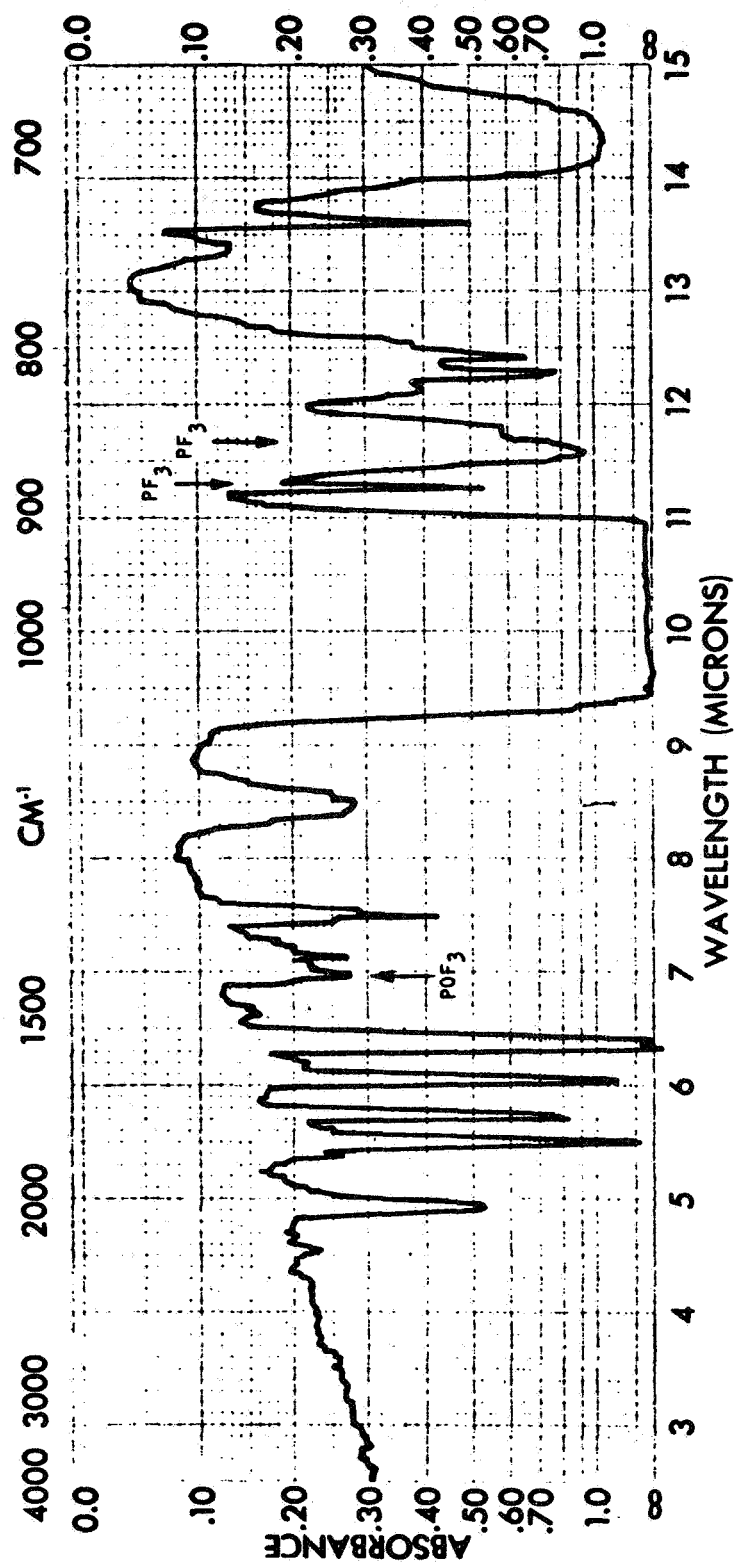


Figure 9. Infrared Spectrum of Phosphorous Pentafluoride (PF₅ #1).

silver chloride windows. The absorption peak at 1420 cm^{-1} is due to POF_3 and the peaks at 860 and 890 cm^{-1} are due to PF_3 . The remaining peaks are those expected for phosphorous pentafluoride (Ref. 20 and 21). A mixture of 20-millimeter phosphorous trifluoride, (Ozark-Mahoning Company, no purity given) and 240-millimeter helium was prepared for calibration purposes. The absorbance at 860 and 890 cm^{-1} was measured as a function of the partial pressure of PF_3 , as shown in Fig. 10a. The PF_3 absorbance in the PF_5 #1 sample corresponds to 2.35 and 1.90 millimeters at 860 and 890 cm^{-1} , respectively, or a concentration of approximately 0.2 percent (by weight).

The spectrum of POF_3 has been reported (Ref. 20 and 22) but no extinction coefficients are available. The preparation of POF_3 with a known purity is very difficult and an indirect method has been employed to determine the extinction coefficient. The intense absorption peak for POF_3 at 1420 cm^{-1} is due to the stretching of the P-O bond. Assuming that POCl_3 and POF_3 have similar characteristics, the extinction coefficient of the P-O bond should be the same for these two species even though the absorption frequency is different due to the differences in the masses of the two species. A mixture of 13 millimeters of phosphorous oxychloride, POCl_3 (Baker analyzed reagent grade), and 700 millimeters of helium was prepared and the absorbance was measured at 1320 cm^{-1} at different pressures. The absorbance of phosphorous oxychloride as a function of its partial pressure is shown in Fig. 10b. The minimum absorbance peak for POF_3 in PF_5 #1 had an absorbance of 0.08 (Fig. 9), which corresponds to 0.3 millimeter of POCl_3 or approximately 300 ppm (by weight) of POF_3 in PF_5 . This absorbance was repeatedly obtained but some spectra showing larger amounts of POF_3 were also found. The larger concentrations in these cases are probably due to the phosphorous pentafluoride reacting with traces of water. The actual POF_3 concentration may actually be less than 300 ppm. The much greater value found for POF_3 by mass spectrometry is due to incomplete passivation of the inlet system.

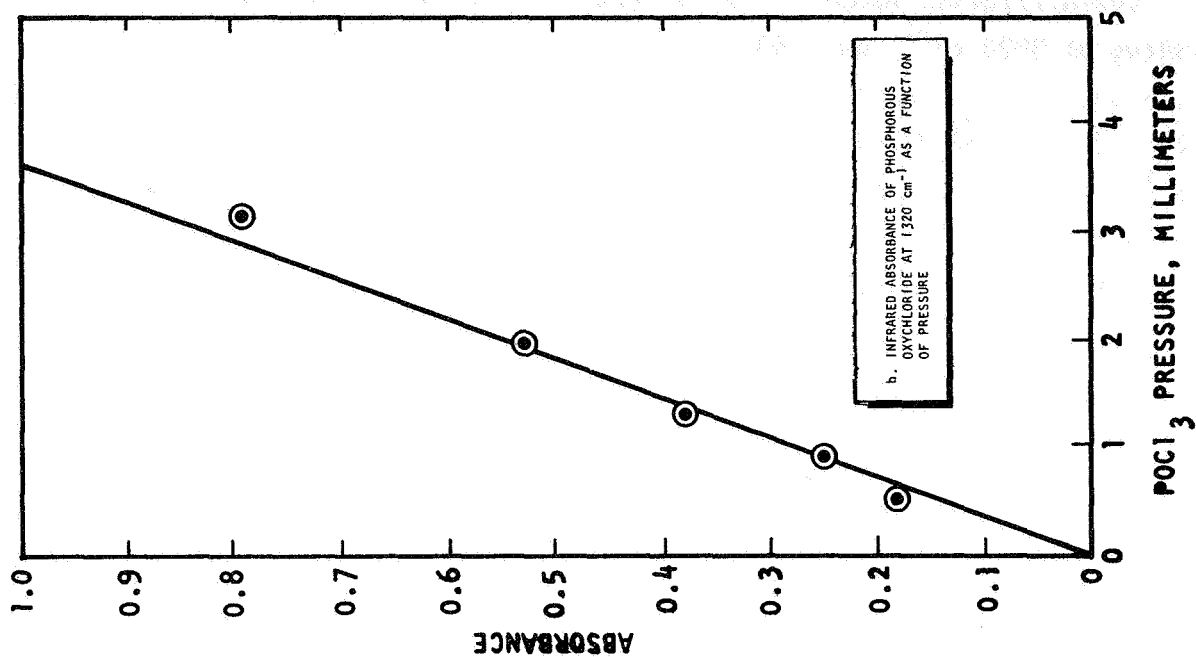
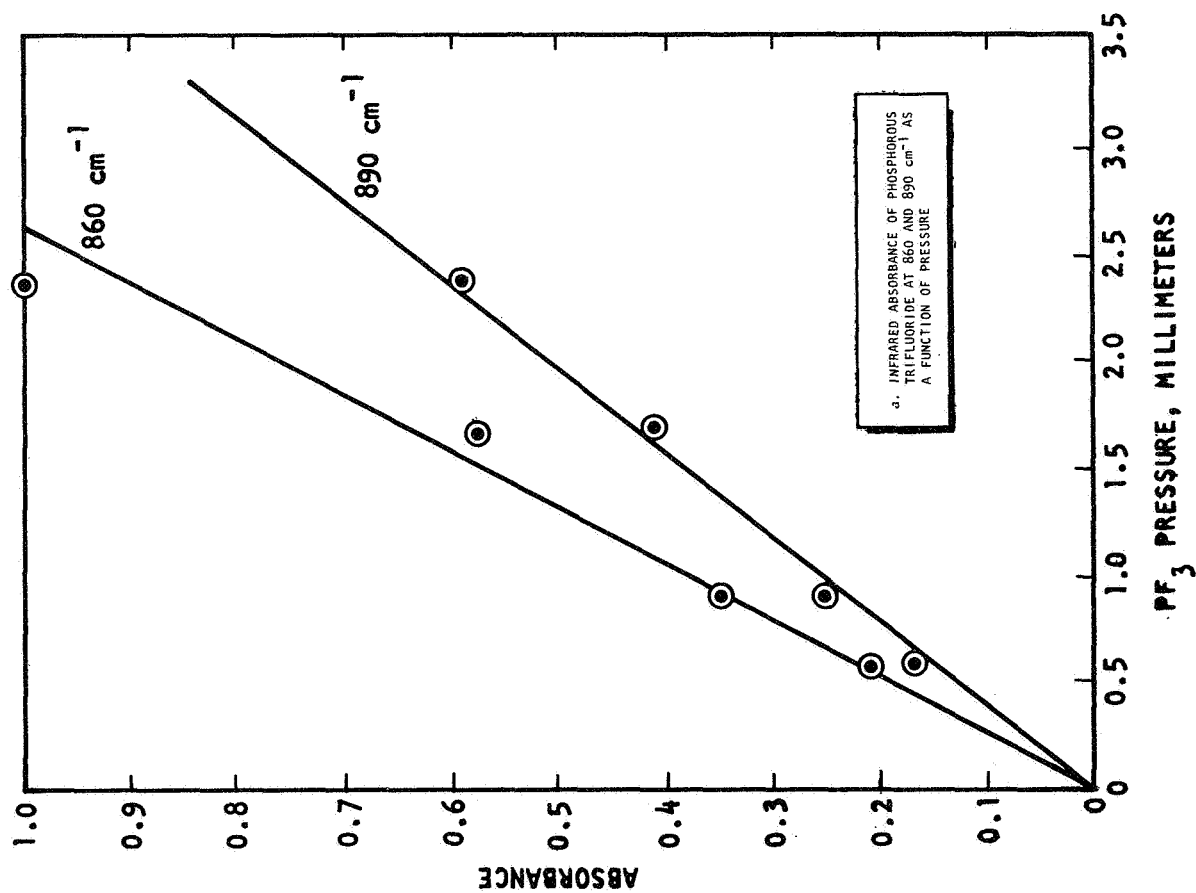


Figure 10. Infrared Absorbance of Phosphorous Trifluoride and Phosphorous Oxychloride as a Function of Pressure

The HF concentration in the PF_5 , determined by measuring the absorbance of a 500-millimeter sample in a 10-centimeter cell with calcium fluoride windows at 3878 cm^{-1} , was 800 ppm.

Water. Deionized distilled water with a typical conductivity of $5 \times 10^{-7} \text{ ohm}^{-1} \text{ cm}^{-1}$ was used throughout the program. A further characterization was not deemed necessary because water was added to the electrolytes only in small amounts, normally at the 1000 ppm level.

Cupric Fluoride. A special grade cupric fluoride product of the Ozark-Mahoning Company, CuF_2 #2, was analyzed by spark source mass spectrography and emission spectrography. The results of Table 19 indicate several impurities at levels above 100 ppm, Fe and Ni being considered the most critical ones. Another special product, CuF_2 #3, was obtained from Ledoux and Company, the analysis results being listed in Table 20. Low impurity levels for metallic impurities were recorded. A large oxygen content of 1.5 percent by weight was revealed by SSMS together with significant amounts of carbon and some sulfur. In the second analysis, which was provided by the supplier of the chemical and was performed by the Associated Electrical Industries, Ltd., England, no figures for O, N, and C are given; nitrogen and oxygen could not be determined because of instrument background, and in the case of carbon, a determination was impossible because the sample was mixed with graphite. The high oxygen content appears to be due to the presence of a copper oxide rather than to an excessive water content because only small amounts of hydrogen were found. CuF_2 #3 was used for measurements despite the relatively high impurity levels; a more satisfactory product did not seem to be available.

In an effort to prepare pure cupric fluoride, the fluorination of copper arsenide was investigated but without success (Ref. 5).

TABLE 19

IMPURITY CONCENTRATIONS IN CuF_2 #2 DETERMINED BY SPARK
SOURCE MASS SPECTROMETRY AND EMISSION SPECTROSCOPY

Impurity	Spark Source Mass Spectrometry			Emission Spectroscopy
	Detection Limit, ppm atomic	Content ppm atomic	Content, ppm per weight	Content, ppm per weight
H	3.0	910.0	27	
Li	0.3	0.5	0.1	
B	1.0	32.0	10.2	
C	1.0	320.0	114	
N	1.0	75.0	31	
O	1.0	2600.0	1230	
Na	0.3	300.0	204	
Mg	0.7	58.0	42	35
Al	0.5	130.0	104	170
P	1.0	12.0	11	
S	5.0	360.0	340	
Cl	2.0	250.0	260	
K	0.3	22.0	25	
Ca	0.7	18.0	21	86
Ti	7.0	N.D.	< 10	
V	1.0	30.0	45	
Cr	1.0	8.5	13	5
Mn	1.0	7.2	12	23
Fe	2.0	740.0	1200	1100
Ni	5.0	430.0	730	970
Zn	5.0	130.0*	250*	
Ga	0.7	1.3	2.7	
As	5.0	N.D.	< 11	
Ag	0.7	8.2	26	6
Cd	3.0	21.0	70	
Sn	3.0	1300.0	4600	400
Te	10.0	N.D.	< 38	
Pb	3.0	44.0	270	120
Bi	3.0	48.0	300	

*May be due to residuals in mass spectrometer

TABLE 20

IMPURITY CONCENTRATIONS IN CuF_2 #3 DETERMINED BY
SPARK SOURCE MASS SPECTROMETRY AND EMISSION SPECTROSCOPY

Element	Spark Source Mass Spectrometry (by Bell & Howell)			Spark Source Mass Spectrometry (by Associated Electronic Industries)		Emission Spectroscopy (by Pacific Spectro-chemical Laboratory)		Emission Spectroscopy (by Ledoux & Company)	
	Detection Limit, ppm atomic	Impurity Concentration, ppm		Detection Limit*	Impurity Concentration, ppm		Impurity Concentration, ppm per Weight	Impurity Concentration, ppm per Weight (?)	
		Atomic	Per Weight		Atomic	Per Weight			
H	3.0	280	8.3						
Li	0.3	0.3	0.06						
Be	1.0	15	4						
B	1.0	14	4		1	0.3			
C	1.0	1500	500						
N	1.0	26	11						
O	1.0	32,000	15,000						
Na	0.3	71	48		2	1			8
Mg					5				3
Al	0.5	46	37		5				3
Si					20				
P					1.5	1.4		2.7	
S	5.0	240	230					<5	
Cl	2.0	93	97		10	10			
K	0.3	36	42		3	3			
Ca	0.7	8.3	10		4	5		6.9	5
Ti	7.0	<7	<10						
Cr	1.0	6.1	9.4						
Mn					0.2	0.3			
Fe	2.0	4.0	7.0		0.3	0.5		<2	5
Co	2.0	4.9	8.5		4	7			
Ni					2	3			5
Zn	5.0	<5	<10						
Ga	0.7	5.5	11						
As	0.7	31	69						
Rb	0.7	2.0	5.0						
Te		<10	<38						
Pb	10.0				5	30			

*Not available

Cupric Chloride. Reagent grade cupric chloride from Fisher Scientific Company, CuCl_2 #2, was analyzed and used for experimental work without purification. Analysis results presented in Table 21 indicate a satisfactory product; the lithium analysis was uncertain because of possible memory effects in the mass spectrometer or because of cross-sparking.

Tetrabutylammonium Tetraphenylboride. Tetrabutylammonium tetraphenylboride was prepared by metathesis of tetrabutylammonium bromide (TBA·Br #1, Columbia Organic Chemicals Company, Inc., polarographic grade) and sodium tetraphenylboride (Na·TPB #1, Baker Adamson Laboratory Chemical, reagent grade) according to a procedure given in Ref. 23. Solutions of TBA·Br and Na·TPB in conductivity water were prepared (0.1 mole in 500 cc). The solution of Na·TPB was allowed to drop through a fine filter into the TBA·Br solution, and the bulky white precipitate was filtered and dried. The material was recrystallized three times from acetone and dried under vacuum at room temperature for 6 days. This material was subsequently recrystallized and dried under vacuum at 50 C for 2 days. It was given the designation of TBA·TPB #1 and was used without analysis for determination of equivalent ion conductances at infinite dilution.

Sodium Tetraphenylboride. Reagent grade sodium tetraphenylboride (Baker and Adamson Laboratory Chemical, reagent grade), NA·TPB #1, was used without analysis and purification to synthesize TBA·TPB #1.

Tetrabutylammonium Bromide. Polarographic grade tetrabutylammonium bromide (Columbia Organic Chemicals Company, Inc.), TBA·Br #1, was used for determination of equivalent ion conductances at infinite dilution and for synthesizing TBA·TPB. This chemical was used without purification and analysis.

Tetramethylammonium Bromide. Polarographic grade tetramethylammonium bromide, TMA·Br #1, was obtained from Southwestern Analytical Chemicals and was used for conductance studies without analysis and purification.

TABLE 21
 IMPURITY CONCENTRATIONS IN CuCl_2 #2
 DETERMINED BY SPARK SOURCE MASS SPECTROMETRY
 AND EMISSION SPECTROSCOPY

Impurity	Spark Source Mass Spectrometry			Emission Spectroscopy
	Detection Limit, ppm atomic	Content, ppm atomic	Content, ppm per weight	Content, ppm per weight
H	3	36	0.8	< 200
Li	0.3	1200*	190*	
C	1	20	5	
N	1	15	5	
O	1	480	170	
F	1	16	7	4.1
Na	0.3	79	41	
Mg	0.7	1.1	0.6	
Al	0.5	2.9	1.7	
Si	5	Not detected	< 3	
Ca				8.0
P	1	1.7	1.2	6.9
S	5	27	19	
K	0.3	31	27	
Ca	0.7	2.9	2.6	
Ti	1	3.8	4.1	
V	1	13	15	34
Cr	1	7.5	8.7	
Mn	1	3.7	4.5	
Fe	1	100	125	
Ni	1	46	60	Trace <10

*May be due to residuals in the mass spectrometer.

TABLE 21
(Concluded)

Impurity	Spark Source Mass Spectrometry			Emission Spectroscopy
	Detection Limit, ppm atomic	Content, ppm atomic	Content, ppm per weight	Content, ppm per weight
Zn	3	6.1	8.9	11
Ga	0.7	6.7	10.4	
As	1	9.7	16.2	
Se	2	5.4	9.5	
Br	1	11	20	
Ag	< 5			<100
Y	0.7	1.4	2.8	
Ru	2	9.7	22	
Cd	3	50	125	
Sn	4	5.2	13.8	
Sb	3	4.4	12.0	26
Pb	3	5.2	24.1	

Lithium Bromide. The optical grade, anhydrous lithium bromide supplied by Gallard-Schlesinger Chemical Mfg. Corp., LiBr #2, was used for conductance studies without analysis and after drying under vacuum at elevated temperatures.

PREPARATION OF SOLUTIONS

Electrolyte solutions were prepared in the dry box as follows. First, the solids were placed in stoppered volumetric flasks and weighed roughly in the inert-atmosphere box. Then, the flasks were removed and accurately weighed on an analytical balance. Finally, the flasks were returned to the dry box where the solvents were added. Some solutions were stirred with a magnetic stirrer in the dry box to achieve complete dissolution. Some flasks were capped with plastic bags or rubber balloons and removed to a constant temperature bath at elevated temperature for faster dissolution of the solids. Special procedures were followed when gaseous solutes were added, or when decomposition required special precautions as in the case of AlCl_3/PC ; these special procedures are discussed below.

The concentrations of solutions given in this report are normally accurate to 1 percent or better (1 M LiClO_4/PC , e.g., actually stands for 1.00 ± 0.01 M LiClO_4/PC). They are normally given in molarities (moles per liter solution) and are based on 25 C.

Solutions Containing Aluminum Chloride

Solutions resulting from dissolution of AlCl_3 in PC have a tendency to discolor when being prepared, and also on standing. The dissolution reaction of AlCl_3 in PC is exothermic, and a strong discoloration is obtained if the solution is allowed to heat up overall or locally when the solution is prepared. It was found that only slightly tinted solution could be made by adding the solute very slowly, grain by grain, under vigorous stirring, and this method had been used to prepare some AlCl_3/PC solutions.

Very light solutions were obtained by preparing a slurry of aluminum chloride, liquid nitrogen, and propylene carbonate and letting this slurry warm very slowly. This procedure was modified because the amount of condensed water introduced with the liquid nitrogen was unknown. In a modification of this procedure, the aluminum chloride was cooled in a volumetric flask to liquid nitrogen temperature, the solvent was added, and the mixture was allowed to thaw with repeated partial refreezing. Solutions which were only slightly discolored were obtained in this way, which was somewhat more convenient than the grain-by-grain addition method.

Some aspects of the preparation of $\text{LiCl} + \text{AlCl}_3/\text{PC}$ solutions with or without copper halide, and of $\text{LiCl} + \text{AlCl}_3/\text{DMF}$ solutions, will be discussed later in the Solubility Determinations section. Because of LiCl solubilities below 1 molar in PC and AN, 0.7 M $\text{LiCl} + 1 \text{ M AlCl}_3$ solutions of these solvents were normally studied; the composition of such mixed solute electrolytes in DMF was usually 1 M $\text{LiCl} + 0.075 \text{ M AlCl}_3$ because of the low solubility of AlCl_3 in this case.

TEA·F Solutions

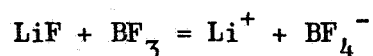
The preparation of $\text{TEA} \cdot \text{F}/\text{PC}$ was discussed earlier. Drying the solid $\text{TEA} \cdot \text{F}$ is impossible because of decomposition, but removal of water from a solution appeared promising. The process which involves distilling off a benzene-water azeotrope was not extended to DMF solutions because it was suspected that adduct formation between H_2O and DMF would prevent success of this approach.

LiAsF_6/MF

Solutions were made by diluting the stock solution supplied by Honeywell's Livingston Electronic Laboratories with methyl formate. The dilution was usually 1:1, and a 1.13 M LiAsF_6/MF was normally used for experimentation. The solvent code designates the methyl formate batch from which MF was added.

Solutions Prepared With BF₃ or PF₅

Lithium tetrafluoroborate solutions were prepared by adding known amounts of gaseous BF₃, under moderate cooling to slurries of LiF in the solvents. A calibrated stainless-steel vacuum line with Teflon traps was used after prepassivation. The BF₃ dissolved readily, and also the LiF "dissolved" in the presence of BF₃ according to the reaction



This reaction requires ample time for completion, and vigorous stirring is beneficial. The composition of the final solutions was checked by analysis for lithium and boron.

PF₅ was added to a slurry of LiF in PC at 0 C using a prepassivated stainless-steel vacuum system. The resulting solution was colored fairly dark with a reddish purple appearance. Such discoloration was also observed by other investigators.

HANDLING OF CHEMICALS AND GLASSWARE

Pure chemicals were handled exclusively in an inert-atmosphere box under a dry nitrogen atmosphere. A dry bag was set up to store bottled chemicals under dry nitrogen to minimize water uptake; this could occur by breathing as the bottles experience temperature fluctuations.

The glassware used for purifying solvents and preparing and storing solutions was treated according to the following procedure. After cleaning in hot nitric acid-water (1:1), the glassware was rinsed thoroughly with deionized water, dried in a regular oven, and finally heated to 250 C in a special oven for several hours under a current of dry nitrogen. After the glassware was dried in such a manner, it was immediately transferred to the inert-atmosphere box.

Glass apparatus such as used for vapor pressure and transference measurements, and NMR sample tubes were subjected to the same treatment. More delicate apparatus such as the calorimeter, conductivity, and dielectric constant cells could not be exposed to higher temperatures and were therefore carefully dried after washing with organic solvents and/or were adequately rinsed with the test solution.

SENSITIVITY TESTING OF PERCHLORATE SOLUTIONS

Lithium perchlorate solutions such as are being prepared on this program are thermodynamically unstable. A potential explosive force can be calculated from thermodynamic data according to Ref. 24(nRT-method). It was calculated, for instance, that 2 M LiClO_4 /DMF has 52.6 percent of the explosive force of TNT.

Sensitivity tests were performed with 2 M LiClO_4 #2/PC #2-11, 3.5 M LiClO_4 #2/DMF #6-3, and saturated LiClO_4 #2/AN #4-2 (less than 2 molar). These solutions were subjected to 250 in.-lb of impact on a modified Jet Propulsion Laboratory impact tester and to 72 inches by 2 pounds on an Olin-Matheson drop weight tester. All responses were negative.

Although these tests seem to indicate that the above solutions can be handled safely, such sensitivity tests are never completely conclusive. The same solutions could give positive results on different types of tests; for example, they could constitute an explosive hazard upon heating, sparking, etc.

STRUCTURAL STUDIES

The structural studies reported here are based upon measurements made with high resolution and broadline nuclear magnetic resonance (NMR) spectrometers and an electron paramagnetic resonance (EPR) spectrometer. These instruments will be briefly described. It is most convenient to divided the discussion of structural findings into four classifications:

1. Electrolytes containing aluminum and lithium ions
2. Electrolytes containing cupric ions
3. Electrolytes containing quarternary ammonium ions, and
4. LiAsF_6/MF electrolytes

INSTRUMENTATION

Early in the program high resolution proton (H^1) and fluorine (F^{19}) measurements were made utilizing a Varian Associated DP-60 NMR spectrometer. About midway in the program, this instrument was modified to include an internal lock feature so that its high resolution capabilities are now equivalent to a model HR-60 IL. Broadline NMR measurements were made with an in-house assembled spectrometer. This spectrometer consisted of a Varian Associates Variable Frequency R.F. Unit, Varian Associates Probes, a Princeton Applied Research Corp. coherent amplifier, Model HR-8, and some auxiliary electronics. The magnet utilized for broadline measurements was a Magnion 12-inch magnet powered with a Varian Associates Field Dial power supply. This magnet was also used for the EPR measurements which were made with a Strand Labs EPR spectrometer. This spectrometer was modified slightly to permit the use of the HR-8 for signal processing.

ELECTROLYTES CONTAINING ALUMINUM AND LITHIUM IONS

AlCl_3 , LiCl , LiClO_4 in DMF

The AlCl_3 /DMF system has been investigated by several workers at this writing. Early work (Ref. 25) reported the observation of peaks, in addition to those found in neat DMF, in the high resolution proton NMR spectrum which have been attributed to DMF molecules, which are being coordinated by Al^{+3} ions. This observation shows that the interaction between DMF molecules and Al^{+3} is sufficiently strong so that the exchange rate between the coordinated molecules and the bulk solvent molecules is slow on an NMR time scale. The work reported in Ref. 25 was done with solutions which had some water added to increase the solubility of AlCl_3 in DMF. Inasmuch as it was inherent in the objectives of the work reported here that very pure, water-free electrolytes be characterized, the type of work that had been reported was repeated using water-free solvents.

Figure 11 shows the high resolution proton spectrum for pure DMF #4-2, while Fig. 12 shows the same spectrum for 0.0528 M AlCl_3 #3/DMF #4-2. The distinguishing features of the latter spectrum as indicated by the vertical arrows are the additional peaks due to coordinated DMF molecules. The down-field shift is greater for the aldehyde proton than for the methyl protons. These shifts are in agreement with previously reported (Ref. 25) values. Thus, the water added in the measurements reported in Ref. 25 apparently had little effect on the measurements. If it is assumed that all the AlCl_3 that is dissolved provides Al^{+3} ions, integration of the areas under the down-field shifted peaks and the bulk DMF peaks gives a coordination number of six. Thus, for AlCl_3 in DMF, the cation species formed is $\text{Al}[\text{DMF}]_6^{+3}$. This is substantiated by the observation that the Al^{27} broadline NMR spectrum is one line that occurs at a field quite near (therefore having a quite small chemical shift relative to) the Al^{27} line

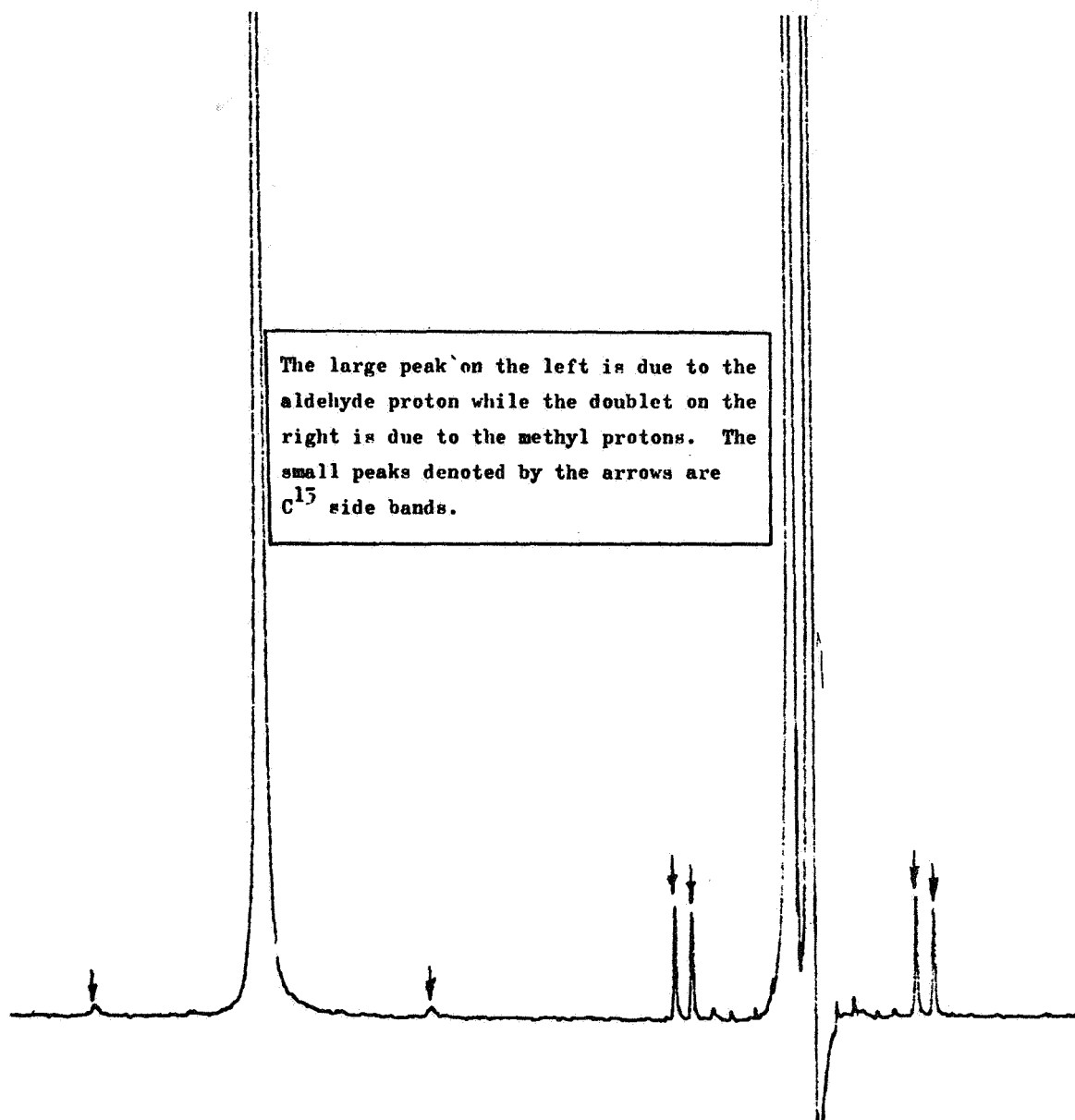


Figure 11. H^1 Spectrum for Pure DMF

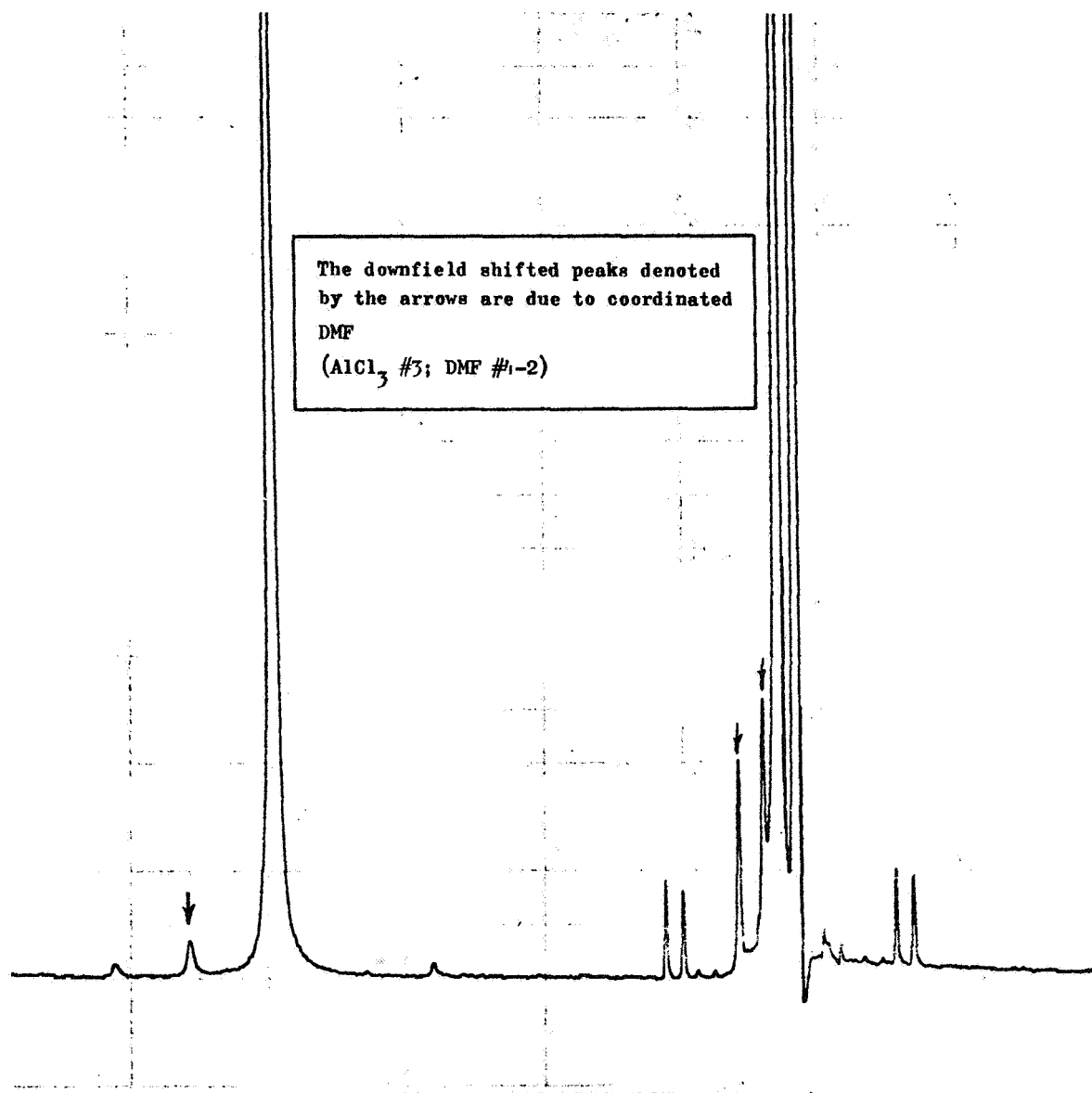


Figure 12. ^1H Spectrum for 0.0528 M AlCl_3/DMF

in a reference solution, consisting of a slightly acidic aqueous AlCl_3 solution. The Cl^{35} line was observed to occur at essentially the same field as the chloride ion (see later discussion) so that the anion species is Cl^- as expected.

The general character of the spectrum shown in Fig. 12 is not changed with the addition of LiCl . Furthermore, the high resolution proton spectrum in pure DMF (no AlCl_3) containing both 0.1 and 1 M LiClO_4 has the same general characteristics as that shown for neat DMF in Fig. 11. Thus, the species obtained on dissolving LiCl and LiClO_4 in pure DMF do not have as large an effect on the solvent proton spectrum as does AlCl_3 . If solvation effects are occurring, the exchange rate at room temperature is high on the NMR time scale.

The Li^7 spectrum in all of the above systems consisted of a single line which saturated quite readily. This saturation behavior which is due to a long spin lattice relaxation time, T_1 , is quite characteristic of Li^7 lines in ionic solids (Ref. 26). It has been shown (Ref. 26) that the generation of paramagnetic impurities in ionic solids appreciably decreases T_1 , thus reducing greatly the saturation effects. Some saturation studies were made on LiCl/DMF solutions with CuCl_2 which contain paramagnetic species (these species are discussed later).

Broadline H^1 and Li^7 spectra were recorded in several of these specimens as a function of radio-frequency power (this was done 2 weeks after sample preparation), to demonstrate the effect of the paramagnetic species on the relaxation time of these resonances. As expected, the saturation behavior of the H^1 resonances in DMF containing LiCl and CuCl_2 differs from that in neat DMF. The line saturates less readily in the DMF containing CuCl_2 as a result of increased relaxation via interaction of protons with the spin of the paramagnetic species. However, the saturation behavior of the Li^7 line in 1 M LiCl + 2 M CuCl_2/DMF is the

same as it is in 1-molar lithium chloride solution (LiCl #2/DMF #5-2). This indicates that the relaxation of the Li resonance is not affected by the paramagnetic species. This may be due to "shielding" of the Li^+ ions from the paramagnetic species by coordinated molecules surrounding the paramagnetic species, and/or molecules coordinated by the Li^+ ions, or because the paramagnetic copper species have structures similar to CuCl_4^{-2} with the paramagnetic electron in the center of the structure. The high resolution H^1 spectra of 1 M LiCl/DMF do not show coordinated peaks; however, Li^+ ions are expected to coordinate less strongly than Al^{+3} ions resulting in much higher exchange rates, which would preclude the observation of coordinated peaks at room temperature.

As discussed later, the EPR measurements in 1 M LiCl + 2 M CuCl_2 /DMF show no solvent complexed copper ion. This indicates that the decrease in saturation effects of the protons may be caused by interaction with the paramagnetic chloride complex. Because this complex is negatively charged, the Li^+ ions should interact at least as readily as the protons. If this is the situation, then the fact that they don't interact would have to be explained on the basis of shielding by DMF molecules, giving indirect evidence of Li^+ solvation in DMF.

The Cl^{35} resonance was also investigated in LiCl/DMF and LiClO_4 /DMF solutions. In 0.1 M and 1 M LiCl/DMF, the Cl^{35} resonance occurs at the same field as the Cl^{35} line from the Cl^- ion in 3 M LiCl/ H_2O , and in 0.1 M and 1 M LiClO_4 /DMF the Cl^{35} line occurs about 975 ppm down-field from this line.

The Cl^{35} line in LiClO_4 /DMF is quite narrow, indicating very little quadrupole interaction. This is as expected for the tetrahedral ClO_4^- ion. Furthermore, the chemical shift of 975 ppm compares quite well with the 970-ppm shift reported (Ref. 27) for the ClO_4^- ion.

As a check on the results for the chemical shift of the Cl^{35} line in 1 M LiCl/DMF , the Cl^{35} spectrum which consists of two Cl^{35} lines as shown in Fig. 13, was observed in a 0.5 M $\text{LiCl} + 0.5 \text{ M LiClO}_4/\text{DMF}$. The narrower line on the left is from the ClO_4^- ion. The broader line is about 955 ± 15 ppm upfield from the ClO_4^- line. This shift is quite close to the shift between ClO_4^- and the Cl^{35} from the Cl^- ion in 3 M LiCl and so corroborates that the anion in LiCl/DMF is the Cl^- ion. This spectrum was taken using the dispersion mode because the saturation behavior of the ClO_4^- line prohibited showing both lines in the same run using the absorption mode.

A recent paper (Ref. 28) has reported some interesting results in the $\text{Al}(\text{ClO}_4)_3$ and AlX_3/DMF systems, where $\text{X} = \text{Cl}, \text{Br}$ and I . Addition of X^- by adding LiX to the systems resulted in increases of the down-field shift of the proton lines of the coordinated DMF. This has been interpreted in terms of a second coordination sphere interaction involving X^- ions and/or pairing of $\text{Al}[\text{DMF}]_6^{+3}$ with X^- ions.

The gross picture, thus, for AlCl_3 dissolved in DMF is the formation of well-defined $\text{Al}[\text{DMF}]_6^{+3}$ species, the only aluminum-containing species as the cation and Cl^- as the anion, with possible interaction and/or ion pairing of these species. Adding LiCl to this system provides Li^+ ions and additional Cl^- ions to possibly increase any interaction between $\text{Al}[\text{DMF}]_6^{+3}$ and Cl^- ions. LiCl and LiClO_4 in DMF produce Li^+ ions plus Cl^- and ClO_4^- ions, respectively. The question of ion pairing of these ions is unanswered. There is indirect evidence, the Li^7 line saturation behavior, for example, and the results of mobility measurements as described elsewhere, that suggests that Li^+ is solvated by DMF; however, no direct evidence has been found to date.

$\text{AlCl}_3, \text{LiCl}, \text{LiClO}_4$ in AN

For completeness, large portions of this section are taken directly from Ref. 29 which is a published account of some of the findings in the $\text{LiCl} + \text{AlCl}_3/\text{AN}$ system.

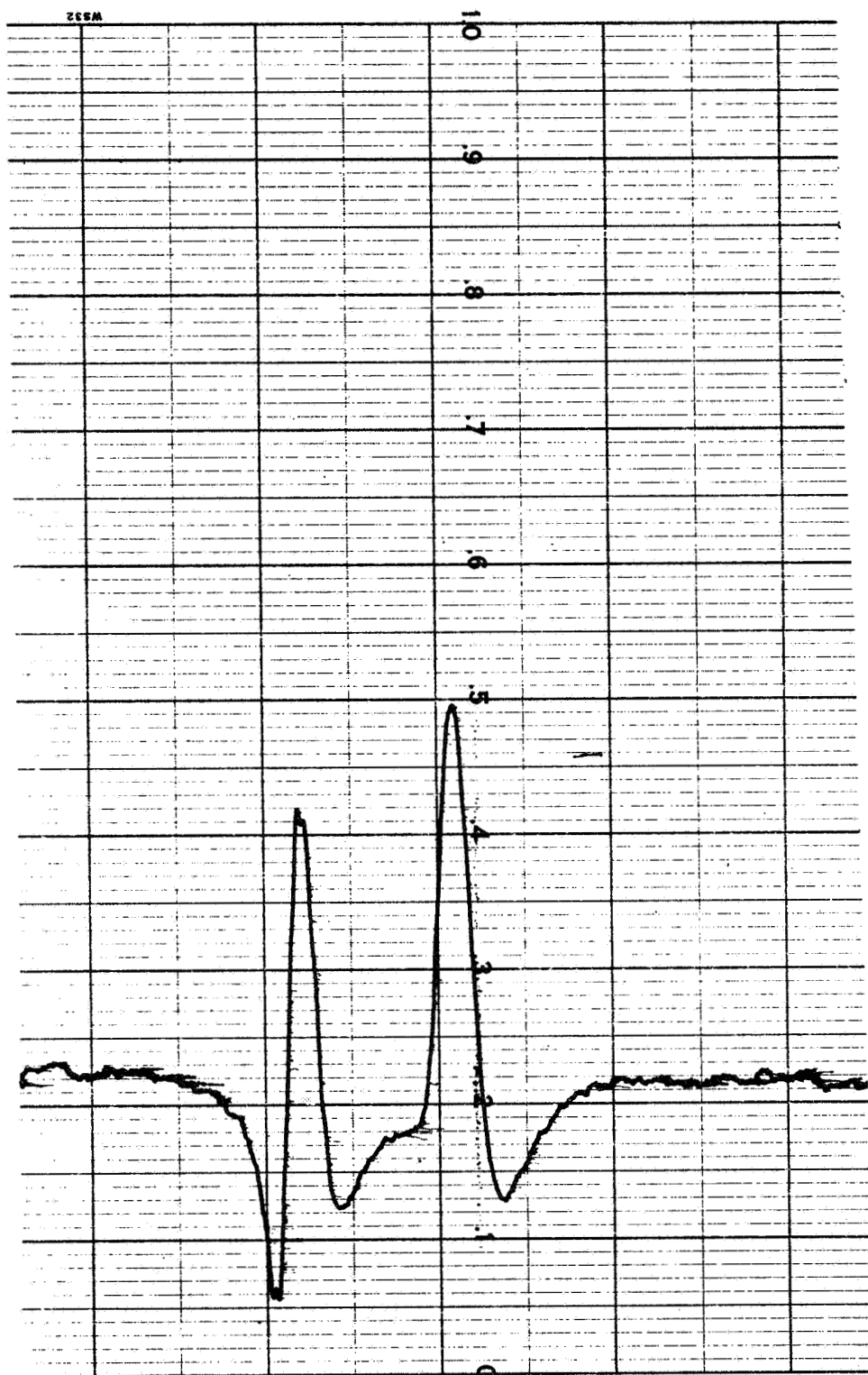


Figure 13. Broadline Cl^{35} Spectrum of 0.5 M LiCl + 0.5 M $\text{LiClO}_4/\text{DMF}$

High resolution proton resonance spectra taken at ambient temperature ($\sim 35^\circ\text{C}$) for pure acetonitrile (AN), 1 M AlCl_3/AN and 1 M AlCl_3/AN saturated with LiCl are shown in Fig. 14, 15, and 16, respectively. Figure 15 shows the down-field shift of coordinated AN which has been previously reported (Ref.30) and a noticeable broadening of both of the resonant lines. Figure 16 shows the result of adding LiCl to 1 M AlCl_3/AN , approximately 0.92 M LiCl is dissolved in 1 M AlCl_3/AN at saturation at room temperature. The addition of chloride ions to 1 M AlCl_3/AN results in a decrease in the population of coordinated AN, while the line width returns to essentially that of pure AN. Broad-line aluminum (Al^{27}) resonances are shown in Fig. 17 for 1 M AlCl_3/AN containing several concentrations of LiCl . The important features of these spectra are that, firstly, there are two Al^{27} lines in all cases except for the specimen that is saturated with LiCl , secondly, both of these lines are quite narrow, and, thirdly, the down-field line is approximately three times as intense as the up-field line in the specimen with no LiCl . Thus, there are apparently two aluminum environments in the 1 M AlCl_3/AN solution.

The simplest explanation is that there are two aluminum-containing species. The relaxation times of the two lines are quite different, with the low-field line relaxing much more slowly than the up-field line. This necessitated recording the spectra at very low R.F. levels. At higher R.F. levels the low-field line saturated and the apparent intensity (peak-to-peak recorder deflections) would appear to be much less than the up-field line. The actual field scan, not shown in Fig. 17, was over 100 gauss in initial observations but no other lines were found.

Chemical shift measurements in these specimens showed that the smaller up-field line and the reference Al^{27} line were nearly superimposed. Thus, the chemical shift of the up-field line relative to the reference was less than 14 ppm. The shift of the down-field line relative to the reference was about 110 ppm.

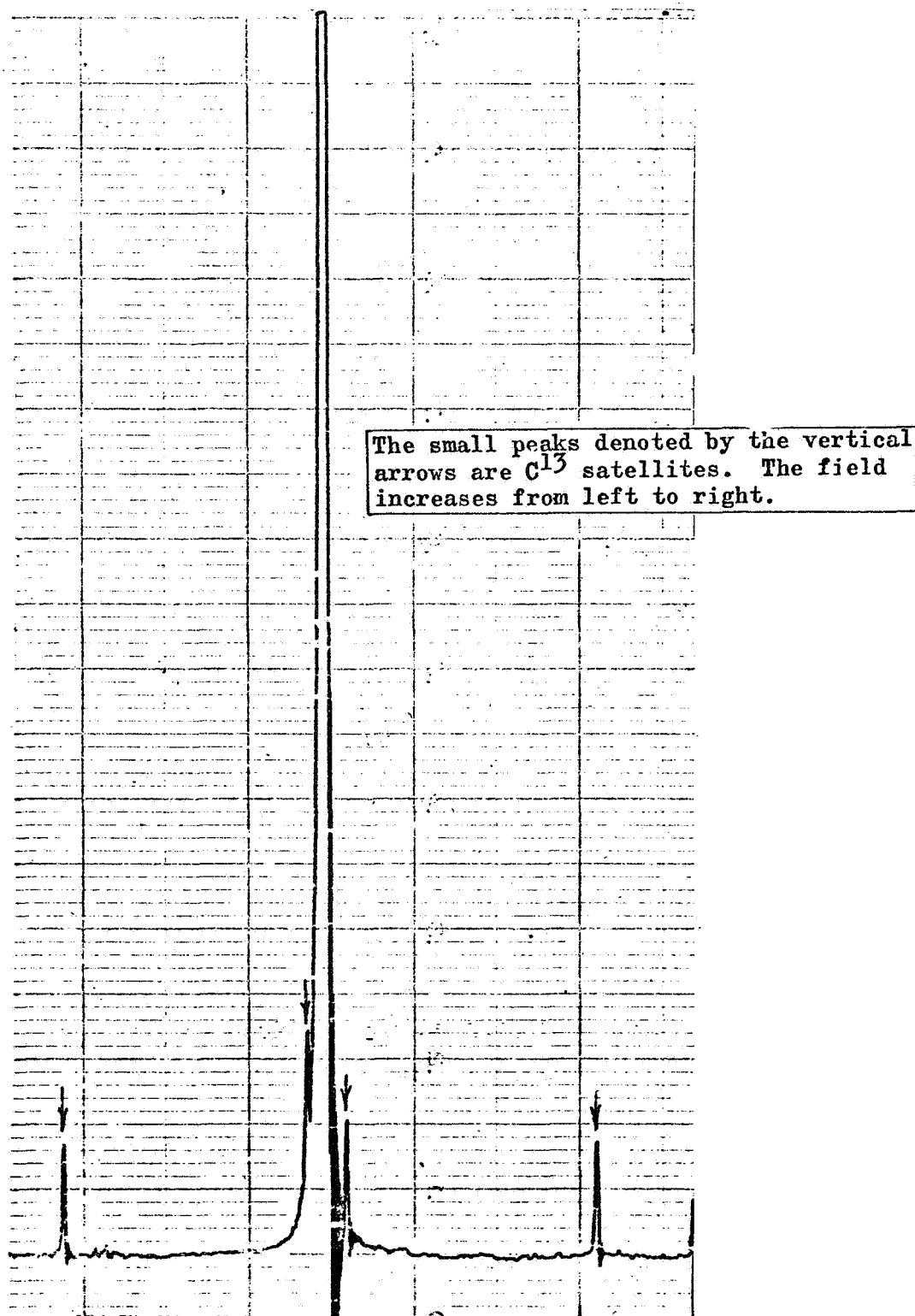


Figure 14. High-Resolution ^1H Spectrum in Pure AN

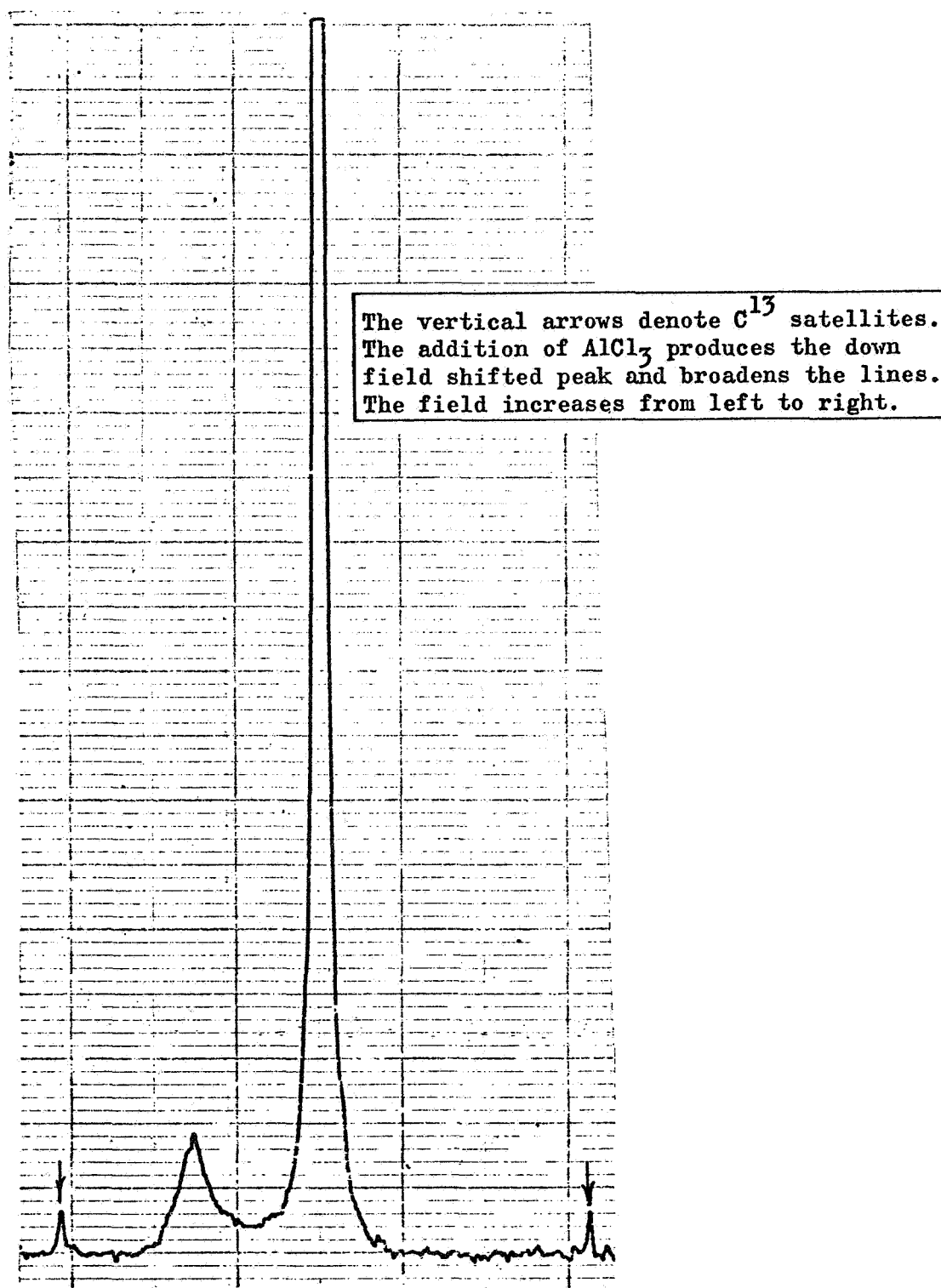


Figure 15. High-Resolution H^1 Spectrum in 0.983 M $AlCl_3/AN$

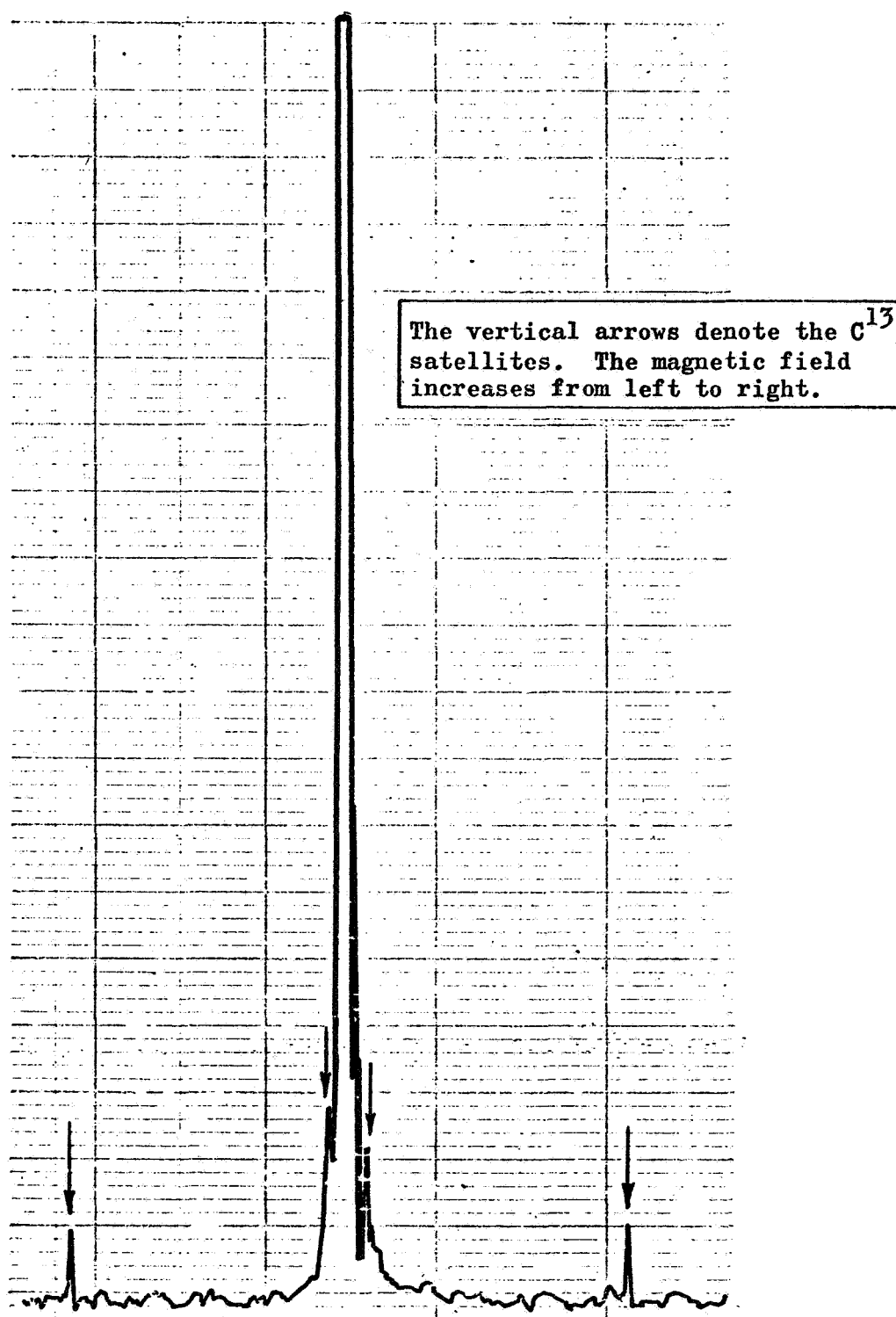


Figure 16. High-Resolution H^1 Spectrum in 0.983 M AlCl_3/AN
Saturated With LiCl

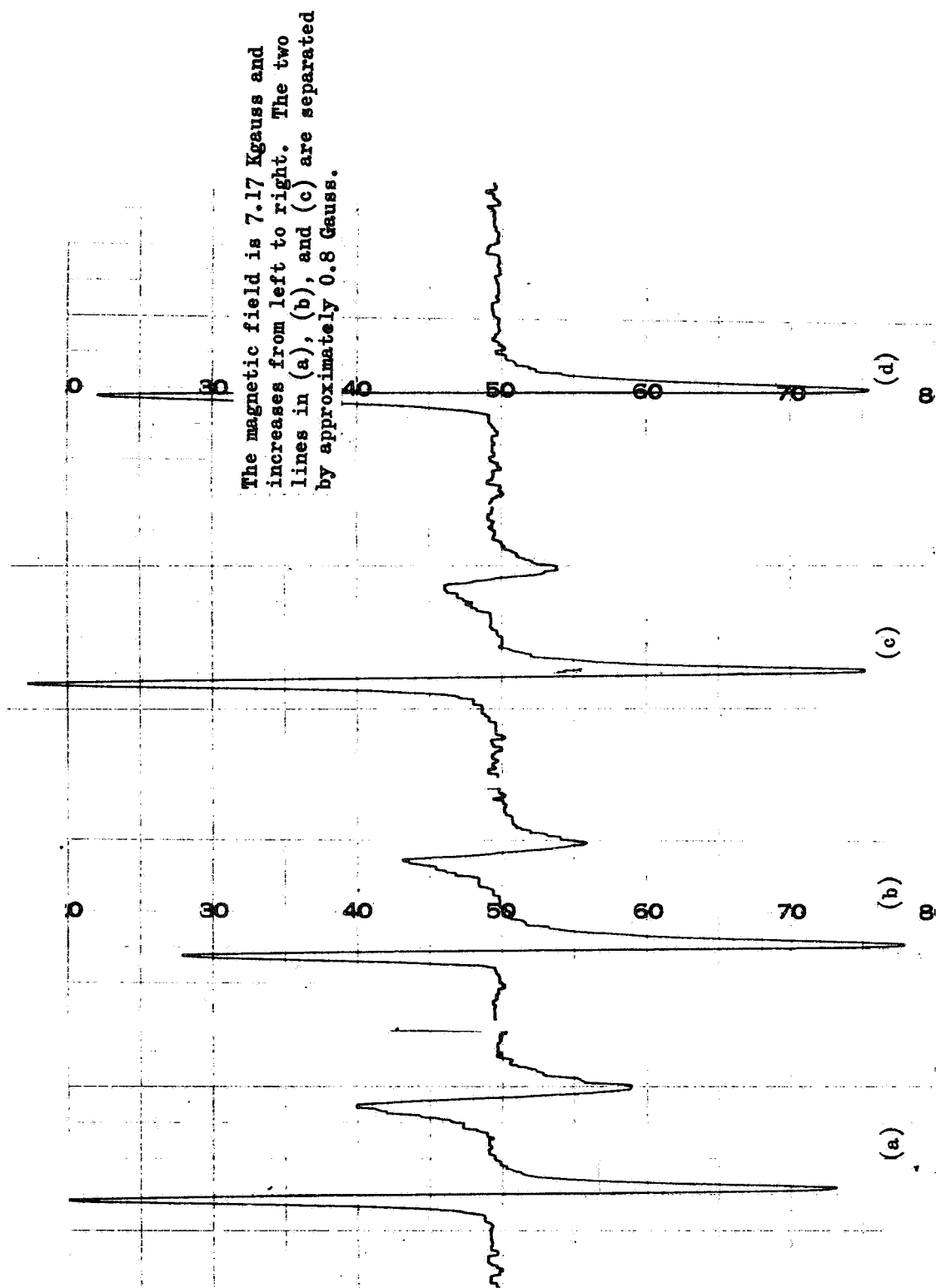
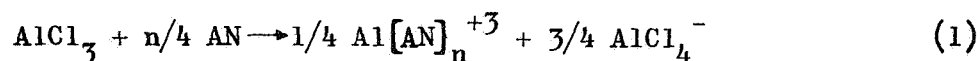


Figure 17. Al^{27} Nuclear Magnetic Resonance in 1 M AlCl_3/AN Containing Various Concentrations of LiCl , (a) No LiCl , (b) 0.25 M LiCl , (c) 0.5 M LiCl , (d) 0.9 M LiCl (saturated at 25°C)

The most important features of these results are, first, that two aluminum species exist in 1 M AlCl_3/AN , only one of which coordinates solvent (AN) molecules, and, secondly, that addition of LiCl changes the relative population of the two species. Both Al^{27} lines are quite narrow, so that both of these species must be such that the symmetry of the aluminum site in the species is high, at least tetrahedral. Because Al^{27} has a quadrupole moment, any lesser symmetry would give rise to a quadrupolar broadened line. It should be noted that these results are concerned with major aluminum-containing species only. Other aluminium species may be present in small, unobservable concentrations.

The following reaction is proposed to occur when AlCl_3 is dissolved in AN:

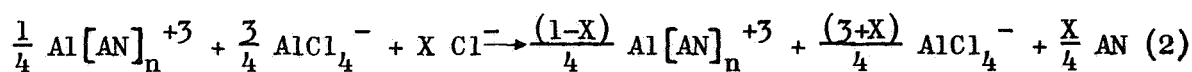


where n denotes the number of coordinated AN. This reaction is selected because it gives rise to a tetrahedral species AlCl_4^- and a solvated species which is highly symmetrical for reasonable values of n . Furthermore, the ratio of coordinating Al species to noncoordinating Al species is $1/3$, which is consistent with the experimental results. Also, this reaction provides results consistent with the qualitative relaxation time observations. It is expected that spin-spin relaxation in the AlCl_4^- would be much slower than in the $\text{Al}[\text{AN}]_n^{+3}$ because of the much lower magnetic moments of Cl^{35} and Cl^{37} compared to that of the protons in AN.

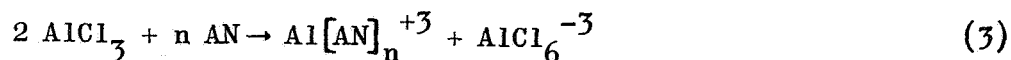
The above reaction can also be used to explain the results obtained when LiCl is added to 1 M AlCl_3/AN . It is assumed that addition of LiCl provides Li^+ and Cl^- ions. Reaction 1 can be considered to be displaying the results of a competition between Cl^- and AN in complexing Al^{+3} in which Cl^- is a stronger complexing agent, when forming AlCl_4^- . (Note that the Cl^- concentration is considerably smaller than that of AN in 1 M AlCl_3/AN .) Because Cl^- is the stronger, AN complexes only those Al^{+3} which remain after

all the Cl^- is utilized. Providing additional Cl^- ions permits the reaction to continue. 1 M LiCl (1 M Cl^-) would allow completion of the reaction. Apparently, the reaction will not go to completion because the saturation concentration of LiCl in 1 M AlCl_3/AN was found to be less than 1 M (0.92 M).

Using the peak-to-peak deflection on the derivative curves shown in Fig. 17 as a rough measure of the relative intensity, the change in concentrations with added LiCl can be approximated. This is shown in Fig. 18 compared with the solid line which is based on the reaction:



where X is the concentration of LiCl added. The error bars in this figure reflect only the error in the ratio of the peak-to-peak deflections of the recorded spectra. These results cannot be considered quantitative because the two lines do not have the same width. Furthermore, as indicated in the results section, the relaxation time of the two lines was quite different, necessitating the recording of the lines at very low R.F. levels. However, the results do agree with the solid curve rather well, thus substantiating reaction 2. Note that the next likely Cl^- complexed species having sufficient symmetry is AlCl_6^{-3} . In this case the reaction equivalent to reaction 1 would be:



where the relative population of $\text{Al}[\text{AN}]_n^{+3}$ would be 1/2, rather than 1/4, and it would take 3 M, rather than 1 M, of LiCl (Cl^-) to complete a reaction of the type shown in reaction 2. Because this is contrary to observation, AlCl_6^{-3} has been discounted as a major species.

One further feature of the spectrum shown in Fig. 15, namely the broadening of the peak due to coordinated AN, is readily explained on the basis of exchange effects if, at ambient temperature, the exchange rate

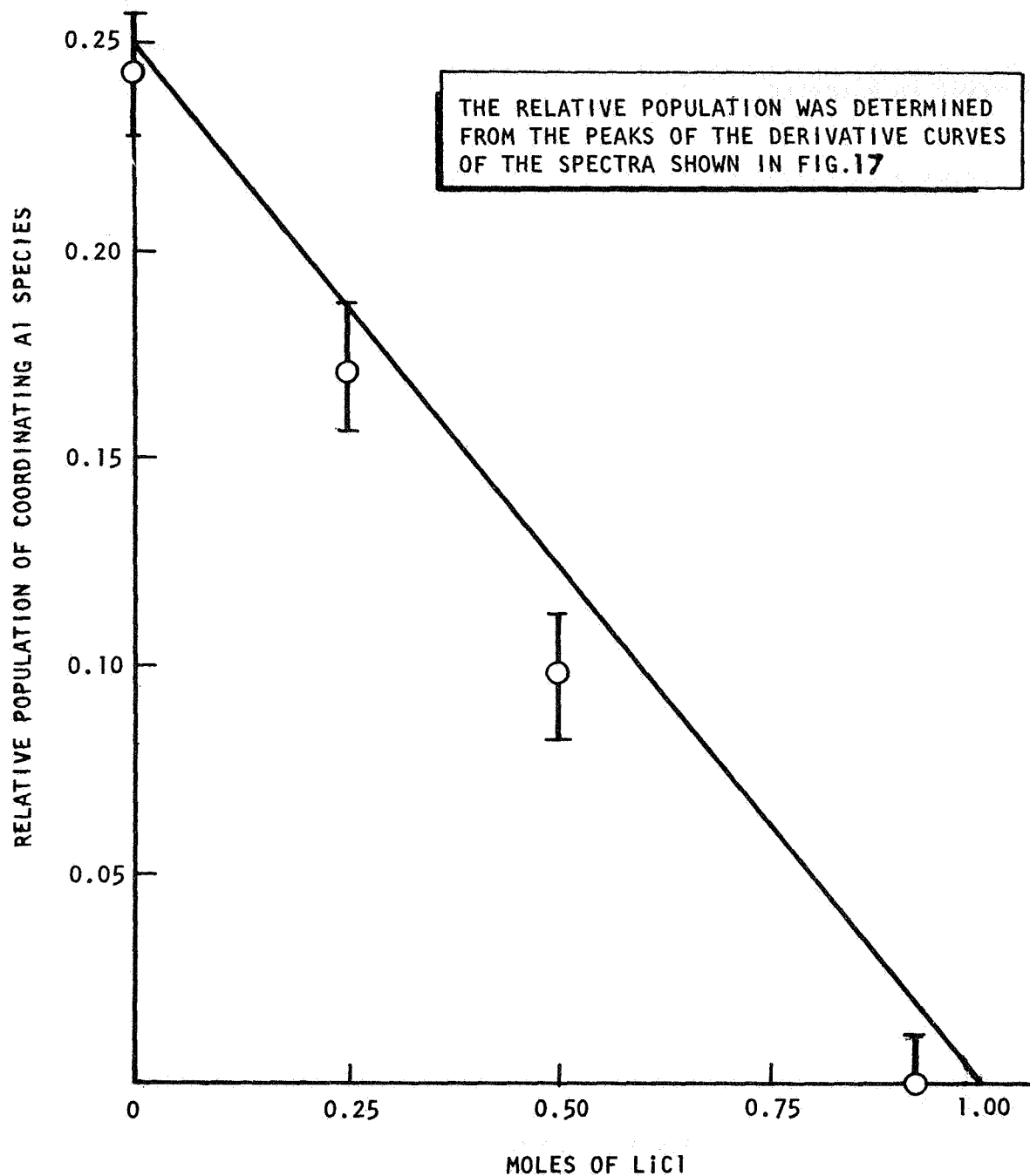
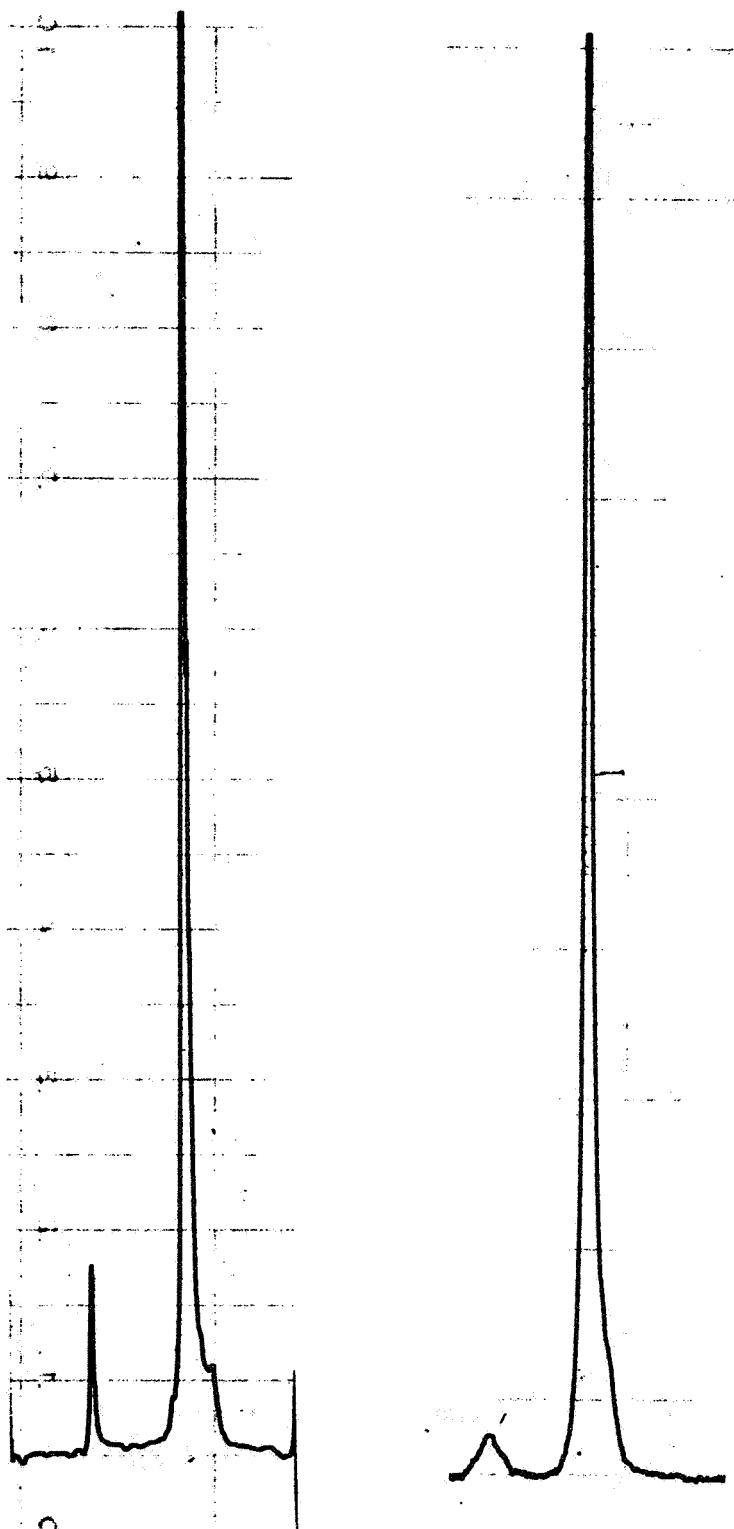


Figure 18. Approximate Relative Population of Coordinating Al Species in 1 M AlCl_3/AN as a Function of Added LiCl.

in the 1 M AlCl_3/AN is of the order of the chemical shift. Figure 19 shows a comparison between the spectra at 30 C and at -23 C. At the lower temperature, the exchange has slowed to the extent that the lines have narrowed as expected.

The results as discussed above can be utilized to obtain a true value for the coordination number, n , by using the area ratio method, taking into account the concentration of coordinating species in contrast to the solute concentration. Because the specimens were essentially free of water, no correction need be considered for the competition between AN and water coordination. Using the ratio of the areas under the bulk AN and coordinated AN proton peaks, and using 1/4 as the ratio of coordinating species concentration to solute concentration, the coordination number of Al^{+3} in 1 M AlCl_3/AN is found to be 6.2. The limits of error in the area ratio are estimated to be about 5 percent. The error in the ratio of 1/4 cannot be determined from the considerations above. It will depend primarily on the extent that reaction 1 is complete. As indicated previously, 1 M LiCl would make reaction 2 complete but 0.92 M LiCl saturates the solution. This suggests that reaction 1 may not be complete. An incomplete reaction would result in a higher concentration of Al^{+3} and would reduce the experimentally determined coordination number. A coordination number of 6 is in good agreement with the findings for Al^{+3} in other solvents (Ref. 31, 32, and 33).

As will be discussed later, when LiClO_4 is dissolved in acetonitrile, ClO_4^- is produced. Two specimens of 1 M AlCl_3/AN were prepared with LiClO_4 added rather than LiCl . It was thought that because no Cl^- ions were formed and because ClO_4^- is a relatively inert ion, that the population of the coordinating species would not be reduced showing the importance of the Cl^- in the depletion of the coordinating species. The Al^{27} line for 0.5 M LiClO_4 #2 + 1 M AlCl_3 #3/AN #4-1 and 1 M LiClO_4 #2 + 1 M AlCl_3 #3/AN #4-1 is shown in Fig. 20. As can be seen, contrary to expectation, these spectra are different from the Al^{27} spectra of 1 M AlCl_3 #3/AN #4-1 shown in Fig. 20a. Also, the H^1 resonance indicates that the



a. Low Temperature (-23 C)

b. Room Temperature (30 C)

Figure 19. High Resolution Proton (H^1) Resonance in 1 M $AlCl_3/AN$

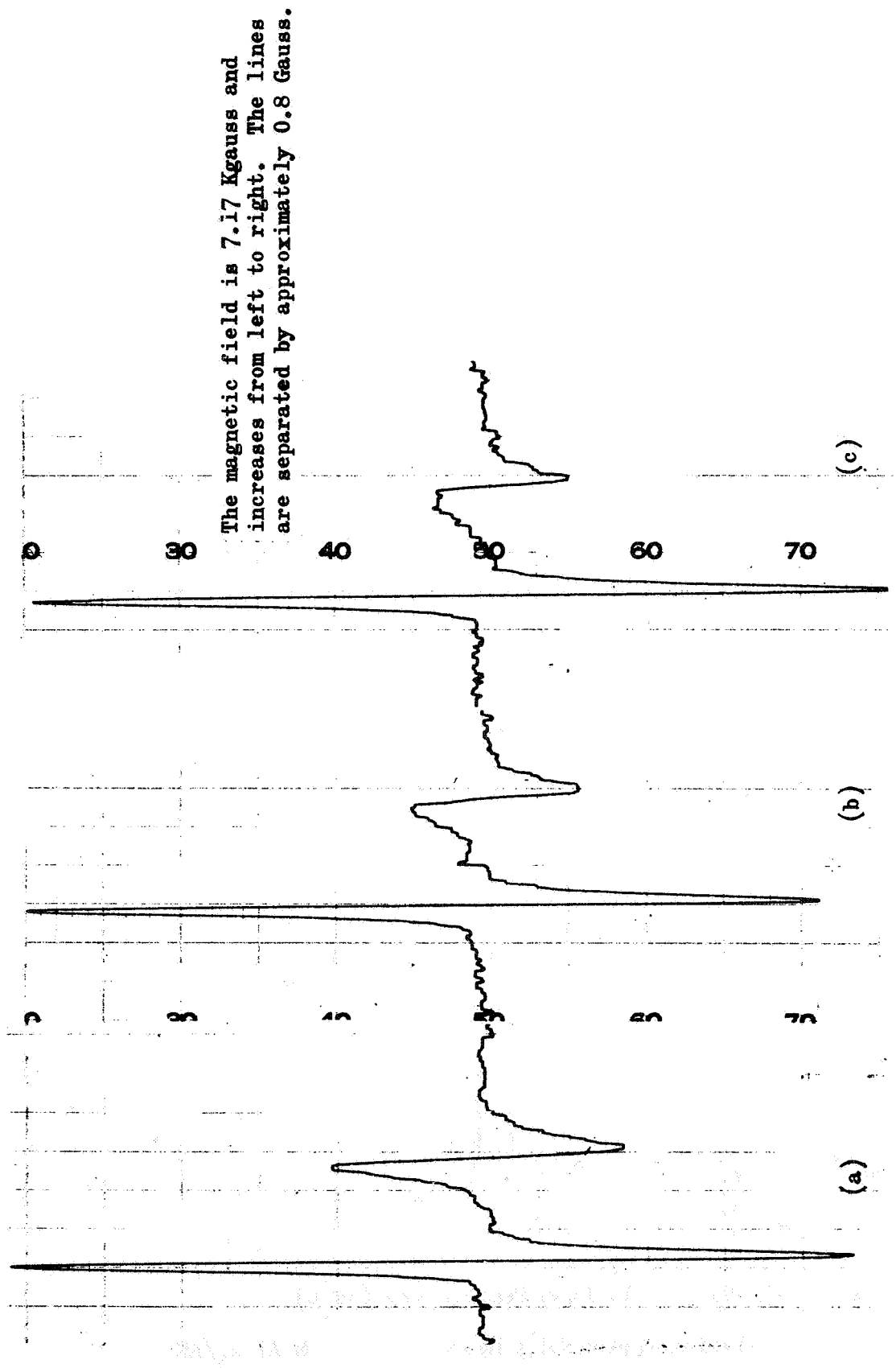


Figure 20. Al^{27} Nuclear Magnetic Resonance in 1 M AlCl_3/AN Containing Various Concentrations of LiClO_4 , (a) No LiClO_4 , (b) 0.5 M LiClO_4 , (c) 1 M LiClO_4

population of the solvent coordinating species is decreased on addition of LiClO_4 . Thus, addition of LiClO_4 to 1 M AlCl_3/AN appears to have a similar effect as LiCl , but LiClO_4 is not as effective. Whereas 0.92 M LiCl reduces the population of the coordinating species to the point where it cannot be observed, 1 M LiClO_4 reduces the population approximately to the same extent as 0.5 M LiCl .

These results might be explained on the basis of the formation of $\text{Al}(\text{ClO}_4)_4^-$ or $\text{Al}(\text{ClO}_4)_6^{3-}$ species, though the ClO_4^- ion is not generally considered to be a complexing species. If these species were formed in the 1 M LiClO_4 + 1 M AlCl_3/AN system, there would be three aluminum-containing species: $\text{Al}[\text{AN}]_n^{+3}$, AlCl_4^- and $\text{Al}(\text{ClO}_4)_4^-$ (or $\text{Al}(\text{ClO}_4)_6^{3-}$) and three Al lines would result but this was not observed. This could be explained if the difference of the chemical shifts of the Al^{27} line in the anionic species were so small that separate lines could not be resolved; however, this seems unlikely.

Alternatively, the results can tentatively be interpreted in terms of a competition between ClO_4^- and AN in the Al^{+3} coordination sphere. The mixed complexes resulting from such a competition would likely be interconverted at the solvation exchange rate. The resulting species would, therefore, be asymmetric and the resonance would be broader but still centered at approximately the same chemical shift value as the pure solvent complex. However, unless more information is obtained, this explanation must remain speculative.

In the LiClO_4/AN system, no down-field shifted peaks in the proton spectrum were observed. Thus, if LiClO_4 in AN has an effect on the solvent, it is smaller than that caused by AlCl_3 .

The Li^7 spectrum in all the $\text{LiCl}+\text{AlCl}_3/\text{AN}$ electrolytes and in both 0.1 M and 1 M LiClO_4/AN consisted of a single, easily saturated line.

A series of measurements was made in 0.1 M AlCl_3/AN , similar to the series made in 1 M AlCl_3/AN . The Al^{27} lines were recorded as a function of LiCl concentration up to 0.1 M, and the results showed qualitatively the same effect as in the 1 M AlCl_3/AN case. In the dilute series, the signal-to-noise ratio was an order of magnitude less so that the results were not as quantitative. The peak due to $\text{Al}[\text{AN}]_6^{+3}$ did reduce with the addition of LiCl and was no longer observed with 0.1 M LiCl added.

The Cl^{35} line in 0.1 M and 1 M LiClO_4/AN was narrow and shifted about 975 ppm down-field from the Cl^{35} line for Cl^- in 3 M $\text{LiCl}/\text{H}_2\text{O}$ and is, therefore, attributed to the ClO_4^- ion. Cl^{35} spectra for all of the $\text{LiCl}+\text{AlCl}_3/\text{AN}$ solutions consisted of a single broadline. When compared to a reference solution containing Cl^- , no chemical shift could be detected. Because of this result, it was earlier reported (Ref. 6) as being due to Cl^- ions in these solutions. However, the intensity of these lines seemed too high to be consistent with this interpretation, so the Cl^{35} spectrum obtained from 1 M LiClO_4+1 M AlCl_3/AN was investigated further. Figure 21 shows this Cl^{35} spectrum taken in the dispersion mode. Because of the quite different relaxation rates of the two lines they could not be recorded on the same scan in the absorption mode. The narrow line on the left is due to the ClO_4^- ion. Note that the remaining line, up-field from the ClO_4^- ion line, is considerably broader than the up-field line for Cl^- in 0.5 M $\text{LiCl} + 0.5$ M $\text{LiClO}_4/\text{DMF}$ shown in Fig. 13. Furthermore, careful measurements of the chemical shift of the righthand line relative to the ClO_4^- line in $\text{LiClO}_4 + \text{AlCl}_3/\text{AN}$ showed it to be 876 ± 15 ppm up-field. This is appreciably less than the Cl^- chemical shift relative to ClO_4^- . Because the line is so intense, because it is considerably broader than the Cl^- line in 1 M LiCl/DMF , and because it has a smaller chemical shift relative to ClO_4^- than the Cl^- line, it is attributed to the chlorines in the AlCl_4^- complex. Chemical shifts and line widths have been reported for several tetrachloride structures (Ref. 34). These structures give relatively broad lines and are shifted

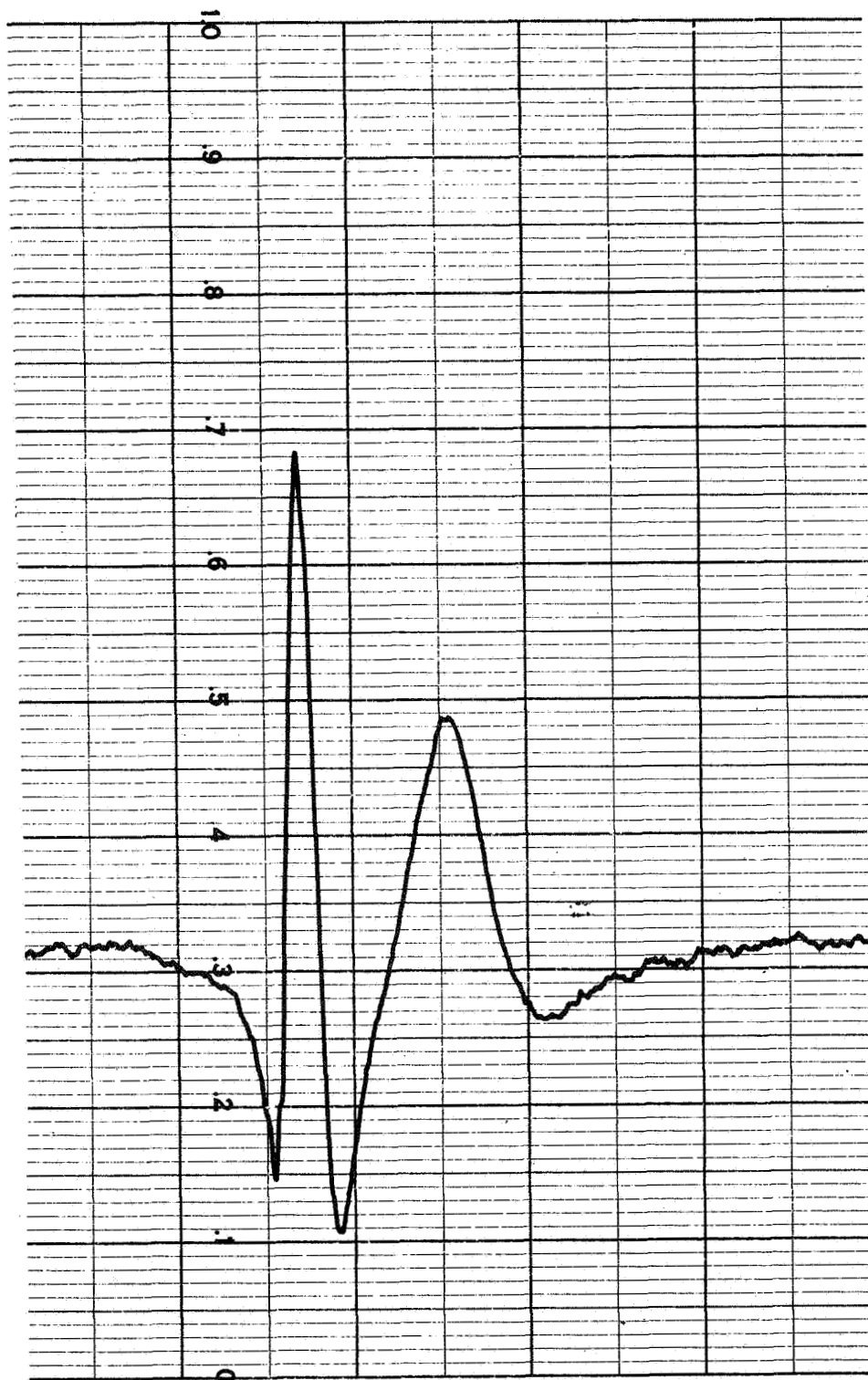


Figure 21. Cl^{35} Magnetic Resonance in 1 M LiClO_4 + 1 M AlCl_3/AN

down-field from the Cl^- line. Because the shift of the AlCl_4^- relative to Cl^- is small compared to the line width, the resonance due to Cl^- in these solutions would be obscured. This interpretation explains why no chemical shift could be found in the earlier measurements and is qualitatively consistent with the intensity of the observed line.

As was discussed earlier, the broadening displayed in the spectrum shown in Fig. 15 (1 M AlCl_3/AN) is a result of exchange between coordinated and bulk AN molecules. When there are two chemically inequivalent sites for the resonating nucleus, in this case H^1 , the spectrum can be very sensitive to the exchange rates between the two sites. An analysis of this situation is described in Ref. 35 under conditions of very slow, very fast, and intermediate rates of exchange. In the case of slow exchange, separate resonances are observed, which is the case in this spectrum. Under these circumstances the transverse relaxation time, τ_2 , of one of the lines (designated by A) is given by

$$\tau_{2A}^{-1} = T_{2A}^{-1} + \tau_A^{-1}$$

where

T_{2A} = relaxation time in site A without exchange

τ_A = first-order lifetime in site A

A similar expression holds for the second site, B:

$$\tau_{2B}^{-1} = T_{2B}^{-1} + \tau_B^{-1}$$

From the recorded spectra, the resonant frequency shift between the two sites, $\omega_A - \omega_B$, is 30.0 Hz, τ_{2B}^{-1} is 3.4 sec^{-1} , and τ_{2A}^{-1} is approximately 3.8 sec^{-1} ; τ_{2B}^{-1} is taken from the line width at half maximum. τ_{2A}^{-1} is estimated from the broadening of the line such that the C^{13}

satellites, clearly shown in the spectrum of neat AN (Fig. 14), are just smeared out as displayed in the spectrum of Fig. 15. From the neat AN spectrum, $T_2^{-1} = 1.8 \text{ sec}^{-1}$. Only approximate values are used here for qualitative discussion. The assignments A and B correspond to the bulk and the coordinated AN molecules, respectively. From these data, $\tau_A \cong 0.54 \text{ second}$. To obtain τ_B^{-1} , T_{2B} for this site is required, but it can only be obtained when no exchange is present. T_{2B} can be obtained from the low-temperature spectrum (Fig. 19) which shows essentially the same line width as the line in the pure solvent. Therefore, T_{2B}^{-1} is taken to be the same as T_{2A}^{-1} . Thus, $\tau_B \cong 0.05 \text{ second}$. This long lifetime of a coordinated AN molecule corresponds to a very slow exchange rate of coordinated AN molecules with bulk AN molecules.

From the above discussion, the species formed when AlCl_3 is dissolved in AN are primarily $\text{Al}[\text{AN}]_6^{+3}$ and AlCl_4^- . Addition of LiCl produces Li^+ and more AlCl_4^- is formed, depleting the concentration of $\text{Al}[\text{AN}]_6^{+3}$. Some free Cl^- may be produced, but it is unobservable because the line width of the Cl^{35} line in AlCl_4^- is large compared to the chemical shift relative to Cl^- . LiClO_4 in AN produces Li^+ and ClO_4^- . Whether or not solvation of Li^+ by AN occurs has not been determined, nor has information on ion pairing been obtained. Answers to these questions require additional work, particularly low-temperature and mixed-solvent experiments.

AlCl_3 , LiCl , LiClO_4/PC

The results obtained for these solutes in PC parallel those obtained in AN in almost all respects. Figure 22 shows the proton spectrum in pure PC. Figure 23 shows the proton spectrum for 1 M AlCl_3/PC in the vicinity of the methyl proton doublet (right side of Fig. 22), and Fig. 24 shows the proton spectrum near the complex pattern (left side of Fig. 22). Additional peaks, in both spectra, due to the addition of AlCl_3 are shown by the vertical arrows. Thus, as in the AlCl_3/AN electrolyte, dissolving AlCl_3 in PC produces coordinated PC as shown by the appearance of the new

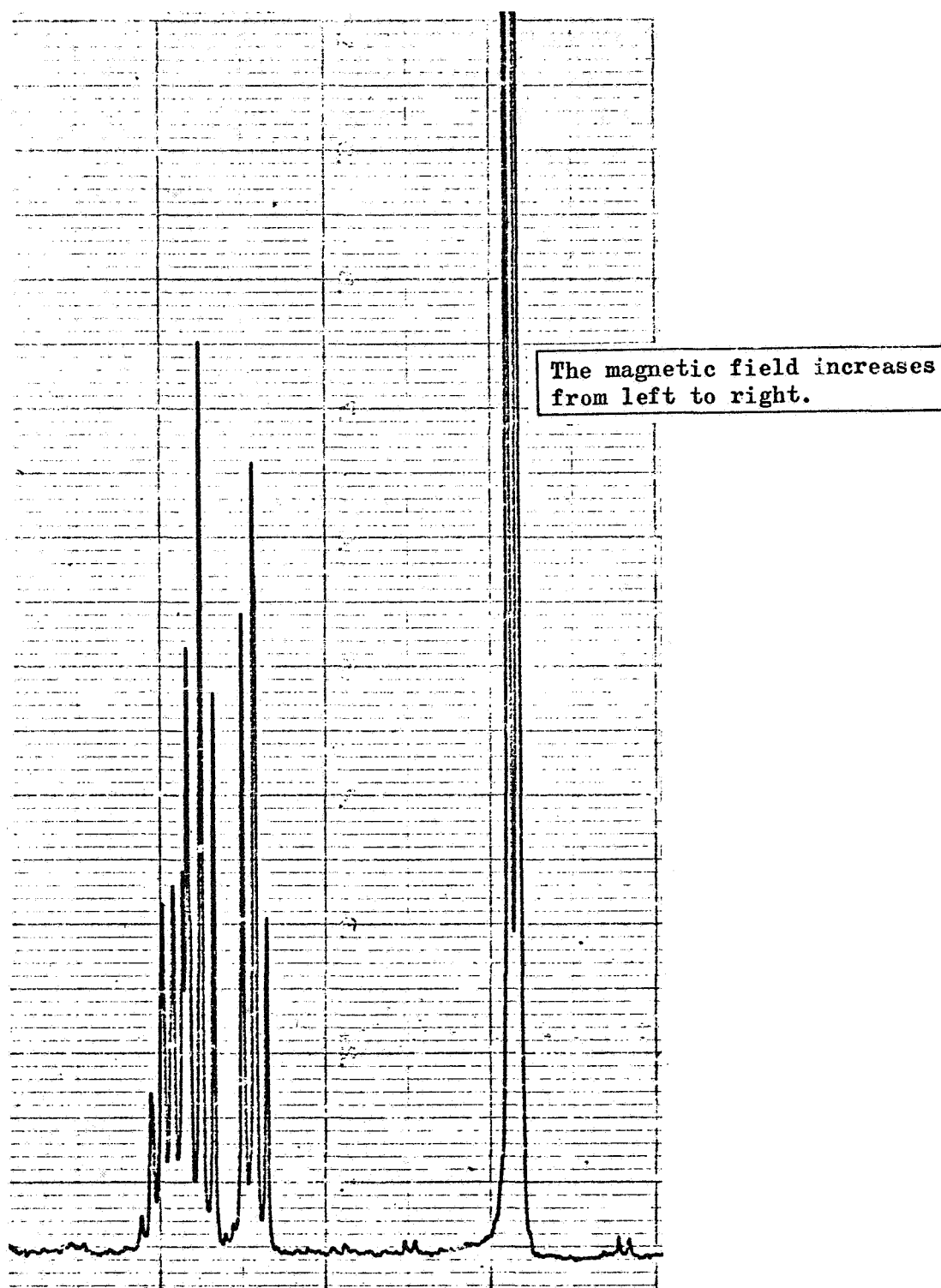


Figure 22. High-Resolution H^1 Spectrum in Pure PC

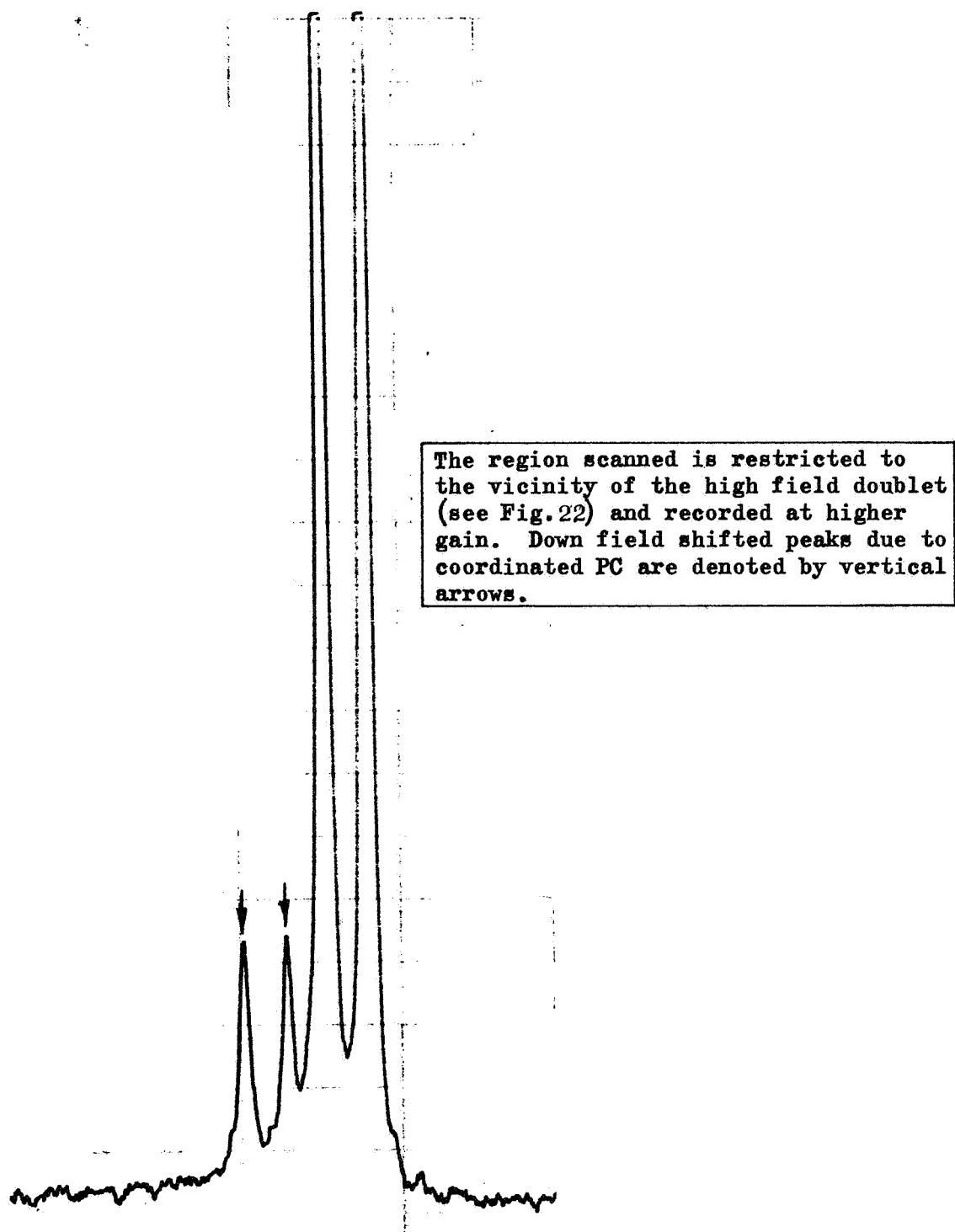


Figure 23. High-Resolution ^1H Spectrum in 1.00 M AlCl_3/PC

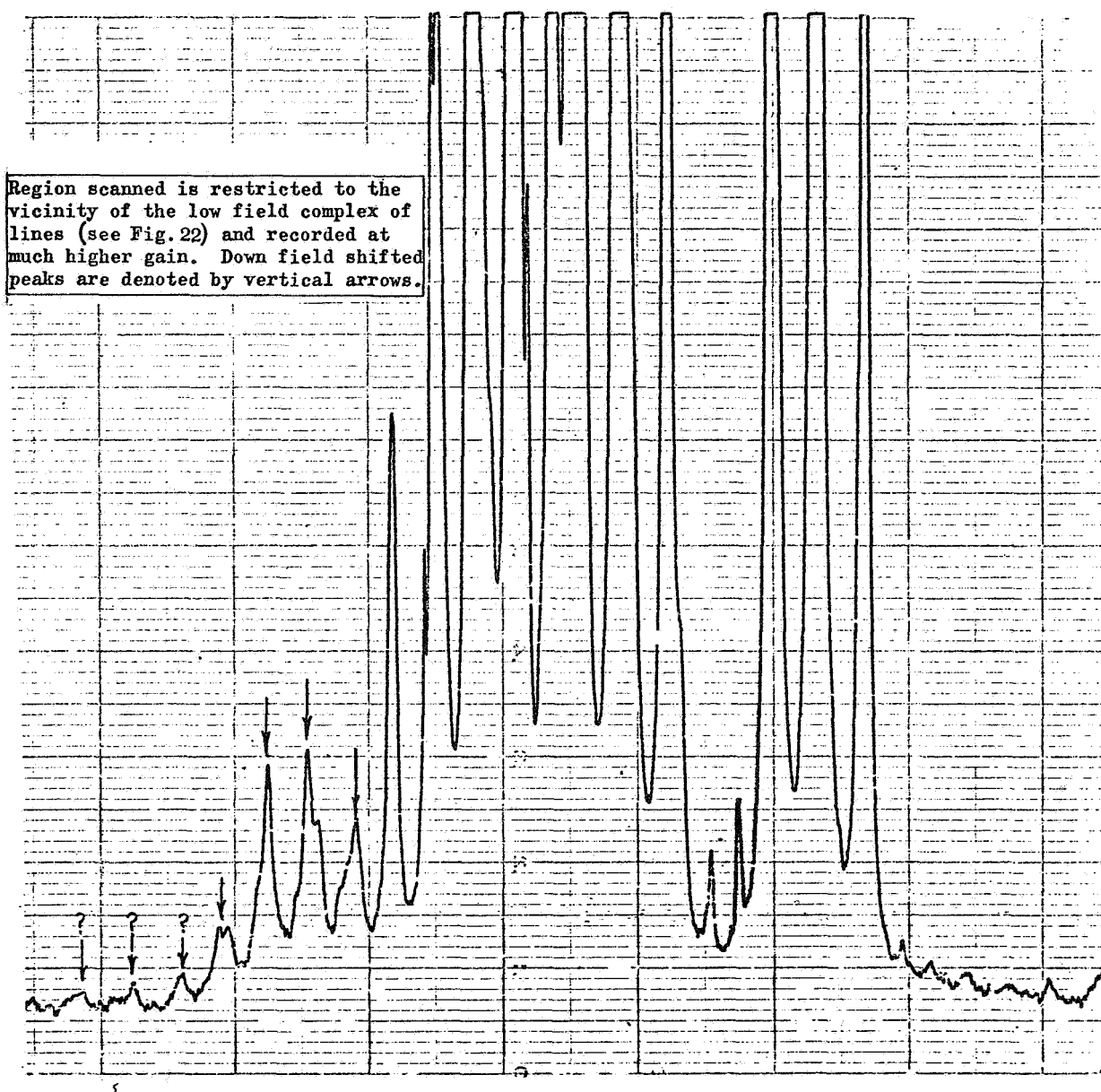
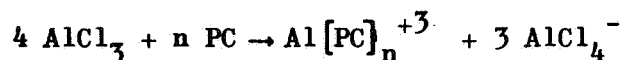


Figure 24. High-Resolution ^1H Spectrum in 1.00 M AlCl_3/PC

down-field shifted peaks. As LiCl is added to 1 M AlCl₃/PC, these down-field peaks reduce in intensity. The Al²⁷ spectra have been recorded for several 1 M AlCl₃ #3/PC #2-12 solutions containing different concentrations of LiCl #2 using the broadline spectrometer. These spectra are shown in Fig. 25. Chemical shift measurements using a 1 M AlCl₃ aqueous solution in the inner tube of a coaxial tube specimen show that the less intense line is that due to the coordinating Al-containing species. These data have been analyzed in the same manner as described above for LiCl + AlCl₃/AN solutions. A plot of the relative concentration of the coordinating Al species as a function of LiCl concentration is shown in Fig. 26. The results are very similar to those obtained for the LiCl + AlCl₃/AN series. Thus, the following major species reaction occurs in the AlCl₃/PC solution as well:



The Al²⁷ spectra were obtained also for 0.1 M AlCl₃ #3/PC #2-12. This is shown in Fig. 27. Because of the much lower signal (one-tenth of that for 1 M AlCl₃/PC) the spectra were recorded much slower with higher gain and longer time constant. The spectra show the same characteristics as those obtained from the 1 M AlCl₃/PC, namely, two aluminum-containing species with relative intensities of 3 to 1. From this result, it appears that the aluminum-containing species present in 0.1 M AlCl₃/PC do not differ from those in 1 M AlCl₃/PC.

Using the Al²⁷ results above and integration of the down-field and bulk methyl proton peaks shown in Fig. 23, a coordination number of 6.3 is obtained for Al⁺³ in PC. Integration of the down-field peaks is somewhat inaccurate in this case because the peaks are fairly broad and there is some interference from the bulk PC peaks. Some measurements were taken at low temperature in an effort to remove the possible broadening effects of exchange. However, in PC, in contrast to the AN results reported

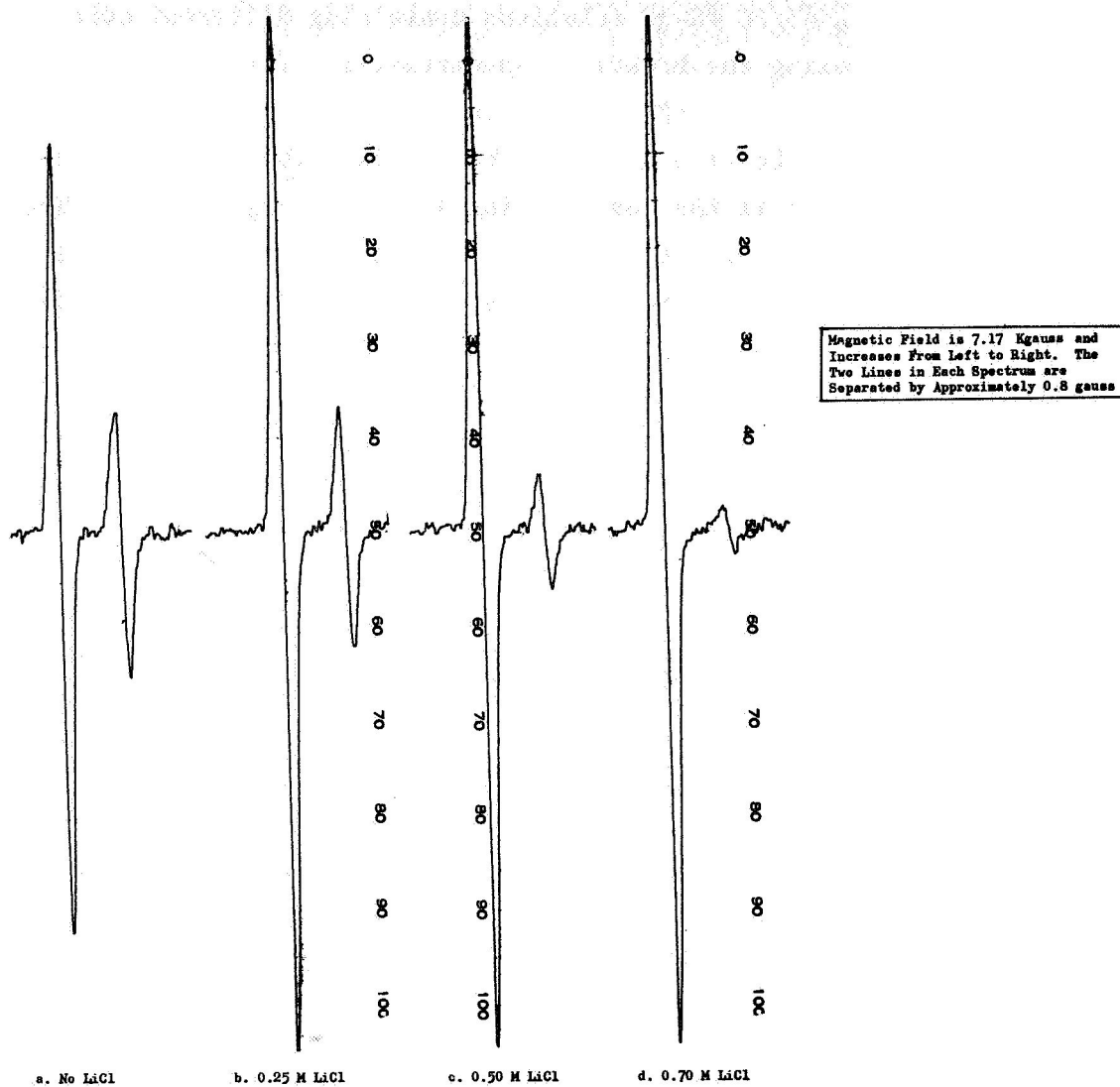


Figure 25. Al^{27} Nuclear Magnetic Resonance in 1 M AlCl_3/PC Containing Various Concentrations of LiCl

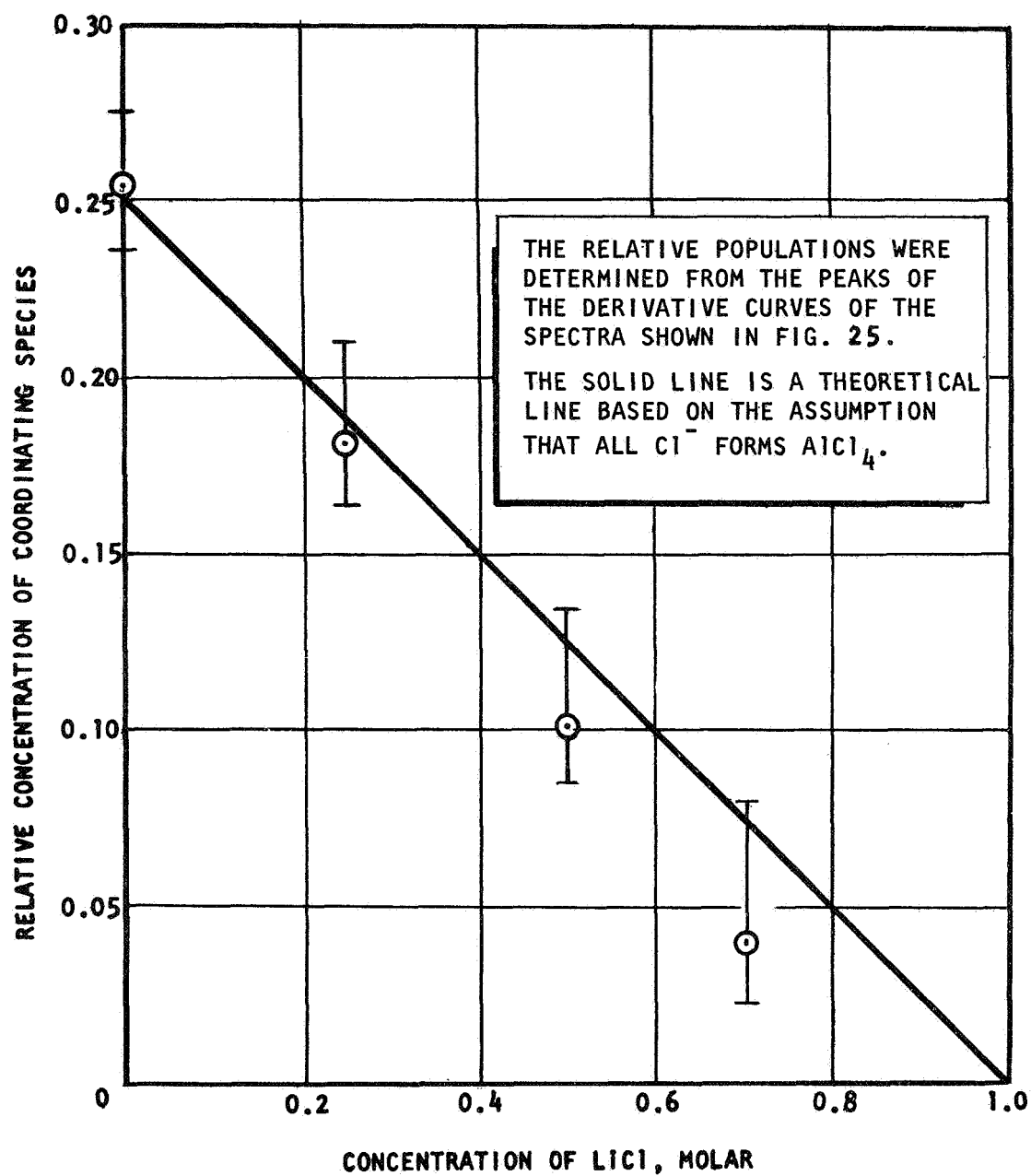


Figure 26. Approximate Relative Populations of Coordinating Al Species in 1 M AlCl_3/PC as a Function of Added LiCl

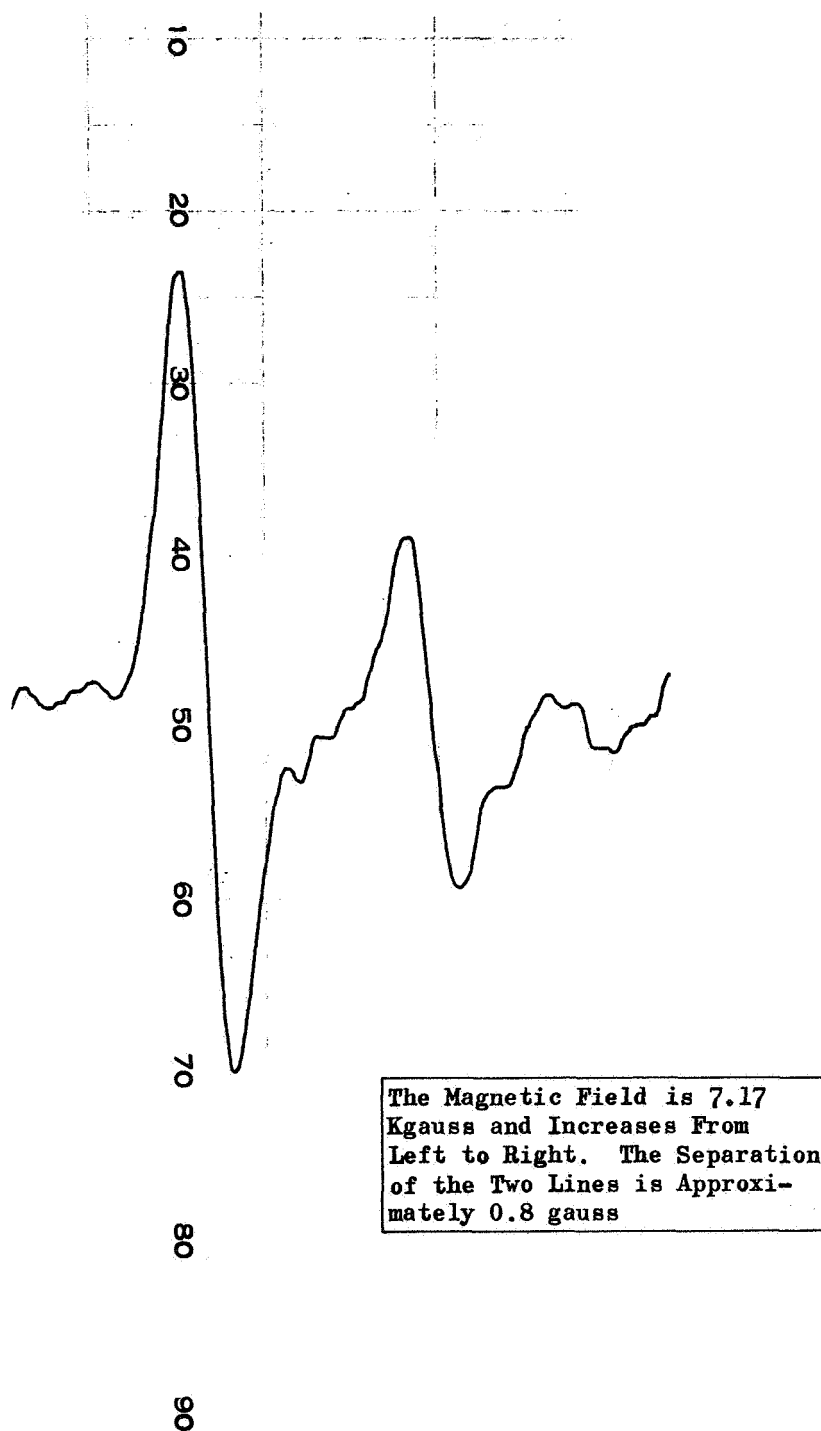


Figure 27. Al^{27} Nuclear Magnetic Resonance in 0.1 M AlCl_3/PC

previously, the peaks due to the coordinated PC broadened further rather than becoming narrow. This can be explained on the basis of increased viscosity effects at lower temperatures. At temperatures higher than room temperatures, the peaks broadened and disappeared as would be expected on the basis of exchange effects.

The spectrum of neat propylene carbonate (PC #2-12) was studied briefly under high resolution conditions. The complexity of the spectrum suggests that the chemical shifts and coupling constants of the ring protons are quite similar in magnitude. This situation results in a very complex spectral pattern which cannot be assigned in terms of simple multiplets for each of the various proton environments. However, the spectral features due to resonance of the methyl protons are well removed from the ring proton signals. For the purpose of determining coordination number, the simple pattern due to the methyl group provided all the necessary information. For the study of possible partial polymerization or other degradation reactions of propylene carbonate under the influence of aluminum species, a further investigation of the spectra due to the ring protons may be advantageous.

Li^7 lines in the $\text{LiCl}+\text{AlCl}_3/\text{PC}$ solutions and in 0.1 and 1 M LiClO_4/PC were single lines and easily saturated as has been the case for all Li^7 lines observed in these studies.

The Cl^{35} line in LiClO_4/PC consisted of the single narrow line of the ClO_4^- ion. This line was somewhat broader than that found for the ClO_4^- ion in DMF and AN. The Cl^{35} line in $\text{LiCl}+\text{AlCl}_3/\text{PC}$ was a single line which is attributed to the Cl in AlCl_4^- . However, in this case the line was much broader than in AN. The increased broadening of the Cl^{35} line in the ClO_4^- ion and the AlCl_4^- ion in PC is most likely due to the effects of viscosity noted in the proton spectrum of 1 M AlCl_3/PC .

Thus, in parallel to the results obtained in AN solutions, the results obtained here indicate that dissolving of AlCl_3 in PC produced the species $\text{Al}[\text{PC}]_6^{+3}$ plus AlCl_4^- . Addition of LiCl to AlCl_3 in PC produced Li^+ and additional AlCl_4^- .

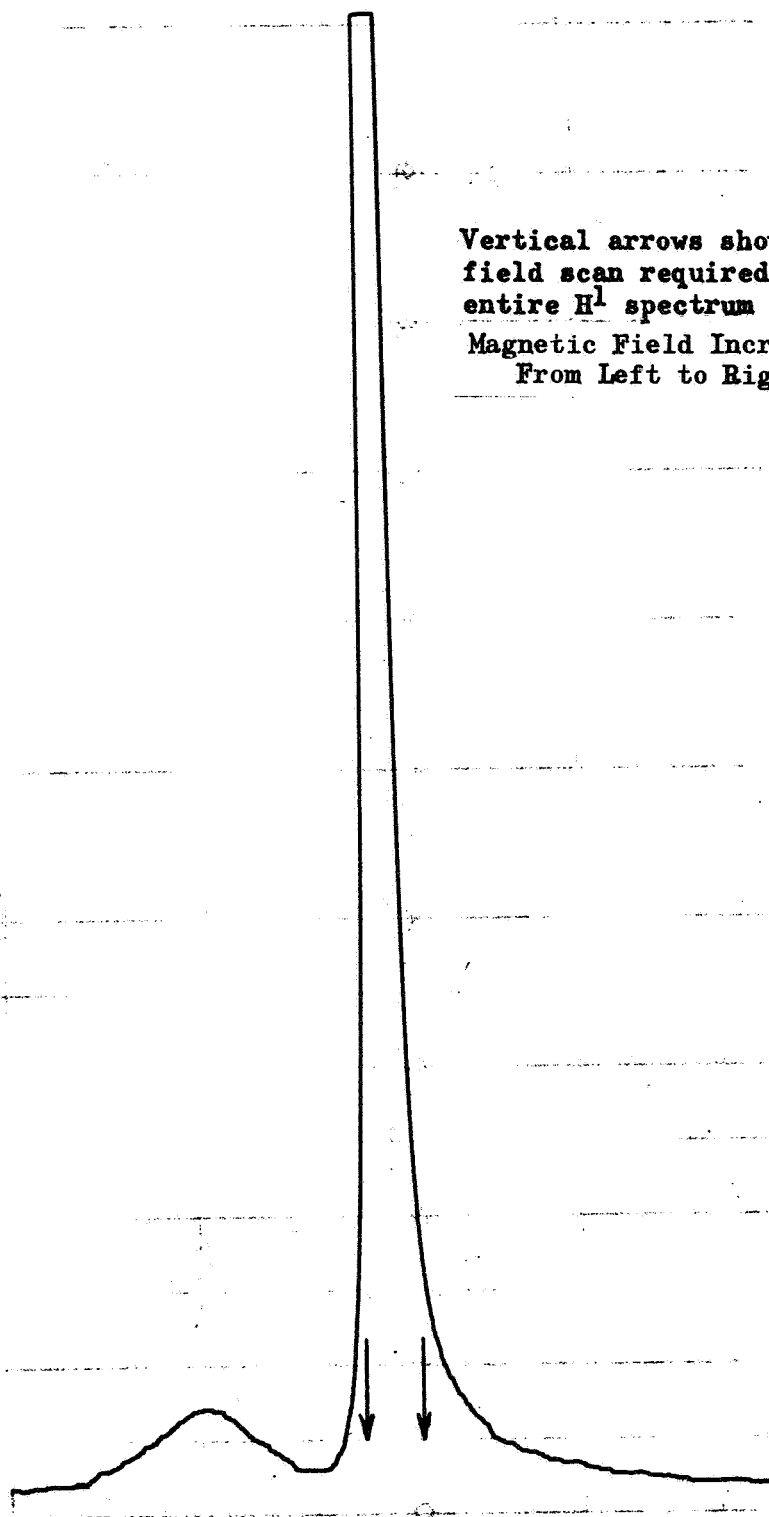
LiClO_4 in PC produces Li^+ and ClO_4^- . Additional measurements at low temperature and in mixed solvents would be required to determine the extent of possible solvation of Li^+ .

ELECTROLYTES CONTAINING CUPRIC SPECIES

Measurements were made in DMF, PC, and MF containing copper halides, with and without electrolyte added. A major effort was directed toward the determination of species in $\text{CuCl}_2 + \text{LiCl}/\text{DMF}$. Work with this system was emphasized because of the favorable solubilities and the possibility of a shift in major species on addition of LiCl , as observed in the $\text{AlCl}_3 + \text{LiCl}$ systems. It was found that the observations on the sparingly soluble systems could be readily interpreted in terms of the CuCl_2/DMF results, as will be shown.

$\text{LiCl} + \text{CuCl}_2/\text{DMF}$

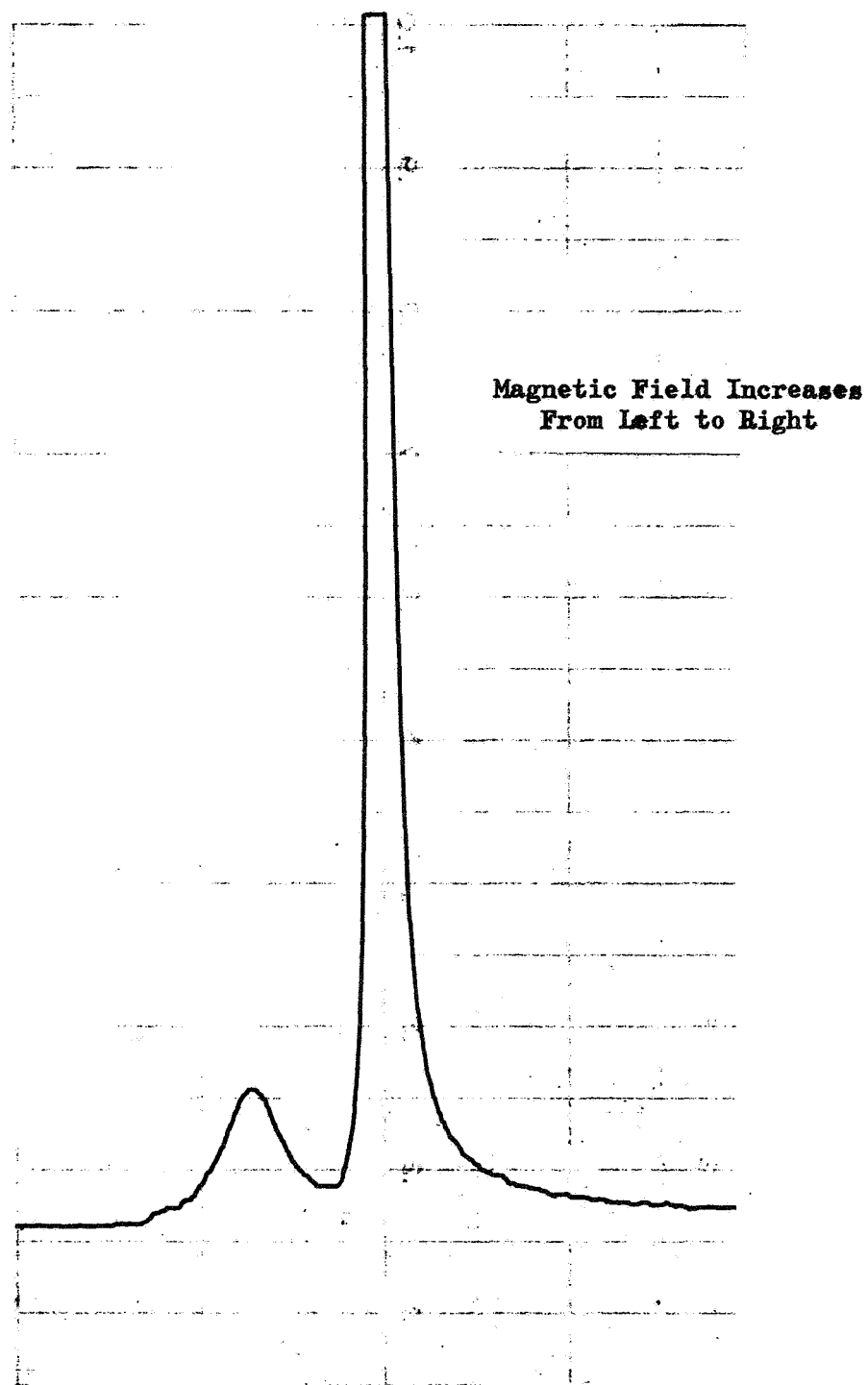
The high resolution proton spectra of solutions of CuCl_2 #2 in DMF #5-2 with various amounts of LiCl #2 were observed over a period of 6 months as reported in Ref. 5. The spectra of a series of freshly prepared solutions (0, 0.5, 1, and 2 M LiCl) are reproduced in Fig. 28, 29, 30, and 31. The primary features of interest in these spectra are the very broad lines and large separation of aldehyde and methyl resonances as compared with the spectrum of neat DMF (Fig. 11) and the decrease in these differences with addition of LiCl . The differences were also observed to decrease with time as may be seen in the series of spectra taken 1 month after preparation (Fig. 32, 33, 34, and 35). In addition,



Vertical arrows show the approximate
field scan required to record the
entire H^1 spectrum in pure DMF.

Magnetic Field Increases
From Left to Right

Figure 28. Proton Spectrum in 1 M $CuCl_2/DMF$,
Freshly Prepared Specimen



**Figure 29. Proton Spectrum in 0.5 M LiCl + 1 M CuCl₂/DMF,
Freshly Prepared Specimen**

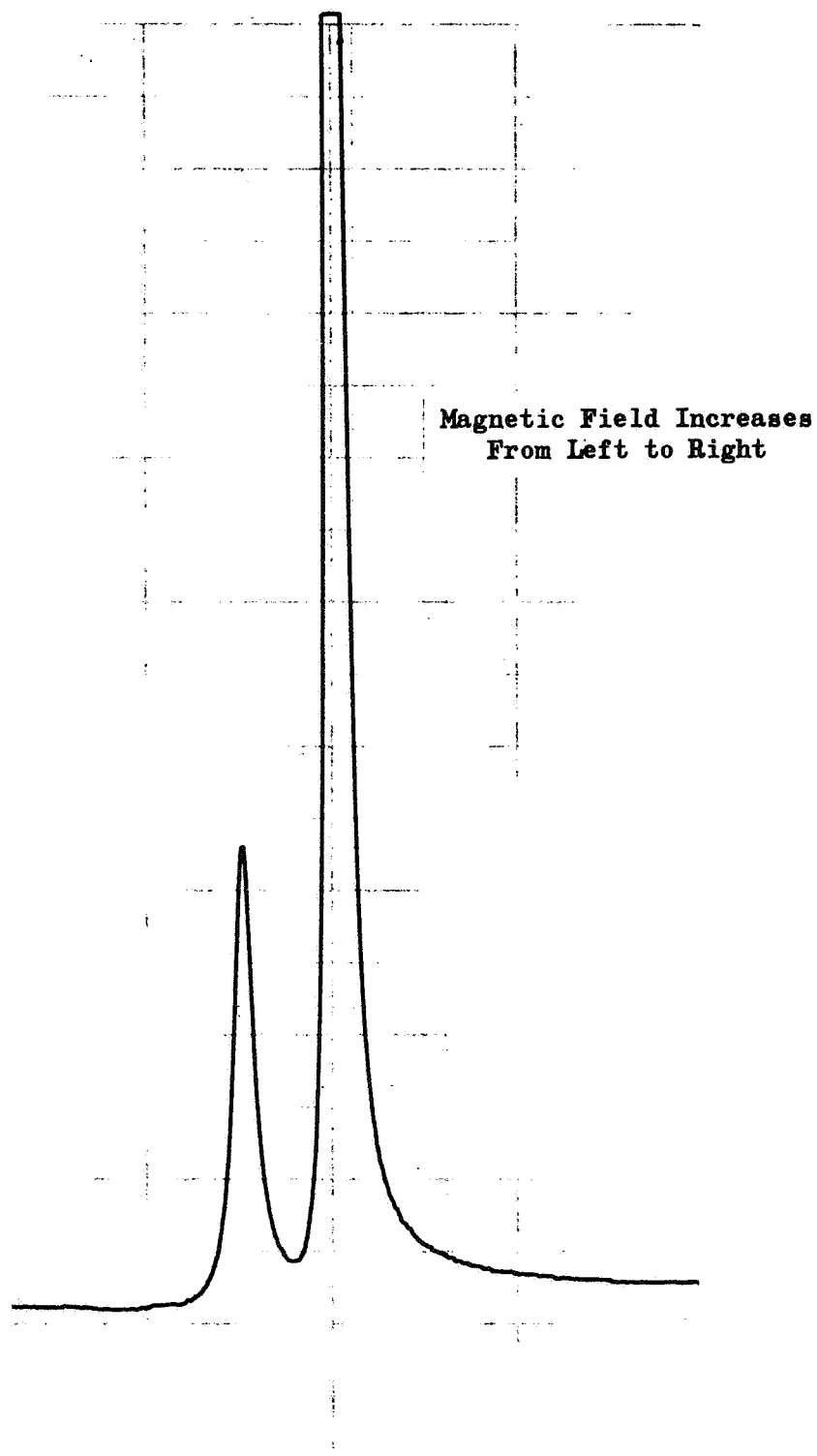
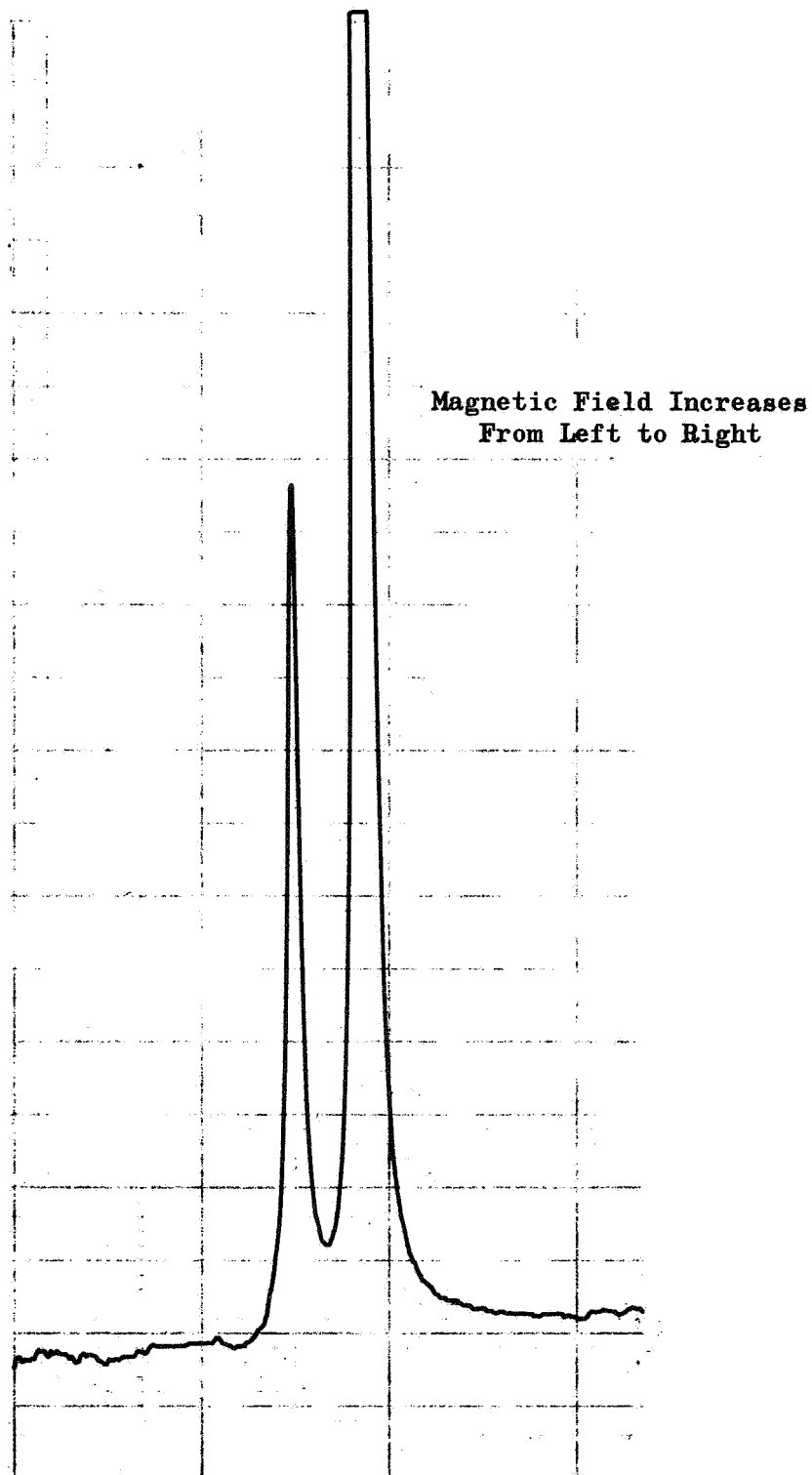


Figure 30. Proton Spectrum in 1 M LiCl + 1 M CuCl₂/DMF,
Freshly Prepared Specimen



**Figure 31. Proton Spectrum in 2 M LiCl + 1 M CuCl₂/DMF,
Freshly Prepared Specimen**

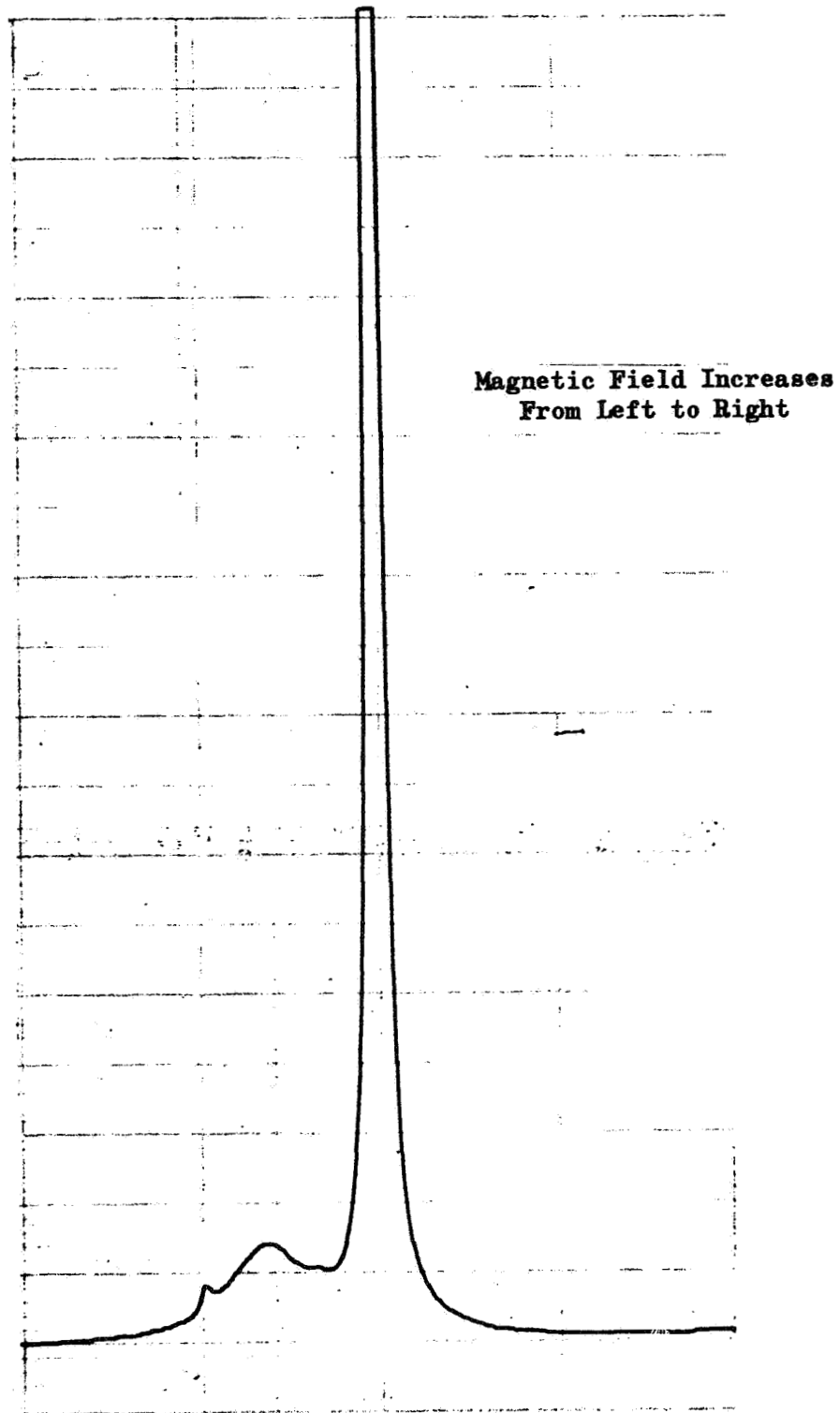


Figure 32. Proton Spectrum in 1 M CuCl_2/DMF , 1 Month After Preparation

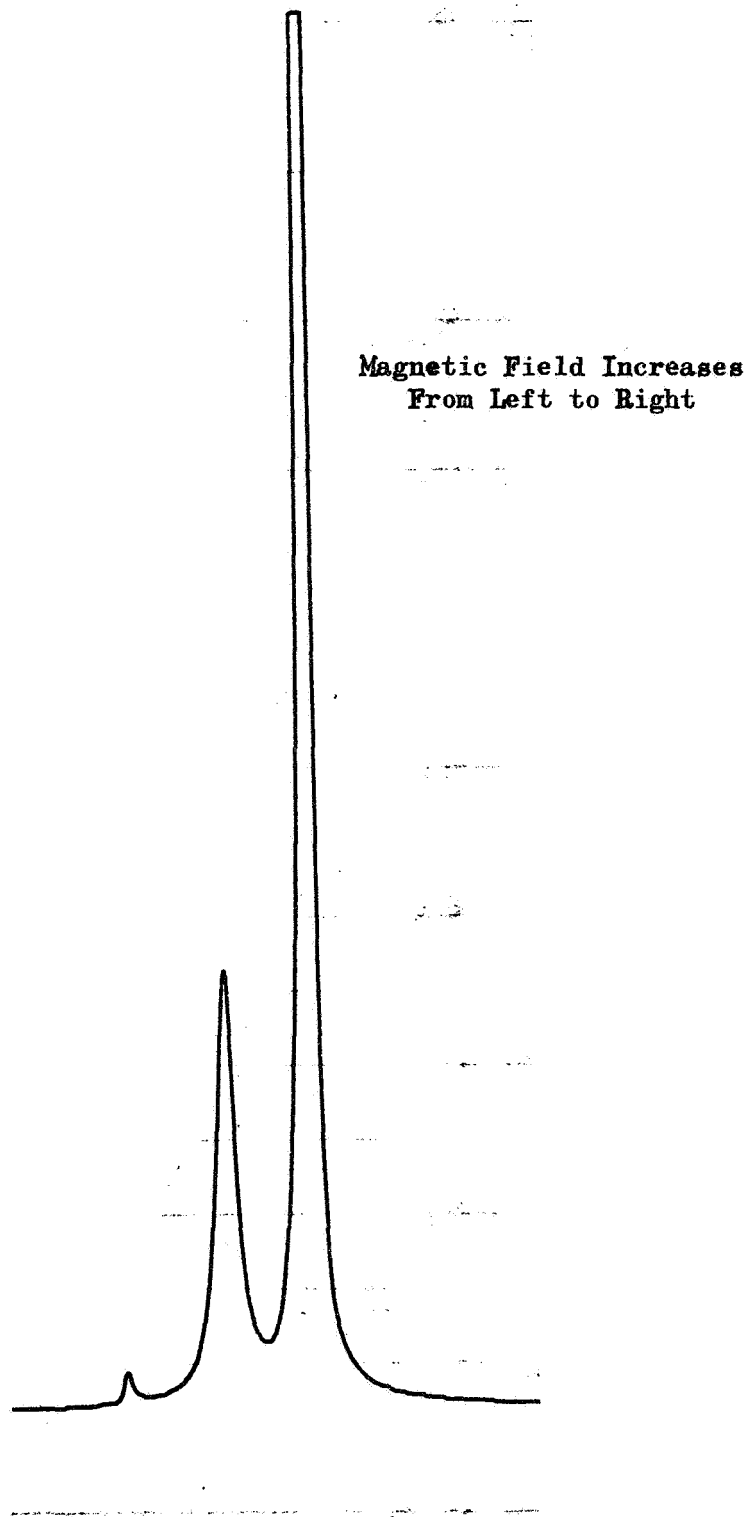


Figure 33. Proton Spectrum in 0.5 M LiCl + 1 M CuCl₂/DMF,
1 Month After Preparation

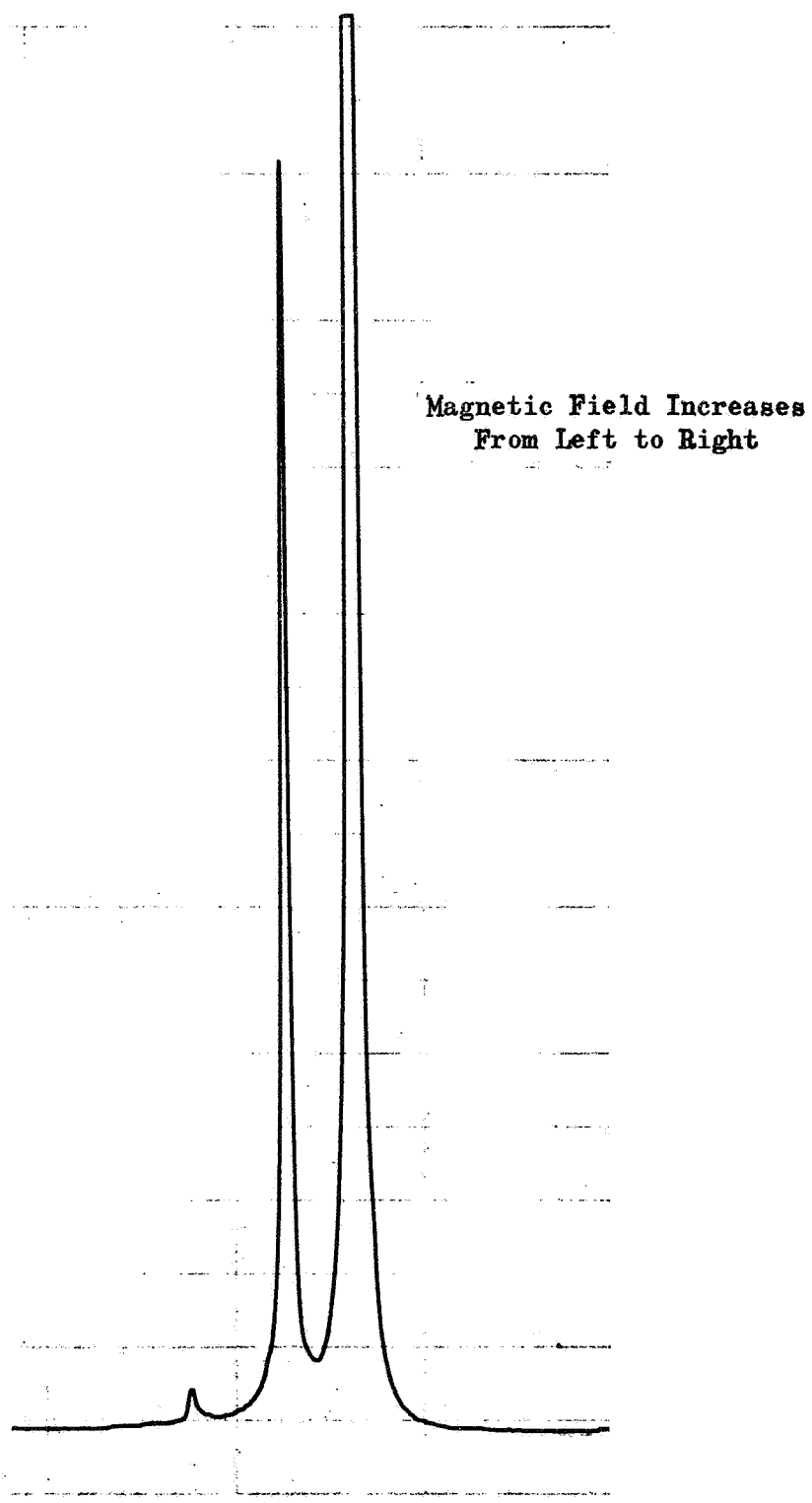


Figure 34. Proton Spectrum in 1 M LiCl + 1 M CuCl₂/DMF,
1 Month After Preparation

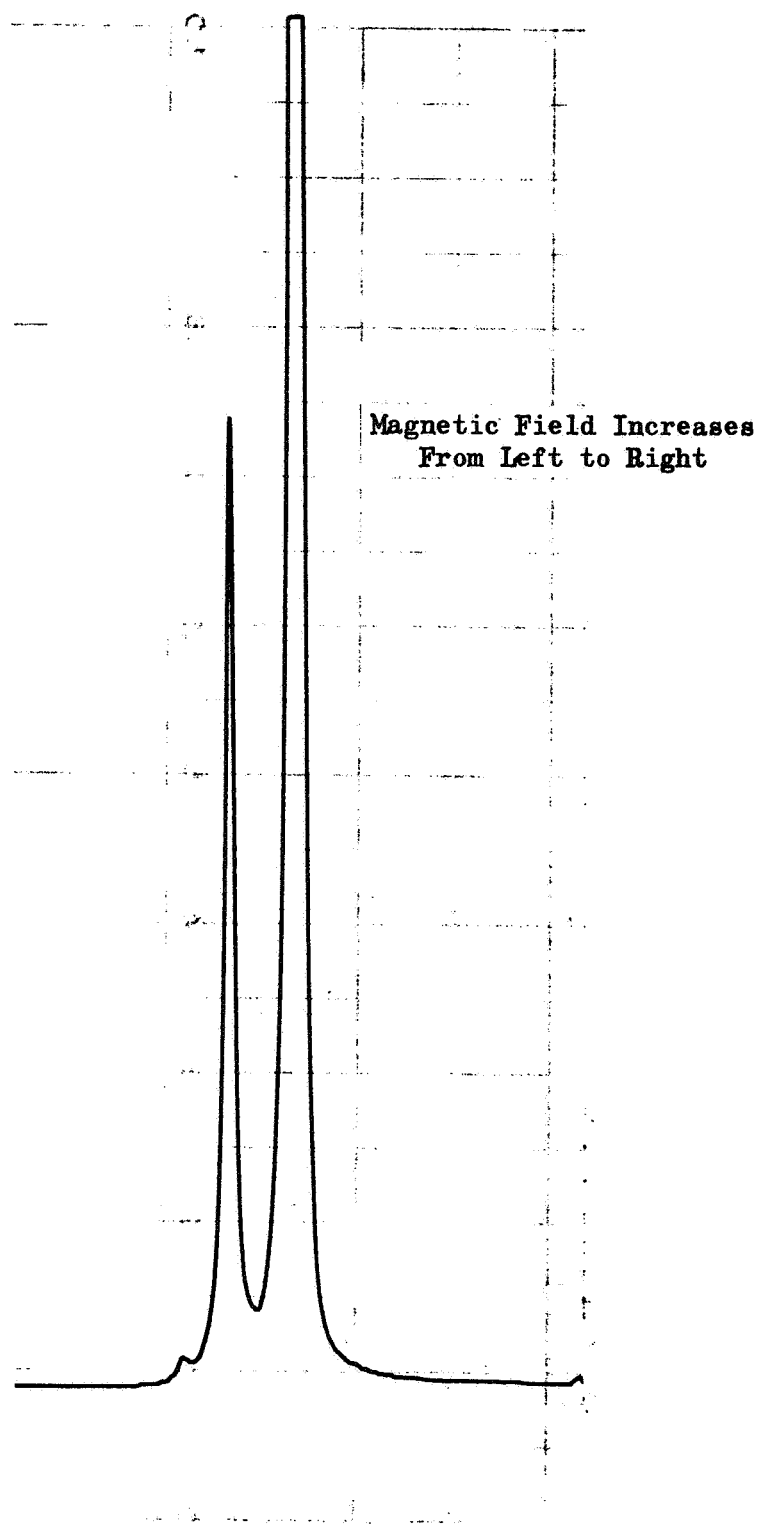


Figure 35. Proton Spectrum in 2 M LiCl + 1 M CuCl₂/DMF, 1 Month After Preparation

a smaller peak appeared down-field of the aldehyde proton resonance a few weeks after sample preparation. The separation of each of these peaks from the methyl group resonance appeared to approach a limiting value several months after preparation, as is shown in Fig. 36 and 37. For all the solutions in this series, the aldehyde resonance position and width approach the values observed in neat DMF. An example of this is shown in the spectrum obtained for a 1 M CuCl_2/DMF 4 months after preparation (Fig. 38). The small down-field peak, however, approaches a different position for each concentration of LiCl.

Electron paramagnetic resonance spectra were recorded for the same $\text{CuCl}_2 + \text{LiCl}/\text{DMF}$ series. Two resonances centered at $g = 2.01$ and $g = 2.16$ were observed. The $g = 2.16$ resonance was observed only in solutions containing less than 1 M LiCl and is ascribed to the solvated cupric ion. This g value is in good agreement with that reported for other solvent Cu^{+2} complexes (Ref. 36). The line at $g = 2.01$ was much stronger in solutions containing added LiCl. It is attributed to tetrahedral CuCl_4^{-2} on the basis of this chloride dependence, a g value near that predicted for a regular tetrahedral complex, and the agreement in color with that discussed by Ballhausen (Ref. 37). Relative intensities of the EPR signals are strongly dependent on the sample history. In particular, in 1 M CuCl_2/DMF evidence of the CuCl_4^{-2} resonance has been observed as a shoulder on the edge of a strong solvent complex line in some samples, whereas only a weak solvent complex line is observed in a sample with a different storage history. Typical EPR spectra of 1 M CuCl_2/DMF solutions with LiCl added are shown in Fig. 39 through 42. Figure 43 shows the spectrum of the same green 1 M CuCl_2/DMF as Fig. 39 recorded at higher gain, to demonstrate the small amount of CuCl_4^{-2} present in this solution. The gain used to record the 1 M LiCl + 1 M CuCl_2/DMF spectrum (Fig. 41) was reduced by a factor of 2 and that for the 2 M LiCl + 1 M CuCl_2/DMF (Fig. 42) by 10. Quantitative comparisons of the EPR signal intensities for these solutions are quite uncertain due to the dependence of the spectrometer sensitivity on the properties of the solution being examined;

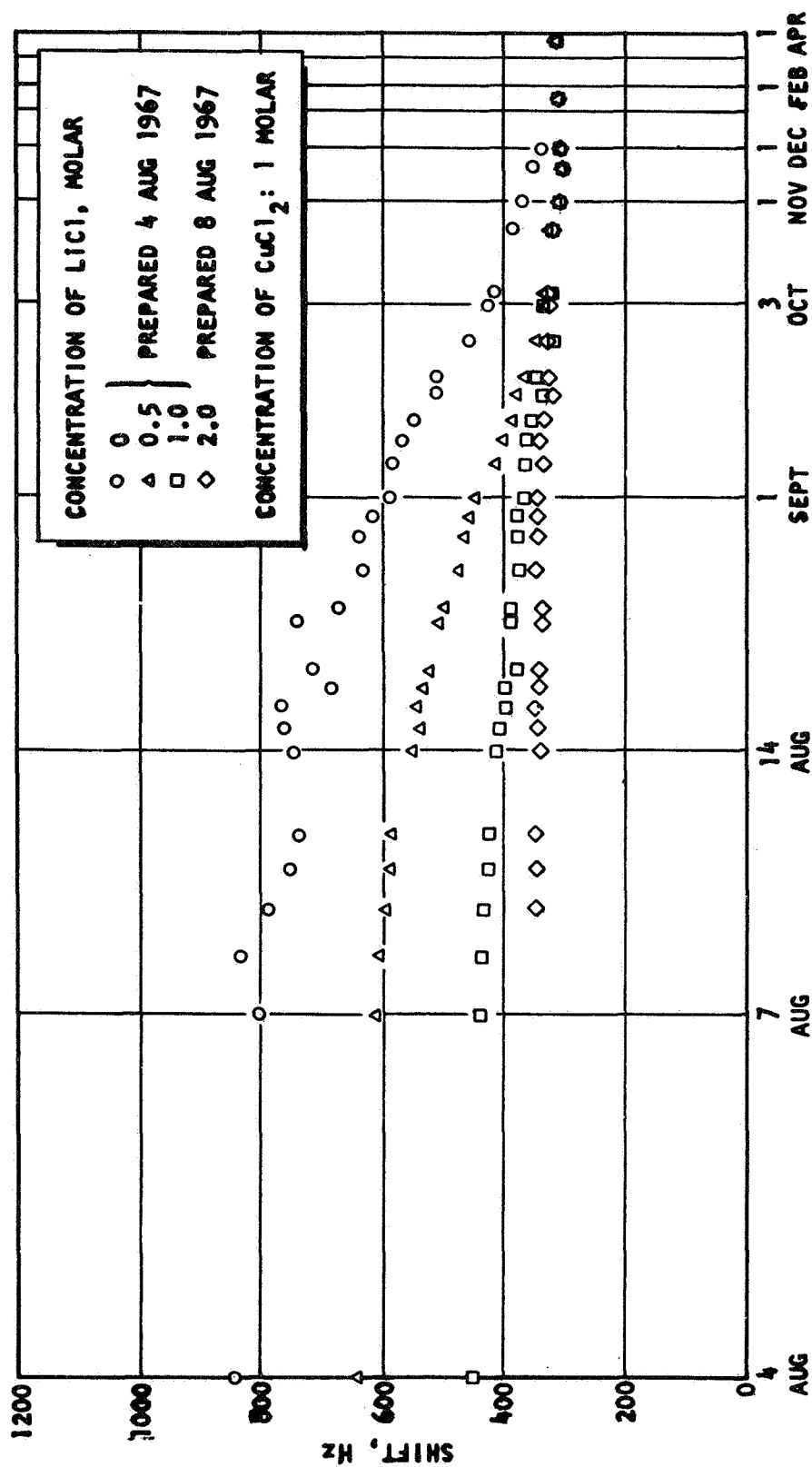


Figure 36. Splitting of Large Proton Peaks as a Function of Time for LiCl + CuCl₂/DMF

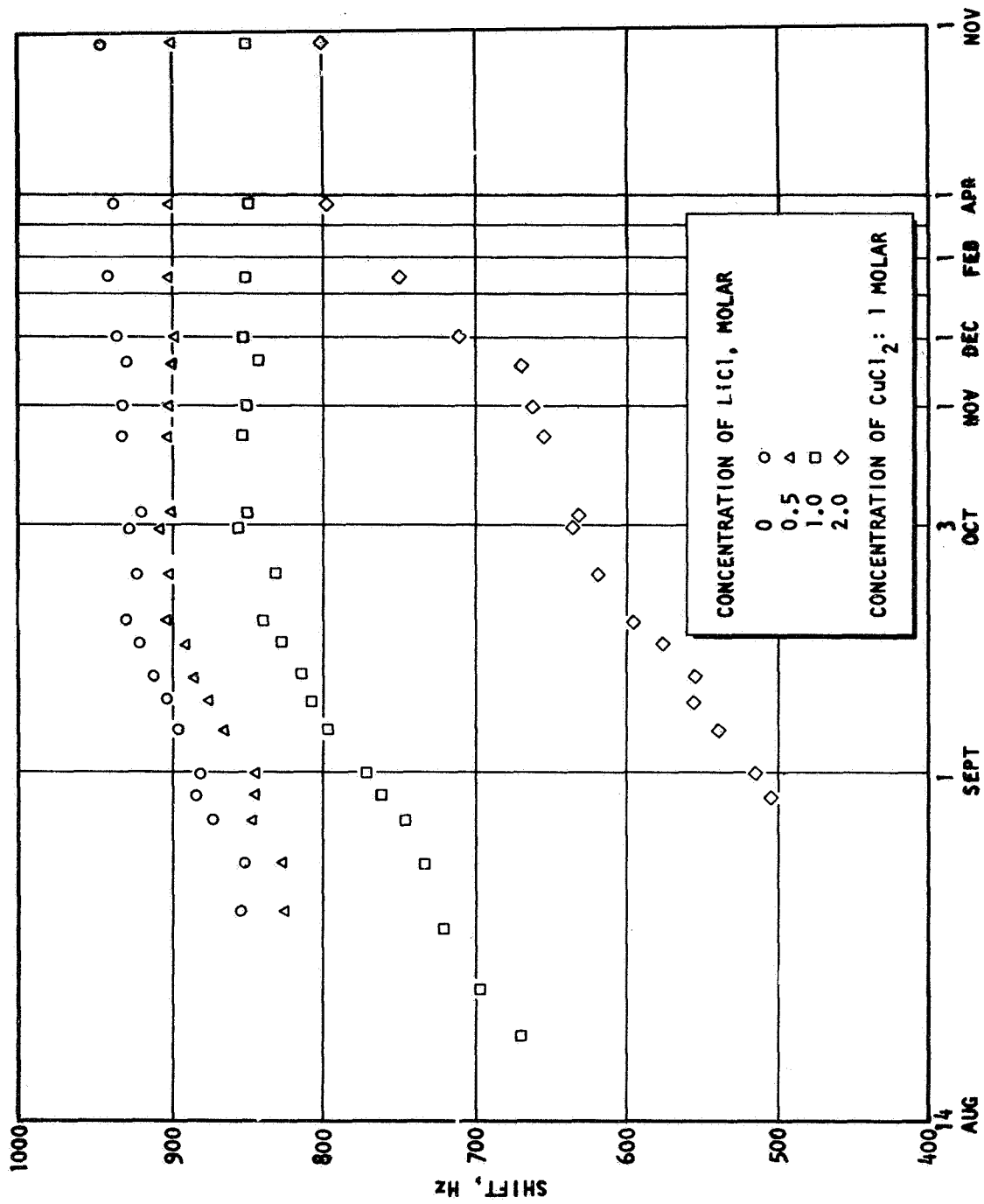


Figure 37. Position of Small Far-Downfield Resonance as a Function of Time for LiCl + CuCl₂/DMF

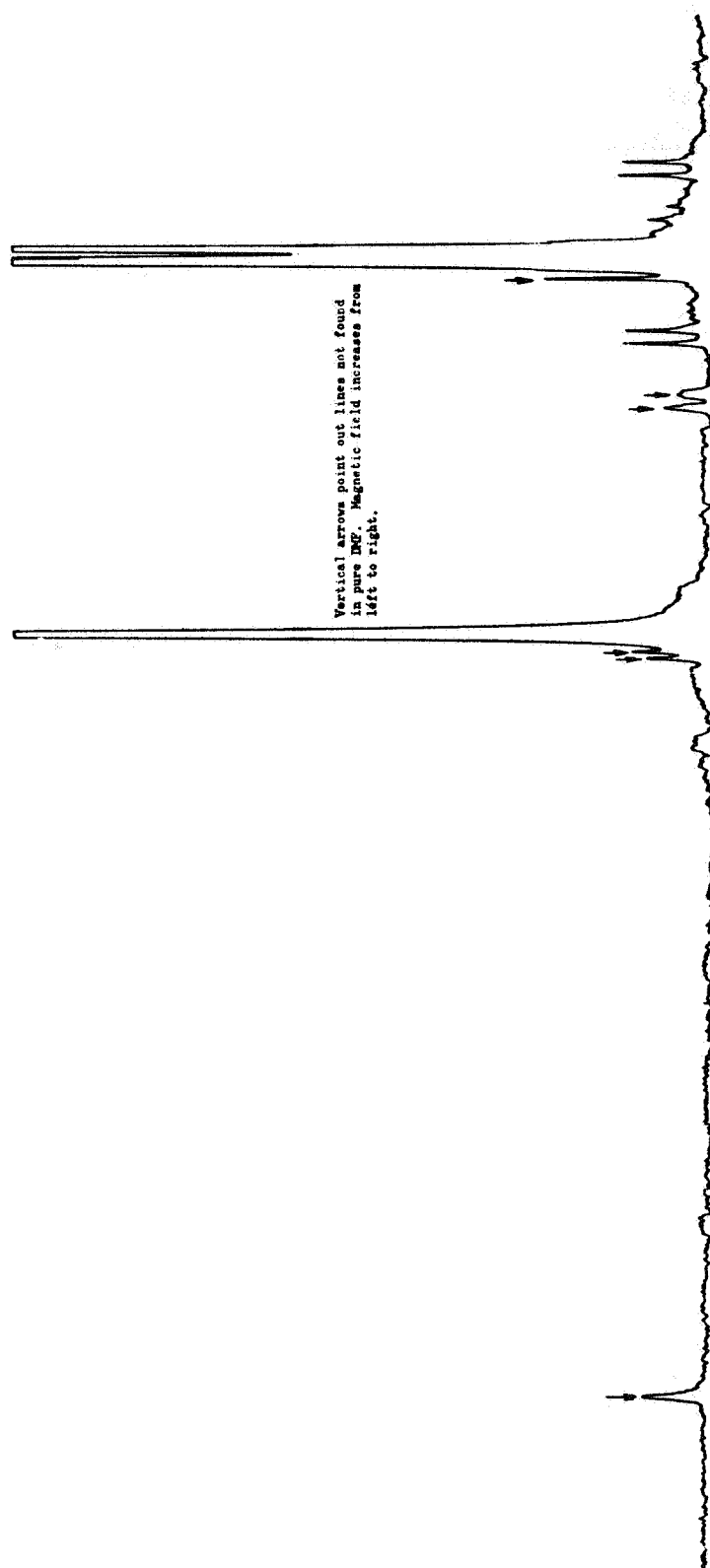


Figure 38. Proton Spectrum (High Resolution) in 1 M CuCl_2/DMF , 4 Months After Preparation

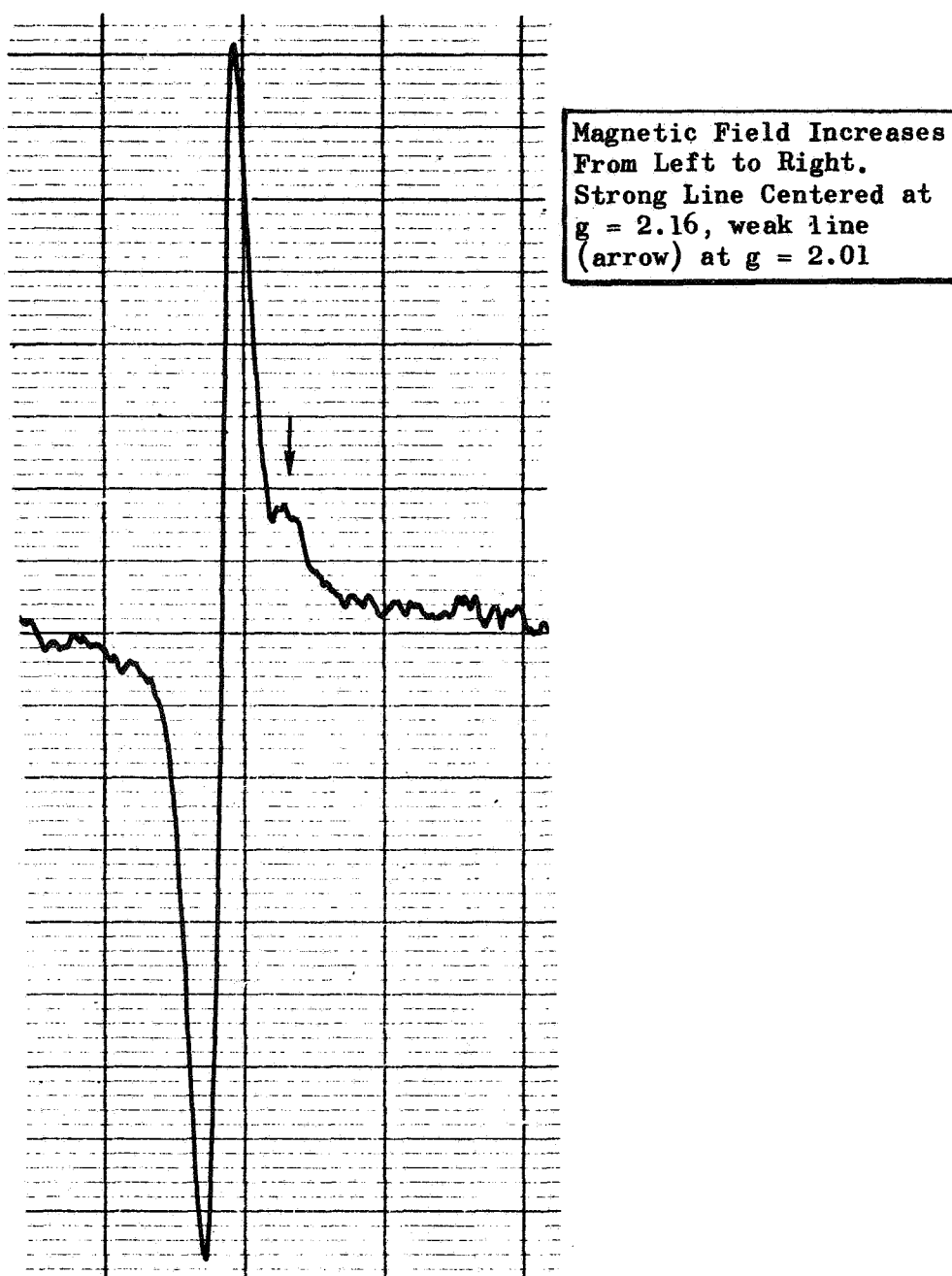


Figure 39. EPR Spectrum of 1 M CuCl_2/DMF

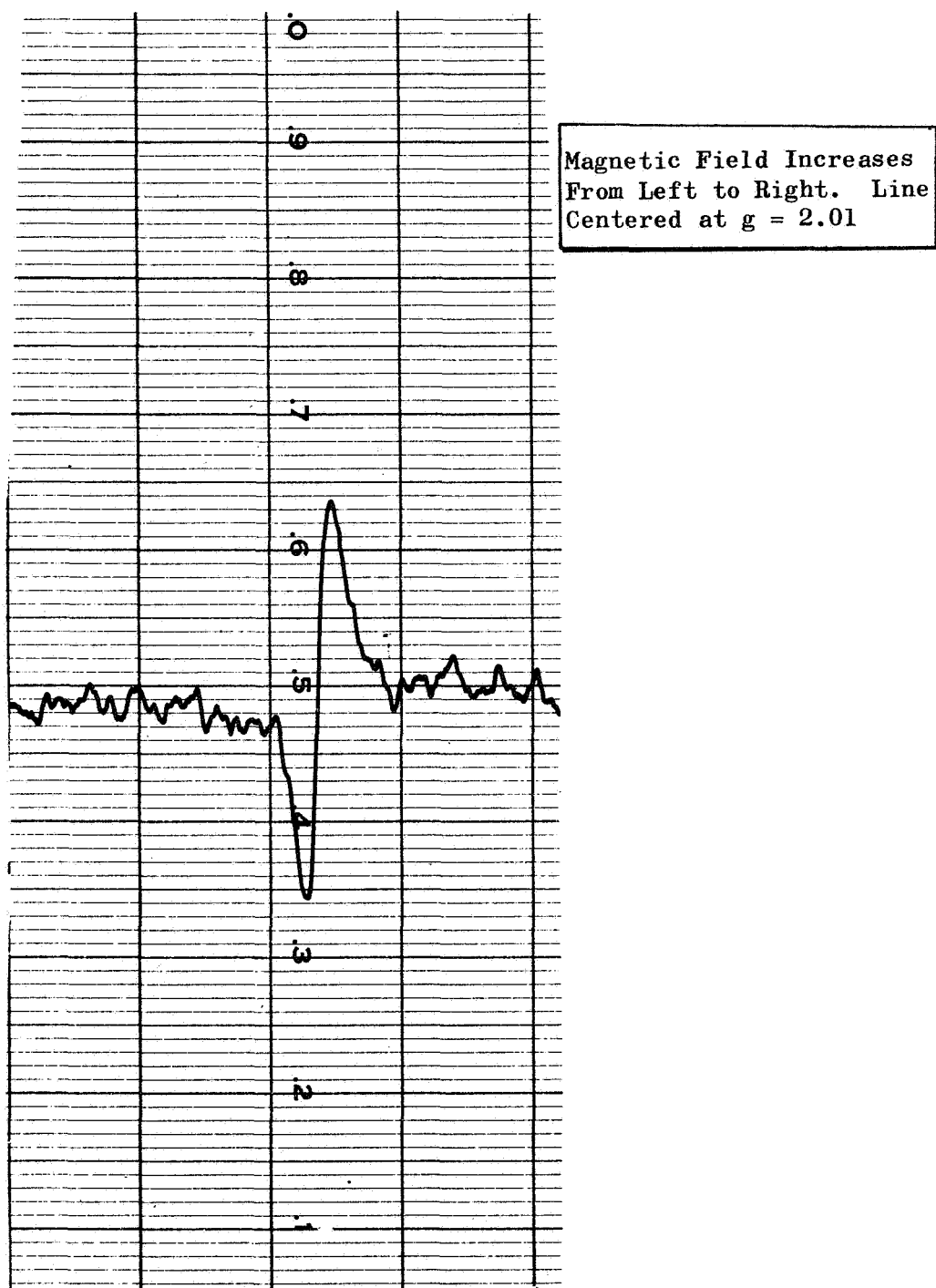


Figure 40. EPR Spectrum of 0.5 M LiCl + 1 M CuCl₂/DMF

Magnetic Field Increases
From Left to Right. Line
Centered at $g = 2.01$

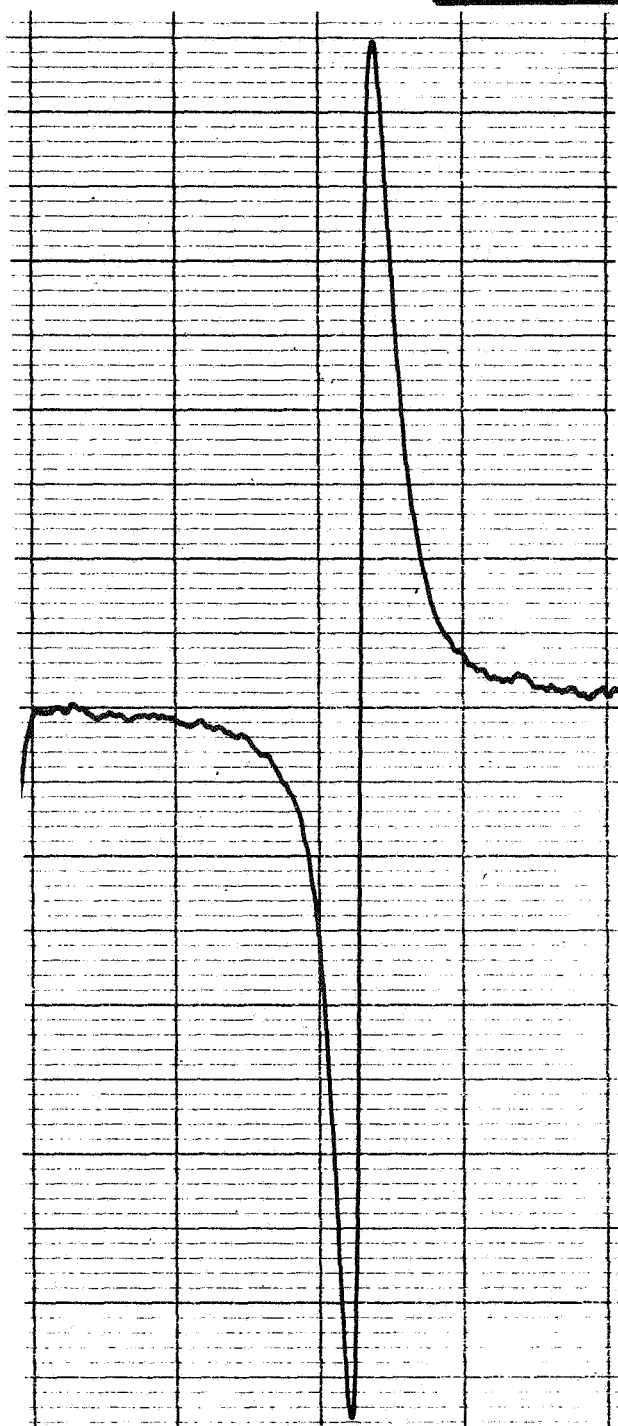


Figure 41. EPR Spectrum of 1 M LiCl + 1 M CuCl₂/DMF

Magnetic Field Increases
From Left to Right. Line
Centered at $g = 2.01$

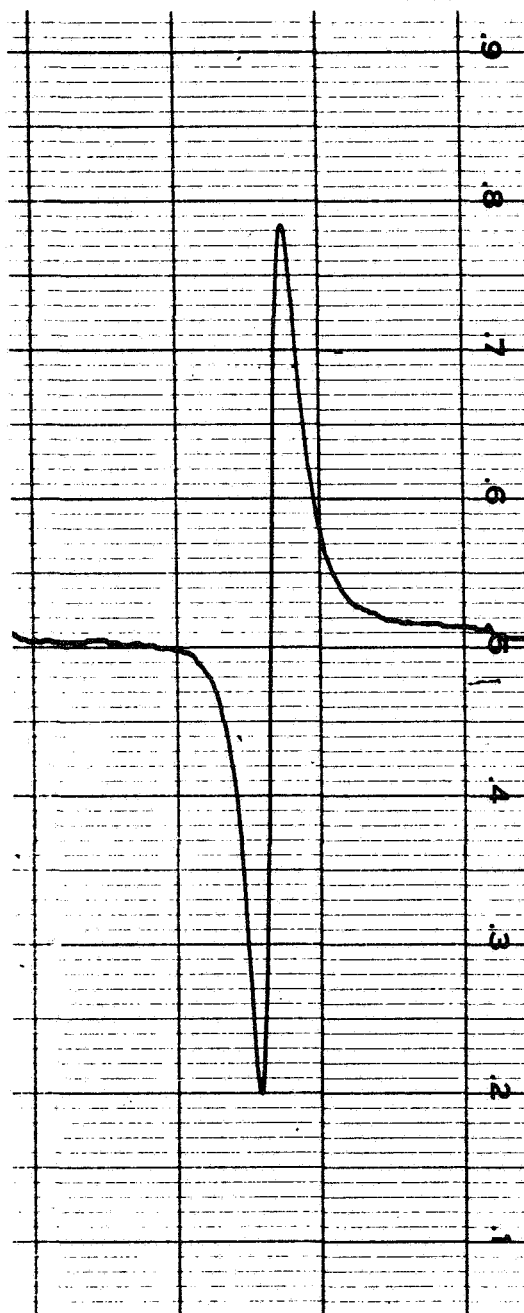


Figure 42. EPR Spectrum of 2 M LiCl + 1 M CuCl₂/DMF

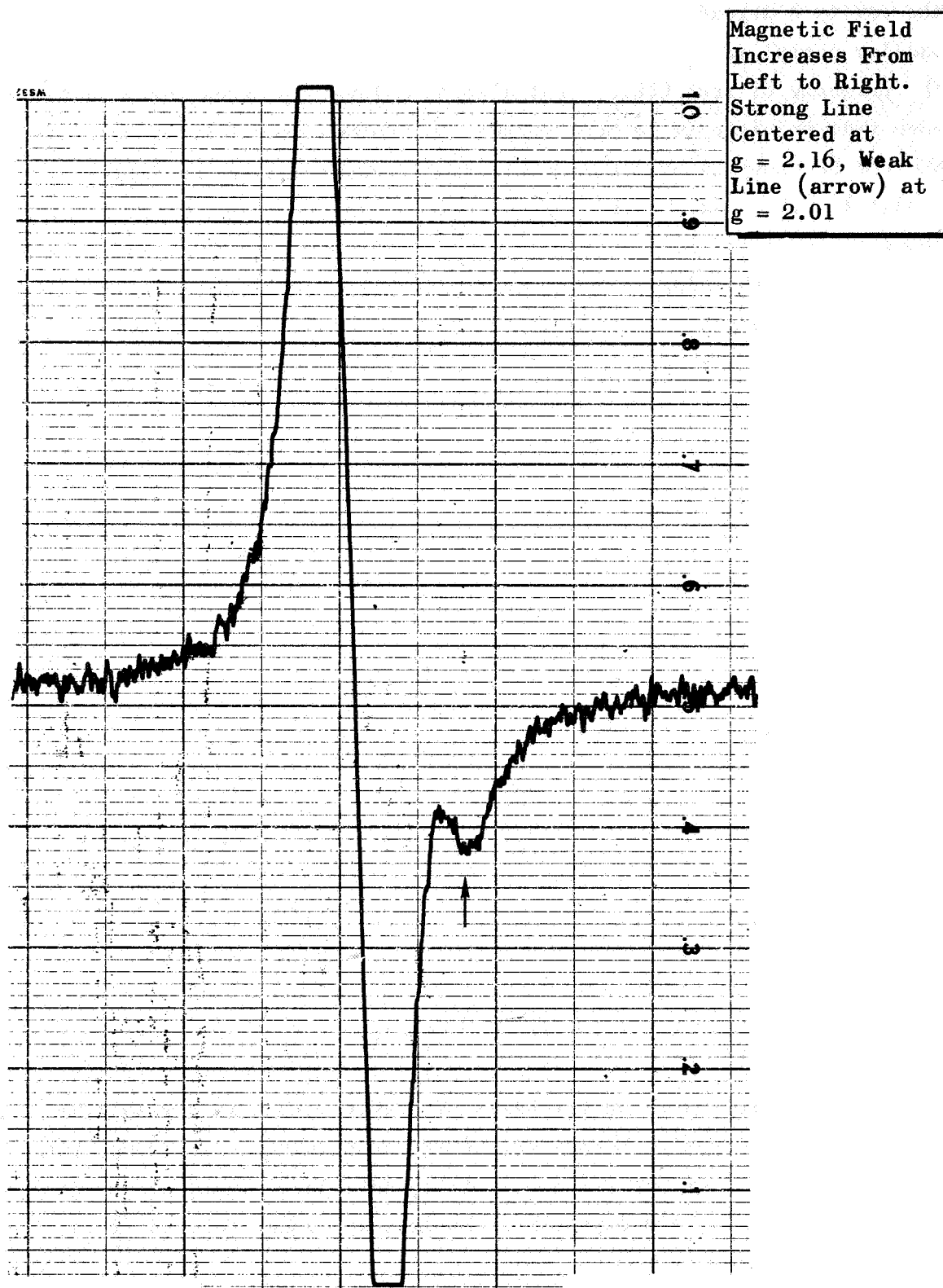


Figure 43. EPR Spectrum of 1 M CuCl_2/DMF at High Gain

the cavity Q depends upon the conductivity of the specimen. Thus, the smaller signal in 1 M LiCl + 1 M CuCl₂/DMF is probably due not only to the presence of less CuCl₄⁻² but also to a lower spectrometer sensitivity when that solution is being observed. Measurements involving both the NMR and EPR spectra of the same electrolyte were made using different physical samples due to the differences in sample volume and sample tube materials required for the measurements. EPR spectra of the aging NMR samples could therefore not be obtained without terminating the sequence of NMR measurements.

Broadline H¹ and Li⁷ magnetic resonance studies performed on these solutions (see previous discussion) indicate that the solvent molecules in 2-week-old solutions are in contact with paramagnetic species while the lithium ion is shielded either by species associated with the paramagnetic center or by its own solvation sphere. No broadline resonance due to Cl³⁵ could be detected in these solutions, indicating that the chloride exists mainly in complexes connected to paramagnetic ions.

A 0.1 M CuCl₂/DMF solution was observed to be yellow in color when freshly prepared. The proton NMR spectrum showed only a slight broadening, but EPR resonances were found at g = 2.16 and g = 2.01 as shown in Fig. 44. On standing a few days, the color faded and no sign of any cupric species could be detected in either the NMR or EPR spectra.

An analysis of the available data leads to the conclusion that several copper-containing species exist in 1 M CuCl₂/DMF and that addition of LiCl results mainly in the formation of CuCl₄⁻². The exact nature of the species remains unclear at this time, although several candidate species can be suggested on the basis of previous work in crystalline materials. For example, both a yellow square-planar and an orange tetrahedral form exist for CuCl₄⁻² in crystals (Ref. 38). In addition, dimeric complexes containing two cupric ions bridged by either chloride ions,

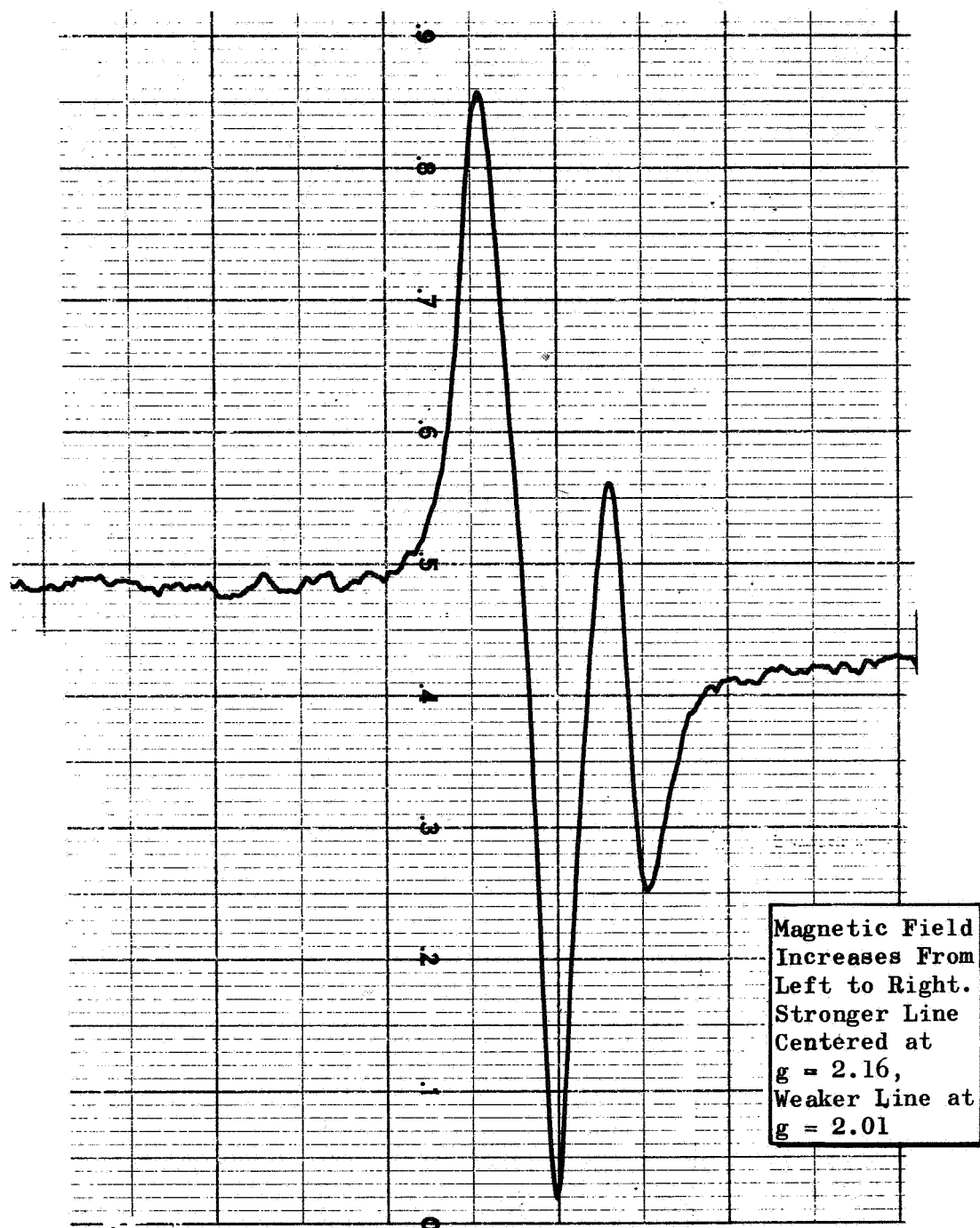
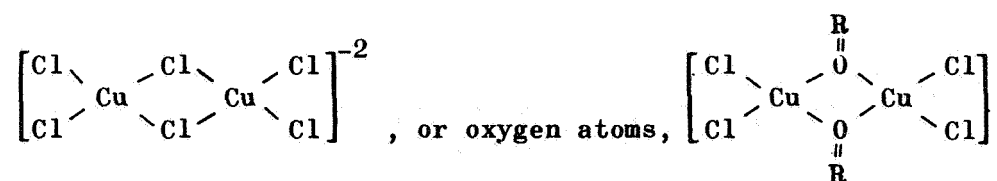


Figure 44. EPR Spectrum of Freshly Prepared 0.1 M CuCl_2/DMF



in solvent molecules have been reported (Ref. 39). The formation of such a dimer could quite possibly account for the slow process by which the paramagnetic ions are removed from contact with the bulk solvent. It would also explain the small down-field peak, because any DMF serving as a bridge would not be expected to exchange with the bulk DMF and the paramagnetic contact shift would be very large. The slow reaction is indicative of a high activation energy for the process, although possible photochemical or surface phenomenon cannot be excluded without further study. An additional feature of this hypothesis is that it makes it possible to account for the dependence of the position of the small down-field peak as a function of added LiCl, by employing an argument similar to that reported in Ref. 28, where the reported frequency of the aldehyde proton in the DMF-AlCl₃ complex depends on the anion present through a second solvation sphere interaction. In their interpretation, the association of chloride ion with the aldehyde proton in the coordinated solvent resulted in a decrease in electron density at the proton and thus gave a further down-field shift. In CuCl₂/DMF systems, the large down-field shift is due to the paramagnetic contact shift rather than a simple shielding effect. A decrease in the electron density at the aldehyde proton in this case would then reduce this contact shift and give an up-field shift. In LiCl + CuCl₂/DMF electrolytes, the principal anionic species formed on addition of LiCl is CuCl₄⁻². The presence of this anion in close proximity to the dimer could produce an up-field shift. Because the energy of this interaction is quite small, a rapid exchange would be expected, the resultant line showing only the statistical average position. Additional LiCl, producing more CuCl₄⁻², would cause the average position to shift up-field as more of the associated species would be present on the average.

$\text{CuF}_2 + \text{LiClO}_4/\text{DMF}$

The low solubility of CuF_2 in pure DMF prevented the observation of any cupric species in that system.

The results on saturating 1 M $\text{LiClO}_4/\text{DMF}$ with CuF_2 are consistent with the precipitation of LiF and the formation of only a blue $\text{DMF} - \text{Cu}^{+2}$ complex. No evidence of any Li^7 broadline resonance was observed and the Cl^{35} resonance was the single sharp line associated with ClO_4^- . The high resolution proton spectrum was a single very broad peak. Because there was no Cl^- present, all of the Cu^{+2} was available to interact with the solvent. As a result, the aldehyde peak was apparently either broadened or shifted beyond detection. EPR measurements on this solution showed only the strong line at $g = 2.16$ which is assigned to the solvent complex.

$\text{CuCl}_2, \text{CuF}_2$ in PC and in $\text{LiCl} + \text{AlCl}_3/\text{PC}$

The high resolution NMR spectra of PC saturated with CuCl_2 or CuF_2 were identical with that of the pure solvent. A detectable EPR signal was found in CuCl_2/PC but not in CuF_2/PC . The line occurred at $g = 2.13$ which again is indicative of a solvent complex.

Saturated solutions of CuCl_2 and CuF_2 in $\text{LiCl} + \text{AlCl}_3/\text{PC}$ were examined but no changes from the spectra previously obtained for this solvent system were observed. Because discrepancies were observed in other measurements on these solutions, the composition of the solutions used is uncertain.

$\text{CuF}_2 + 1.1 \text{ M LiAsF}_6/\text{MF}$

A saturated solution of CuF_2 #3 in 1.1 M LiAsF_6 #1/MF #2-4 exhibited only an EPR line at $g = 2.16$ in addition to the unperturbed solvent proton NMR spectrum.

ELECTROLYTES CONTAINING QUARTERNARY AMMONIUM IONS

The electrolytes investigated were tetramethylammonium hexafluorophosphate ($\text{TMA} \cdot \text{PF}_6$) in DMF, AN, and PC, and tetramethylammonium fluoride ($\text{TMA} \cdot \text{F}$) in DMF and PC. Some measurements were also made on tetraethylammonium fluoride ($\text{TEA} \cdot \text{F}$ #1) in PC #6-2. It is expected that dissolving $\text{TMA} \cdot \text{PF}_6$ and $\text{TMA} \cdot \text{F}$ would result in the formation of TMA^+ and PF_6^- , and TMA^+ and F^- ions, respectively. To verify this, both the H^1 and F^{19} resonances were investigated in DMF, AN, and PC solutions containing $\text{TMA} \cdot \text{PF}_6$, and in DMF and PC containing $\text{TMA} \cdot \text{F}$.

The F^{19} resonance in PC, DMF, and AN containing $\text{TMA} \cdot \text{PF}_6$ was an equal intensity doublet. No other F^{19} lines were observed. Because P^{31} has a spin of $1/2$, the spin-spin interaction with the spin of F^{19} should lead to an equal intensity doublet. Furthermore, all F's in PF_6^- are chemically equivalent; therefore, complex spectra (more than one line) would occur only because of P-F spin-spin interactions. Thus, the finding of only an equal intensity doublet is consistent with the assumption that the ion containing F^{19} is the PF_6^- ion.

The P-F splittings for PF_3 , PF_5 , PF_6^- , and HPF_6 have been reported (Ref. 40) as 1441, 916, 710, and 710 Hz, respectively. Also, the P-F splitting for PF_5 complexed with amides has been reported as 740 Hz (Ref. 41). Particularly because of the latter, the P-F splitting was carefully measured for $\text{TMA} \cdot \text{PF}_6$ in DMF and found to be 711 Hz which agrees well with that reported for PF_6^- . No evidence of F-F or H-F splittings could be observed. If HPF_6 were formed, such splittings would occur. Thus, the remote possibility of the formation of HPF_6 is ruled out.

Because of the relatively low solubility, these F^{19} lines from the PF_6^- ion were rather weak. The even lower solubility of $\text{TMA} \cdot \text{F}$ in PC and DMF and the smaller number of fluorine atoms per solute molecule resulted in no F^{19} line being observed in these solutions.

In contrast, the proton line due to the addition of $\text{TMA} \cdot \text{PF}_6$ and $\text{TMA} \cdot \text{F}$ was observed in every case. It should be noted that $\text{TMA} \cdot \text{F}$ contains the same number of protons as $\text{TMA} \cdot \text{PF}_6$. Therefore, the low solubility of $\text{TMA} \cdot \text{F}$ did not prevent the proton resonance line from being observed as was the case with the F^{19} resonance. In all cases, the proton line consisted of an equal intensity triplet with a splitting of 0.6 Hz. A typical spectrum is shown in Fig. 45. For comparison, note that the proton spectrum obtained for NH_4^+ (Ref. 42) consists of an equal intensity triplet with a splitting of 46 ± 2 Hz. This pattern is explained on the basis that all protons are equivalent and the line is split into a triplet by virtue of the spin-spin interaction with N^{14} which has a spin of 1. By analogy, because all protons are equivalent in the TMA^+ ion, and because interaction with N^{14} would yield a triplet as observed, the observations are consistent with what is expected for a TMA^+ ion. The splitting in TMA^+ should be, and is, much less than that in NH_3 because the interaction must go through an additional bond due to the carbon in the methyl groups.

Measurements on the proton resonance of $\text{TMA} \cdot \text{PF}_6/\text{AN}$ were hindered by the C^{13} side band of the solvent resonance line. The near coincidences of these resonances can be seen in Fig. 46 for four different solutions. An interesting feature is the change in position with addition of tetramethylsilane, TMS, a supposedly inert internal standard. No evidence for this type of interaction has been detected in any other of the systems studied in this work, although a similar effect has been reported elsewhere (Ref. 43). Thus, the species obtained when dissolving $\text{TMA} \cdot \text{PF}_6$ in DMF, AN, and PC are the TMA^+ and PF_6^- ions. In the case of $\text{TMA} \cdot \text{F}$ dissolved in DMF and AN, the TMA^+ ion is obtained. No direct data were obtained regarding the anionic species in this case because of the lack of observable signals.

Solutions of $\text{TEA} \cdot \text{F}$ #1 in PC #6-2 were examined at 0.1 and 1 molar. The H^1 spectrum clearly shows the quartet expected for the methylene group resonances (Fig. 47), but the triplet due to the methyl group is partially obscured by the methyl group resonance of the solvent. Two additional

This spectrum was obtained from
0.075 M TMA·PF₆/PC solution
(TMA·PF₆ #1, PC #2-5)

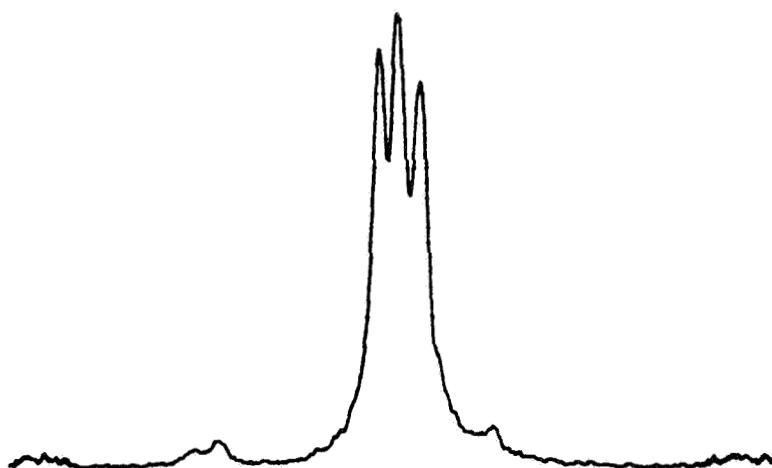


Figure 45. H^1 Spectrum of TMA^+ in Propylene Carbonate

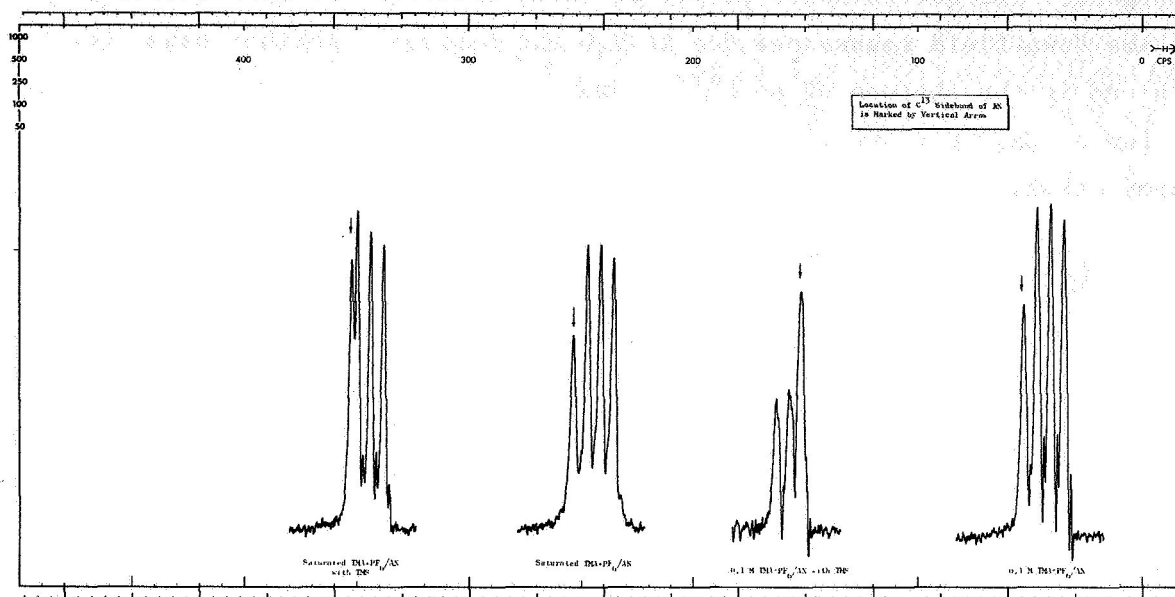


Figure 46. H^1 Spectrum of TMA^+ in Acetonitrile

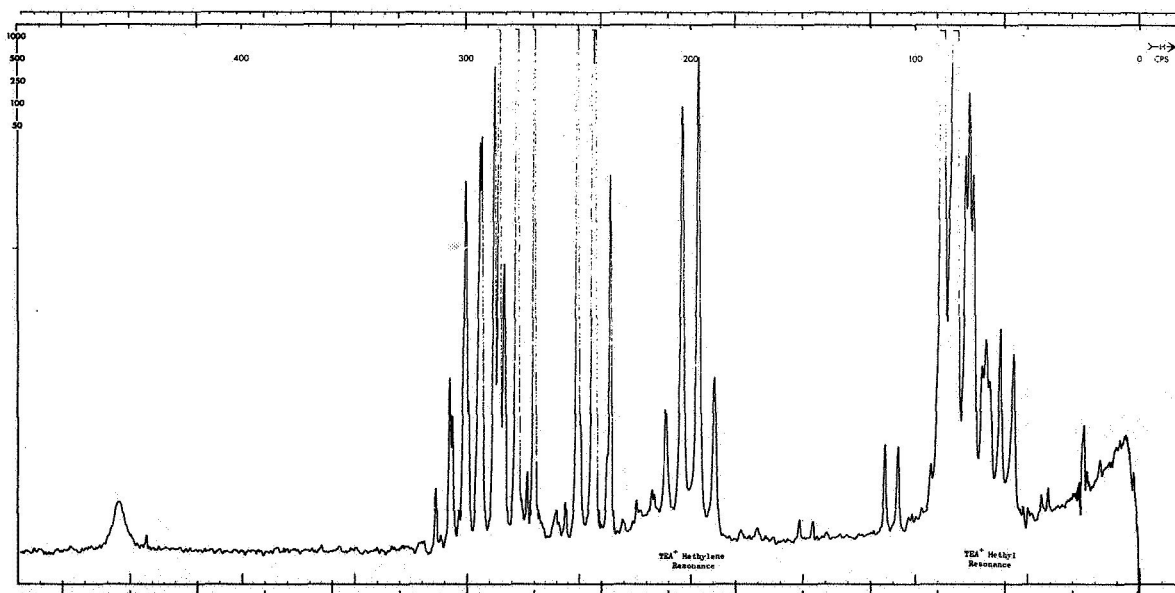


Figure 47. H^1 Spectrum of $\text{TEA} \cdot \text{F}$ in Propylene Carbonate

peaks which appear up-field from the methyl triplet have not been assigned. The questionable purity of these solutions is also evidenced by the down-field resonances due to H_2O and benzene. Another cause for concern is the absence of an F^{19} resonance. Further studies on the composition of this electrolyte are necessary to confirm the presumed chemical formulation.

LiAsF_6/MF ELECTROLYTES

Some exploratory measurements were made in LiAsF_6/MF electrolytes. The H^1 NMR spectra of these systems have been partially described elsewhere in this report. An interesting feature of these spectra is the down-field shift of the resonance frequencies as LiAsF_6 is added. This shift may be due to solvation of the lithium ion. However, further studies on this system are required. Temperature variations, for example, may provide more direct evidence on the solvation of lithium ions.

Broadline As^{75} and high resolution F^{19} spectra were obtained for the AsF_6^- ion. An As-F coupling constant of approximately 950 Hz derived from the As^{75} spectra shown in Fig. 48 is in good agreement with that reported by Muetterties and Phillips (Ref. 40).

The high resolution F^{19} spectrum consisted of only a broad unresolved line in 1.1 M LiAsF_6/MF at ambient temperature. This is consistent with the results on AsF_6^- reported by Packer and Muetterties (Ref. 44).

Saturation of this solution with CuF_2 #3 produced no observable change in any of the NMR spectra.

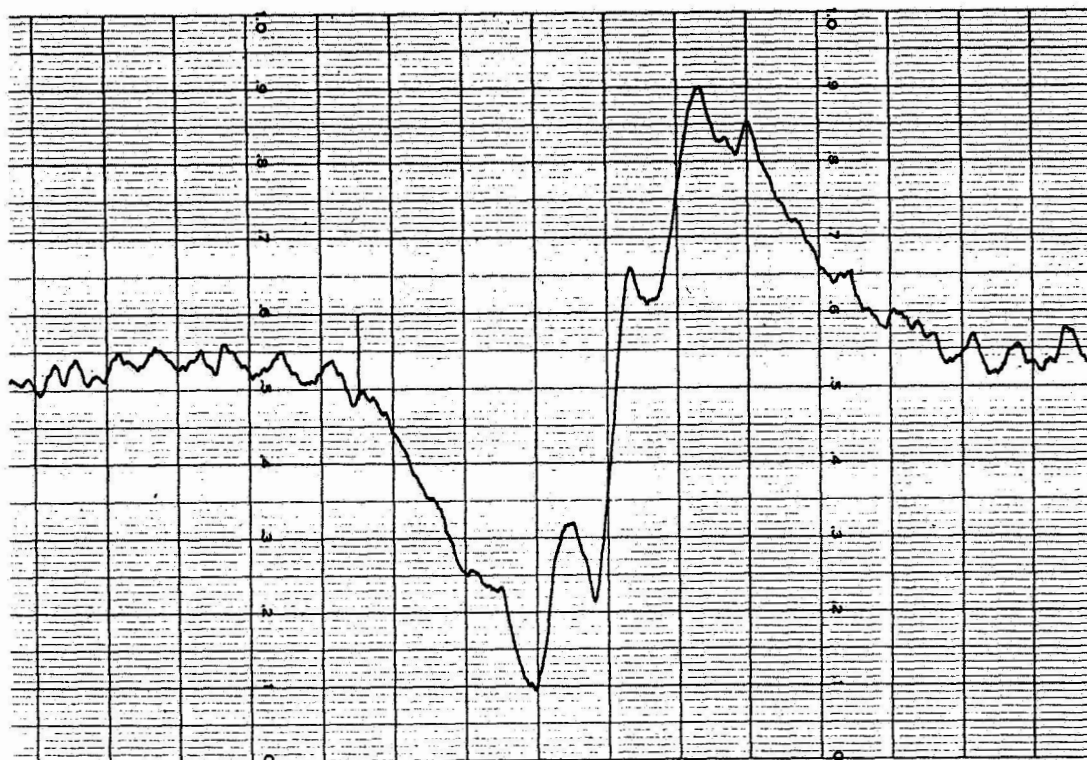


Figure 48. As^{75} Magnetic Resonance in 1.1 M LiAsF_6/MF

PHYSICAL PROPERTY DETERMINATIONS

SOLUBILITIES

Solubility studies were made in the following systems: (1) electrolyte solutes in various solvents, (2) electroactive materials (i.e., cupric fluoride and cupric chloride) in the solvents and in some electrolytes, and (3) potential battery discharge products (i.e., lithium fluoride and lithium chloride) in selected electrolytes.

Procedure

Saturated solutions were prepared by adding in the dry box an excess of solute to the solvent or solution of interest. Often, a Teflon-coated stirring bar was added. The flasks were then sealed with a glass stopper and the neck of the flask enclosed in a polyethylene bag containing dry nitrogen. The flasks were removed from the dry box and placed in a bath which was held at a temperature well above the final sampling temperature; magnetic stirring was possible in this bath. The samples were normally removed from this bath after 1 to 2 days and placed in other constant-temperature baths to equilibrate at 25 or 60 C, respectively, for several days with occasional stirring. In the case of sensitive systems, exposure to elevated temperatures had to be limited.

For sampling purpose, the flasks remained in the constant-temperature bath and were opened. A sample of the supernatant liquid was taken very quickly, the pipette being prewarmed to above the bath temperature if necessary.

In some cases, a different procedure was used. A LiAsF_6/MF solution was concentrated up to saturation by bubbling nitrogen through the solution. A saturated LiBF_4/DMF was directly synthesized by adding sufficient amounts of LiF and BF_3 to DMF. An attempt to get a saturated LiPF_6/PC solution was made by evaporating off the solvent under reduced pressure.

Several analytical methods were used to determine solute contents in the samples. Except in the case of NMR methods which were used, e.g., to determine TMA·F and TMA·PF₆ contents, the samples were diluted with water. Atomic absorption was the method used most frequently, for determination of lithium, aluminum, boron, and copper. Chloride ion concentrations were determined by a silver nitrate titration used routinely on another program (Ref. 45).

Results

The results are given in Table 22 for electrolyte solutes including potential cell discharge products, and in Table 23 for electroactive materials.

Uncertainties. There are several sources for uncertainties. (1) Solubility values were not verified, as it is sometimes done, by approaching saturation at a certain temperature also from below this temperature to eliminate uncertainties caused by possible oversaturation as well as incomplete saturation. (2) Dissolution rates were often very slow in these systems. This is particularly severe in systems which undergo changes with time. Such changes were obvious in AlCl₃/PC solutions and were studied in some detail in CuCl₂/DMC systems. If sample preparation time is too short, saturation may not be reached; on the other hand, solubility may be affected significantly by solvent decomposition or other slow reactions occurring during a prolonged experiment, particularly if it involves exposure to higher temperatures. (3) The presence of more than one solute may complicate the situation further.

LiCl + AlCl₃/PC. Somewhat erratic results were found in this system. An early result showed a solubility of 0.78 M LiCl in a 1 M AlCl₃/PC solution. Later, only 0.66 M LiCl was determined in a 1.2 M AlCl₃ solution. Based on the first result, however, a composition of 0.7 M LiCl + 1 M AlCl₃/PC was selected for extensive studies and such solutions were made up routinely with complete dissolution of the lithium chloride.

TABLE 22

SOLUBILITIES OF ELECTROLYTES

Solute	Solvent	Other Solution Components	Solubility at 25 C, moles/liter	Solubility at 60 C, moles/liter
LiClO ₄ #2	PC #2-7		2.1	3.1
LiClO ₄ #2	PC #2-7	1000 ppm H ₂ O	3.1	3.1
LiClO ₄ #2	DMF #3-3		4.4	4.8
LiClO ₄ #2	DMF #3-3	1000 ppm H ₂ O	3.5	4.9
LiClO ₄ #3	AN #4-3		1.06	
LiCl #2	PC #2-2		0.038	0.031
LiCl #2	PC #2-10	1 M LiClO ₄ #2 + 1000 ppm H ₂ O	0.071	
LiCl #2	DMF #4-1		2.42	3.76
LiCl #3	DMF #6-18	0.88 M LiF #2 + 0.88 M BF ₃ #1	1.94	
LiCl #2	AN #1-2		0.026	0.014
LiCl #1	PC #1-4	1 M AlCl ₃ #2	0.78	0.80
LiCl #2	PC #2-6	1.2 M AlCl ₃ #3	0.66	0.75
AlCl ₃ #3	DMF #1-4	1 M LiCl #2	0.088	
LiCl #2	AN #3-1	1 M AlCl ₃ #3	0.92	
LiF #2	PC #2-4		$<5 \times 10^{-6}$	$<5 \times 10^{-6}$
LiF #2	PC #4-5	1 M LiClO ₄ #3	1.3×10^{-4}	
LiF #2	DMF #1-2		3.2×10^{-5}	5.3×10^{-5}
LiF #2	DMF #6-13	1 M LiCl #2	$<1 \times 10^{-4}$	
LiF #2	AN #1-2		2.2×10^{-5}	3.2×10^{-5}
LiF #2 + BF ₃ #1	DMF #6-16		1.60	
LiF #2 + PF ₅ #1	DMF #6-17		1.6	
TMA·F #1	PC #2-3		0.065	
TMA·F #1	DMF #4-2		0.028	
TMA·PF ₆ #1	PC #2-4		0.15	0.22
TMA·PF ₆ #1	PC #2-6	1000 ppm H ₂ O	0.15	0.23
TMA·PF ₆ #1	DMF #4-2		0.24	0.36
TMA·PF ₆ #1	DMF #3-3	1000 ppm H ₂ O	0.21	0.32
TMA·PF ₆ #1	AN #1-2		0.10	0.18
LiAsF ₆ #1	MF(stock)		4.64	

TABLE 23

SOLUBILITIES OF COPPER HALIDES

Solute	Solvent	Other Solution Components	Solubility at 25 C, moles/liter	Solubility at 60 C, moles/liter
CuF ₂ #3	PC #2-11		2×10^{-4}	4×10^{-4}
CuCl ₂ #2	PC #2-4		4.9×10^{-3}	4.2×10^{-3}
CuF ₂ #3	DMF #5-6		1×10^{-4}	2×10^{-4}
CuCl ₂ #2	DMF #1-2		1.30	2.68
CuF ₂ #3	PC #2-11	1 M LiClO ₄ #2	4.7×10^{-3}	6.3×10^{-3}
CuF ₂ #3	PC #4-5	1 M LiClO ₄ #3 + 1000 ppm H ₂ O	2.2×10^{-2}	2.4×10^{-2}
CuCl ₂ #2	PC #2-7	1 M LiClO ₄ #2	1.9×10^{-3}	4.2×10^{-3}
CuCl ₂ #2	PC #2-8	1 M LiClO ₄ #2 + 1000 ppm H ₂ O	1.1×10^{-2}	1.9×10^{-2}
CuF ₂ #3	DMF #6-13	1 M LiClO ₄ #2	0.49	0.50
CuF ₂ #3	DMF #6-13	1 M LiClO ₄ #2 + 1000 ppm H ₂ O	0.50	0.45
CuCl ₂ #2	DMF #3-3	1 M LiClO ₄ #2	0.82	1.57
CuCl ₂ #2	DMF #3-5	1 M LiClO ₄ #2	0.87	2.2
CuF ₂ #3	DMF #5-1	1 M LiCl #2	0.53	0.52
CuCl ₂ #2	DMF #4-2	1 M LiCl #2	1.04	1.34
CuF ₂ #3	PC #4-5	0.7 M LiCl #3 + 1 M AlCl ₃ #4	0.183	
CuF ₂ #3	PC #5-5	0.7 M LiCl #3 + 1 M AlCl ₃ #4	0.063	0.11
CuF ₂ #3	PC #5-5	Excess LiCl #3 + 1 M AlCl ₃ #4	0.39	
CuCl ₂ #2	PC #2-8	Sat. LiCl #2 + 1 M AlCl ₃ #3	0.37	0.57
CuCl ₂ #2	PC #5-5	0.7 M LiCl #3 + 1 M AlCl ₃ #4	0.0094	0.0063
CuCl ₂ #2	PC #5-5	Excess LiCl #3 + 1 M AlCl ₃ #4	0.54	
CuF ₂ #3	DMF #6-2	1 M LiCl #2 + 0.075 M AlCl ₃ #3	0.44	0.44
CuCl ₂ #3	DMF #6-2	1 M LiCl #2 + 0.075 M AlCl ₃ #3	1.89	
CuF ₂ #3	MF #2-4	1.1 M LiAsF ₆ #1	7.5×10^{-4}	

LiCl + AlCl₃/DMF. A solubility value of 0.088 molar was determined for AlCl₃ in 1 M LiCl/DMF. Solutions of 1 M LiCl + 0.075 M AlCl₃/DMF were used for most experiments. In a solution which was left standing for several weeks, the formation of a crystalline precipitate was observed. This precipitate was analyzed and found to contain lithium and aluminum in stoichiometric amounts.

Because NMR results and a high exothermic heat of solution for AlCl₃ in DMF both indicated very strong complex formation, it was somewhat surprising that the solubility of AlCl₃ in DMF was relatively low. In an attempt to establish whether or not the precipitation of a compound containing lithium and aluminum was responsible for the low solubility, 1 gm of AlCl₃ #4 was added to 15 to 20 ml 1 M LiCl #3/DMF #7-2 solution. A white, fluffy precipitate formed, and the concentration of lithium in the supernatant liquid was found to have increased to 1.35 molar. The precipitate evidently contained dimethyl formamide and may have been a compound of the formula Al[DMF]₆Cl₃ rather than a compound which contains both lithium and aluminum. This compound may not necessarily be identical to the crystalline precipitate obtained after prolonged standing as mentioned above.

LiPF₆/PC. A 1 M LiPF₆/PC solution was made by adding PF₅ to a slurry of LiF in PC, and a dark solution resulted. A sample of this solution was concentrated by evaporating about half of the solvent at 60 C under vacuum; evaporation occurred slowly because of the low vapor pressure. The lithium content of the resulting solution was 1.31 molar, and the solution appears to have been saturated, although no precipitate could be distinguished in the dark solution.

Solubility of LiF. The solubility of LiF was found to be very low in the three solvents, PC, DMF, and AN. The lithium content of a saturated LiF/PC solution was actually below the detection limit of the atomic

absorption spectroscopic method; i.e., below 5×10^{-6} molar. This value is lower than the value of 6×10^{-5} molar which had been estimated by other investigators from conductance data (Ref. 46).

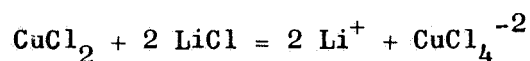
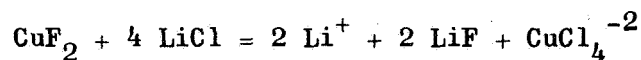
The solubility of LiF in a 1 M LiClO_4/PC solution was determined by means of a fluoride ion activity electrode (Orion Research, Incorporated). The potentials of such an electrode were measured across a calomel electrode in samples which had been diluted 10:1 with water. A sample of the saturated solution and blank 1 M LiClO_4/PC samples, with and without the addition of known amounts of LiF, were used. A value of 1.3×10^{-4} molar resulted for the solubility of LiF in 1 M LiClO_4/PC at 25 C. This is higher than was found for the pure solvent. According to solubility product consideration, the solubility of LiF should be lower in an electrolyte containing lithium ions than in the pure solvent. This does not necessarily have to be the case, however, because activity effects may be predominant.

It was attempted to determine the solubility of LiF in a 1 M LiCl/DMF solution at 25 C. A saturated solution was prepared and a sample diluted 10 to 1 with water. This sample was also analyzed by means of an Orion fluoride ion activity electrode. It was found that the potentials drifted with time in the presence of dimethyl formamide. Because of this, no reliable results could be obtained below a fluoride ion concentration of 10^{-5} molar, which therefore is the limit of detection for fluoride ion in this particular system. This corresponds to a LiF concentration of 10^{-4} molar for the original saturated solution. The solubility of LiF in 1 M LiCl/DMF was therefore $< 1 \times 10^{-4}$ molar. Hence, it was verified that the LiF solubility was also very low in this case, although it could not be decided whether it was considerably lower or even somewhat higher than in the pure solvents.

The low solubility of LiF is very significant because it indicates the formation of LiF at the cathode in Li-CuF_2 cells under discharge. This will lead to starvation of, e.g., LiClO_4 electrolytes at the cathode if sufficiently high currents are applied.

CuF₂ and CuCl₂ Systems. Slow changes were demonstrated in structural studies of the CuCl₂/DMF system. It is quite conceivable that such changes are accompanied by solubility changes.

The presence of more than one solute may complicate the situation. Studies of the solubility of CuF₂ and CuCl₂ in 0.7 M LiCl + 1 M AlCl₃/PC were made, with and without excess LiCl. The results of lithium, aluminum, and copper analyses are given in Table 24. They show that CuCl₂ as well as CuF₂ are soluble to a much greater extent in the presence of excess LiCl. On the other hand, the presence of the copper halides enhances the solubility for LiCl. Possible reactions are:



The fact that solubilities of the copper halides are smaller in the absence of excess LiCl indicates that chloride is more strongly complexed by aluminum than by copper, whereby the formation of the copper complex induces solubilization of the copper halide.

TABLE 24

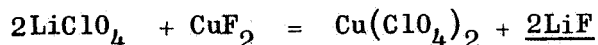
SOLUBILITY OF CuF₂ AND CuCl₂ IN LiCl #3 + AlCl₃ #4/PC #5-5

Solutes Added	Temperature, C	Lithium Content, molar	Aluminum Content, molar	Copper Content, molar
None		0.68	1.00	0
CuF ₂ #3	25	0.66	0.92	0.063
CuCl ₂ #2	25	0.75	1.00	0.0094
CuF ₂ #3 + LiCl #3	25	1.15	0.85	0.39
CuCl ₂ #3 + LiCl #3	25	1.73	0.99	0.54
CuF ₂ #3	60	0.62	0.80	0.11
CuCl ₂ #2	60	0.63	0.99	0.0063

The aluminum content of all solutions to which CuF_2 had been added was slightly decreased. A possible, but still very speculative explanation would be the formation of an insoluble aluminum or lithium-aluminum fluoride species. Another explanation can be based on the assumption that the presence of fluoride catalyzes in some way the formation of polymerization products which precipitate and contain aluminum.

When a 0.04 M CuF_2 #3 + 0.7 M LiCl #3 + 1 M AlCl_3 #4/PC #6-3 solution was made up for use in a Hittorf experiment, some interesting observations were made which relate to the above comments about uncertainties of solubility. The solvent was added to the solutes; a solution with a dark appearance formed, and a black copper-containing precipitate which was readily soluble in water could be filtered off, leaving an amber solution. On standing, more of a black precipitate formed, and the final concentration of the dissolved copper was considerably below the value given in Table 23. The reactions involved and the composition of the black, water-soluble copper species are not known.

The solubility of CuF_2 was largely determined by the anion of the lithium salt electrolyte. It should be noted that the term "solubility of CuF_2 " is used very loosely in this report; the fluoride from the CuF_2 precipitates as LiF if lithium ions are available because LiF has a very low solubility. In the case of LiClO_4 , e.g., copper perchlorate was actually present in solution, because of the reaction



The dissolution of CuF_2 was stoichiometric if copper compounds of sufficient solubility resulted.

Effect of H_2O . The addition of 1000-ppm water appeared to have only a significant effect in cases of compounds with low solubilities. The solubility of CuF_2 , e.g., was increased in 1 M LiClO_4 /PC from 4.7×10^{-3} to 2.2×10^{-2} molar at 25 C upon the addition of 1000-ppm H_2O . This water content corresponds to approximately 7×10^{-2} M H_2O . This result is in line with the results of a more detailed investigation (Ref. 47).

HEATS OF SOLUTION

Differential heats of solution in concentrated solutions were measured at 25 C in a precision calorimetry system procured from the LKB-Produkter AB Corporation (Stockholm, Sweden). This calorimetry system, Model 8700, is a general purpose instrument designed for reaction and solution calorimetry.

The calorimeter is one of the nonisothermal, constant-temperature environmental type. Figure 49 shows the 100-ml pyrex reaction vessel. A heater can be seen on the left side, and a thermistor temperature sensor on the right side. The combined sample-holder stirrer is located in the center. By downward movement of the stirrer toward the sapphire spike, breakage of the sealed ampoule (not shown in the photograph) containing the solute sample can be initiated without discontinuing the stirring. Because the calorimeter must not be exposed to elevated temperatures, it was carefully washed with water and acetone and flushed with dry nitrogen rather than cleaned according to the regular procedure for glassware. The calorimeter was filled in the dry box, and special precautions were taken not to expose the solute sample to the laboratory atmosphere while sealing the fragile sample container.

The calorimeter was placed in a 12-liter precision thermostat equipped with proportional control which maintained a constant temperature to within ± 0.001 C. An electronic console includes an electronic timer and a precision potentiometer for calibration, and a resistance bridge for temperature measurement. An electronic galvanometer is used as a null indicator for both the potentiometer and the resistance bridge. A precision power supply is incorporated into the system as a power source for the instrumentation.

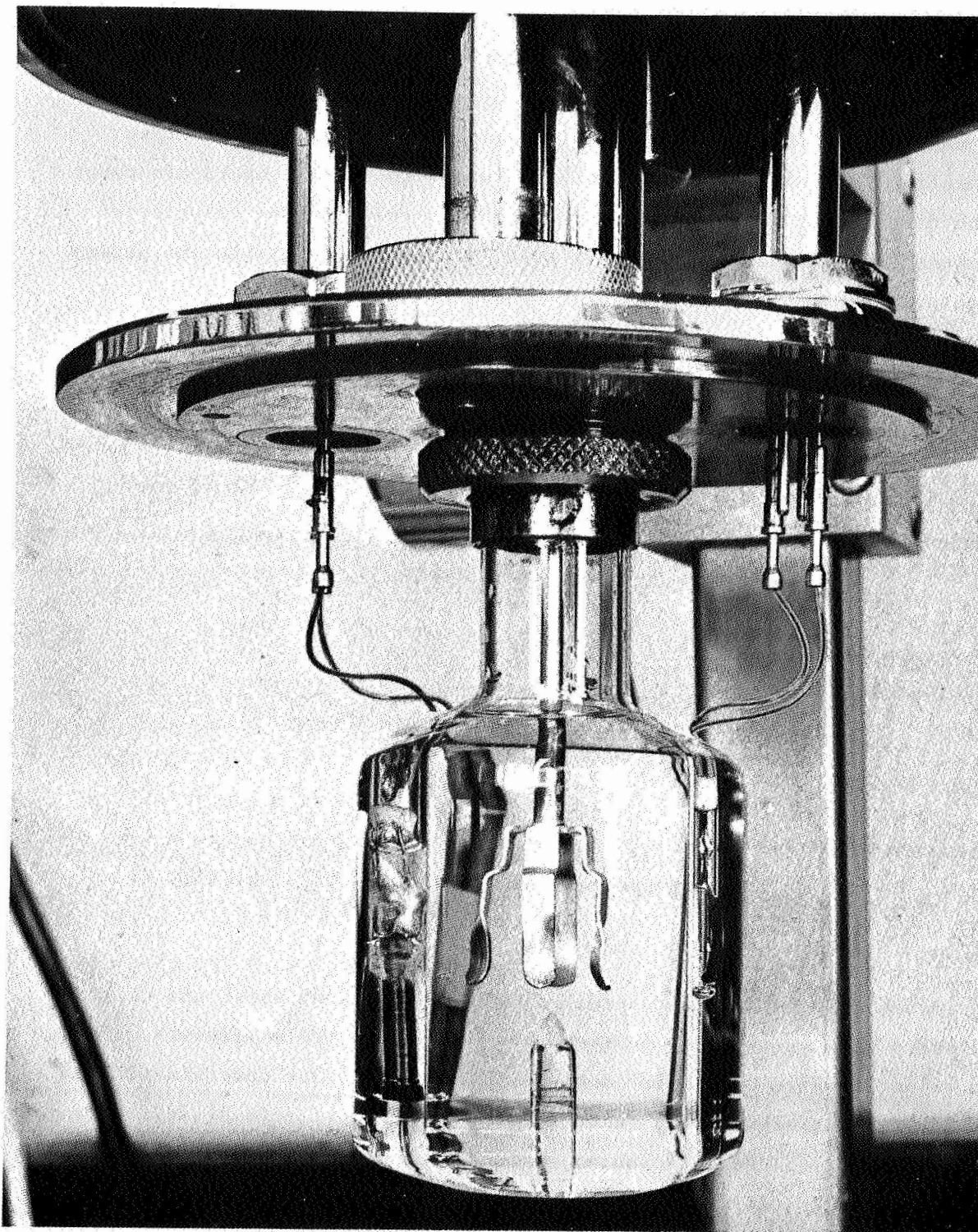


Figure 49. Heat of Solution Calorimeter

Precise energy measurements with the calorimeter are made possible by the accurate determination of the corrected temperature change and the heat capacity of the system (the calibration constant). The electric calibration heating was carried out over about the same temperature range as the dissolution experiment. For exothermic reactions the calorimeter was cooled by directing a stream of cold, dry nitrogen between the jacket and calorimeter.

Among the most useful methods for evaluating the corrected temperature change are the Dickinson and the Regnault-Pfaundler techniques (Ref. 48). The latter was used for the current tests. The expression taken proportional to ΔT was $(\Delta R/R_m)$. The calibration constant (\mathcal{E}) was obtained from the expression

$$\mathcal{E} = \frac{Q_{\text{calib.}}}{\left(\frac{\Delta R}{R_m}\right)_{\text{calib.}}}$$

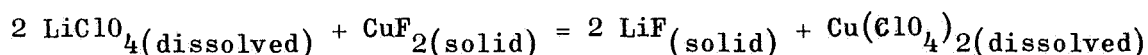
where $Q_{\text{calib.}}$ was an accurately defined quantity of heat in calories supplied electrically. ΔR is the change in thermistor resistance in ohms attributable to the calibration heat and R_m is the mean value of the resistance in ohms. Thermistor resistance could be read on the bridge to 0.01 ohm (~ 0.125 millidegrees C) and interpolated graphically to 0.001 ohm.

Calorimeter constants were determined with 100 grams of water and calibration heats of 2 calories at heating rates of 50 and 100 milliwatts. The mean value was 2718 ± 9 . Experiments with empty ampoules demonstrated no measurable "heat of breaking" effect, although heat effects of as little as 5 millicalories are detectable. Calibration measurements of the heat of solution of KCl in water yielded values well within 1 percent of the value selected by the National Bureau of Standards (Ref. 49).

The results obtained are listed in Table 25. In general, the results have an estimated precision of ± 0.1 kcal/mole. Most solutes dissolved within less than 30 minutes. Some dissolved more slowly, and in two cases complete dissolution was apparently not achieved (in these cases, the exothermic value represents a lower limit).

The dissolution of CuCl_2 in LiCl/DMF was endothermic, presumably because of the formation of the CuCl_4^{2-} complex. This complex formation still appears to take place after stoichiometric amounts of CuCl_2 had been added, possibly indicating the presence of significant amounts of free Cl^- ions (a delayed equivalent point was also found in a conductometric titration).

The dissolution of CuF_2 in 1 M $\text{LiClO}_4/\text{DMF}$ was only slightly exothermic. A solid was noticed upon dissolution of the CuF_2 , but an analysis indicated that at least 75 percent of the copper went into solution. In this dissolution process, LiF forms and precipitates, and the heat of solution listed in Table 25 is actually a heat of reaction according to:



It appears that at least two processes occur simultaneously which compensate each other: the dissolution of CuF_2 and the formation of solid LiF .

The dissolution of $\text{TMA} \cdot \text{PF}_6$ in all three solvents was found to be an endothermic reaction, in contrast to the dissolution of LiCl or LiClO_4 . There the heat evolved is mainly due to the solvation of the lithium ion. The difference in heat of solution between LiCl and LiClO_4 in DMF points to a strong tendency to ion pair formation in the case of LiCl .

A very negative value was found for the dissolution of AlCl_3 in a $\text{LiCl} + \text{AlCl}_3/\text{DMF}$ electrolyte. This indicates a very strong solute-solvent interaction as has been found in NMR studies. It was somewhat surprising that the solubility of AlCl_3 in this system is very limited, but it was shown that an aluminum solvate actually precipitated.

TABLE 25

HEATS OF SOLUTION AT 25 C

Solute Added	Electrolyte Solution	Concentration in Added Solute, molar		Heat of Solution ΔH_{solute} , kcal/mole
		Initial	Final	
LiClO ₄ #3	1 M LiClO ₄ #3/PC #4-3	1.000	1.008*	-7.4
LiClO ₄ #2	1 M LiClO ₄ #2/DMF #6-16	1.000	1.007	-18.3
LiClO ₄ #2	1 M LiClO ₄ #2/AN #4-4	1.000	1.007	-6.3
LiCl #2	1 M LiCl #3/DMF #6-13	1.000	1.015	-8.9
LiCl #3	0.5 M LiCl #3+1 M AlCl ₃ #4/PC #5-5	0.500	(0.520)**	(-2)
LiCl #2	0.7 M LiCl #3+1 M AlCl ₃ #3/AN #4-4	0.700	0.717	-3.2
AlCl ₃ #3	1 M LiCl #3+0.04 M AlCl ₃ #3/DMF #6-17	0.0408	0.0449	-48.8
TMA·PF ₆ #1	0.1 M TMA·PF ₆ #1/PC #4-5	0.100	0.107	+4.6
TMA·PF ₆ #1	0.16 M TMA·PF ₆ #1/DMF #6-17	0.160	0.174	+2.9
TMA·PF ₆ #1	0.07 M TMA·PF ₆ #1/AN #4-4	0.063	0.070	+4.5
CuF ₂ #3	1 M LiClO ₄ #3/DMF #7-1	0	(0.0089)**	-0.2
CuCl ₂ #2	1 M LiCl #3/DMF #6-17	0	0.010	-13.1
CuCl ₂ #2	0.5 M CuCl ₂ #2+1 M LiCl #3/DMF #7-1	0.499	0.508	-10.9

*Slow dissolution

**Very slow, or incomplete dissolution

VAPOR PRESSURES

Vapor pressures of solvents and solutions were measured at 25 C and 60 C. A gas-saturation method as described in Ref. 50 was used, and the apparatus is shown in Fig. 50. Dry nitrogen was bubbled through the saturator which was immersed to the level of the glass wool wad into a constant-temperature bath. The nitrogen was saturated with the solvent, and the solvent was collected in a liquid nitrogen trap. The connection between saturator and trap was maintained above the temperature of the constant-temperature bath, if necessary, by means of heating tapes. The gas flow was measured by a soap-bubble flowmeter. To minimize the error caused by evaporation of water in the flowmeter, a 2:1 mixture of glycol and glycerol containing approximately 7-1/2 percent of Ultrawet 60L was used. Typical nitrogen flowrates were 1 to 2 ml/sec.

To elucidate the experimental procedure, the measurement of the vapor pressure of a 1 M LiCl/DMF solution at 60 C is selected as an example. The gas flow was kept as constant as possible, at 1.4 ml/sec. It was monitored and the average product of inverse flowrate in sec/ml and room temperature (i.e., temperature of the soap-bubble flowmeter) in K was determined. This product was 21.63 sec ml⁻¹K, and 1.9781 gm of DMF was collected during a 250-minute period. The total gas flow was 23,100 ml of N₂ at 60 C plus 750 ml of DMF, corresponding to 2.706 x 10⁻² mole at 740 mm Hg. The partial pressure of DMF was:

$$P_{\text{DMF}} = 2.706 \times 10^{-2} \times \frac{0.082 \times 333.2}{23.85} \times 760 \text{ mm Hg} = 23.55 \text{ mm Hg}$$

At the low vapor pressure values of propylene carbonate at 25 C, relatively small amounts of solvent were collected; in these cases, the limits of this gas saturation method were approached. On the other hand, saturation will eventually become only partial at higher vapor pressures, and limits of the method were approached because of the relatively high vapor pressures of acetonitrile.

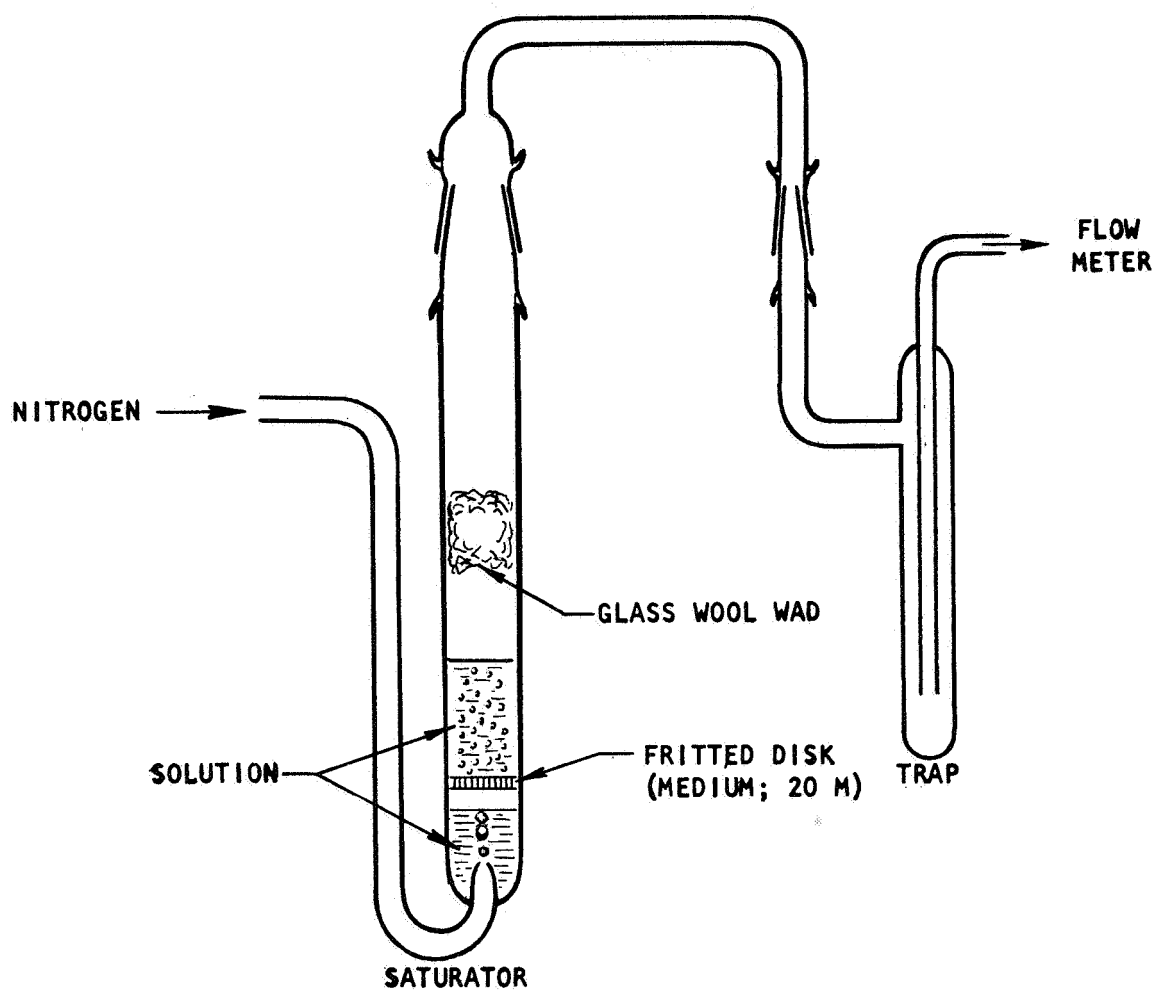


Figure 50. Apparatus for Measuring Vapor Pressures by Gas Saturation Method

For the above reason, a different method was used for measuring vapor pressures of methyl formate solutions. Samples were placed in a 25 C constant-temperature bath, and the vapor pressure was determined with a mercury manometer (a correction was made to take into account the different densities of mercury at room temperature and 0 C). The entire apparatus was kept at the bath temperature or above. Before taking the final value, the samples were frozen in liquid nitrogen and degassed on a vacuum line.

The results of the vapor pressure measurements are listed in Table 26. The vapor pressures of the four solvents increase in the order $PC < DMF < AN < MF$, the differences between two solvents being at least an order of magnitude. Because of its very low volatility, propylene carbonate would be the best solvent for practical usage if only vapor pressures were considered. Methyl formate can be used in most cases in sealed systems only.

Vapor pressures were generally about 20 percent lower in 1-molar propylene carbonate and dimethyl formamide solutions than in the respective pure solvents. The vapor pressure reduction by addition of solutes was relatively lower in acetonitrile and methyl formate, because of the lower molecular weight of these solvents; i.e., because of the lower solute to solvent mole ratio in solution of the same concentration (in moles per liter).

VISCOSITIES AND DENSITIES

Viscosities were determined by a conventional technique involving measurement of the efflux time of the solutions through a capillary. Depending on the viscosity of the solution, various commercial Ubbelohde viscometers were used; in the case of methyl formate a modified closed type was employed. The viscometers were calibrated with water and appropriate standard solutions from Cannon Instrument Company.

TABLE 26

VAPOR PRESSURES

Solvent	Solute(s)	Temperature, C	Vapor Pressure, mm Hg
PC #2-12, 4-3	None	25	0.069
PC #2-11		60	0.80
PC #4-3	1 M LiClO ₄ #3	25	0.052
PC #2-11	#2	60	0.66
PC #4-5	0.7 M LiCl #3 + 1 M AlCl ₃ #4	25	0.035
PC #4-5		60	0.42
PC #2-11	0.125 M TMA·PF ₆ #1	25	0.062
PC #2-11		60	0.52
DMF #5-2, 5-5, 6-18	None	25	3.88
DMF #5-2, 5-5		60	26.3
DMF #5-1	1 M LiClO ₄ #2	25	3.16
DMF #5-1		60	22.6
DMF #6-13	1 M LiCl #2	25	3.35
DMF #5-1		60	23.55
DMF #6-2	1 M LiCl #2 + 0.075 M AlCl ₃ #3	25	3.32
DMF #6-2		60	22.80
DMF #7-1	1 M LiClO ₄ #3 + 0.5 M CuF ₂ #3	25	3.27
DMF #7-1		60	23.60
DMF #6-13	1 M LiCl #2 + 0.5 M CuCl ₂ #2	25	3.31
DMF #6-13		60	23.4
DMF #6-13	0.20 M TMA·PF ₆ #1	25	3.50
DMF #6-13		60	25.5
AN #4-2	None	25	89.0
AN #4-2	1 M LiClO ₄ #2	25	79.4
AN #4-4	0.7 M LiCl #3 + 1 M AlCl ₃ #3	25	77.8
MF #2-1	None	25	590
MF #2-1	1 M LiClO ₄ #3	25	561
MF #2-1	1.1 M LiAsF ₆ #1	25	550

Densities were measured either with pycnometers or with a chainomatic density balance. The latter method has an accuracy to about three decimal places, the former method is even more accurate. The results for viscosities and densities are given in Table 27.

The solvent viscosity decreased in the order $PC > DMF > AN \approx MF$. In general, 1-molar solutions had a 2 to 3 times greater viscosity than the respective solvents. Extremely high viscosities were found for saturated $LiClO_4/PC$ (2.1 molar) and $LiClO_4/DMF$ (4.4 molar). The high viscosity is reflected in the lower specific conductance of these saturated solutions as compared to 1-molar solutions.

SONIC VELOCITIES

The apparatus illustrated in Fig. 51a was used to measure the velocity of sound in various solutions. The electronic equipment consisted of a Sperry-type UR Reflectoscope, a Tektronix model 535A oscilloscope, and a 10 MHz pulse-modulated radio-frequency signal which was fed simultaneously to the transducer and the oscilloscope. The sound waves, emanating from the transducer, traveled through a known distance of liquid to the bottom of the cell at which point they were reflected back to the transducer. The initial and reflected waves were displayed on the oscilloscope where they produced a trace as shown in Fig. 51b (a first reflection was caused by the introduction of the cover protecting the transducer). The time, τ , required for the ultrasonic waves to traverse the known distance of the test fluid was measured and the velocity calculated. The adiabatic compressibility, $\beta = dV/VdP$, was obtained from this velocity and the solution density.

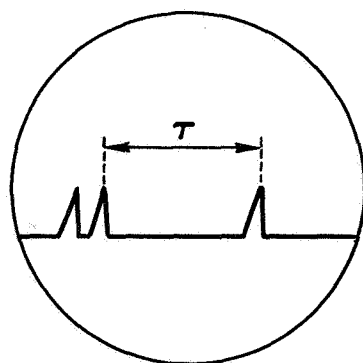
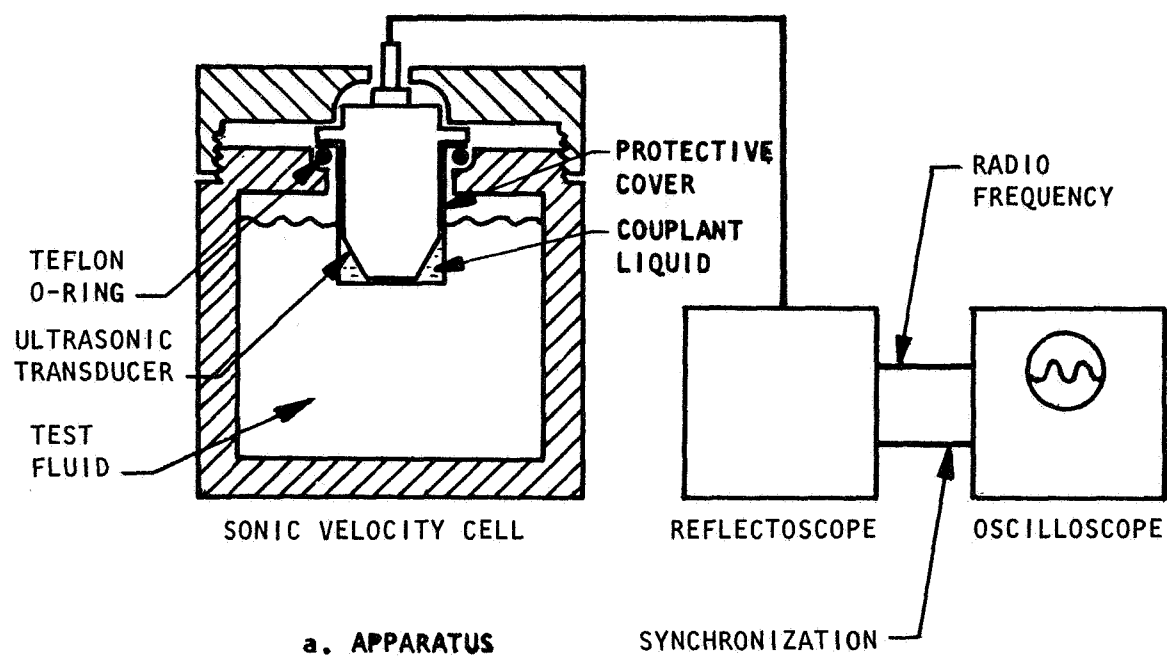
The cell was filled in the dry box and a seal provided by a Teflon O-ring. Because the transducer material was attacked by some of the solutions, the transducer was not immersed directly into the solution as conventionally done. A stainless-steel cup was constructed to be placed over the transducer face, and glycerin was used as a couplant.

TABLE 27

VISCOSITIES AND DENSITIES

Solvent	Solute	Temperature, C	Density, gm/cm ³	Viscosity, millipoises
PC #2-6		25	1.203	24.8
PC #2-7		60	1.161	13.3
PC #2-6	1 M LiClO ₄ #2	25	1.254	70.8
PC #4-5	Sat.* LiClO ₄ #3	25	1.380	3868
PC #2-6	Sat.* M LiCl #2 + 1.03 M AlCl ₃ #3	25	1.257	71.6
PC #2-6	1.03 M AlCl ₃ #3	25	1.257	57.2
PC #2-4	Sat.* TMA·PF ₆ #1	25	1.209	26.6
DMF #4-1		25	0.944	7.93
DMF #5-1		60	0.910	5.35
DMF #3-5	1 M LiClO ₄ #2	25	1.019	18.9
DMF #6-15	Sat.* LiClO ₄ #3	25	1.291	5770
DMF #4-1	1.02 M LiCl #2	25	0.984	18.15
DMF #6-15	Sat.* LiCl #3	25	1.023	54.7
DMF #3-2	1 M LiCl #2 + Sat.* AlCl ₃ #3	25	0.984	22.8
DMF #4-2	Sat.* TMA·PF ₆ #1	25	0.964	8.99
AN #1-2		25	0.777	3.36
AN #3-1		60	0.737	2.63
AN #3-2	1 M LiClO ₄ #2	25	0.863	6.60
AN #4-3	Sat.* LiClO ₄ #3	25	0.868	7.09
AN #3-1	Sat.* LiCl #2 + 1 M AlCl ₃ #3	25	0.879	
AN #1-2	Sat.* TMA·PF ₆ #1	25	0.787	3.57
MF #2-5		25	0.968	3.38
MF #2-4	1.1 M LiAsF ₆ #1	25	1.137	8.06

*Saturated



b. SIGNAL

Figure 51. Determination of Sonic Velocities

The distance between the metal cup wall and the bottom of the cell was determined by calibration using distilled water as a standard (Ref. 51). All measurements were made at 25 ± 0.02 C, with the cell being placed in a constant temperature oil bath. The estimated accuracy of the values determined is 0.2 percent.

The results at 10 MHz are given in Table 28 for 25 C. Two measured values were obtained for PC, namely 1.440×10^5 and 1.446×10^5 cm/sec, and the average value was entered in Table 28. The average value for 1 M LiClO_4 /PC was derived from two measured values also, 1.481×10^5 and 1.493×10^5 cm/sec.

A method to determine primary solvation numbers from compressibility data is mentioned in Ref. 52. Passynsky (Ref. 53) estimated solvation numbers based on the assumption that the molecules in the primary solvation sheath had zero compressibility. These molecules very near to the ions were responsible for the lower compressibility of the solutions, as compared to the compressibility of the pure solvent, and a direct proportionality was assumed between adiabatic compressibility and concentration of "compressible molecules." The total concentrations of solvent molecules in the solution, C , in mole/cm³, is

$$C = \frac{\rho - C_d M_d}{M_o}$$

whereby ρ (gm/cm³) is the solution density, C_d the concentration of the solute, M_d (gm/mole) the formula weight of the solute, and M_o the molecular weight of the solvent.

The concentration of unsolvated solvent molecules in the solution, C_u , is

$$C_u = \frac{\beta}{\beta_o} \cdot C_o = \frac{\beta}{\beta_o} \cdot \frac{\rho_o}{M_o}$$

with β being the measured compressibility of the solution, β_o the one of the pure solvent, ρ_o the density of the pure solvent, and C_o the solvent concentration in the pure solvent.

TABLE 28

SONIC VELOCITIES AT 25 C

Solvent	Solute	Sonic Velocity, cm sec ⁻¹
PC #2-11 PC #4-5		1.443×10^5
PC #2-11 PC #4-3	1 M LiClO ₄ #2 1 M LiClO ₄ #3	1.487×10^5
PC #4-5	0.7 M LiCl #3 + 1 M AlCl ₃ #4	1.435×10^5
PC #2-11	0.02 M TMA·F #2	1.443×10^5
PC #2-11	0.125 M TMA·PF ₆ #1	1.438×10^5
PC #6-2	1 M TEA·F #1	1.505×10^5
DMF #7-1		1.451×10^5
DMF #6-18	1 M LiClO ₄ #3	1.537×10^5
DMF #7-1	1 M LiClO ₄ #3 + 0.5 M CuF ₂ #3	1.490×10^5
DMF #6-17	1 M LiCl #3	1.539×10^5
DMF #7-2	1 M LiCl #3 + 0.075 M AlCl ₃ #4	1.571×10^5
DMF #7-1	1 M LiCl #3 + 0.5 M CuCl ₂ #2	1.464×10^5
DMF #7-1	0.20 M TMA·PF ₆ #1	1.471×10^5
AN #4-7		1.275×10^5
AN #4-4	1 M LiClO ₄ #2	1.339×10^5
AN #4-4	0.7 M LiCl #3 + 1 M AlCl ₃ #3	1.297×10^5
MF #2-6		1.148×10^5
MF #2-5	1.1 M LiAsF ₆ #1	1.142×10^5

The concentration of solvated solvent molecules, C_* , is

$$C_* = C - C_u = \frac{(\rho - C_d M_d)}{M_o} - \frac{\beta}{\beta_o} \frac{\rho_o}{M_o}$$

The solvation number, Z , is therefore

$$Z = \frac{C_*}{C_d} = \left(\rho - C_d M_d - \frac{\beta}{\beta_o} \rho_o \right) \frac{1}{C_d M_o}$$

This formula is essentially identical to the one given in a recent paper by Kaurova and Roshchina (Ref. 54) which was taken from a monograph (Ref. 55).

The correlation between compressibility, β , and sonic velocity, v , is

$$v = 1/\sqrt{\beta \cdot \rho}$$

The solvation numbers of Table 29 have been calculated from sonic velocity data. It appears that these solvation numbers cannot be accepted with confidence because they are not in the right order of magnitude and are inconsistent within themselves. It appears that higher numbers were obtained with solvents of lower molecular weights; it may be that the method is applicable only to solvents with low molecular weights, such as water or methanol.

CONDUCTANCE MEASUREMENTS

Measurement Technique

Specific conductances, λ , of solutions were determined at 1000 Hz a-c using an E.S.I. impedance bridge and capacitance compensation. Freas cells with platinized platinum electrodes were filled with exactly 10 milliliters of solution. Cell constants were determined accurately with standard aqueous KCl solutions and were approximately 0.4 cm^{-1} . Measurements were made in constant-temperature oil baths at $25 \pm 0.02 \text{ C}$ and at $60 \pm 0.1 \text{ C}$.

TABLE 29

SOLVATION NUMBERS CALCULATED FROM SONIC VELOCITY DATA

Solution	Sonic Velocity, cm/sec	Density, gm/cm ³	Compressi- bility, gm ⁻¹ cm sec ²	Solvation Number
PC	1.443×10^5	1.203	3.992×10^{-9}	
1 M LiClO ₄ /PC	1.487×10^5	1.254	3.606×10^{-9}	0.61
0.7 M LiCl + 1 M AlCl ₃ /PC	1.435×10^5	1.257	3.863×10^{-9}	-0.70
0.125 M TMA·PF ₆ /PC	1.438×10^5	1.209	4.000×10^{-9}	-1.9
DMF	1.451×10^5	0.944	5.031×10^{-9}	
1 M LiClO ₄ /DMF	1.537×10^5	1.019	4.154×10^{-9}	1.82
1 M LiCl/DMF	1.539×10^5	1.023	4.127×10^{-9}	2.84
1 M LiCl + 0.075 M AlCl ₃ /DMF	1.571×10^5	0.984	4.118×10^{-9}	2.08
0.20 M TMA·PF ₆ /DMF	1.471×10^5	0.964	4.794×10^{-9}	1.37
AN	1.275×10^5	0.777	7.917×10^{-9}	
1 M LiClO ₄ /AN	1.339×10^5	0.863	6.463×10^{-9}	3.00
0.7 M LiCl + 1 M AlCl ₃ /AN	1.297×10^5	0.879	6.763×10^{-9}	1.28
MF	1.148×10^5	0.968	7.839×10^{-9}	
1.1 M LiAsF ₆ /MF	1.142×10^5	1.137	6.744×10^{-9}	1.24

To determine the conductivity of pure solvents and of very dilute solutions, the cell was washed several times with the solvent. It was found that leaving the cell overnight filled with the solvent was more effective for this purpose than repeated washings for short intervals.

Specific Conductances of Pure Solvents

Conductivities of pure solvents were not investigated extensively nor used as a criterion for the purity of distilled solvent batches. The specific conductances of some solvent batches are given in Table 30. The values are representative only and were selected more or less at random. The specific conductance appears to change with aging of the solvent. Slow drifts of conductivities were observed with dimethyl formamide, probably because of a decomposition process catalyzed by the platinized platinum of the conductivity cell.

Specific Conductances of 1-Molar and Saturated Solutions

The specific conductances of 1-molar and saturated solutions are listed in Table 31.

Equivalent Conductances at Infinite Dilution

Specific conductances of dilute solutions were measured, and the equivalent (molar) conductances, Λ , calculated. These values were extrapolated to concentration zero to obtain the equivalent conductance at infinite dilution, Λ_0 . A simple procedure was selected, namely a graphical extrapolation of the equivalent conductance (corrected for the solvent contribution to the solution conductance) plotted versus the square root of the concentration.

TABLE 30

SPECIFIC CONDUCTANCES OF PURE SOLVENTS

Solvent	Specific Conductance at 25 C, ohm ⁻¹ cm ⁻¹	Specific Conductance at 60 C, ohm ⁻¹ cm ⁻¹
PC #2-3	1.78×10^{-7}	3.19×10^{-7}
PC #2-6	1.24×10^{-7}	2.36×10^{-7}
PC #2-10	8.56×10^{-7}	1.46×10^{-6}
PC #6-3	5.88×10^{-7}	9.97×10^{-7}
DMF #1-2	1.38×10^{-6}	1.88×10^{-6}
DMF #3-4	3.30×10^{-7}	4.49×10^{-7}
DMF #5-2	6.87×10^{-7}	9.75×10^{-7}
AN #1-2	1.65×10^{-6}	1.84×10^{-6}
AN #3-1	4.69×10^{-7}	6.34×10^{-7}
AN #4-1	7.75×10^{-7}	1.00×10^{-6}
AN #5-1	1.63×10^{-7}	5.52×10^{-7}
MF #2-6	1.07×10^{-7}	

TABLE 31

SPECIFIC CONDUCTANCE OF 1-MOLAR AND SATURATED SOLUTIONS

Solvent	Solute	Temperature, C	Specific Conductance, $\text{ohm}^{-1} \text{cm}^{-1}$
PC #4-5	1 M LiClO_4 #3	25	5.11×10^{-3}
PC #2-6	1 M LiClO_4 #2	25	5.36×10^{-3}
		60	1.06×10^{-2}
PC #4-5	1 M LiClO_4 #3 + 1000 ppm H_2O	25	5.22×10^{-3}
		60	9.87×10^{-3}
PC #2-2	Saturated LiCl #2	25	1.91×10^{-4}
	0.027 M LiCl #2	25	1.46×10^{-4}
	0.027 M LiCl #2	60	2.72×10^{-4}
PC #2-5	Saturated LiCl #2 + 1 M AlCl_3 #3	25	6.58×10^{-3}
	Saturated* LiCl #2 + 1 M AlCl_3 #3	60	1.29×10^{-2}
PC #5-5	1 M LiF #2 + 1 M PF_5 #1	25	6.2×10^{-3}
		60	1.2×10^{-2}
PC #2-3	1 M AlCl_3 #3	25	6.96×10^{-3}
		50	1.31×10^{-2}
PC #2-5	Saturated $\text{TMA} \cdot \text{PF}_6$ #1	25	2.71×10^{-3}
		60	6.75×10^{-3}
PC #6-2	1 M $\text{TEA} \cdot \text{F}$ #1	25	6.15×10^{-3}
		60	1.21×10^{-2}
DMF #3-5	1 M LiClO_4 #2	25	2.03×10^{-2}
		60	3.09×10^{-2}
DMF #4-1	1 M LiCl #2	25	8.50×10^{-3}
		60	1.12×10^{-2}
DMF #3-2	1 M LiCl #2 + Saturated* AlCl_3 #3	25	7.77×10^{-3}
		60	1.19×10^{-2}

*Saturated at 25 C

TABLE 31
(Concluded)

Solvent	Solute	Temperature, C	Specific Conductance, ohm ⁻¹ cm ⁻¹
DMF #6-12	Saturated LiF #2	25	1.27 x 10 ⁻⁶
		60	2.25 x 10 ⁻⁶
DMF #6-17	0.88 M LiF #2 + 0.88 M BF ₃ #1	25	2.07 x 10 ⁻²
		60	2.96 x 10 ⁻²
DMF #1-2	Saturated TMA·PF ₆ #1	25	1.11 x 10 ⁻²
		60	1.93 x 10 ⁻²
DMF #1-2	Saturated CuCl ₂ #2	25	5.95 x 10 ⁻³
		60	9.06 x 10 ⁻³
AN #3-2	1 M LiClO ₄ #2	25	3.18 x 10 ⁻²
		60	3.91 x 10 ⁻²
AN #3-1	Saturated* LiCl #2 + 1 M AlCl ₃ #3	25	5.09 x 10 ⁻²
		60	6.75 x 10 ⁻²
AN #5-1	Saturated LiF #2	25	2.17 x 10 ⁻⁶
		60	3.30 x 10 ⁻⁶
AN #1-2	Saturated TMA·PF ₆ #1	25	1.14 x 10 ⁻²
		60	2.26 x 10 ⁻²
MF #2-5	2.27 M LiAsF ₆ #1	25	4.65 x 10 ⁻²
MF #2-5	1.13 M LiAsF ₆ #1	25	3.37 x 10 ⁻²
MF #2-6	1 M LiClO ₄ #3	25	1.28 x 10 ⁻²

*Saturated at 25 C

The data collected with LiClO_4 #2/PC #2-6 is given in Table 32 and graphically represented in Fig. 52 and 53. The data of Fig. 52 is replotted on an expanded scale in Fig. 53 to permit an accurate extrapolation. Data on LiCl #2/PC #2-2 and $\text{TMA}\cdot\text{PF}_6$ /PC #2-5 are represented in Fig. 54 through 57. The extrapolation in the above cases did not present any problems.

A reasonable extrapolation is impossible, however, in the case of AlCl_3 /PC, shown in Fig. 58. For this system, two sets of measurements were taken, AlCl_3 #3/PC #2-3 and AlCl_3 #3/PC #2-5. In the first set, the dilution series was initiated with a 1-molar solution which was brownishly discolored; in the second set, the dilution was initiated with a 0.1-molar solution which was only slightly tinted. A maximum and a minimum of the equivalent conductance was observed for AlCl_3 /PC with decreasing solute concentration, although in one case the minimum was only fragmentally indicated as a slight change in the slope of the curve. Such a behavior has been reported also by other investigators (Ref. 46). An unambiguous interpretation has not been found; the occurrence of the minimum at low concentrations may be connected with the water content of the solvent, which was approximately 20 ppm (corresponding to a concentration of 0.001 molar). A study of this effect as a function of the water content could result in clarification, but such a study was beyond the scope of the present work.

A comparison of three electrolytes LiCl #2/PC #2-2, AlCl_3 #3/PC #2-3, and LiCl #2 + AlCl_3 #3/PC #2-5 is illustrated in Fig. 59. A starting solution of saturated LiCl (0.8M) in 1 M AlCl_3 was used, and the concentrations indicated are in respect to AlCl_3 . There appears to be an additive effect in the molar conductances when LiCl was added to AlCl_3 /PC. At low concentrations, the high conductance of LiCl /PC predominated; at higher concentrations, the conductance curves of AlCl_3 /PC and of the mixed electrolyte approached each other because the contribution of LiCl became small. The formation of new species as indicated by the increase

TABLE 32

SPECIFIC CONDUCTANCE (λ) AND EQUIVALENT CONDUCTANCE (Λ)
OF LiClO_4 #2/PC #2-6 AT 25 AND 60 C

Concentration (C), molar	\sqrt{C} , molar ^{1/2}	λ (25 C), ohm ⁻¹ cm ⁻¹	Λ^* (25 C), ohm ⁻¹ equ cm ²	λ (60 C), ohm ⁻¹ cm ⁻¹	Λ^* (60 C), ohm ⁻¹ equ cm ²
0.9996	0.9999	5.363×10^{-3}	5.64	1.055×10^{-2}	10.55
0.09996	0.3161	1.697×10^{-3}	16.98	2.872×10^{-3}	28.73
0.009996	0.09999	2.178×10^{-4}	21.78	3.686×10^{-4}	36.85
0.004998	0.07067	1.123×10^{-4}	22.45	1.903×10^{-4}	38.04
0.002499	0.04999	5.796×10^{-5}	23.15	9.825×10^{-5}	39.22
0.001250	0.03535	2.974×10^{-5}	23.70	5.058×10^{-5}	40.27
0.0006250	0.02500	1.522×10^{-5}	24.16	2.587×10^{-5}	41.01
0.0003125	0.01768	7.842×10^{-6}	24.70	1.326×10^{-5}	41.66
0.0001562	0.01250	3.924×10^{-6}	24.33	6.705×10^{-6}	41.41
0		1.241×10^{-7}		2.359×10^{-7}	
			Extrapolated: $\Lambda_0 = 25.6$	Extrapolated: $\Lambda_0 = 43.1$	

* Equivalent conductance, corrected for conductance of pure solvent

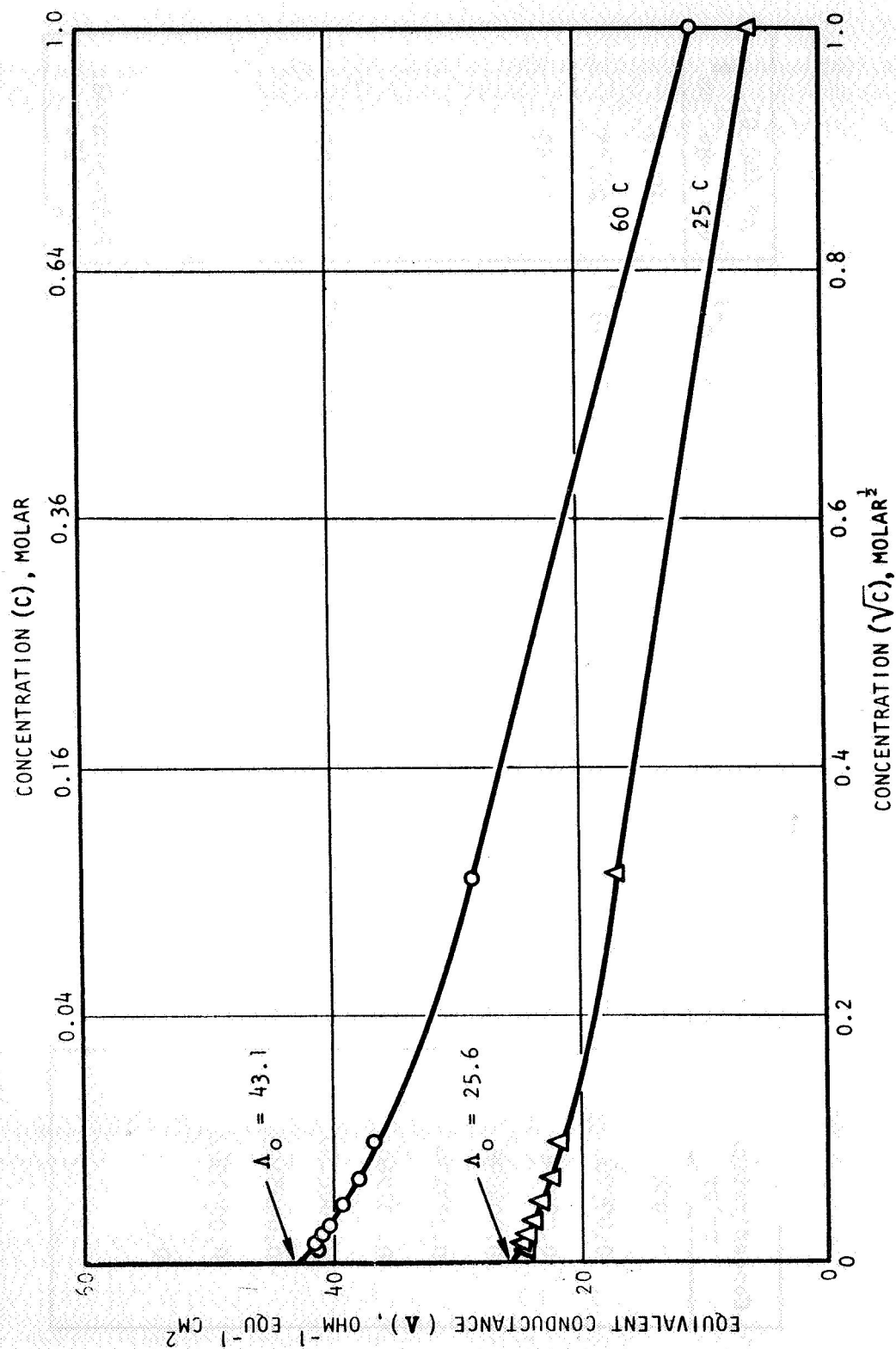


Figure 52. Equivalent Conductance of LiClO_4 in Propylene Carbonate at 25 and 60 C

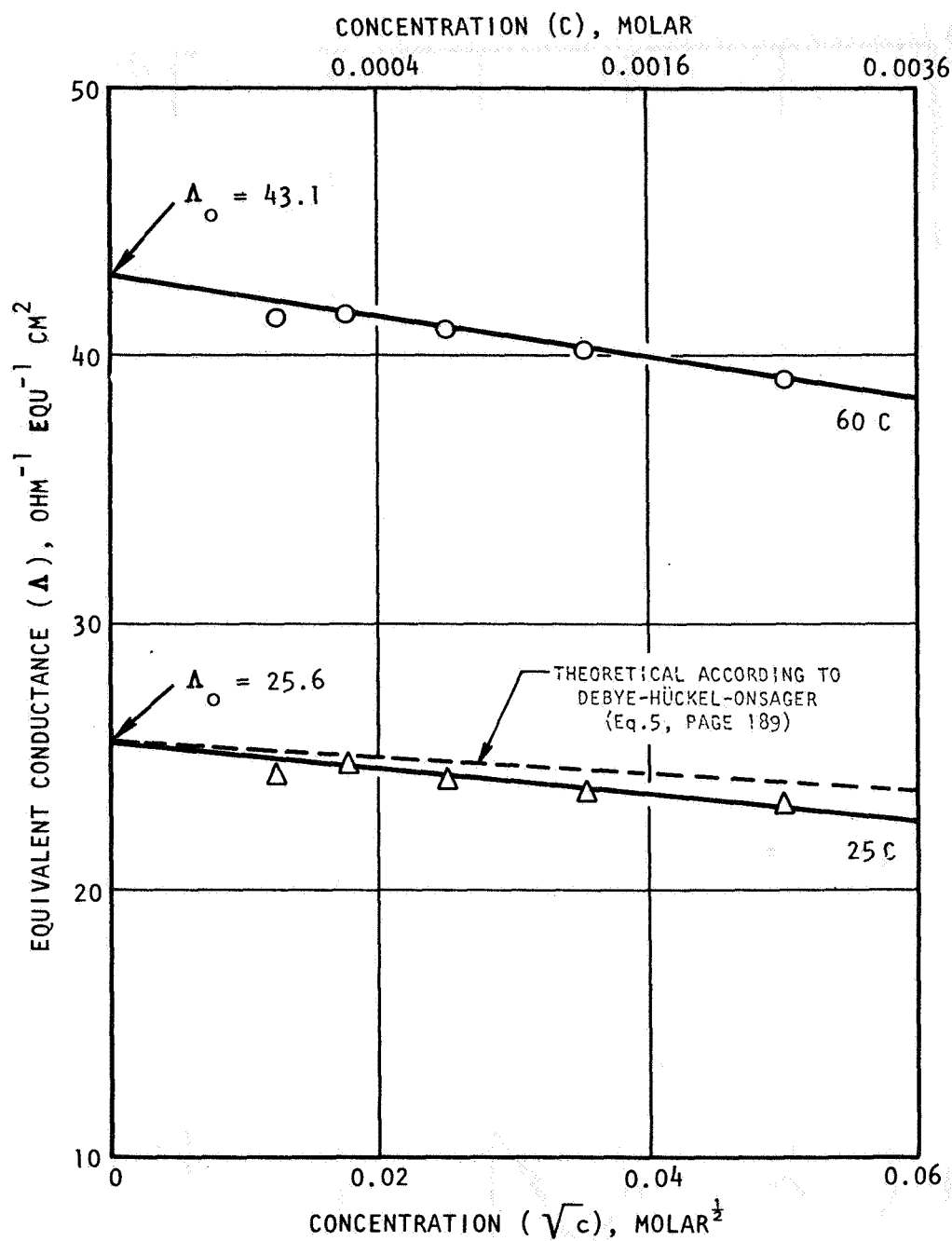


Figure 53. Equivalent Conductance of LiClO_4 in Propylene Carbonate at 25 and 60 C.

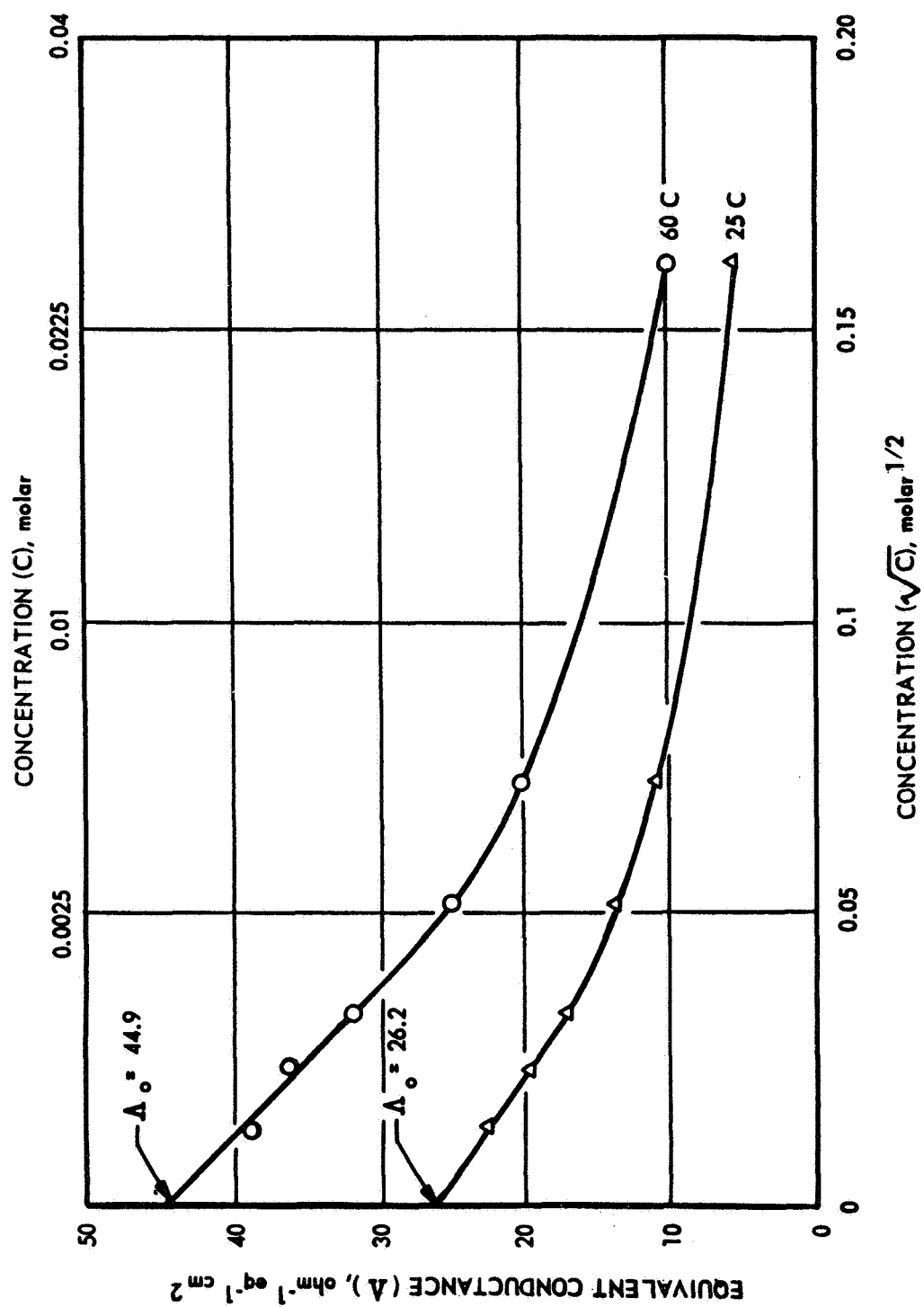


Figure 54. Equivalent Conductance of LiCl in Propylene Carbonate at 25 and 60 C

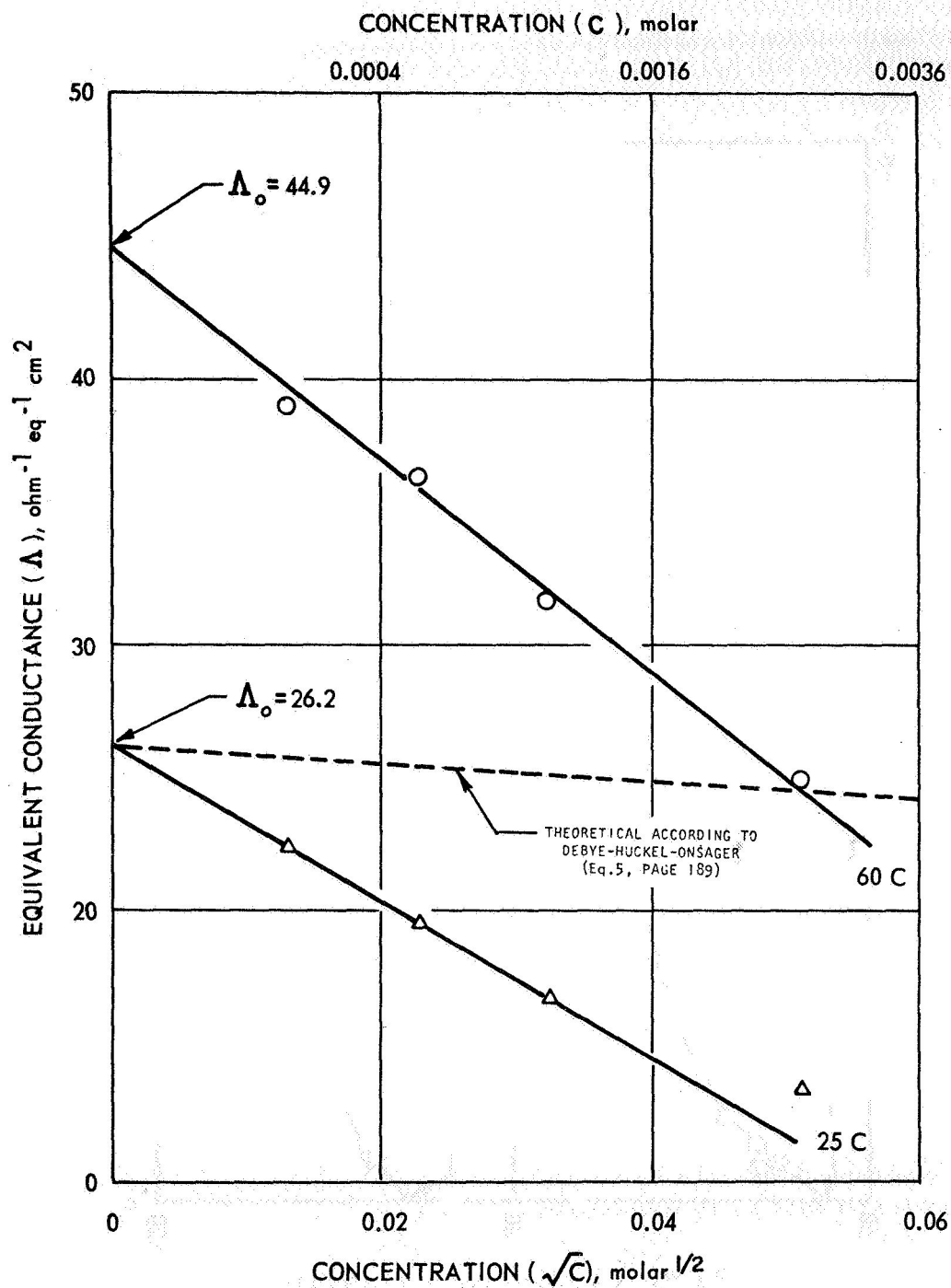


Figure 55. Equivalent Conductance of LiCl in Propylene Carbonate at 25 and 60 C

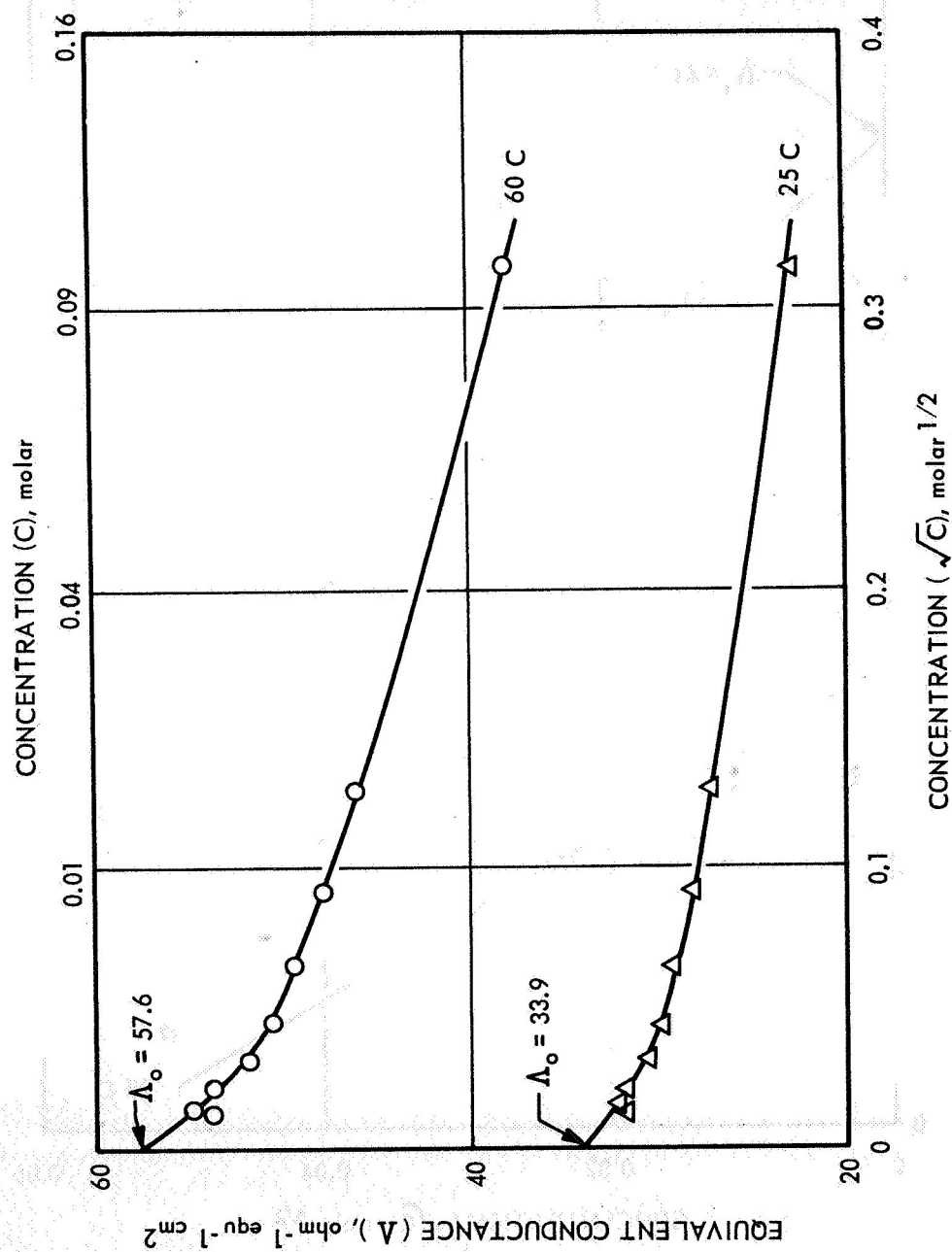


Figure 56. Equivalent Conductance of $\text{TMA} \cdot \text{PF}_6$ in PC at 25 and 60 C

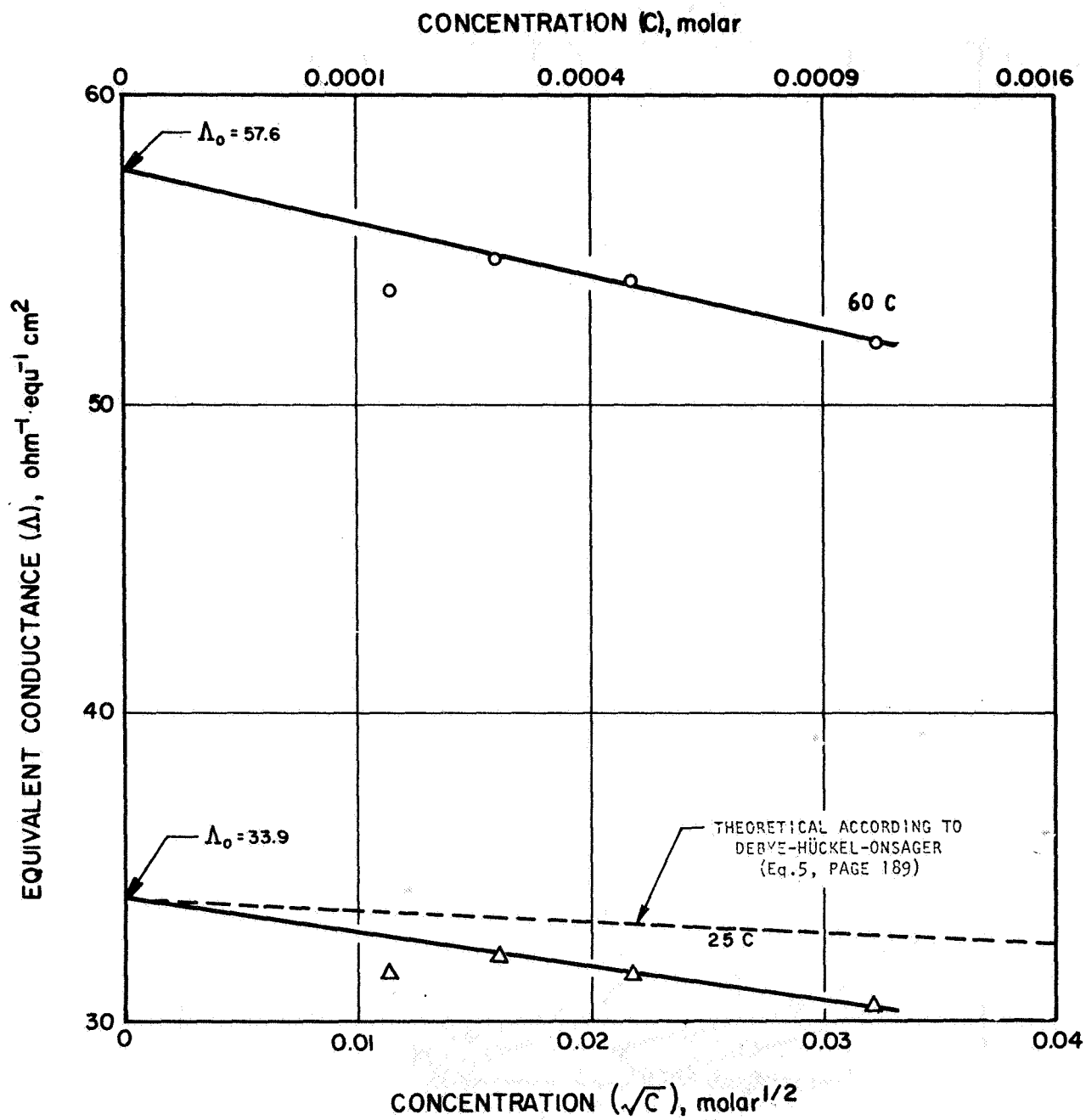


Figure 57. Equivalent Conductance of $\text{TMA} \cdot \text{PF}_6$ in PC at 25 and 60 C

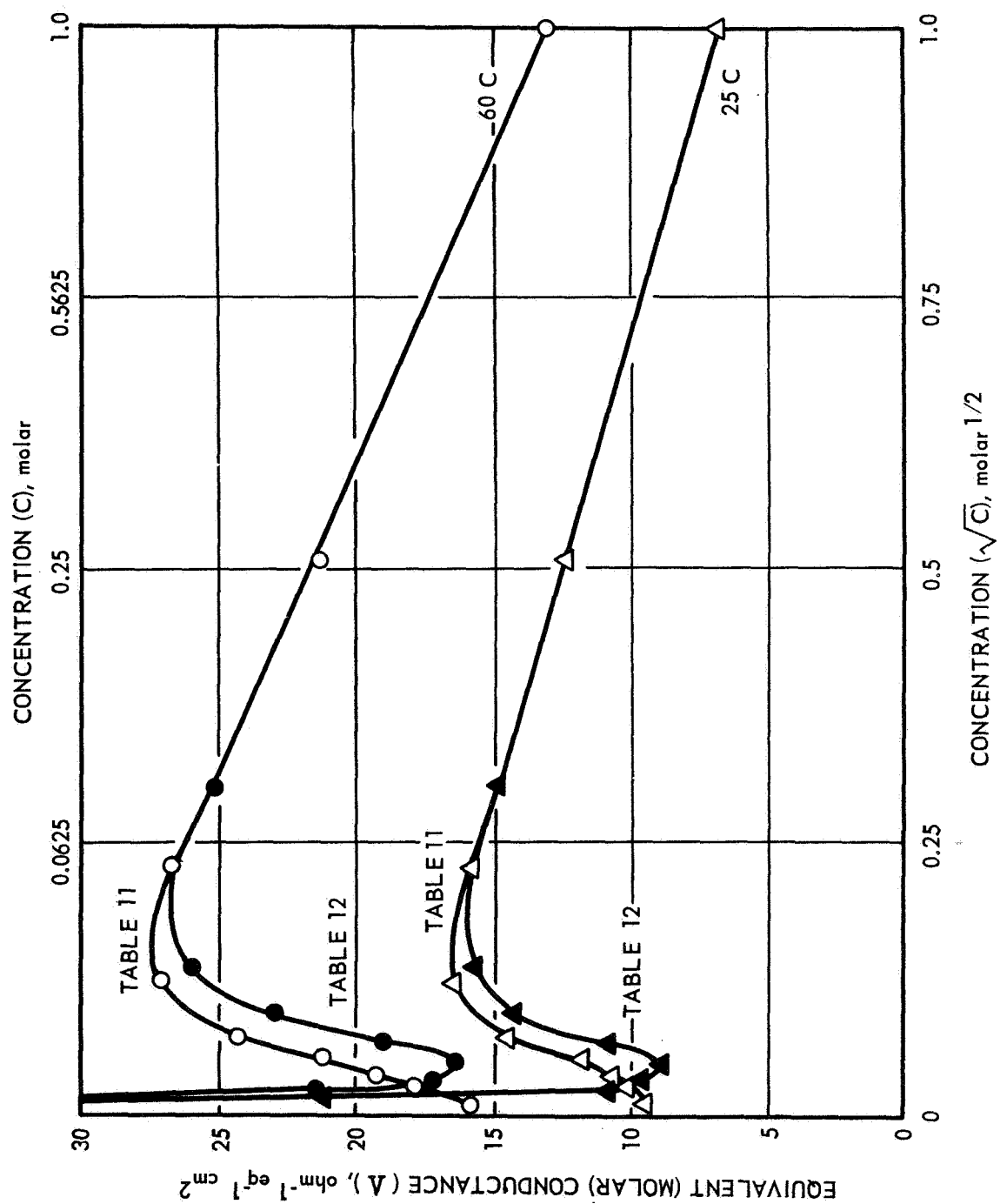


Figure 58. Equivalent (Molar) Conductance of AlCl_3 in Propylene Carbonate at 25 and 60°C

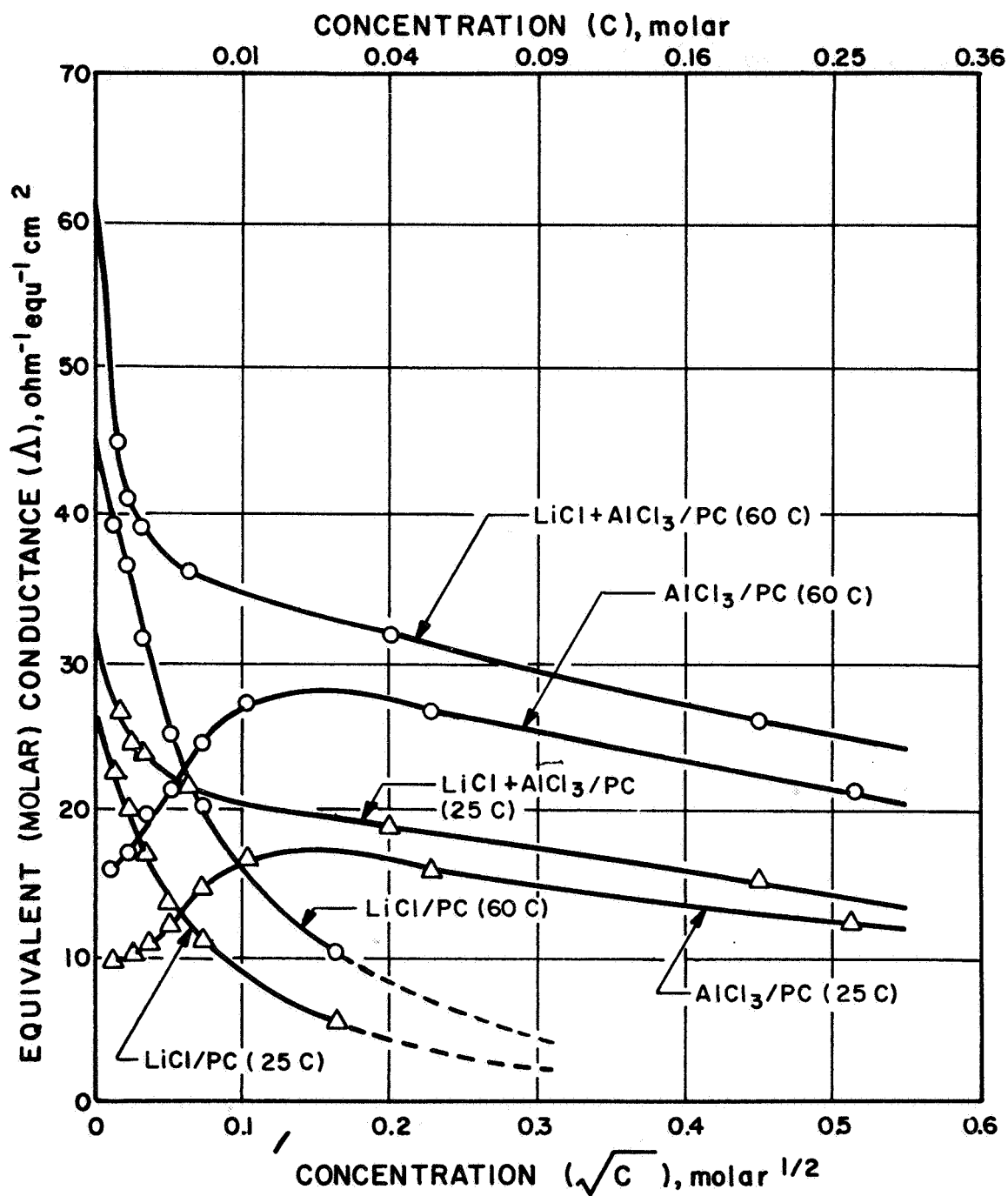


Figure 59. Comparison of Equivalent (Molar) Conductances of Electrolytes Containing LiCl and/or AlCl₃ in PC at 25 and 60 C.

of the solubility of LiCl and demonstrated by NMR studies does not seem to be reflected in these conductance results. The interpretation of these results is, however, complicated because changes in ionic strength of the solution by formation of new species may have a similar effect on conductance as an increase in conductive species.

Conductance data obtained in DMF solutions are represented in Fig. 60 through 65. The extrapolation of the equivalent conductance is straightforward in the cases of LiClO_4 #2/DMF #5-2, LiCl #2/DMF #4-1 and $\text{TMA} \cdot \text{PF}_6$ #1/DMF #1-2 (Fig. 60, 62, and 64). For AlCl_3 #3/DMF #3-2 and LiCl #2 + AlCl_3 #3/DMF #3-2 (Fig. 65), the extrapolation is somewhat uncertain because a straight line was not obtained; it yielded values of $\Lambda_0 = 220 \text{ ohm}^{-1} \text{ equ}^{-1} \text{ cm}^2$ at 25 C and $\Lambda_0 = 280 \text{ ohm}^{-1} \text{ equ}^{-1} \text{ cm}^2$ and 60 C for AlCl_3 /DMF, and $\Lambda_0 = 260 \text{ ohm}^{-1} \text{ equ}^{-1} \text{ cm}^2$ at 25 C and $\Lambda_0 = 325 \text{ ohm}^{-1} \text{ equ}^{-1} \text{ cm}^2$ at 60 C for an equimolar LiCl + AlCl_3 /DMF mixed electrolyte solution. An additive effect in regard to solution conductance is indicated by these results but cannot be considered entirely certain.

Results on acetonitrile solutions are given in Fig. 66 through 70. In the case of the LiCl #2 + AlCl_3 #3/AN #3-1 solution, the starting solution was a 1 M AlCl_3 solution saturated with LiCl, and the concentration of LiCl in all diluted solutions was therefore 0.92 times the concentration of AlCl_3 . The Λ_0 - value at 25 C resulting from the extrapolation was $148 \text{ ohm}^{-1} \text{ equ}^{-1} \text{ cm}^2$ which compares to $172 \text{ ohm}^{-1} \text{ equ}^{-1} \text{ cm}^2$ for LiClO_4 #2/AN #3-2. This indicates that only 2 ions were formed from LiCl + AlCl_3 , and that $\text{Li}^+ + \text{AlCl}_4^-$ were the main species existing in a LiCl + AlCl_3 /AN electrolyte even at low concentrations approaching infinite dilution. The results for $\text{TMA} \cdot \text{PF}_6$ #1/AN #1-2 appears too high. Because a good extrapolation was obtained, an error appears likely to have occurred in preparing the initial solution used for the dilution series.

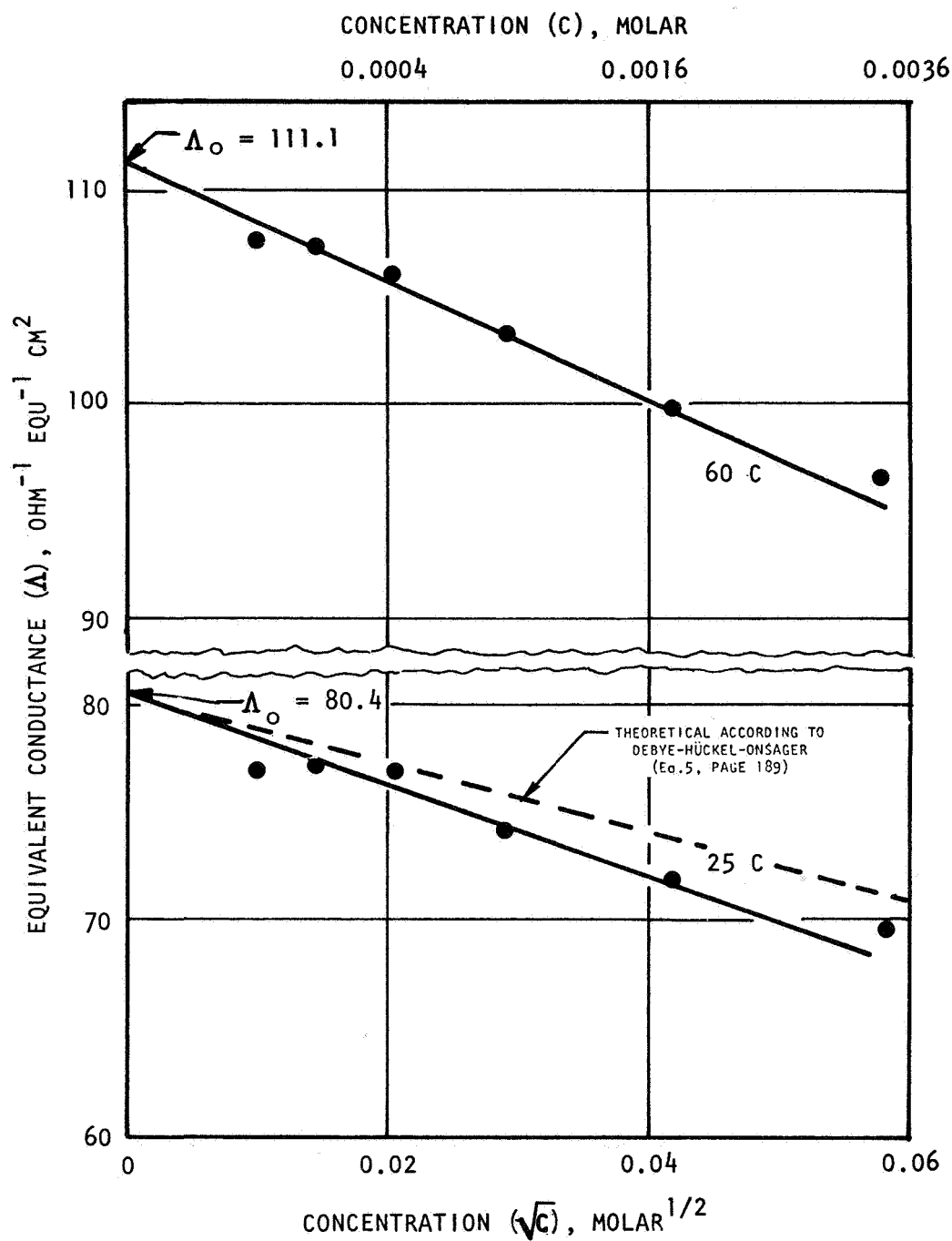


Figure 60. Equivalent Conductance of LiClO_4 in DMF at 25 and 60 C

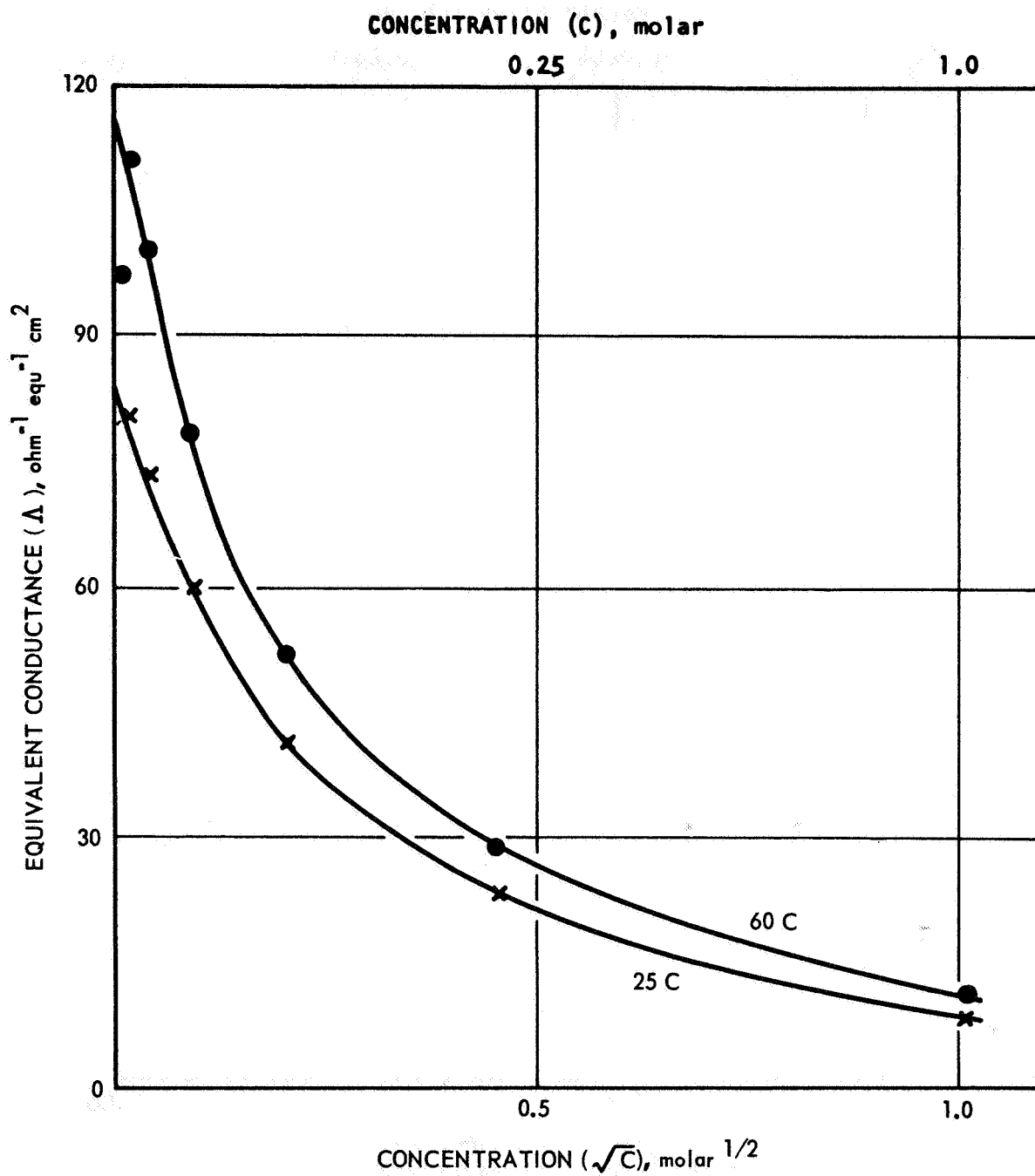


Figure 61. Equivalent Conductance of LiCl in DMF at 25 and 60 C

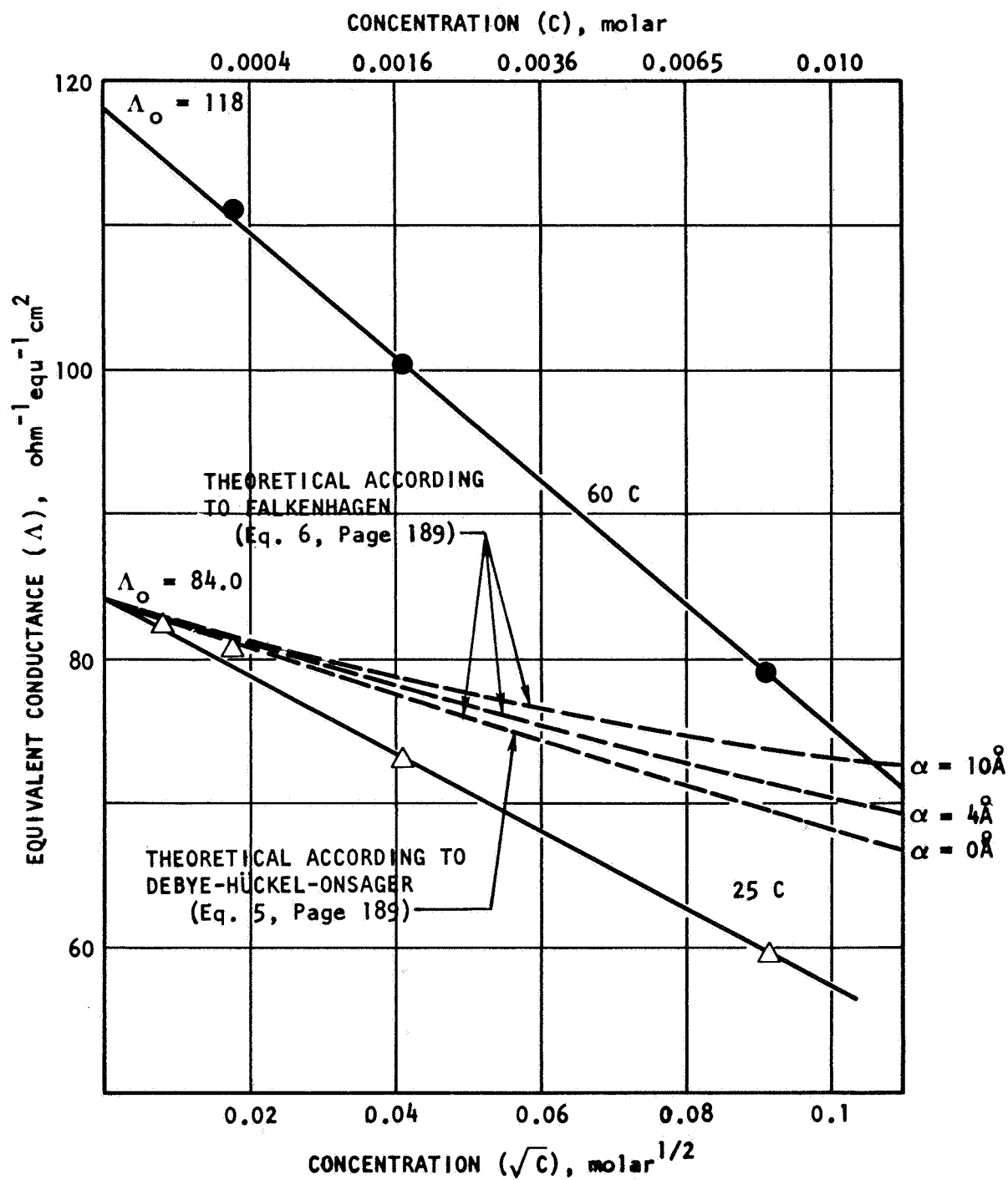


Figure 62. Equivalent Conductance of LiCl in DMF at 25 and 60 C

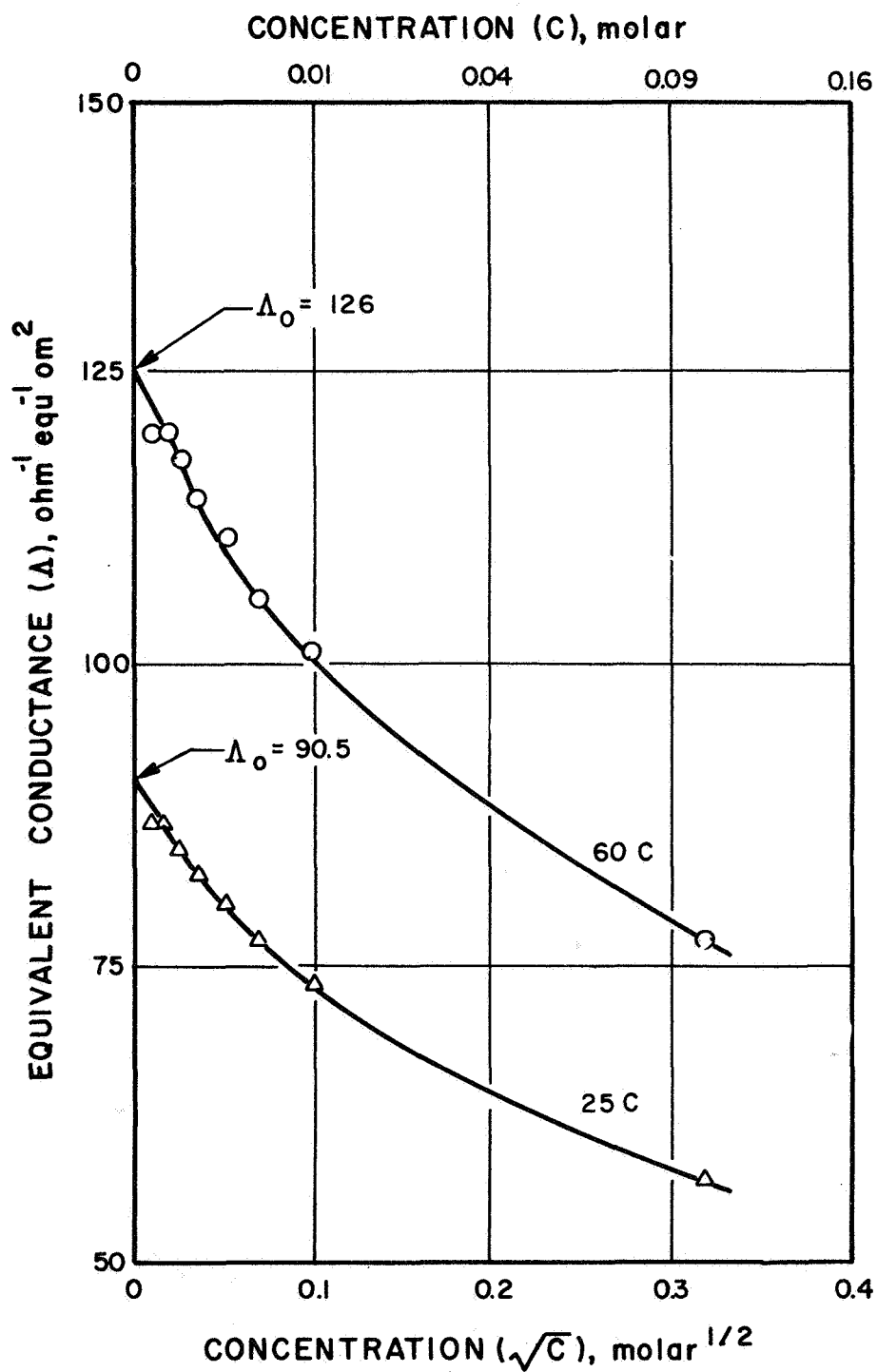


Figure 63. Equivalent Conductance of $\text{TMA} \cdot \text{PF}_6$ in DMF at 25 and 60 C

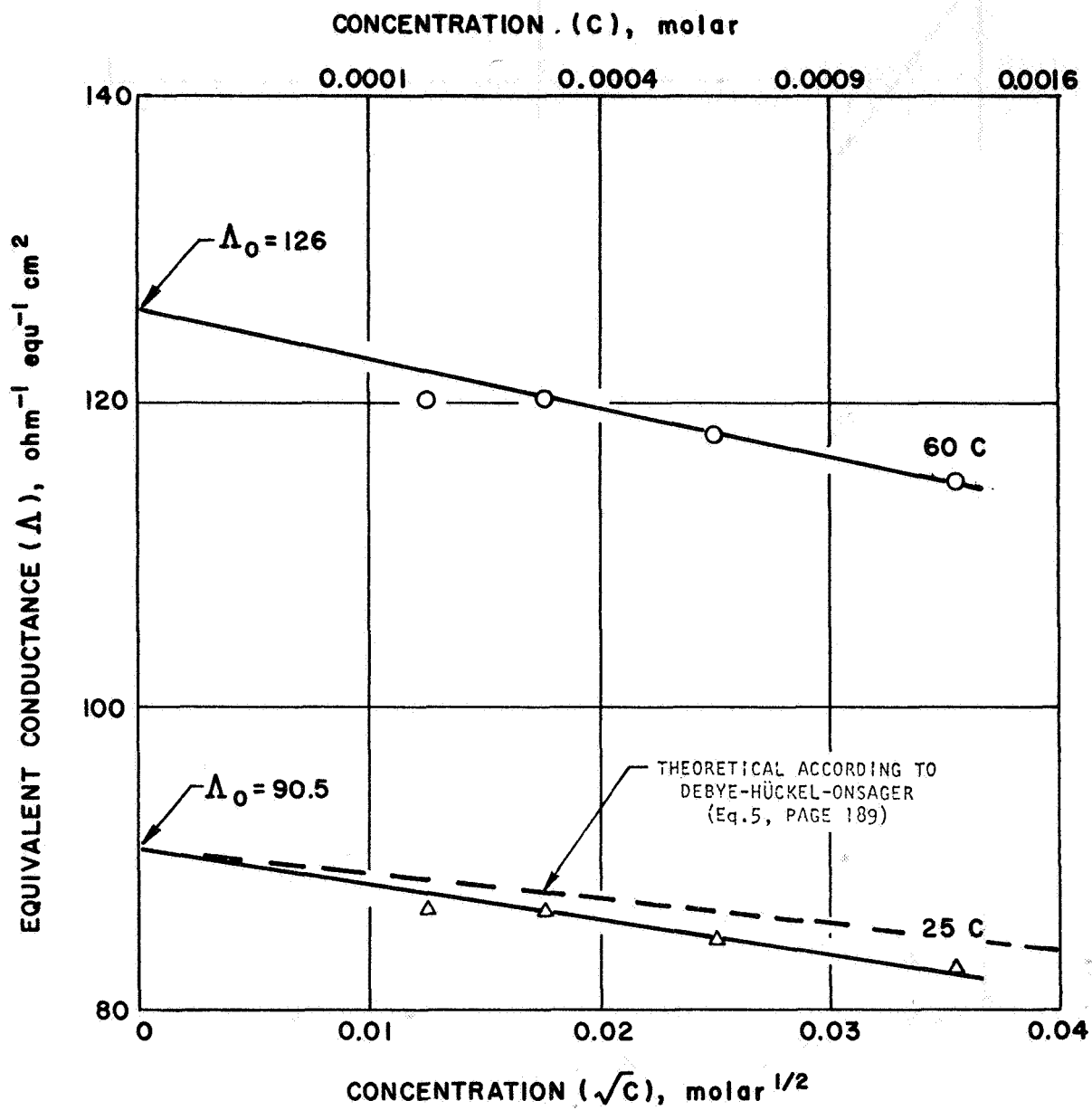


Figure 64. Equivalent Conductance of $\text{TMA} \cdot \text{PF}_6$ in DMF at 25 and 60 C

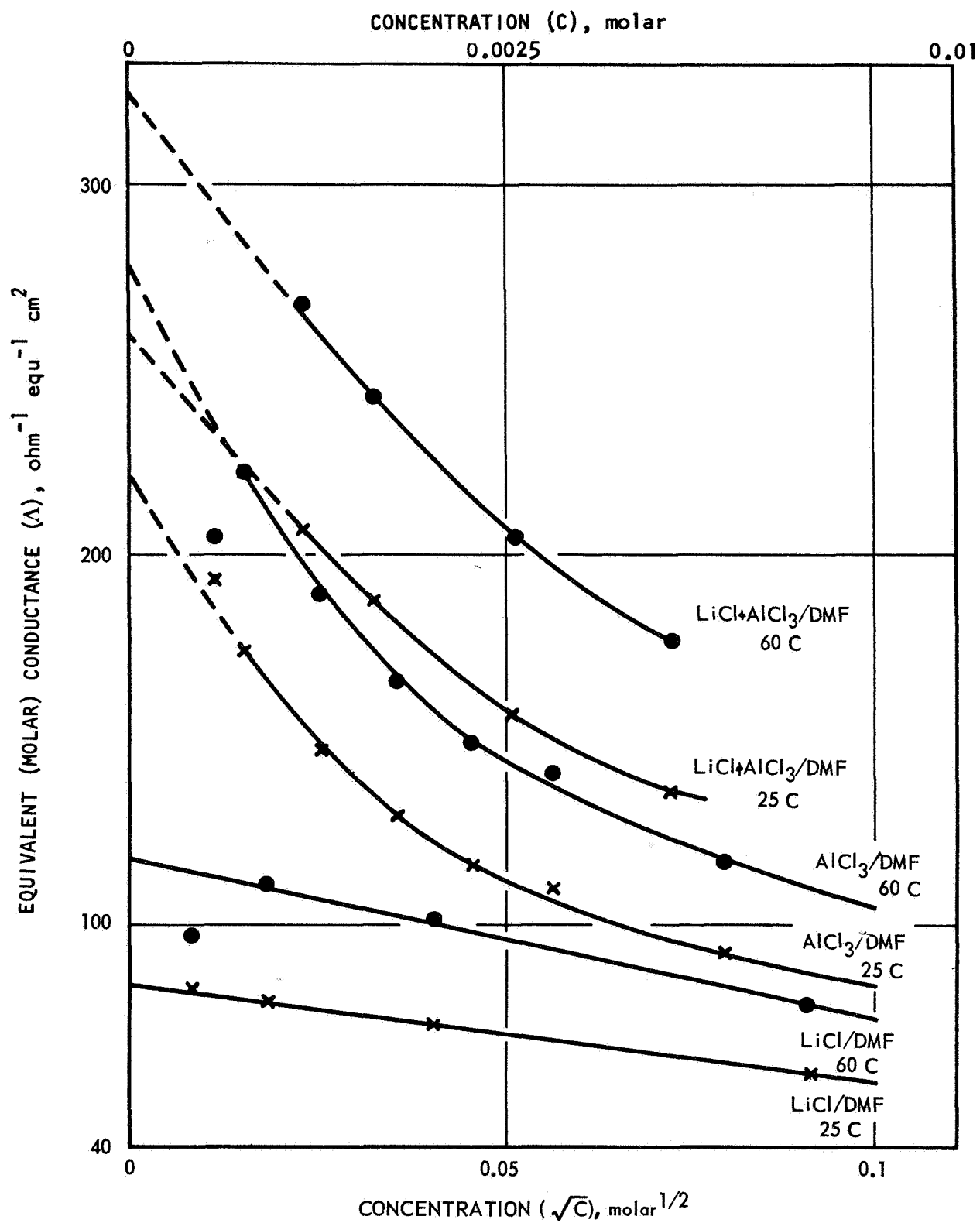


Figure 65. Equivalent (Molar) Conductance of LiCl/DMF , AlCl_3/DMF , and $\text{LiCl}+\text{AlCl}_3/\text{DMF}$ at 25 and 60 C

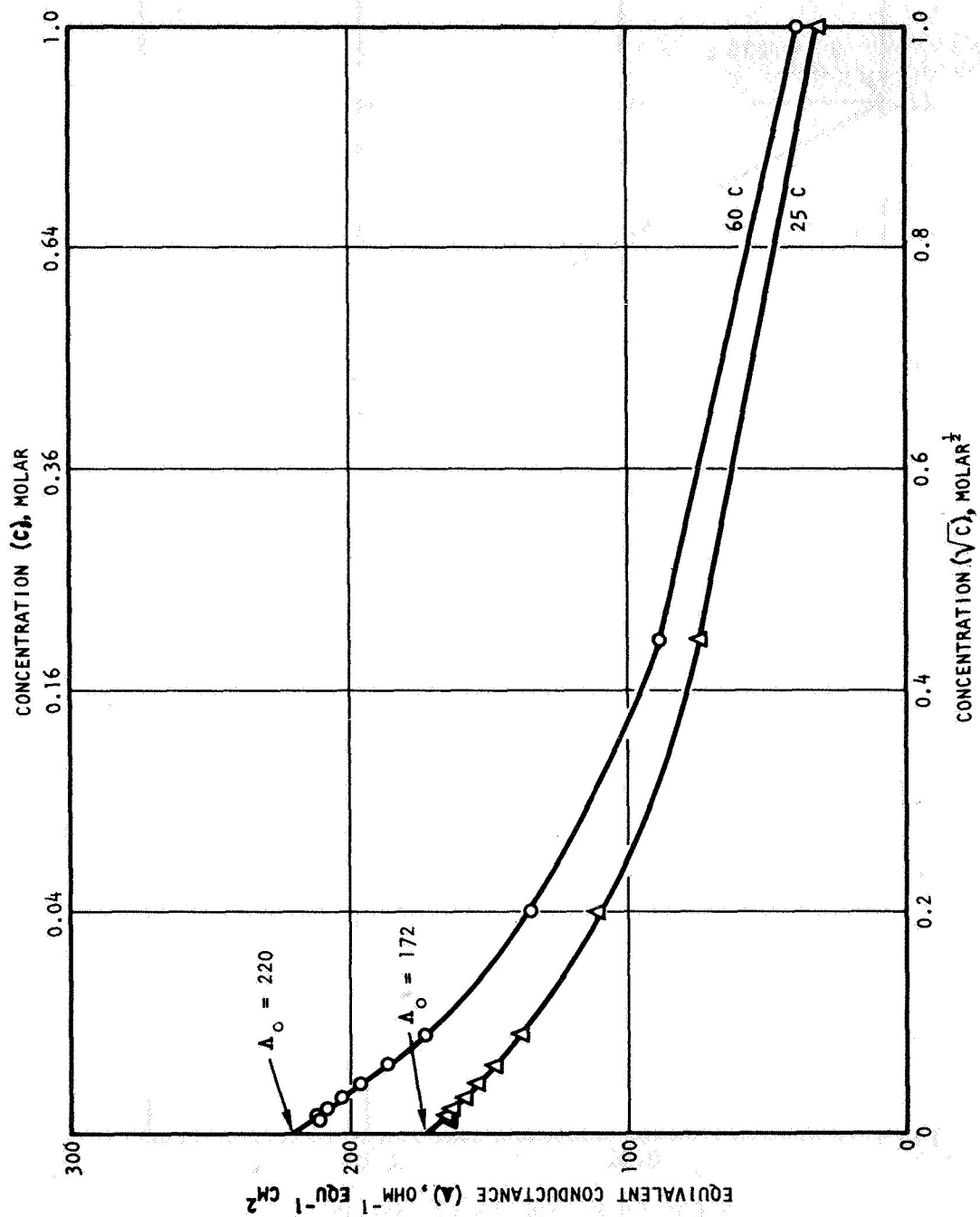


Figure 66. Equivalent Conductance of LiClO_4 in Acetonitrile at 25 and 60 C

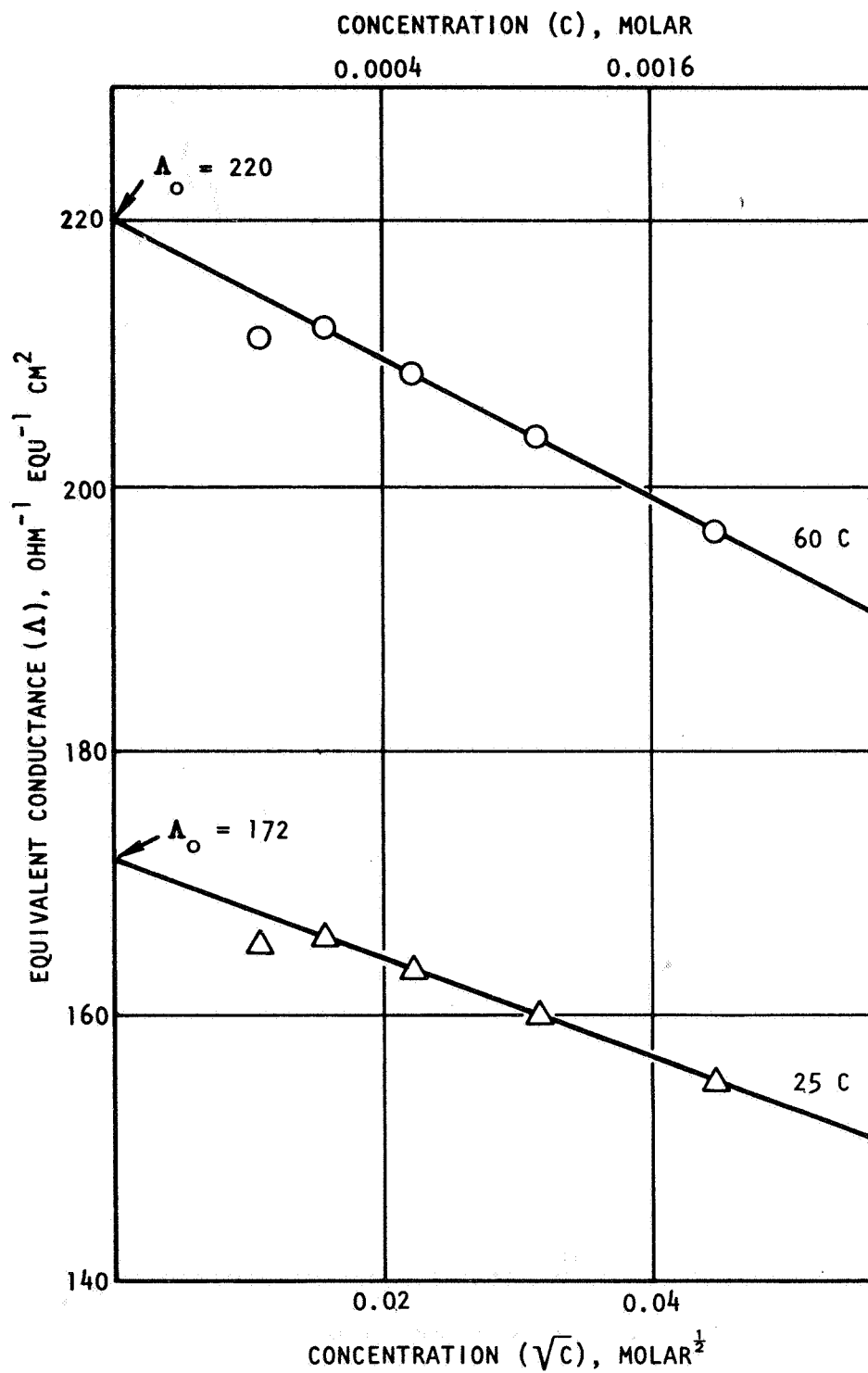


Figure 67. Equivalent Conductance of LiClO_4 in Acetonitrile at 25 and 60 C.

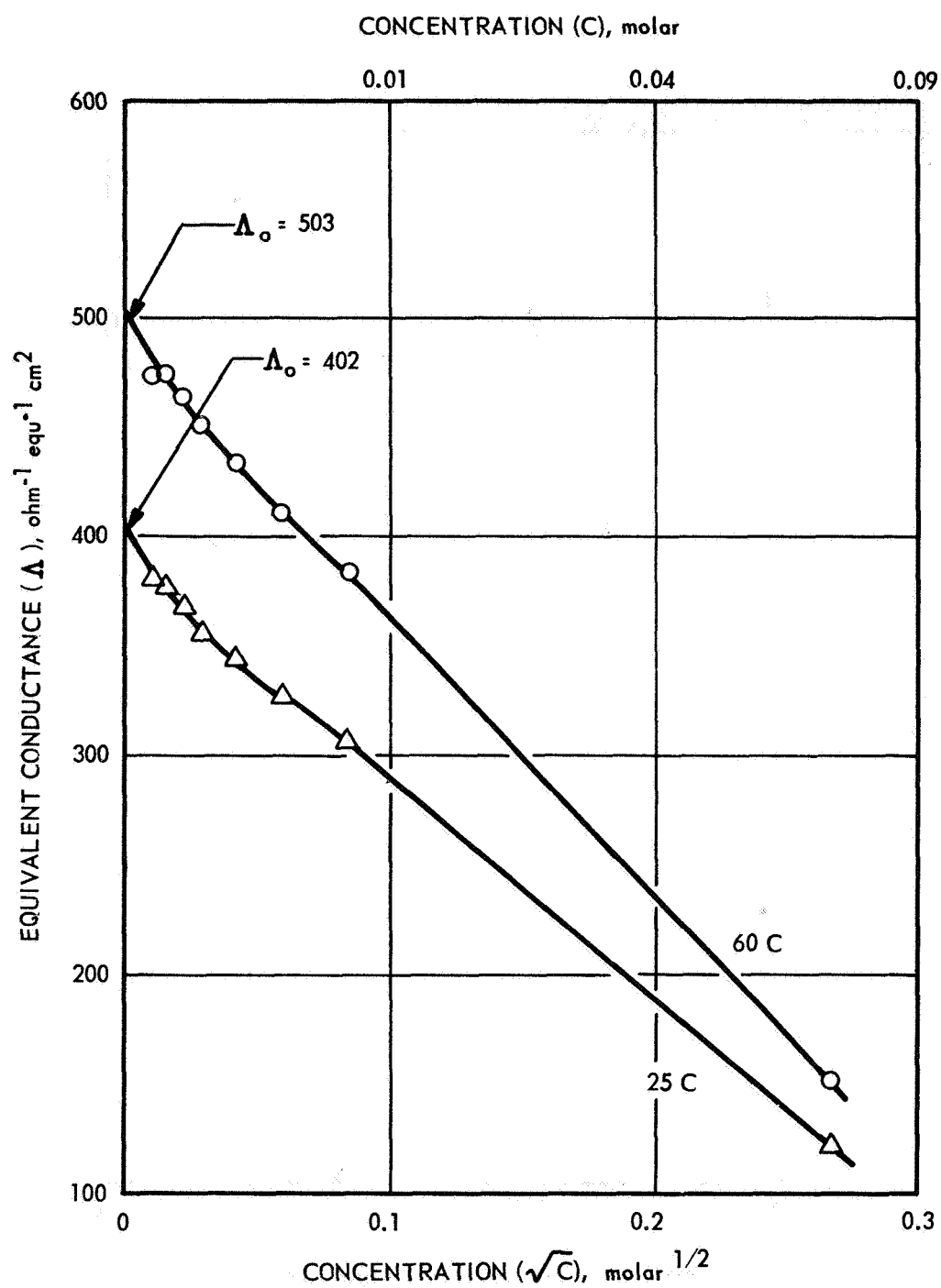


Figure 68. Equivalent Conductance of $\text{TMA} \cdot \text{PF}_6$ in AN at 25 and 60 C

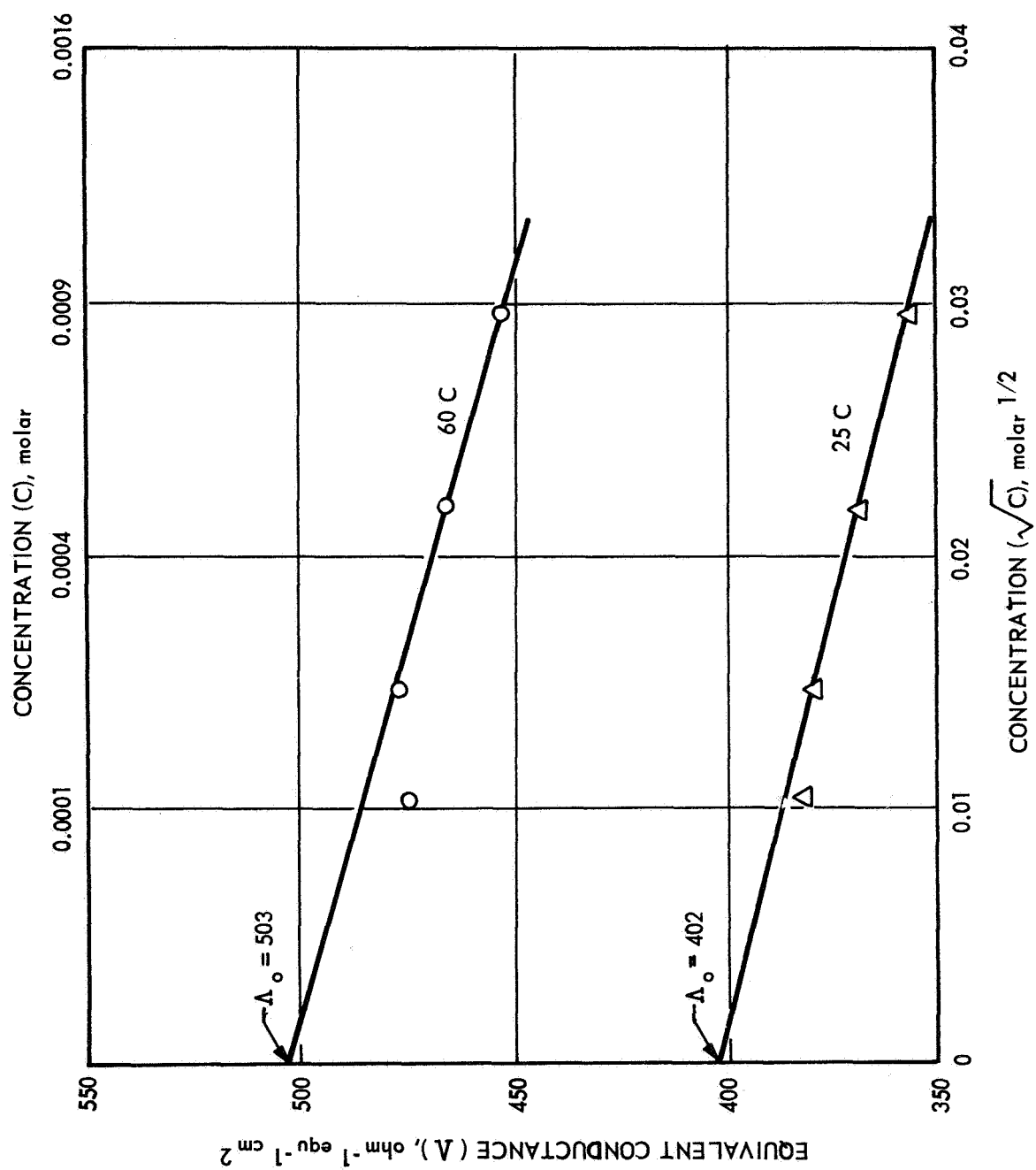


Figure 69. Equivalent Conductance of TMA·PF₆ in AN at 25 and 60 C

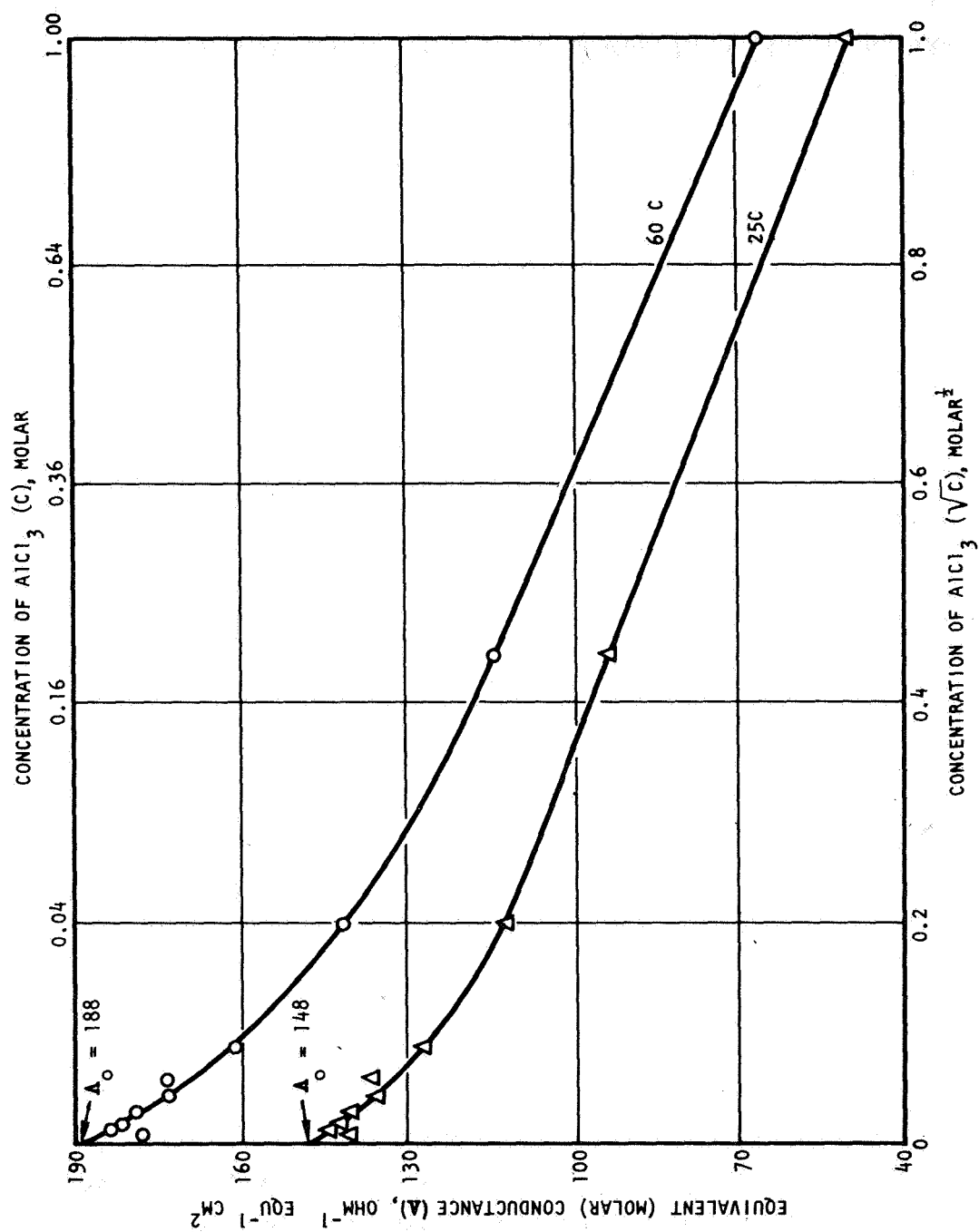


Figure 70. Equivalent (Molar) Conductance of $\text{LiCl}+\text{AlCl}_3$ in Acetonitrile at 25 and 60 C

An abnormal behavior was found with methyl formate solutions. The data on LiClO_4 #3/MF #2-6 and LiAsF_6 #1/MF #2-5 are presented in Tables 33 and 34, and in Fig. 71. A minimum value for the equivalent conductance was indicated at a low concentration, somewhere between 0.01 and 0.1 molar. The Λ -value at that point has to be considered relatively very low because of the low viscosity of the solvent. After the minimum, the equivalent conductance increased rapidly upon further decrease of the concentration. The $\Lambda - \sqrt{C}$ relationship at these low concentrations was not linear, however, and an extrapolation to infinite dilution was not attempted.

The average value of the Walden product, $\Lambda_0 \cdot \eta$, for the LiClO_4 solutions in the three other solutions is $0.617 \text{ ohm}^{-1} \text{ equ}^{-1} \text{ cm}^2$ poises for 25 C (LiClO_4/PC : $\Lambda_0 \cdot \eta = 25.6 \times 24.8 \times 10^{-3} = 0.635$; $\text{LiClO}_4/\text{DMF}$: $\Lambda_0 \cdot \eta = 80.4 \times 7.93 \times 10^{-3} = 0.638$; LiClO_4/AN : $\Lambda_0 \cdot \eta = 172 \times 3.36 \times 10^{-3} = 0.578$). If LiClO_4/MF should furnish a Walden product in the same order, Λ_0 would be $182 \text{ ohm}^{-1} \text{ equ}^{-1} \text{ cm}^2$, η being 3.38×10^{-3} poises.

For LiAsF_6/MF , a decrease of Λ at higher concentration above 1 molar was indicated.

Aside from some rather speculative attempts, the relationships between equivalent conductance and the electrolyte concentration has not been interpreted for these methyl formate solutions. With its low dielectric constants, methyl formate is the unique solvent of the four investigated. A similar shape of the $\Lambda - \sqrt{C}$ curve, incidentally, has been found also in AlCl_3/PC , but it is doubtful if there is any correlation.

Equivalent conductances at infinite dilution were also determined for a series of electrolytes which were not studied otherwise. Values of tetrabutylammonium tetraphenylboride (TBA·TPB), tetrabutylammonium bromide, and lithium bromide solutions permit the calculation of individual ionic mobilities in the main electrolytes studied. It has been suggested by

TABLE 33

SPECIFIC CONDUCTANCE (λ) AND EQUIVALENT CONDUCTANCE (Λ)
OF LiClO_4 #3/MF #2-6 AT 25 C

Concentration (C), molar	\sqrt{C} , molar ^{1/2}	$\lambda(25\text{ C})$, ohm ⁻¹ cm ⁻¹	$\Lambda^*(25\text{ C})$, ohm ⁻¹ equ ⁻¹ cm ²
1.000	1.000	1.281×10^{-2}	12.81
0.0400	0.2000	8.044×10^{-5}	2.01
0.00320	0.0566	1.202×10^{-5}	3.72
0.00128	0.0358	7.135×10^{-6}	5.49
0.000512	0.0226	4.346×10^{-6}	8.28
0.000204	0.0143	2.744×10^{-6}	12.93
0		1.067×10^{-7}	

Λ^* : Equivalent conductance, corrected for conductance of pure solvent

TABLE 34

SPECIFIC CONDUCTANCE (λ) AND EQUIVALENT CONDUCTANCE (Λ)
OF LiAsF_6 #1/MF #2-5 AT 25 C

Concentration (C), molar	\sqrt{C} , molar ^{1/2}	λ (25 C), ohm ⁻¹ cm ⁻¹	Λ^* (25 C), ohm ⁻¹ equ ⁻¹ cm ²
2.27	1.503	4.648×10^{-2}	20.6
1.13	1.060	3.365×10^{-2}	29.8
0.113	0.336	1.853×10^{-3}	16.4
0.0113	0.106	1.416×10^{-4}	12.4
0.00452	0.0672	7.055×10^{-5}	15.4
0.00181	0.0425	3.879×10^{-5}	20.9
0.000723	0.0269	2.167×10^{-5}	28.6
0.000289	0.0170	1.239×10^{-5}	39.6
0	---	9.572×10^{-7}	---

Λ^* : Equivalent conductance, corrected for conductance of pure solvent

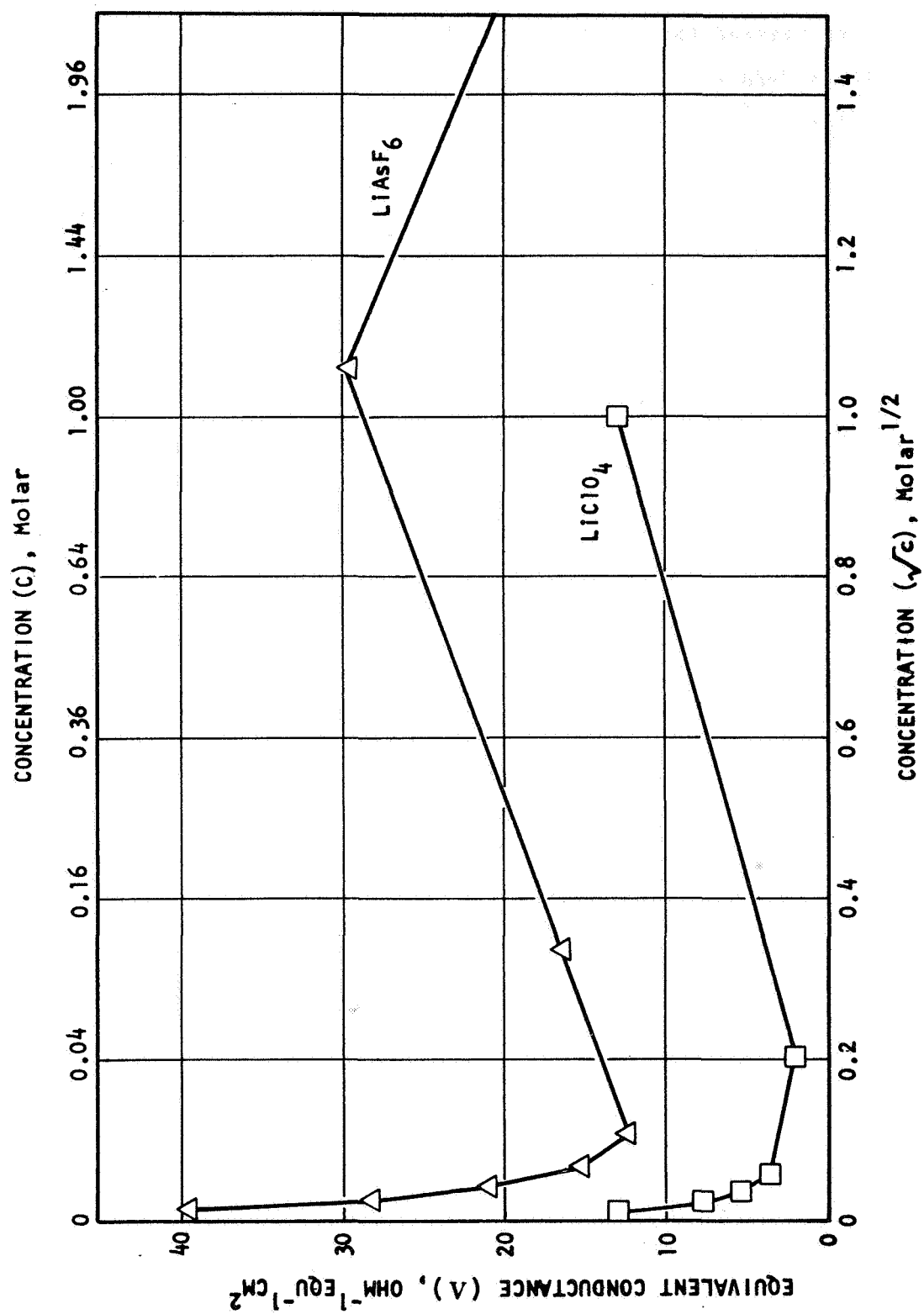


Figure 71. Equivalent Conductance of LiAsF_6 and LiClO_4 in Methyl Formate at 25 C

Fuoss and Hirsch (Ref. 56) that the cation and anion in TBA·TPB are of equal size and have equal mobility, and they claim that this is much closer approximated than in the case of tetrabutylammonium triphenylborofluoride suggested by Fowler and Kraus (Ref. 57) and used by Prue and Sherrington (Ref. 58).

The equivalent conductances at infinite dilution for these special electrolytes are given in Table 35. Most of these results have been presented earlier in detail (Ref. 4 and 5).

The equivalent conductances at infinite dilution calculated for individual ions from the preceding data are listed in Table 36 for propylene carbonate, in Table 37 for dimethyl formamide, and in Table 38 for acetonitrile. The values for compounds from which the values for individual ions were calculated are also listed.

It should be noted that these ion mobility values are fairly sensitive to experimental errors. A first possible source for such errors is an inaccurate extrapolation, another source are inaccurate starting solutions. No time was allocated in general to duplicate the measurements. An error, for instance, is suspected in the TBA·Br/DMF results (a higher Λ_0 - values for TBA·Br than for TMA·Br is unlikely), and may be reflected in the entire series of ion mobilities in DMF.

Ionic radii were calculated from the ion mobility data of Tables 36 through 38. It was assumed that Stokes law applies; i.e., that the ions move through the solvent as spheres with the electric force equaling the frictional force. The frictional force, F_f , for an ion of the radius r , moving at the speed v , in a solvent with the viscosity η , is according to Stokes law

$$F_f = 6\pi r\eta v$$

TABLE 35

EQUIVALENT CONDUCTANCES AT INFINITE DILUTION (Λ_0) FOR SPECIAL SOLUTIONS USED TO DETERMINE INDIVIDUAL ION MOBILITIES

Solvent	Solute	Λ_0 at 25 C, ohm ⁻¹ equ ⁻¹ cm ²	Λ_0 at 60 C, ohm ⁻¹ equ ⁻¹ cm ²
PC #2-11	TBA·TPB #1	17.2	30.0
PC #2-10	TBA·Br #1	27.5	47.3
PC #6-3	TMA·Br #1	33.8	58.9
PC #2-7; 2-8	LiBr #2	26.2	44.8
DMF #5-1	TBA·TPB #1	51.0	72.6
DMF #5-2	TBA·Br #1	87.0	122.4
DMF #6-18	TMA·Br #1	83.2	116.4
DMF #3-4	LiBr #2	79.1	111
AN #4-1	TBA·TPB #1	119.6	154.6
AN #4-1	TBA·Br #1	161.6	207.8
AN #4-7	TMA·Br #1	217.2	278.9
AN #4-7	LiBr #2	170.1	216.0

TABLE 36

EQUIVALENT CONDUCTANCE AT INFINITE DILUTION (Λ_0) FOR SEVERAL
SOLUTES AND INDIVIDUAL IONS IN PROPYLENE CARBONATE

Solute	25 C.		60 C	
	Λ_0 , ohm ⁻¹ equ ⁻¹ cm ²	Λ_0^+ or Λ_0^- , ohm ⁻¹ equ ⁻¹ cm ²	Λ_0 , ohm ⁻¹ equ ⁻¹ cm ²	Λ_0^+ or Λ_0^- , ohm ⁻¹ equ ⁻¹ cm ²
TBA·TPB	17.2		30.0	
TBA ⁺		8.6		15.0
TPB ⁻		8.6		15.0
TBA·Br	27.5		47.3	
Br ⁻		18.9		32.3
LiBr	26.2		44.8	
Li ⁺		7.3		12.5
LiClO ₄	25.6		43.1	
ClO ₄ ⁻		18.3		30.6
LiCl	26.2		44.9	
Cl ⁻		18.9		32.4
TMA·PF ₆	33.9		57.6	
TMA·Br	33.8		58.9	
TMA ⁺		14.9		26.6
PF ₆ ⁻		19.0		31.0

TABLE 37

EQUIVALENT CONDUCTANCE AT INFINITE DILUTION (Λ_0) FOR SEVERAL
SOLUTES AND INDIVIDUAL IONS IN DIMETHYL FORMAMIDE

Solute	25 C		60 C	
	Λ_0 , ohm ⁻¹ equ ⁻¹ cm ²	Λ_0^+ or Λ_0^- , ohm ⁻¹ equ ⁻¹ cm ²	Λ_0 , ohm ⁻¹ equ ⁻¹ cm ²	Λ_0^+ or Λ_0^- , ohm ⁻¹ equ ⁻¹ cm ²
TBA·TPB	51.0		72.6	
TBA ⁺		25.5		36.3
TPB ⁻		25.5		36.3
TBA·Br	87.0(?)		122.4(?)	
Br ⁻		61.5		86.1
LiBr	79.1		111.0	
Li ⁺		17.6 25.0 (Ref. 58)		24.9
LiClO ₄	80.4		111.1	
ClO ₄ ⁻		62.8		86.7
LiCl	84.0		118.0	
Cl ⁻		66.4		93.0
TMA·Br	83.2		116.4	
TMA ⁺		21.7		30.3
TMA·PF ₆	90.5		126.0	
PF ₆ ⁻		68.3		86.3

TABLE 38

EQUIVALENT CONDUCTANCE AT INFINITE DILUTION (Λ_o) FOR SEVERAL
SOLUTES AND INDIVIDUAL IONS IN ACETONITRILE

Solute	25 C		60 C	
	Λ_o , ohm ⁻¹ equ ⁻¹ cm ²	Λ_o^+ or Λ_o^- , ohm ⁻¹ equ ⁻¹ cm ²	Λ_o , ohm ⁻¹ equ ⁻¹ cm ²	Λ_o^+ or Λ_o^- , ohm ⁻¹ equ ⁻¹ cm ²
TBA · TPB	119.6		154.6	
TBA ⁺		59.8		77.3
TPB ⁻		59.8		77.3
TBA · Br	161.6		207.8	
Br ⁻		101.8		130.5
LiBr	170.1		216.0	
Li ⁺		68.3		85.5
LiClO ₄	172		220	
ClO ₄ ⁻		104		134
TMA · Br	217.2		278.9	
TMA ⁺		115.4		148.4
TMA · PF ₆	402(?)		503(?)	
PF ₆ ⁻		287		355

The electric force, F_e , in the field E , on the ion carrying the charge q , is

$$F_e = q \cdot E$$

The equivalent conductance, Λ , is

$$\Lambda = \frac{q \cdot N \cdot v}{E} \quad (4)$$

N being Avogadro's number. Setting $F_f = F_e$ and substituting for v from Eq. 4, the following equation results

$$r = \frac{q^2 \cdot N}{6 \pi \eta \cdot \Lambda}$$

The ionic radii calculated accordingly are listed in Table 39. Only the lithium ion appears to have a considerably larger radius than the crystal ionic radii. This indicates that only Li^+ is solvated to a significant extent.

A solvation number can be calculated by dividing the volume of the solvation sheath by the volume which a solvent molecule occupies in the liquid. The volume of the solvation sheath, V_{solv} , is

$$V_{\text{solv}} = \frac{4\pi}{3} (r^3 - r_o^3)$$

r being the radius of the migrating ion, and r_o the crystal ion radius. The volume of one solvent molecule, $V_{\text{solv.molec.}}$, is calculated from the solvent density, ρ , and the molecular weight, M.W.:

$$V_{\text{solv.molec.}} = \frac{\text{M.W.}}{\rho \cdot N}$$

This figure is $1.41 \times 10^{-22} \text{ cm}^3$ for PC, $1.29 \times 10^{-22} \text{ cm}^3$ for DMF, and $8.8 \times 10^{-23} \text{ cm}^3$ for AN, all at 25 C.

TABLE 39

IONIC RADII CALCULATED FROM ION MOBILITIES

Ion	Radius ₀ in PC, Å	Radius ₀ in DMF, Å	Radius ₀ in AN, Å	Crystal Ionic Radii	Temperature, C
Li ⁺	4.55	5.90 (4.15*)	3.58	0.68	25
Cl ⁻	1.75	1.59		1.81	
Br ⁻	1.75	1.69	2.41	1.96	
ClO ₄ ⁻	1.81	1.65	2.35		
PF ₆ ⁻	1.75	1.52	0.85		
TMA ⁺	2.23	4.8	2.12		
TBA ⁺ , TPB ⁻	3.86	4.07	4.10		
Li ⁺	4.95	6.19	3.66	0.68	60
Cl ⁻	1.91	1.66		1.81	
Br ⁻	1.92	1.79	2.40	1.96	
ClO ₄ ⁻	2.02	1.78	2.34		
PF ₆ ⁻	2.60	1.79	0.88		
TMA ⁺	2.32	5.18	2.11		
TBA ⁺ , TPB ⁻	4.10	4.25	4.05		

*Calculated from $\Lambda_0 = 25.0$ (Ref.58)

For the Li^+ ion, the following solvation numbers result for these three solvents at 25 C: 2.8 for PC, 6.7 (3.02, if $r = 4.15 \text{ \AA}$) for DMF, and 2.16 for AN. Solvation numbers between 2 and 3 seem unlikely, however. As discussed, for instance, in Ref. 59, the meaning of solvation number values as determined above have their limits. Assuming smaller volumes for the solvent molecules would increase the solvation numbers, or there may be rapid exchange between solvent molecules in the solvation sheath and those in the bulk solvent.

In summarizing the above results on ion mobilities at infinite dilution, it may be stated that, in general, no unusual behavior was exhibited by PC, DMF, or AN solutions. The ion mobility at infinite dilution is largely determined by size of the ion and viscosity of the solvent (the Walden product for individual ions is fairly constant). The well-known conductance maximum with increasing concentration of nonaqueous, aprotic electrolytes is therefore governed by activity effects. It occurs at specific conductances which are a magnitude lower in nonaqueous aprotic electrolytes than in aqueous solutions. Activity effects seem to be aggravated by the larger size of the solvent molecules. In some cases (e.g., in the case of LiCl), ion pair formation appears to depress the conductance maximum further.

A very significant result, which is also of great practical importance, is the low mobility of the lithium ion in all of the three major solvents. From ion mobilities, transference numbers for the Li^+ ion in LiClO_4 solutions can be calculated:

$t_+ = 0.28$ and 0.29 in propylene carbonate at 25 and 60 C, respectively

$t_+ = 0.22$ in dimethyl formamide at 25 and 60 C

$t_+ = 0.40$ and 0.39 in acetonitrile at 25 and 60 C, respectively

In addition to Λ_0 -values, information on ion pair formation can be obtained from the relationship of the equivalent conductance to the square root of the concentration. The Debye-Hückel-Onsager equation predicts this relationship for low concentrations, taking into account a relaxation and an electrophoretic effect. This equation is represented for a uni-univalent electrolyte, as given in Ref. 60:

$$\Lambda = \Lambda_0 - \left[\frac{82.4}{(\epsilon T)^{1/2} \eta} + \frac{8.20 \times 10^5}{(\epsilon T)^{3/2}} \Lambda_0 \right] \sqrt{C} \quad (5)$$

or

$$\Lambda = \Lambda_0 - [B_1 + B_2 \Lambda_0] \sqrt{C}$$

In Eq. 5, ϵ is the dielectric constant, and η the viscosity of the solvent, T is the absolute temperature, and C the solute concentration in moles per liter.

Calculations using this relationship were made for a number of cases, and the theoretical curves according to Eq. 5 are represented for 25 C in Fig. 53, 55, 57, 60, 62, and 64. A strong deviation of the actually measured curve from the theoretical one was found particularly for LiCl/PC, and also for LiCl/DMF. Such deviations are usually interpreted as being due to a strong ion pair formation. The low solubility of LiCl in PC may be related to this effect.

Investigations by Falkenhagen and others have led to a refinement of the Debye-Hückel-Onsager equation to the form as given in Ref. 59:

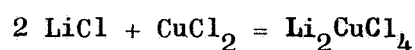
$$\Lambda = \Lambda_0 - \left[\frac{8.204 \times 10^5}{(\epsilon T)^{3/2}} \Lambda_0 + \frac{82.5}{\eta (\epsilon T)^{1/2}} \right] \frac{\sqrt{C}}{1 + 50.29 \alpha (\epsilon T)^{-1/2} \sqrt{C}}, \quad (6)$$

α being the mean ionic diameter. This relationship was calculated for various values of α in the case of LiCl/DMF; the curves are represented in Fig. 62. It can be seen that the correction introduced resulted in smaller slopes of the theoretical curves, and the above remarks in regard to ion pair formation are still valid.

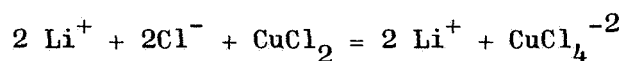
CONDUCTOMETRIC TITRATIONS

CuF₂ Added to LiCl/DMF

The conductometric titration of LiCl with CuCl₂ in DMF was performed by adding small amounts of solid CuCl₂ #2 to 10 ml of LiCl/DMF solution placed in a conductivity cell. The results of Fig. 72 and 73 were derived. An obvious break in the conductance curve occurred when the mole ratio of CuCl₂ to LiCl was approximately 1:2. The reaction appeared to be:



or rather



The breaking point in both curves seems somewhat delayed in reference to the stoichiometric equivalence point. This shift may be due to the existence of free chloride ions in considerable amounts or to a systematic error of the weighing of the CuCl₂ (e.g., incomplete transfer of the weighed samples).

In the case of 1 M LiCl #2/DMF #6-13, the specific conductance increased at first upon the additions of CuCl₂ #2. After the equivalence point, the conductance of the solution decreased. The ions which presumably existed before, at, and after the equivalence point are given in Table 40. The addition of CuCl₂ before the equivalence point causes a replacement of 2 Cl⁻ ions by CuCl₄⁻². It is not easy to predict a priori if this should cause an increase or a decrease in specific conductance; it is not known whether Cl⁻ or 1/2 CuCl₄⁻² would exhibit a higher equivalent conductance. The increase in ionic strength by substituting 1/2 CuCl₄⁻² for Cl⁻ possibly had a significant effect at this high concentration. A further factor likely to cause an increase was the breaking up of LiCl ion pairs.

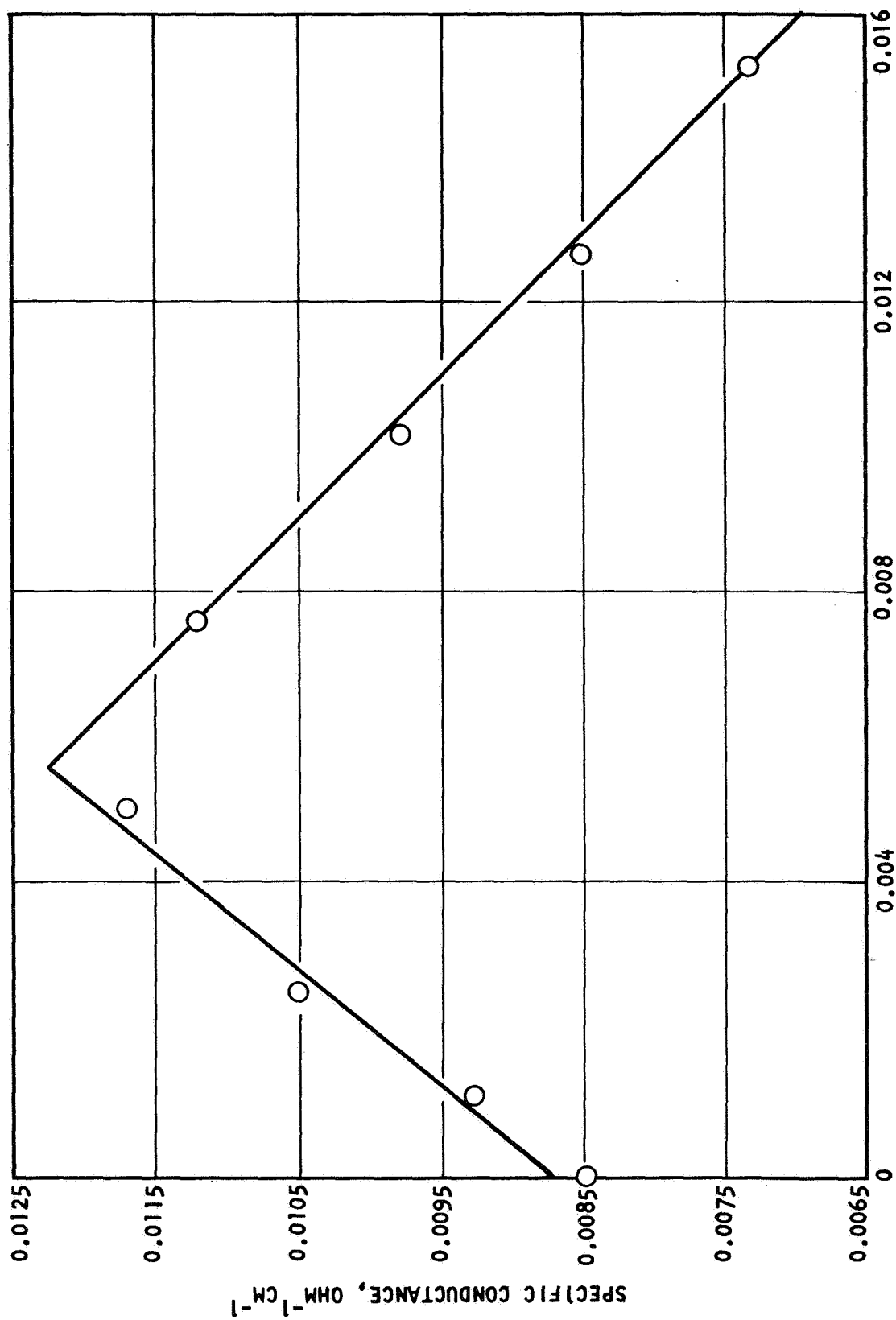


Figure 72. Conductometric Titration of 1.0 M LiCl/DMF With CuCl₂ at 25 C

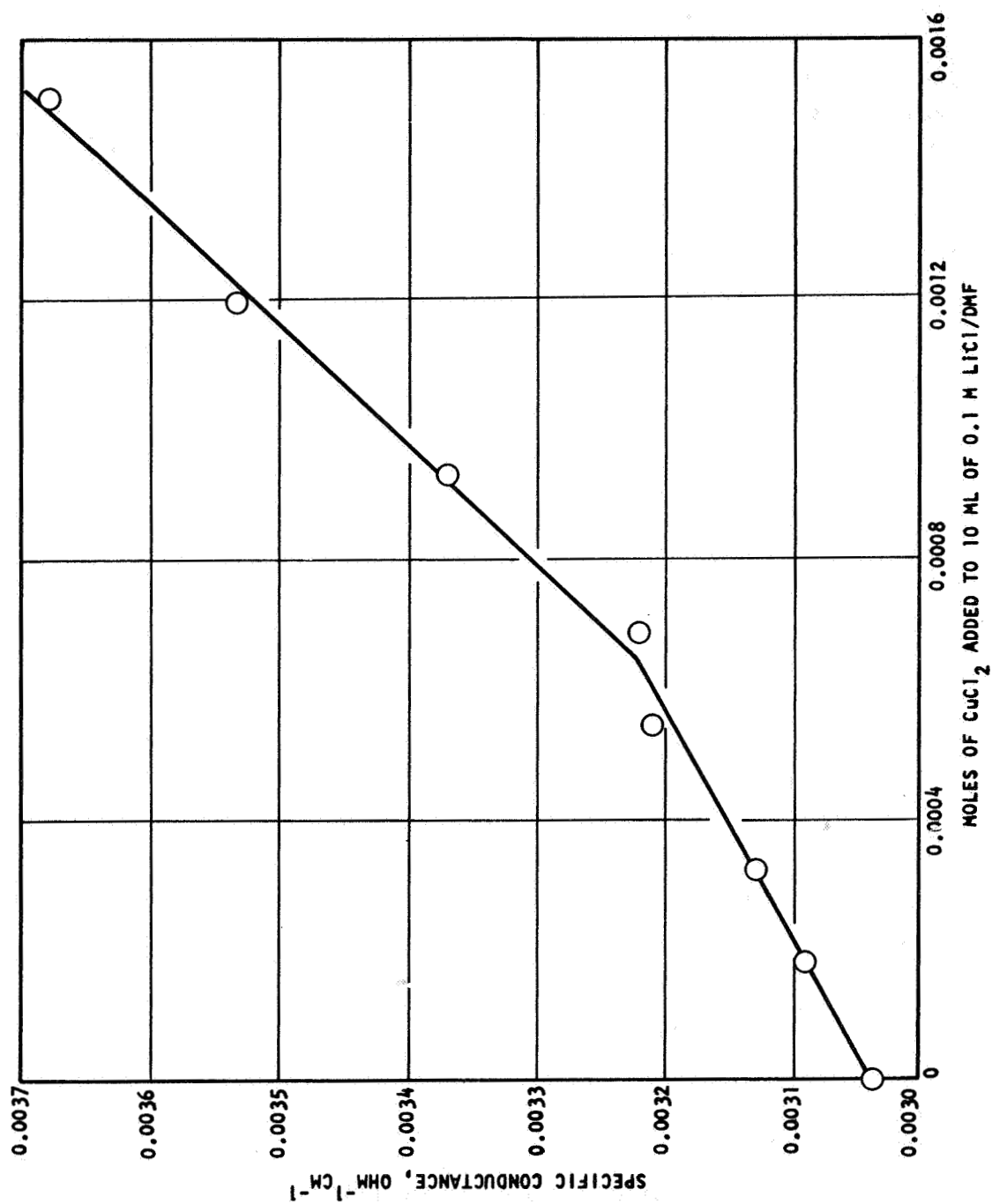
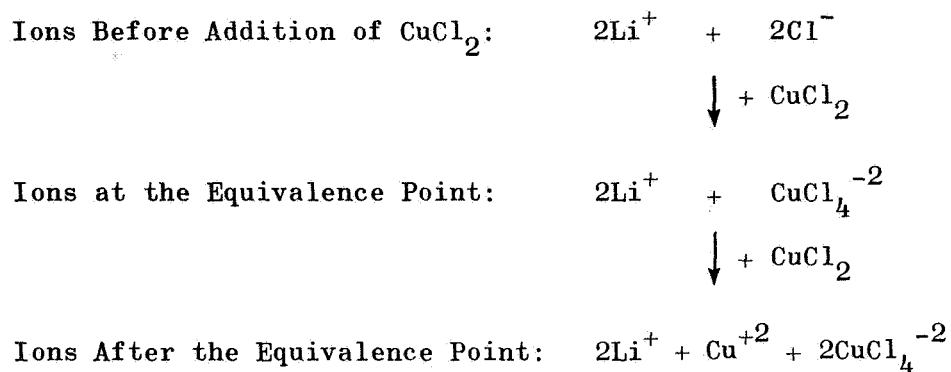


Figure 73. Conductometric Titration of 0.1 M LiCl/DMF With CuCl_2 at 25°C

TABLE 40

IONS INVOLVED IN THE CONDUCTOMETRIC TITRATION
OF LiCl/DMF WITH CuCl₂



CuCl₂ dissolved passed the equivalence point, and it is assumed that the additional CuCl₂ formed Cu⁺² and CuCl₄⁻² ions. An increase in the concentration of conductive species resulted, and an increase in specific conductance would be expected, accordingly. In actuality, however, a decrease was observed, and this must be ascribed to activity effects. A conductance maximum had been reported for LiCl/DMF solutions at about the concentration of 1 molar (Ref. 61).

To ascertain that an activity effect was reversing the tendency to have higher specific conductances with higher concentrations of conductive species, the experiment was repeated with a less concentrated (i.e., a 0.1 M LiCl #2/DMF #6-17) solution. Indeed, the specific conductance kept increasing past the equivalence point, which is indicated by a change of slope of the titration curve.

CuF₂ Added to LiClO₄/DMF

The results shown in Fig. 74 were obtained by titrating LiClO₄ #3/DMF #7-2 with solid CuF₂ #3. The following observations should be made: (1) Relative changes in conductance were smaller than those in the CuCl₂ + LiCl/DMF case. (2) The dissolution rate of CuF₂ appeared to be very slow, and only

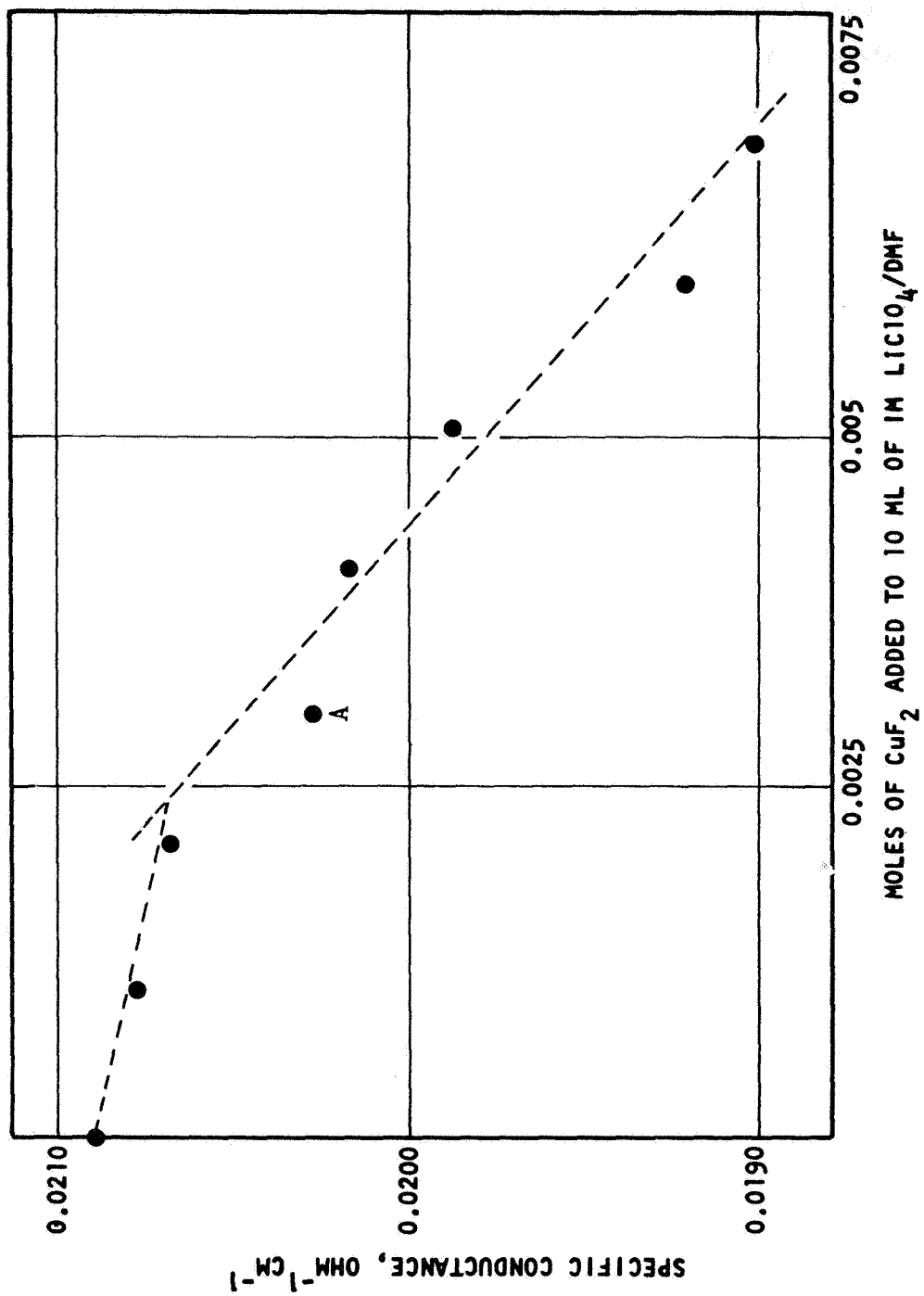


Figure 74. Conductometric Titration of 1 M LiClO₄/DMF With CuF₂ at 25 C

apparently stable values were actually measured. Point A, e.g., was determined after an overnight period whereas the others usually 1 hour after the addition. (3) Instead of a slow dissolution of CuF_2 , a slow copper complex formation could have been involved; the appearance of a blue discoloration was observed but not immediately after addition of the CuF_2 .

From solubility data, a reaction according to



was indicated. The equivalence point would occur when 1/2 mole of CuF_2 had been added to 1 mole of LiClO_4 , and CuF_2 would not dissolve past this point. No such equivalence point is indicated in Fig. 74. The decrease of the specific conductance past the predicted point may indicate that dissolution of CuF_2 previously added still took place. An apparent equivalence point is indicated at a lower concentration, but it is believed to be delusive because of the reasons named above.

H_2O Added to LiClO_4/PC

The specific conductance of a 1 M LiClO_4 #3/PC #4-5 solution increased from $5.11 \times 10^{-3} \text{ ohm}^{-1} \text{ cm}^{-1}$ to $5.22 \times 10^{-3} \text{ ohm}^{-1} \text{ cm}^{-1}$ when 1000-ppm H_2O was added; the increase was proportional to the amount of water added. The change in conductance probably reflected the formation of hydrated lithium ions which had a greater mobility than lithium ions solvated with propylene carbonate.

HITTORF EXPERIMENTS

Apparatus

The cell employed for these experiments is shown in Fig. 75 and 76. The design of Wall, Stent, and Ondrejcin (Ref. 62) was modified to allow easy immersion of the lower parts of the cell into an oil bath. The experiments were performed at room temperature; the electrolyte warmed under current flow because of the relatively low specific conductance of the electrolytes under study, which prevented performing the experiment at a completely controlled, constant temperature. It appears that cooling of the lower cell parts in a bath was efficient enough, however, to prevent excessive temperature increases in the cell. Cooling of only the lower parts of the cell also furnished a stable density distribution in the electrolyte. The three compartments were filled with a total of approximately 90 milliliters of electrolyte and the electrolyte was raised to the desired level by applying suction to the center arm. A constant current was maintained, typically about 10 milliamperes for a period of 400 minutes. At the conclusion of the experiment, the stopcock was reopened to separate catholyte and anolyte from the electrolyte contained in the middle compartment. Solute concentration changes in the cathode and anode compartment were then determined by analysis.

A platinum cathode and a silver anode were first selected as electrodes. However, platinum forms an alloy with electro-deposited lithium, and nickel or molybdenum cathodes were substituted. The anodic dissolution of silver appeared to be perfectly coulometric in some systems; but silver, as well as copper, were found to react in some solutions containing copper halides; molybdenum was therefore very often substituted as anode material.

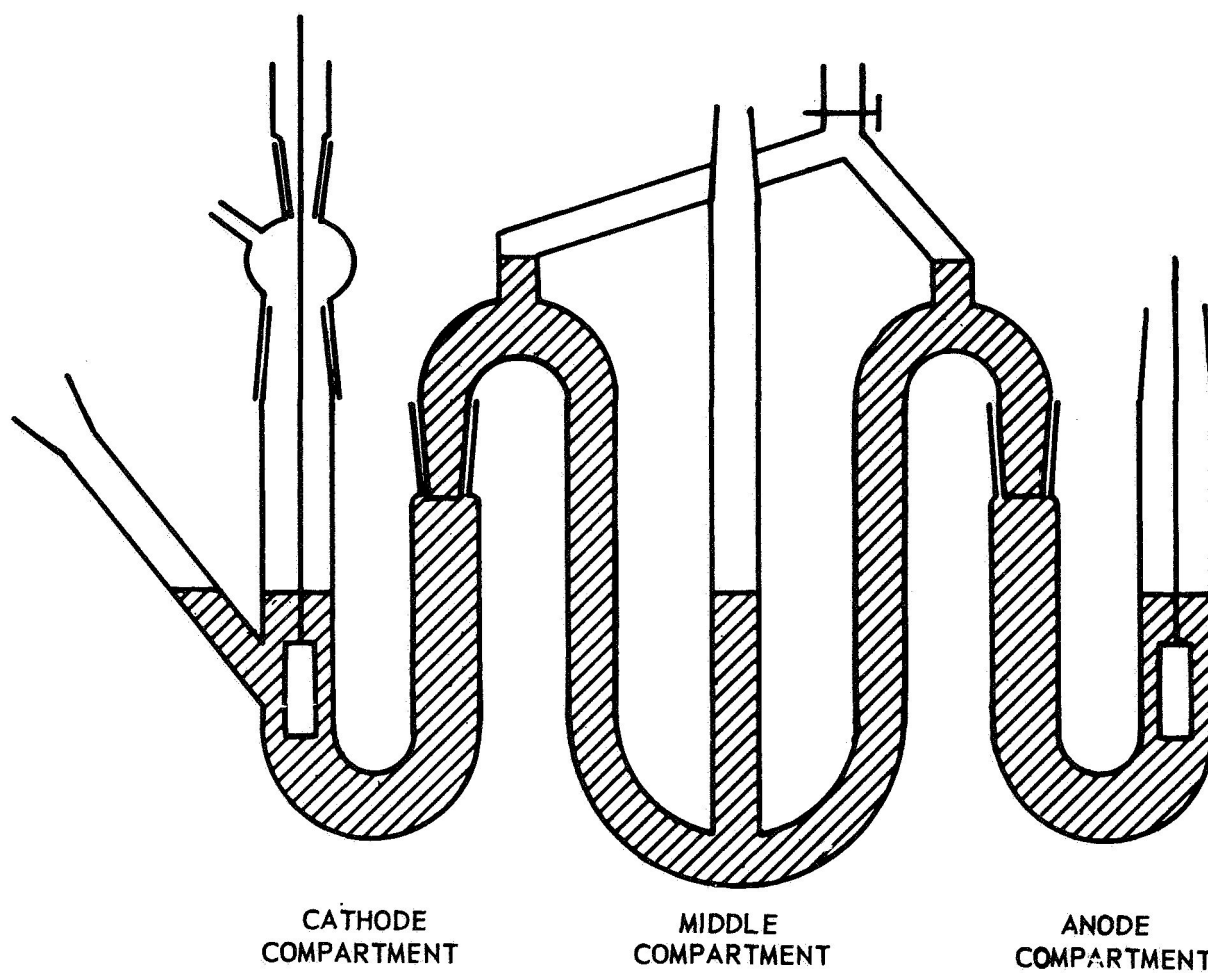
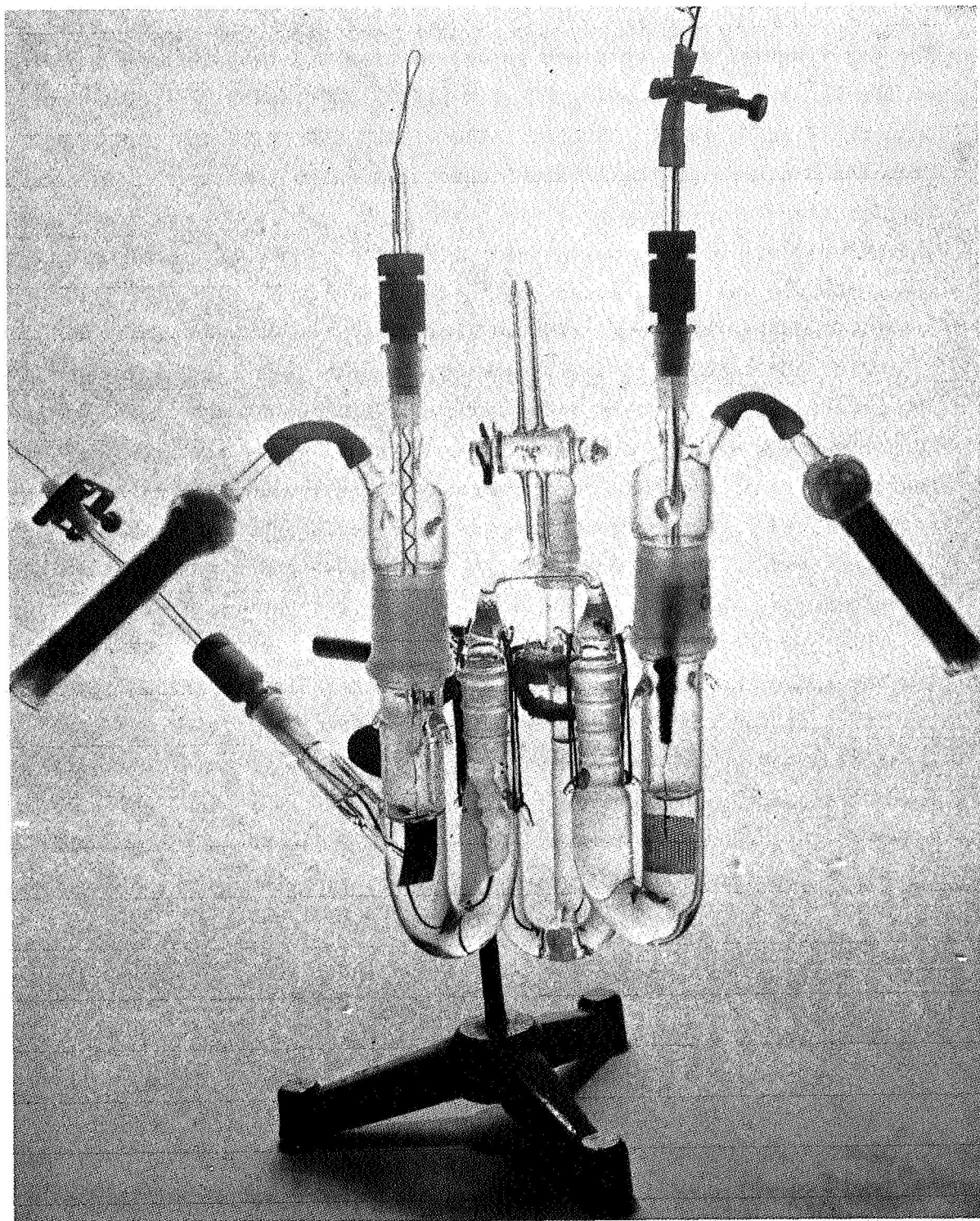


Figure 75. Hittorf Cell Schematic



5AL21-3/16/67-C1B

Figure 76 . Hittorf Cell

Measurement of Transference Numbers

The experimental data obtained in determining the transference numbers of the Li^+ ion in 1 M LiClO_4/PC , 1 M $\text{LiClO}_4/\text{DMF}$, and 1 M LiClO_4/AN are summarized in Table 41. Nickel cathodes and silver anodes were used. From the decrease of the lithium concentration in the anolyte, one value for the transference number of the cation, t_+ , was obtained. Because of the uncertainty of the coulometric efficiency of the lithium deposition, the catholyte was not examined in the case of 1 M LiClO_4/PC . In the other two cases, the total lithium content of the cathode compartment, including the cathodic deposit, was determined; such a lithium deposit apparently did not form in acetonitrile. From the change in the cathode compartment, a second value for t_+ was obtained. The divergence within the two pairs of t_+ values, for DMF and AN, is indicative of the limits of the method. Because small concentration changes in the order of 3 to 5 percent had to be determined by an atomic absorption method which had an accuracy of about 1 percent, a considerable experimental uncertainty resulted for the loss or gain of lithium in the electrode compartments, and hence for the transference numbers. Another factor further limits the exactness of the results. The ions can be heavily solvated and carry along a number of solvent molecules when migrating in an electric field. An imbalanced transport of solvent may result if cation and anion are solvated to a different extent. Taking this into consideration, the agreement between values obtained by Hittorf experiments and those calculated for ion mobilities (at infinite dilution) is good.

As indicated by the data given in Table 42, the chloride content rather than the lithium content was determined in the case of LiCl/DMF electrolytes. According to weight loss determinations, the anodic dissolution of the silver anode was quantitative. The silver chloride was soluble in the electrolyte but precipitated on dilution with water. The chloride remaining in solution was titrated and the numbers are listed as "Adjusted Loss of Cl in the Anolyte." In some cases, a lithium deposit at the cathode was not observed, and spurious analysis results appeared to have resulted in such cases (such data was omitted in Table 42).

TABLE 41

DETERMINATION OF TRANSFERENCE NUMBERS, t , FOR LiClO_4
ELECTROLYTES BY THE HITTORF METHOD

Solute	Solvent	Total Charge, Coulombs	Loss of Li in Anolyte, moles	t_+ From Anolyte Data	Gain of Li in Cathode Compartment, moles	t_+ From Catholyte Data	t_+ Average From Hittorf Data	t_+ From Λ_0 Values
1 M LiClO_4 #2	PC #2-7	386	7.5×10^{-4}	0.19			0.19	0.28
1 M LiClO_4 #2	DMF #3-4	434	1.00×10^{-3}	0.22	1.2×10^{-3}	0.27	0.25	0.22
1 M LiClO_4 #2	AN #3-1	370	1.46×10^{-3}	0.38	9.9×10^{-4}	0.26	0.32	0.40

TABLE 42

DETERMINATION OF TRANSFERENCE NUMBERS, t , IN LiCl/DMF BY THE HITTORF METHOD

Solute	Solvent	Total Charge, Coulombs	Cell Current, milliamperes	Adjusted Loss of Cl in Anolyte, moles	t_+ From Anolyte, Data	Loss of Cl in Catholyte, moles	t_+ From Catholyte, Data	t_+ Average Value
1.25 M LiCl #2	DMF #3-1	216	10	6.1×10^{-4}	0.27	1.6×10^{-3}	0.27	0.27
1 M LiCl #2	DMF #3-1	398	12	6.2×10^{-4}	0.15			0.15
1 M LiCl #2	DMF #4-2	486	15	7.6×10^{-4}	0.15			0.15
1 M LiCl #2	DMF #3-3	344	12	9.0×10^{-4}	0.25			0.25
0.1 M LiCl #2	DMF #4-2	63.4	2.2	1.6×10^{-4}	0.24	4.6×10^{-4}	0.30	0.27

Average Value From Hittorf Data: $t_+ = 0.22$ Value From Λ_0 Values: $t_+ = 0.21^*$ * $t_+ = 0.30$ From Λ_0 -Values of Ref. 58

A value of $t_+ = 0.22$ was obtained as the average from these measurements with LiCl/DMF. This compares with $t_+ = 0.21$ calculated from our ion mobility data, or $t_+ = 0.30$ if the value of $\Lambda_0 = 25.0 \text{ ohm}^{-1} \text{ cm}^2$ of Ref. 58 is preferred.

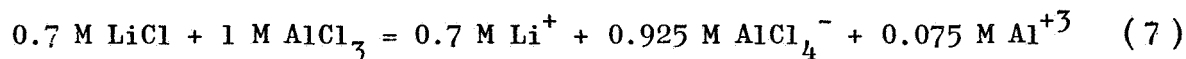
Two attempts were made to determine the transference number of the Li^+ ion in LiAsF_6/MF . No conclusive results could be obtained with either solution, 1.1 M LiAsF_6 #1/MF #2-1, or 1.1 M LiAsF_6 #1/MF #2-5. Slight increases in lithium content were determined in both anode and cathode compartment. Although no volume changes were apparent, some solvent may have had evaporated during the experiment, thus distorting the concentration changes caused by ion migration.

Study of Solutions Containing LiCl and AlCl_3

Hittorf experiments were made with various solutions containing both LiCl and AlCl_3 ; the results are summarized in Table 43. The interpretation of the results is qualitative because these systems are not defined well enough. Transference numbers were not calculated.

Aluminum was found to accumulate and the lithium concentration, as expected, to decrease in the anolyte during experiments with PC and AN solutions. The charge corresponding to the observed concentration changes was calculated, assuming a single lithium and aluminum species, with n as the number of electrons per ion. The catholyte was not studied because of the ill-defined cathode process.

In the case of PC and AN, the results are consistent with the quantitative formation of AlCl_4^- from Cl^- ions introduced by the LiCl with some positive Al species remaining, according to



Because of the presence of some positively charged aluminum species in addition to the negatively charged one, the number of coulombs carried by

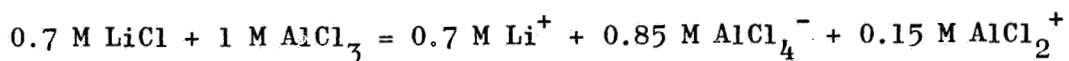
TABLE 43

HITTORF EXPERIMENTS WITH ELECTROLYTES CONTAINING LiCl AND AlCl_3

Solutes	Solvent	Total Charge, coulombs	Change of Lithium Content in Anolyte	Change of Aluminum Content in Anolyte	Change of Aluminum Content in Catholyte
0.7 M LiCl #2 + 1 M AlCl_3 #3	PC #2-10	432	-5.8×10^{-4} mole (corresponds to n x 56 coulombs)	$+3.3 \times 10^{-3}$ mole (corresponds to n x 318 coulombs)	
0.7 M LiCl #2 + 1 M AlCl_3 #3	PC #2-10	461	-9.5×10^{-4} mole (corresponds to n x 92 coulombs)	$+2.52 \times 10^{-3}$ mole (corresponds to n x 244 coulombs)	
1 M LiCl #2 + 0.05 M AlCl_3 #3	DMF #3-3 + DMF #3-4	345		Not determined	$+4.5 \times 10^{-5}$ mole (corresponds to n x 4.3 coulombs)
0.5 M LiCl #2 + 0.05 M AlCl_3 #3	DMF #3-5	251		-4.6×10^{-5} mole (corresponds to n x 4.4 coulombs)	$+8.9 \times 10^{-5}$ mole (corresponds to n x 8.6 coulombs)
0.7 M LiCl #2 + 1 M AlCl_3 #3	AN #4-1	461	-1.75×10^{-3} mole (corresponds to n x 175 coulombs)	$+3.04 \times 10^{-3}$ mole (corresponds to n x 294 coulombs)	

lithium and aluminum as determined from concentration changes, theoretically should not be equal to the total charge passed.

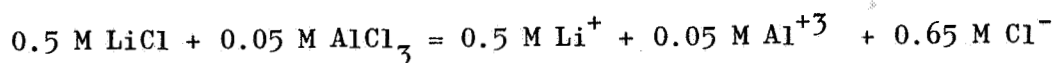
From these Hittorf measurements it cannot be decided whether Eq. 7 or a somewhat different one applies, such as e.g.,



NMR measurements, however, confirmed Eq. 7.

In the case of $\text{LiCl} + \text{AlCl}_3/\text{DMF}$, a decrease of the aluminum concentration was noticed in the anolyte. An increase was found in the catholyte which was examined under the assumption that no aluminum was cathodically deposited. The lithium concentrations were not determined because they were much higher than the aluminum concentrations. The changes of the aluminum content of anolyte and catholyte were not found equal as it should have been; the concentration changes, however, were small and not too far beyond the detection limit of the analysis method.

The results in DMF indicate the presence of a positively charged aluminum species. The $0.5 \text{ M LiCl} + 0.05 \text{ M AlCl}_3/\text{DMF}$ electrolyte had probably the following composition:

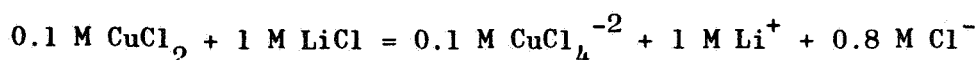


Assuming a three times lower mobility for the Li^+ ion than for the Cl^- ion, and a relatively low mobility for Al^{+3} because of heavy solvation, it can be estimated that the aluminum species should have carried approximately 6 to 15 percent of the current. This is fulfilled reasonably well by the present data ($n = +3$), although the presence of another, additional aluminum species cannot be ruled out.

Study of Solutions Containing Copper Halides

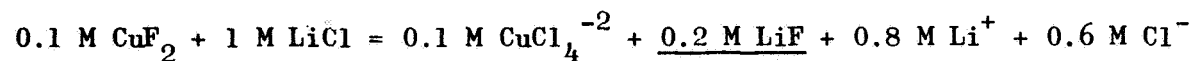
In all cases where copper halide had been added to LiCl or LiClO₄ electrolytes, the copper content in the anode compartment appeared to increase during Hittorf experiments as indicated in Table 44. This indicates that negatively charged copper complex ions were present.

The contribution to the current transport was relatively high in the case of 0.1 M CuCl₂ + 1 M LiCl/DMF. This is consistent with a quantitative formation of CuCl₄⁻² ions according to



Assuming an equivalent conductance for the Li⁺ ions in the order of 25 percent of the one for Cl⁻ ions, and assuming the same equivalent conductance for 1/2 CuCl₄⁻² as for Cl⁻ (in analogy to aqueous solutions), the copper species would transport about 1/6 of the total current. The figures found in the Hittorf experiments would correspond to 15 and 19 percent, respectively.

The contribution according to the observed concentration change was 18 x n percent in the case of 0.1 M CuF₂ + 1 M LiCl/DMF, n being the (average) charge of the copper species. Again, it is likely that a quantitative formation of CuCl₄⁻² occurred, which was accompanied by the precipitation of LiF; the composition was accordingly:



The contribution of the copper species to the current transport in such a system was higher than in the case of the CuCl₂ dissolved in 1 M LiCl/DMF, although it would not be expected to be quite as high as the experimental data, 18 x n percent, indicates.

TABLE 44

HITTORF EXPERIMENTS WITH ELECTROLYTES CONTAINING COPPER HALIDES

Solute	Solvent	Total Charge, Coulombs	Change of Cu Content in Anolyte, moles	Corresponding Charge, Coulombs
0.1 M CuF_2 #3 + 1 M LiClO_4 #3	DMF #6-12	288	$+6.2 \times 10^{-5}$	$6.0 \times n^*$
0.1 M CuF_2 #3 + 1 M LiCl #3	DMF #6-12	288	$+5.5 \times 10^{-4}$	$53 \times n$
0.0094 M CuF_2 #3 + 0.7 M LiCl #3 + 1 M AlCl_3 #4	PC #6-3	288	0	**
0.00016 M CuF_2 #3 + 1.1 M LiAsF_6 #1	MF #6-2	274	$+9.2 \times 10^{-6}$	**
0.0011 M CuCl_2 #2 + 1 M LiClO_4 #2	PC #2-7 + PC #2-8	347	$+1.0 \times 10^{-5}$	$1.0 \times n$
0.1 M CuCl_2 #2 + 1 M LiClO_4 #2	DMF #3-4	288	$+1.85 \times 10^{-4}$	$18 \times n$
0.1 M CuCl_2 #2 + 1 M LiCl #2	DMF #4-2	288	$+2.16 \times 10^{-4}$	$21 \times n$
0.1 M CuCl_2 #2 + 1 M LiCl #2	DMF #4-2	398	$+3.92 \times 10^{-4}$	$38 \times n$
0.006 M CuCl_2 #2 + 0.7 M LiCl #3 + 1 M AlCl_3 #4	PC #6-3	288	-1.9×10^{-5}	**

*Charge (average) of copper species

**Result inconclusive: see text

The accumulation of copper in the anolyte was relatively much smaller in the case of CuF_2 dissolved in 1 M $\text{LiClO}_4/\text{DMF}$ solution than in 1 M LiCl/DMF . The presence of a negatively charged copper species is still indicated, but there appears to have existed a mixture of positively charged (or neutral) copper species and negatively charged copper species. The tendency of Cu^{+2} to form complexes with ClO_4^- seems to exist but to be considerably weaker than with Cl^- .

A formation of negative copper complex ions was also indicated in the case of 0.0011 M CuCl_2 + 1 M LiClO_4/PC . Considering the small ratio of CuCl_2 to LiClO_4 , a relatively large portion of the current was carried by copper species, according to the concentration changes in the anolyte. Not enough Cl^- ions were available to form CuCl_4^{2-} quantitatively, but the tendency to form perchlorate complexes such as $\text{Cu}(\text{ClO}_4)_4^{2-}$ may have been sufficient. Such perchlorate complexes should form more easily in PC than in DMF because of the lower tendency to form solvent complexes.

Experiments with $\text{LiCl} + \text{AlCl}_3/\text{PC}$ electrolytes were inconclusive. Copper containing sediments which formed during the experiment indicated that the systems were not stable. In one case, it was established that the copper content in the anolyte as well as in the catholyte decreased. Concentration changes caused by migration changes could not be separated from concentration changes caused by this precipitation, and evaluation of the results is impossible.

In the case of $\text{CuF}_2 + \text{LiAsF}_6/\text{MF}$, increases in copper concentration were found in anolyte and catholyte. This may have been caused by evaporation of solvent, or by a slight copper impurity in the molybdenum electrodes. These results therefore did not permit any conclusions.

DIFFUSION COEFFICIENTS

Two methods were applied to determine diffusion coefficients. In the porous disk method, molecular diffusion coefficients were measured, whereby anions and cations were constrained by electro-neutrality to diffuse at the same rate. Diffusion coefficients determined by chronopotentiometry are those of the species actually undergoing electrolysis, normally in the presence of excess electrolyte.

Determination by Porous Disk Method

A method described by Wall et al (Ref. 63, 64, and 65) was employed to measure the diffusion coefficients of solutes at 25 C. A porous disk is filled with the solution to be studied and suspended in a large volume of pure solvent. The apparent weight is measured as a function of time, and the integral diffusion coefficient, D , determined using the equation

$$\log [W(t) - W(\infty)] = -\alpha Dt + b$$

where $W(t)$ is the apparent weight of the suspended disk at time t , $W(\infty)$ is the weight after equilibrium has been reached. α is an apparatus constant which was determined for two disks using an aqueous 1.5 M KCl solution ($D = 1.87 \times 10^{-5} \text{ cm}^2 \text{ sec}^{-1}$ at 25 C, according to Ref. 66).

The recommended micro-porous filter disks (2-inch diameter, 1/4 inch thick; porosity No. 10) were obtained from the Selas Corporation of America. They were filled after evacuation with the solution to be studied and allowed to soak overnight. The disks were suspended on a fine wire from the arm of an analytical chainomatic balance. The container with about 1-1/2 liter of solvent was placed in the 25 C temperature bath underneath the balance, and a flow of nitrogen was swept over the solvent.

The results are given in Table 45. The composition of the solution used to fill the disk is listed in the first column, the bulk pure solvent in

TABLE 45
DIFFUSION COEFFICIENTS AT 25 C

Solution	Solvent	Diffusion Coefficient, cm ² sec ⁻¹
1 M LiClO ₄ #3/PC #4-3	PC #4-1, 4-2, 4-4	2.58 x 10 ⁻⁶
0.7 M LiCl #3 + 1 M AlCl ₃ #4/PC #4-5	PC #5-1, 5-2, 5-4	3.04 x 10 ⁻⁶
1 M LiClO ₄ #2/DMF #5-1	DMF #5-1	7.30 x 10 ⁻⁶
1 M LiCl #2/DMF #6-1	DMF #6-2	{ 5.87 x 10 ⁻⁶
1 M LiCl #2/DMF #6-2	DMF #6-1, 6-2, 6-4	
1 M LiCl #2 + 0.075 M AlCl ₃ #3/DMF #6-2	DMF #6-3, 6-5	5.72 x 10 ⁻⁶
1 M LiClO ₄ #2/AN #4-4	AN #5-5, 5-6, 5-7	1.71 x 10 ⁻⁵
0.7 M LiCl #3 + 1 M AlCl ₃ #3/AN #4-4	AN #5-1, 5-2, 5-3	1.69 x 10 ⁻⁵
1 M LiClO ₄ #3/MF #2-1	MF #2	1.68 x 10 ⁻⁵
1.1 M LiAsF ₆ #1/MF #2-1	MF #2-2, 2-3, 2-4	1.54 x 10 ⁻⁵

the second column. The diffusion coefficients listed are integral values for the diffusion of the solute into the pure solvent. A logarithmic plot of the apparent disk weight versus time produced a straight line in all cases, usually with some deviation during the first 10 minutes after immersion of the disk.

As expected from viscosity considerations, the diffusion coefficients measured with propylene carbonate solutions were generally a factor of about 2 lower than values obtained with dimethyl formamide solution. These in turn were another factor of two lower than electrolytes based on acetonitrile or methyl formate.

In an effort to establish a way to estimate diffusion coefficients for electrolytes where no measured data are available, the measured diffusion coefficients of Table 45 are compared in Table 46 with the specific conductance and the viscosity of the respective solution, and also with the solvent viscosity. A constant number for all electrolytes was approached best by the products of diffusion coefficient and solvent viscosity, $D \times \eta$ solvent. The diffusion coefficients for new electrolytes may, therefore, be estimated by dividing 6×10^{-8} by the solvent viscosity. It should be noted, however, that the present comparison was based on (1) lithium salt solution, and (2) 1-molar solutions.

Determination by Chronopotentiometry

Technique. The chronopotentiometric technique was employed in an attempt to determine the diffusion coefficient of some electroactive species. Unfortunately, the systems selected were not sufficiently electrochemically characterized and an unambiguous determination of diffusion coefficients was not possible.

TABLE 46

COMPARISON OF DIFFUSION COEFFICIENT, D , WITH SOLUTION CONDUCTANCE, λ ,
AND VISCOSITY, η SOLUTION, AND SOLVENT VISCOSITY, η SOLVENT, AT 25 C

Solution	D , $\text{cm}^2 \text{sec}^{-1}$	$\frac{D}{\lambda}$ $\text{ohm cm}^3 \text{sec}^{-1}$	$D \times \eta$ solution, dyne	$D \times \eta$ solvent, dyne
1 M LiClO_4/PC	2.58×10^{-6}	5.04×10^{-4}	1.83×10^{-7}	6.40×10^{-8}
0.7 M $\text{LiCl} + 1 \text{ M AlCl}_3/\text{PC}$	3.04×10^{-6}	4.63×10^{-4}	2.18×10^{-7}	7.55×10^{-8}
1 M $\text{LiClO}_4/\text{DMF}$	7.30×10^{-6}	2.30×10^{-3}	1.38×10^{-7}	5.78×10^{-8}
1 M LiCl/DMF	5.87×10^{-6}	6.90×10^{-4}	1.07×10^{-7}	4.65×10^{-8}
1 M $\text{LiCl} + 0.075 \text{ M AlCl}_3/\text{DMF}$	5.72×10^{-6}	7.36×10^{-4}	1.31×10^{-7}	4.54×10^{-8}
1 M LiClO_4/AN	1.71×10^{-5}	5.37×10^{-4}	1.13×10^{-8}	5.75×10^{-8}
0.7 M $\text{LiCl} + 1 \text{ M AlCl}_3/\text{AN}$	1.69×10^{-5}	3.32×10^{-4}	1.13×10^{-8}	5.68×10^{-8}
1 M LiClO_4/MF	1.68×10^{-5}	1.31×10^{-3}		5.68×10^{-8}
1.1 M LiAsF_6/MF	1.54×10^{-5}	4.58×10^{-4}	1.24×10^{-8}	5.21×10^{-8}

In constant current chronopotentiometry, a constant current density, i_0 , is impressed upon an electrode and its potential is measured as a function of time. The transition time, τ , the time at which the reductant concentration is zero at the electrode surface, is given by the Sand equation:

$$\tau^{1/2} = \frac{nFC(\pi D)^{1/2}}{2i_0}$$

where C is the concentration of the electro-active species, D is its diffusion coefficient, n is the number of electrons involved in the electrode reaction, and F is the Faraday constant. Diffusion coefficients can be calculated from the transition time, provided the concentration of the electroactive species and the other experimental parameters are known.

The chronopotentiograms were recorded on a Beckman Electroscan. The indicating and auxiliary electrodes were placed in opposite arms of an H-cell and were separated by a porous glass frit. The indicating electrode was a Beckman platinum inlay electrode with a projected area of 0.25 cm². The reference electrode was a Ag/AgBr(0.5 M LiBr) electrode.

Lithium Ion in TMA·PF₆/PC. The supporting electrolyte, 0.1 M TMA·PF₆ #1/PC #4-3, was first examined to determine the effect of water and to determine if the background potential was sufficiently cathodic to allow lithium reduction. A cathodic wave was found at -2.21 volts; it was very sharp, stepping to -5.0 volts after the wave. No oxidation wave was found upon reversing the current and, hence, the reduction was irreversible. The $i_0\tau^{1/2}$ -product for this wave was 5.88 ma sec^{1/2} cm⁻² and was constant for current densities of 0.800 to 2.24 ma/cm². The addition of 10 μ l of water (~ 0.017 M) increased the transition time but did not change the shape of the wave; thus, the wave appears to be due to the reduction of water. From the increase in the $i_0\tau^{1/2}$ product, the original solution contained approximately 0.011 M water or 160 ppm. Approximately 20 mg

of LiClO_4 #3 were added to the TMAPF_6/PC solution to give a lithium concentration of 0.0073 M, as verified by atomic absorption. No reduction wave was observed for lithium and, hence, its diffusion coefficient could not be calculated. However, the added lithium perchlorate affected the water wave. A prewave appeared which merged with the water wave. The transition time for the prewave and water wave was identical to the transition time found for water prior to the addition of lithium perchlorate.

The prewave was probably due to the reduction of water with the subsequent precipitation of the reduction product by lithium. The precipitate would be lithium hydroxide or lithium oxide. A gray film built up on the electrode which could be removed by wiping the electrode. Even though the lithium did not undergo direct reduction, it would be possible to calculate a diffusion coefficient for lithium from the Sand equation if the prewave were sufficiently separated from the water wave and the transition time could be determined accurately. Unfortunately, the two waves merged without any definite potential break and no accurate transition time could be measured.

Lithium Ion in $\text{TMA}\cdot\text{PF}_6/\text{DMF}$. No reduction waves for lithium were found in a 0.01 M LiClO_4 #3 + 0.2 M $\text{TMA}\cdot\text{PF}_6$ #1/DMF #6-8 solution because of a too positive background potential.

Copper Fluoride in LiClO_4/PC . A sufficient amount of CuF_2 #3 was added to a 1 M LiClO_4 #3/PC #4-5 solution to make a 0.01 M copper solution. However, not all of the copper dissolved despite stirring for several hours, its concentration being only 3.3×10^{-4} M, as determined by atomic absorption. Only a reduction wave was found which was very irreversible and did not seem to correspond to copper. Therefore, a value for the diffusion coefficient could not be calculated.

Copper Chloride in LiClO_4/PC . A sufficient amount of CuCl_2 #2 was added to a 1 M LiClO_4 #3/PC #4-3 solution to make a 0.01 M copper solution. However, a precipitate was found in the solution, and the solution was decanted into the electrolysis cell. The copper content was analyzed by atomic absorption and found to be 0.0028 M. Four cathodic waves were found; the two most negative waves represented the reduction of water and lithium, the two more positive waves may be due to reduction of copper. The ratio of the transition times of the two waves was not the value expected for two 1-electron reduction steps. The reduction waves appeared to be irreversible and, indeed, upon reversing the current, no oxidation waves appeared at the potentials at which reduction had previously occurred. No diffusion coefficient could be calculated.

Copper Chloride in LiCl/DMF . Chronopotentiograms were obtained with a 0.01 M CuCl_2 #2 + 1 M LiCl #2/DMF #5-1 and a 0.01 M CuCl_2 #2 + 1 M LiCl #2/DMF #6-15 solution. A wave was obtained which was suspected to represent two different reduction processes, i.e., the reduction of a copper complex and of water. More than one copper wave was found, but none of them was reversible. It appears that the complexity of the $\text{CuCl}_2 + \text{LiCl}/\text{DMF}$ system observed in the structural studies is reflected in its electrochemical behavior and a determination of reliable diffusion coefficients was not possible.

Chronopotentiograms obtained with CuCl_2 #2 in 1 M LiClO_4 #2/DMF #6-15 presented the same difficulties as above in assigning waves and determining diffusion coefficients.

DIELECTRIC CONSTANTS

The determination of the dielectric properties of conducting solutions requires the separation of the effects of dielectric relaxation and conductance. Because of the high conductances of the solutions of interest, it was necessary to make the measurements in the microwave region of the frequency spectrum to satisfactorily separate the two factors. The method selected was based on the technique described by Harris and O'Konski (Ref. 67) which involves measurement of the complex propagation constant of the solution, $k = k' + i k''$, where k' represents the effect of dispersion and k'' represents the effect of absorption. Experimental values of k'' , $k''_{\text{EXP.}}$, were corrected for conductivity effects by subtracting a frequency dependent term as suggested by Hasted, Titson, and Collie (Ref. 68) $k'' = k''_{\text{EXP.}} - \frac{4\pi\sigma}{\omega}$. Note that this correction factor $\frac{4\pi\sigma}{\omega}$ decreases with the frequency of measurement, ω . Because of the high conductivity, σ , of the solutions to be measured, reduction of this correction factor to obtain reasonable accuracy dictates that measurements be made at microwave frequencies. Some approximate calculations indicated that measurements should be made at frequencies higher than 1 GHz.

Instrumentation

Standard microwave components are generally available for 8.5 GHz (X-band) and 25 GHz (K-band), so these two frequencies were selected and a microwave bridge apparatus was set up at both of these frequencies. The 8.5 GHz apparatus is shown schematically in Fig. 77. The 25 GHz setup was essentially the same except for the use of a directional coupler rather than an E-H tee for separation of the bridge arms. A correction for standing waves due to internal reflections in the standing wave detector was applied as described in Ref. 6. All measurements were made at room temperature.

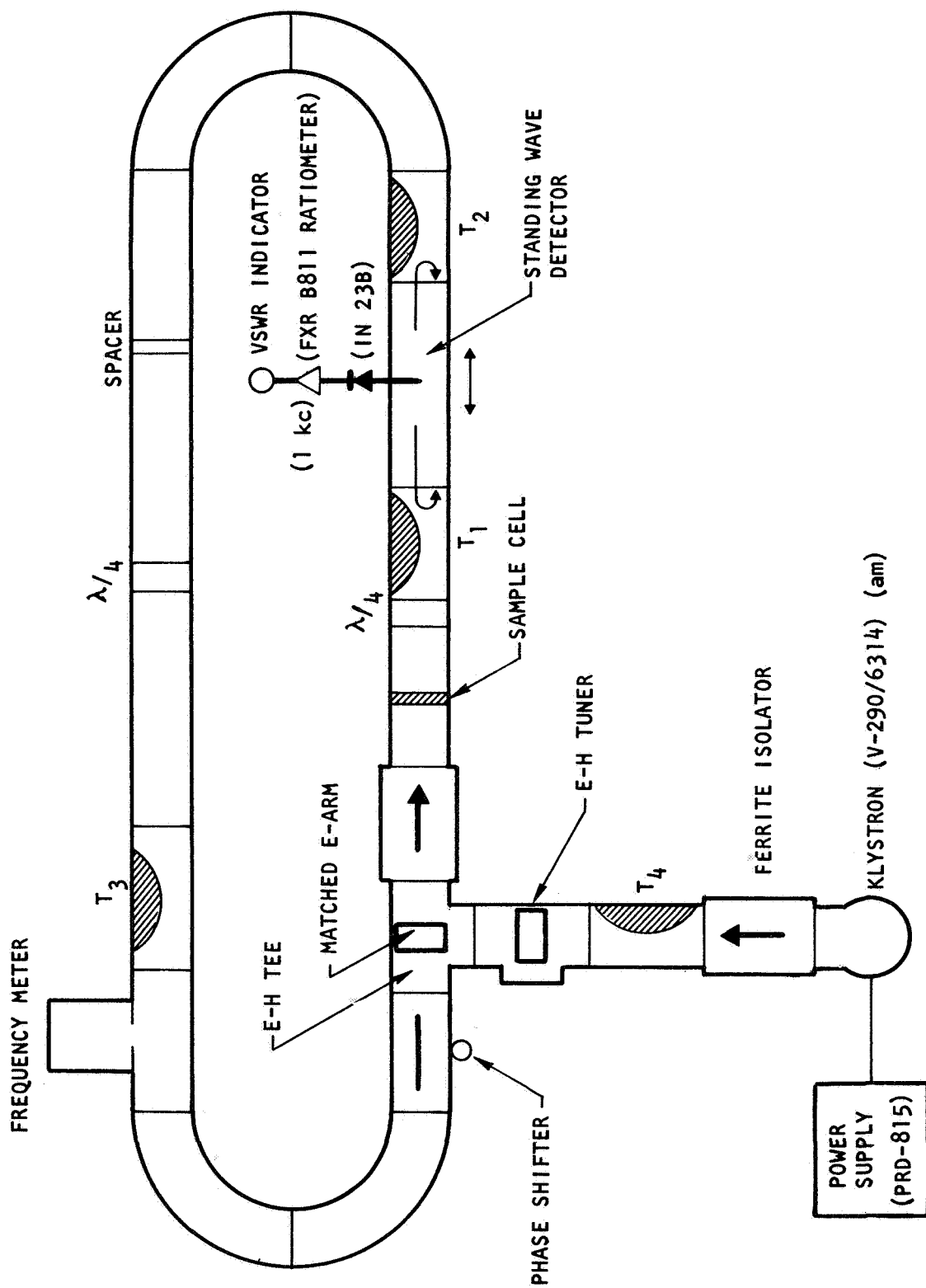


Figure 77. Microwave Setup at 8.5 GHz, $TE_{0,1}$ Mode

Data Reduction

A series of four computer programs were written to assist with the various phases of the data reduction. To minimize errors in data manipulation, a procedure was developed which eliminated manual copying of the data prior to input to the computer. The first program converted the measured standing wave amplitudes and positions into phase shift and attenuation data. A second program was used to correct these data for the effects of the internal waves generated by the standing wave detector. These corrections were particularly important in the 8.5 GHz setup. The resulting phase shifts and attenuations were then compared with those calculated for an array of k' and k'' values using a third program. A series of liquid cell lengths were used at each measurement frequency to unambiguously determine the appropriate k' and k'' . The extrapolation (see below) to obtain the static value of the dielectric constant, k_0 , was also programmed for the computer. Use of these computer programs reduced greatly the time required to reduce the large amount of data required for each measurement.

Extrapolations to obtain the static dielectric constants were performed on the basis of a Cole-Cole plot (Ref. 69). The curves were fit to the values obtained at 8.5 and 25 GHz and the square of the optical index of refraction (equivalent to infinite frequency).

Results

The results are presented in Table 47 along with the data for each solution. Because all three observed data points are required to obtain the circular curve fit, the effect of uncertainties in the data can be quite large. To obtain an indication of the sensitivity of the extrapolation to data fluctuations, the computerized curve fit was repeated for 0.2 increments in each of the data points. The resultant variations in k_0 are included in Table 47.

The Cole-Cole plots for the acetonitrile solutions are shown in Fig. 78. Agreement between the extrapolated value of 39.3 and the literature value of 37.5 is well within the limits of the technique when only three data

TABLE 4/

DIELECTRIC CONSTANTS

Sample	n_D^2	25 GHz			8.5 GHz			k_o
		k'	$k''_{EXP.}$	k''	k'	$k''_{EXP.}$	k''	
AN #4-3, #4-2	1.80	28.7	13.0	13.0	35.1	8.2	8.2	39.3 ± 0.6
1 M LiClO ₄ #2/AN #4-2	1.84	20.3	13.5	11.2	26.0	14.8	8.0	30.5 ± 0.4
1 M AlCl ₃ #3 + 0.7 M LiCl #3 in AN #4-4	1.86	18.2	13.6	9.9*	24.3	16.3	5.5*	26.6 ± 0.3
DMF #6-18	2.04	13.4	14.7	14.7	29.1	15.3	15.3	41.9 ± 0.5
1 M LiCl #3/DMF #6-17	2.08	9.5	10.0	9.4	19.7	15.0	13.2	41.4 ± 1.4
1 M LiCl #2 + 0.075 AlCl ₃ #3 in DMF #6-10	2.10	8.8	8.7	8.1	18.6	13.8	12.2	41.8 ± 1.6
1 M LiClO ₄ #3/DMF #6-18	2.07	9.4	9.3	7.0	17.5	12.9	6.1	22.6 ± 0.4
PC #4-5	2.02	7.2	9.9	9.9	16.5	20.8	20.8	
1 M LiClO ₄ #3/PC #4-3	2.03	6.6	5.7	5.3	11.2	10.3	9.2	
1 M AlCl ₃ #4 + 0.7 M LiCl #3 in PC #4-5	2.05	7.1	5.5	5.0	11.2	10.3	8.9	
1 M TEA·F #1/PC #6-2	1.97	6.9	6.8	6.4	12.1	15.6	14.3	
MF #2-6	1.80	7.5	2.5	2.5	8.2	1.3	1.3	8.4 ± 0.5
1.1 M LiAsF ₆ #1/MF #2-5	1.82	6.3	5.1	2.7	9.1	10.8	3.7	27.4 ± 6.0

*Because no conductance measurement was available for this solution, the conductance was assumed to be 0.051 ohm⁻¹cm⁻¹, the value obtained for 1 M AlCl₃ #3 + 0.92 M LiCl #2/AN #3-1.

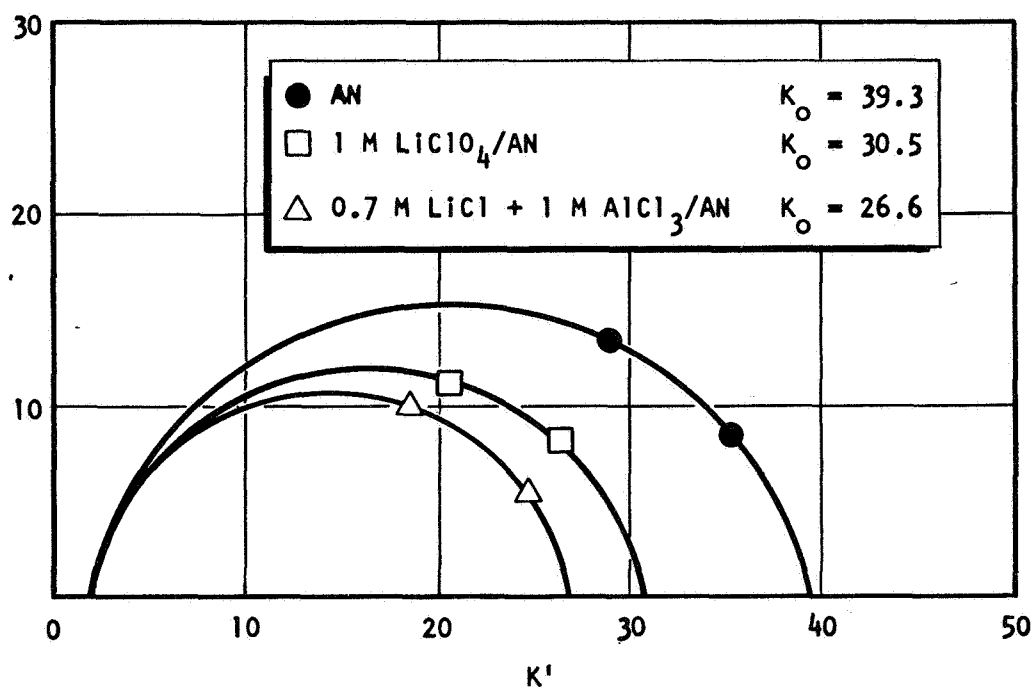


Figure 78. Cole-Cole Plots for AN Solutions

points are available. The extrapolated values for the electrolytes are both lower than for the pure solvent and are significantly different. All three curves have their maxima at a frequency higher than 25 GHz, implying relatively little change (compare with following discussion) in the dielectric relaxation process with addition of salts to AN.

A similar set of plots for DMF solutions is shown in Fig. 79. The agreement with the literature value for the pure solvent, 41.9 as compared to 37.2 (Ref. 13), is again acceptable. Addition of LiCl or LiCl + AlCl₃ to DMF produced a very small change in the extrapolated value of the dielectric constant, but the observed shift of the maximum to lower frequency implies a slower relaxation process in these electrolytes. A 1 M LiClO₄ solution on the other hand shows no change in relaxation time but a drastic decrease in the extrapolated dielectric constant. The above results are consistent with the indications from conductivity data that ion-pairing occurs in LiCl electrolytes but not (or to a much smaller extent) in LiClO₄ electrolytes.

The data for PC taken at 8.5 GHz lies well to the origin side of the semi-circular plot, as shown in Fig. 80, thus indicating that the relaxation process in PC is very slow compared to AN or DMF. This is not surprising because the NMR results in PC indicated that viscosity effects in PC were rather pronounced; the same effects would be expected to hinder dielectric relaxation. Because of the slow dielectric relaxation, the extrapolations based on these data were found to have no significance, and meaningful values of k_0 could not be obtained. Extension of the measurements to lower frequencies would allow an accurate extrapolation in the case of the pure solvent. However, because the conductivity correction increases inversely with frequency it would become essentially equal to k''_{EXP} at a frequency near the midpoint of the curve in the electrolytes. This would render such measurements useless.

The results of MF solutions are shown in Fig. 81. Good agreement with the literature value of 8.5 (Ref. 14) was obtained and the uncertainty in the extrapolation was small due to the very fast relaxation process in the

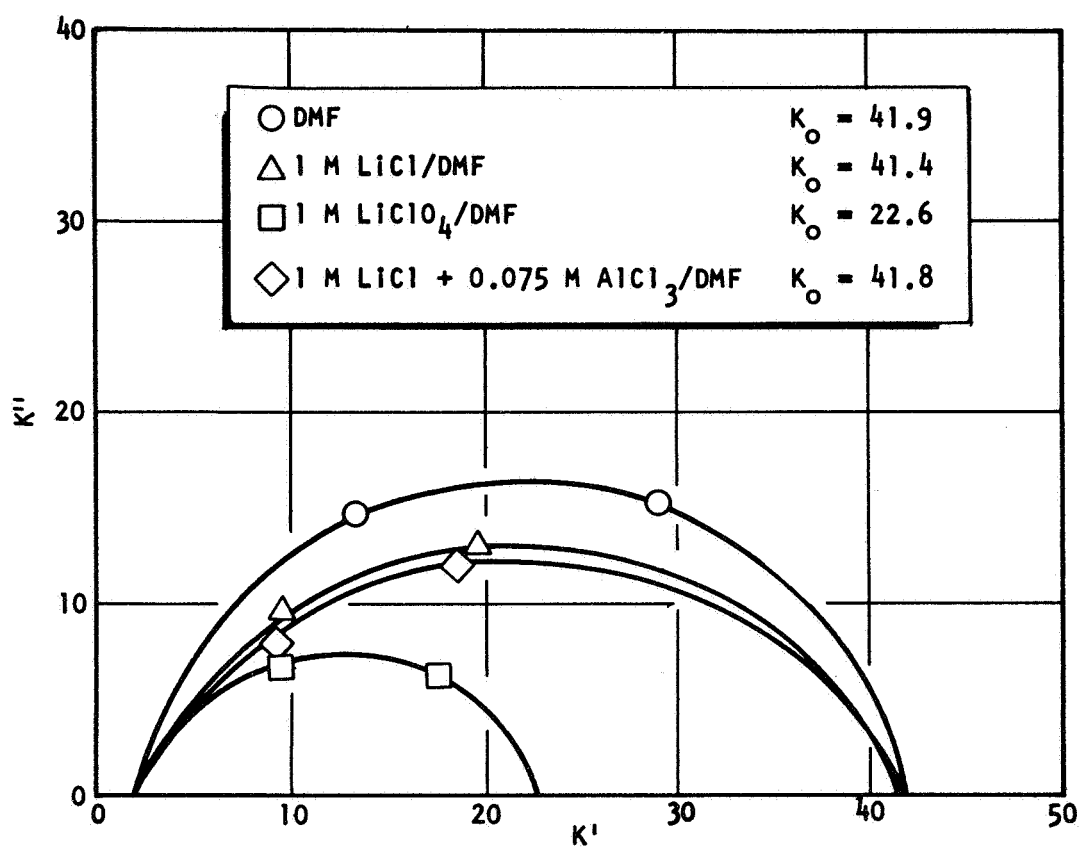


Figure 79. Cole-Cole Plots for DMF Solutions

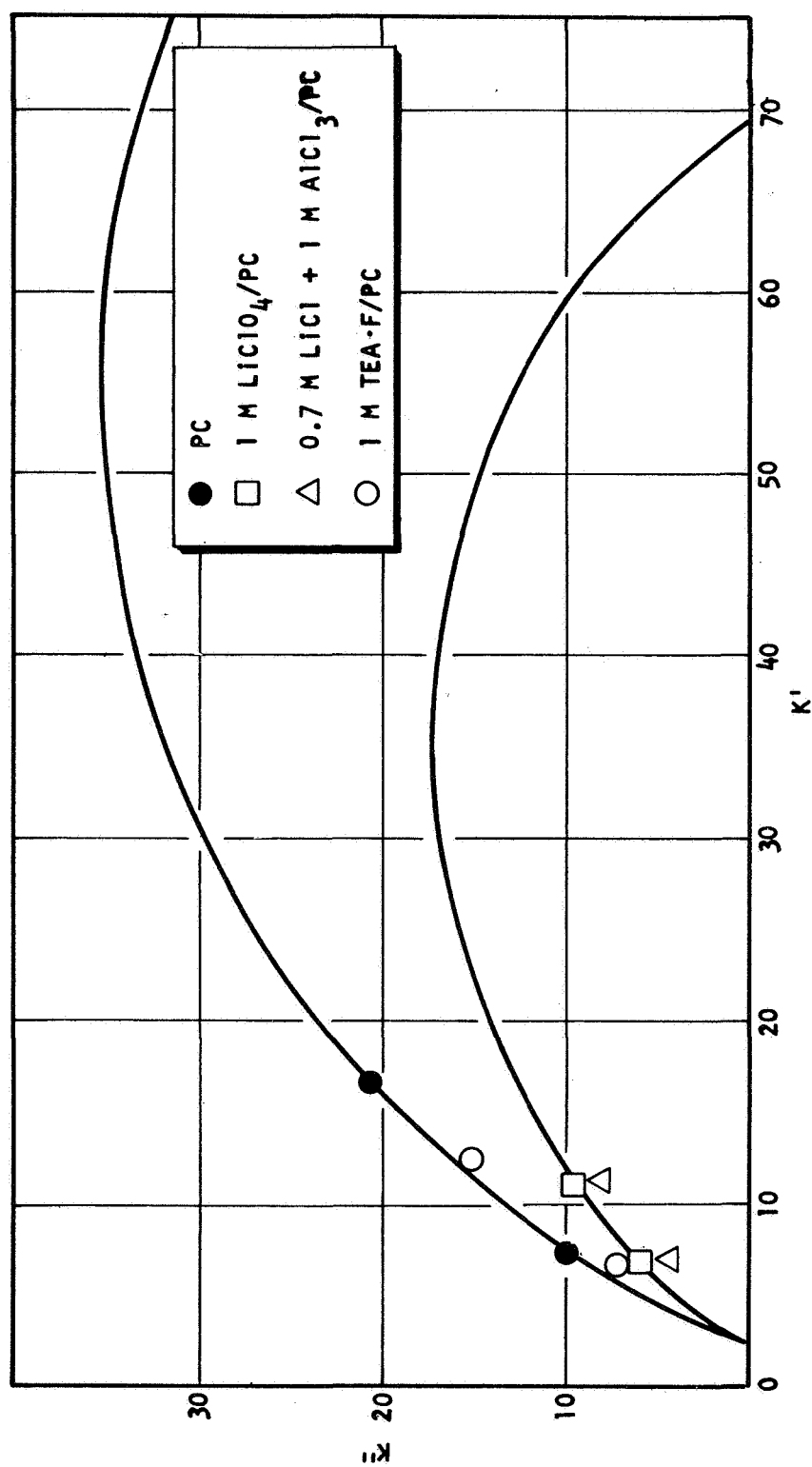


Figure 80. Cole-Cole Plots for PC Solutions

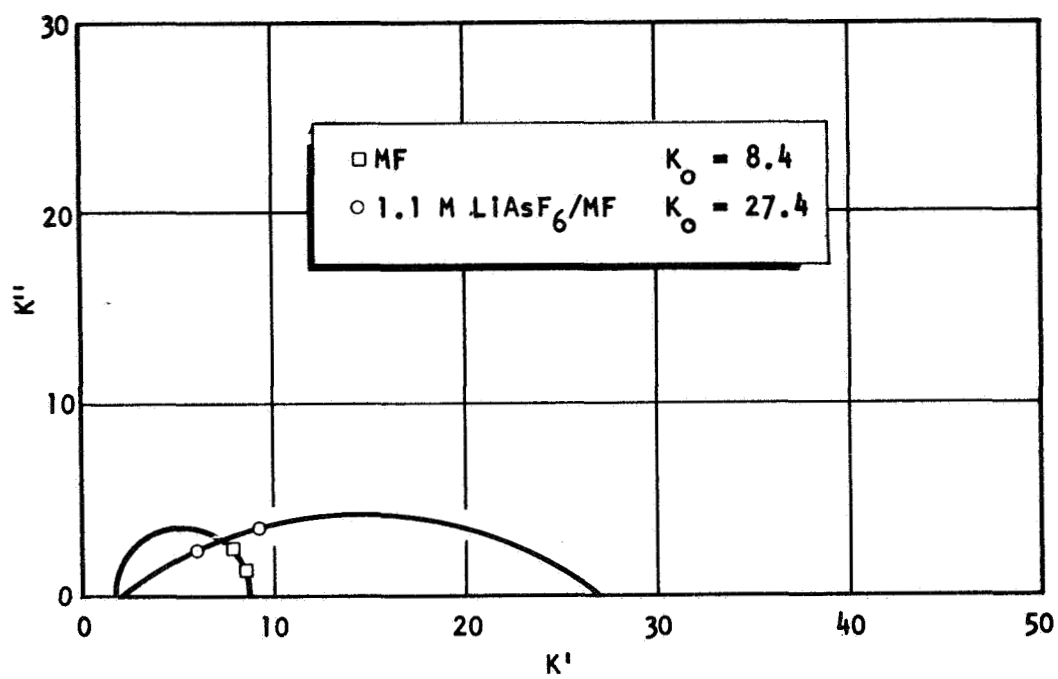


Figure 81. Cole-Cole Plots for MF Solutions

pure solvent. Addition of 1.1 M LiAsF_6 resulted in a much longer relaxation time and a large increase in the extrapolated value of the dielectric constant. This increase in dielectric constant with addition of an electrolyte is contrary to the effects observed in the other solvents. A more comprehensive study of these MF systems, including effects of concentration and possible impurities, would be required to fully interpret this unusual result. A large uncertainty in the extrapolation again arises from the adverse relationship of measurement frequency to relaxation time but a more suitable relaxation time would be predicted for intermediate salt concentrations.

DISCUSSION OF RESULTS

ELECTROLYTE SOLUTIONS

Uni-univalent Electrolytes

Ions Formed. According to structural studies by NMR and indications from physical property determinations, ions appeared to form as expected in the uni-univalent electrolytes: LiClO_4 formed Li^+ and ClO_4^- , LiCl formed Li^+ and Cl^- , and $\text{TMA}\cdot\text{PF}_6$ formed TMA^+ and PF_6^- ions. The tetraalkylammonium ion was found in $\text{TMA}\cdot\text{F}$ and $\text{TEA}\cdot\text{F}$ solutions, but the existence of the fluoride ion was not verified in such solutions. It appears that Li^+ and BF_4^- or PF_6^- formed in solutions made up by adding BF_3 or PF_5 , respectively, to a slurry of LiF ; this was concluded because stoichiometric amounts of lithium and boron or phosphorous were found. The existence of Li^+ and AsF_6^- ions was indicated by NMR measurements of LiAsF_6/MF solutions.

Solvation. Of the monovalent ions, only lithium appeared to solvate to a significant extent according to conductivity studies. Reliable solvation numbers could not be obtained. For the lithium ion, solvation numbers between 0.6 and 3 were calculated from sonic velocity data, and from ion mobility figures values of 2 to 3 were obtained. Indirect evidence for the solvation of the Li^+ ion was also found by NMR.

Ion Pairing. Equivalent conductance data at low concentrations appeared to indicate that ion pair formation was significant in LiCl/PC and LiCl/DMF electrolytes; it seemed to be somewhat stronger in PC than in DMF. The ion pair formation probably caused the specific conductance at 25 C of a 1 M LiCl/DMF solution to be considerably lower ($8.50 \times 10^{-3} \text{ ohm}^{-1} \text{ cm}^{-1}$) than that of a 1 M $\text{LiClO}_4/\text{DMF}$ solution ($2.03 \times 10^{-2} \text{ ohm}^{-1} \text{ cm}^{-1}$).

Interactions in AlCl_3 Systems

Solvent and Chloride Complexes. Strong interactions were observed when AlCl_3 (or rather Al_2Cl_6) was dissolved. The high exothermic heat of solution is indicative of strong complex formation. Such complexes, $\text{Al}[\text{PC}]_6^{+3}$, $\text{Al}[\text{DMF}]_6^{+3}$, and $\text{Al}[\text{AN}]_6^{+3}$ were indeed found by NMR studies; a similar complex, $\text{Al}[\text{H}_2\text{O}]_6^{+3}$, is known to exist in acidic aqueous solution.

Chloride ions from AlCl_3 or from an additional source such as LiCl also form aluminum complexes, mainly AlCl_4^- . In the case of PC and AN, this complex formation is stronger than the formation of the solvent complex; and chloride ions replace solvent molecules in the coordination sphere to form AlCl_4^- . Provided sufficient chloride is present, aluminum will predominantly exist as AlCl_4^- in PC and AN. In the case of DMF, the solvent complex, $\text{Al}[\text{DMF}]_6^{+3}$, is more stable and free chloride ions exist in a AlCl_3/DMF solution.

In Hittorf experiments with solutions containing LiCl and AlCl_3 , the aluminum was indeed found to migrate to the anode in PC and AN, but to the cathode in DMF.

Complexing Property of Solvents

A brief summary of the species found in Al and Li containing electrolytes is shown in Table 48 along with a listing of some solvent properties. To aid and enlarge the intercomparison of solvents, water is included in the table. As this table indicates, the type of species that is formed on dissolving AlCl_3 in the various solvents does not correlate with either the dielectric constant or the electric dipole moment. Note that the dielectric constants of DMF and AN are virtually the same, yet on dissolving AlCl_3 the species $\text{Al}[\text{DMF}]_6^{+3}$ is the preferred species in DMF while AlCl_4^- is the preferred species in AN. Also note that the dielectric constant of PC is much different than that of AN, yet in both solvents the preferred species is AlCl_4^- .

TABLE 48
SUMMARY OF COMPLEXING PROPERTY OF SOLVENTS

	DMF	AN	PC	Water
Solvent Structure	$\begin{array}{c} \text{H} \\ \\ \text{O}=\text{C} \\ \\ \text{N}-\text{CH}_3 \\ \\ \text{CH}_3 \end{array}$	$\begin{array}{c} \text{N} \\ \\ \text{C} \\ \\ \text{H}-\text{C}-\text{H} \\ \\ \text{H} \end{array}$	$\begin{array}{c} \text{O} \\ \\ \text{C} \\ / \quad \backslash \\ \text{O} \quad \text{O} \\ \quad \\ \text{CH}_3-\text{C}-\text{C}-\text{H} \\ \quad \\ \text{H} \quad \text{H} \end{array}$	$\begin{array}{c} \text{H} \\ \backslash \\ \text{O} \\ / \\ \text{H} \end{array}$
Dielectric Constant	~35	~35	~65	~80
Dipole Moment	3.9	2.7	~4 (?)	1.8
Basicity	High	Low	Low (?)	---
Species in AlCl_3 Solution	$\text{Al}[\text{DMF}]_6^{+3}$ + Cl^-	$\text{Al}[\text{AN}]_6^{+3}$ + AlCl_4^- + $\text{Cl}^- (?)$	$\text{Al}[\text{PC}]_6^{+3}$ + AlCl_4^- + $\text{Cl}^- (?)$	$\text{Al}[\text{H}_2\text{O}]_6^{+3}$ or $\left[\text{Al}(\text{OH})_4 \right]^-$ + Cl^-
Change in Species on addition of LiCl	As Above + $\text{Li}^+ + \text{Cl}^-$	$\text{Al}[\text{AN}]_6^{+3} \rightarrow \text{AlCl}_4^-$ + Li^+	$\text{Al}[\text{PC}]_6^{+3} \rightarrow \text{AlCl}_4^-$ + Li^+	
Change in Species on Addition of LiClO_4	As Above + $\text{Li} + \text{ClO}_4^-$	$\text{Al}[\text{AN}]_6^{+3} \rightarrow [\text{Al}(\text{AN})_x(\text{ClO}_4)_y]^{+3-y} (?)$ + $\text{Li}^+ + \text{ClO}_4^-$		

The dipole moments of DMF and AN are different; the dipole moment of PC is not known, but it is expected to be near that of DMF. If this is true, again there is a lack of correlation. Note further that the dipole moment of water is small, even less than that of AN, yet water behaves more like DMF than AN in interacting with aluminum ions.

Because the species $\text{Al}[\text{solvent}]_6^{+3}$ represent very close range effects, it is reasonable to try to correlate such species formation with some chemical behavior (in contrast to a physical or bulk property) of the solvent. Because Al^{+3} is a strong Lewis acid, short-range interactions should correlate with the ability of the solvent to act as an electron donor. Thus, the summary chart indicates the known high basicity for DMF and the low basicity for AN. PC is likely to show a low basicity relative to DMF by virtue of a rather strong tendency of the ring structure to withdraw electrons from the "carbonyl" oxygen. On this basis, AN and PC should show similar characteristics in species formation, while DMF could be different with DMF having a stronger interaction with Al^{+3} than AN or PC. This is in accordance with the observed results.

Complexing by Perchlorate. The perchlorate ion is expected to be a weaker complexing ion than chloride. But because AN is relatively weakly solvating, ClO_4^- may also compete with AN in the first solvation sphere of Al^{+3} . Thus, the results obtained when LiClO_4 was added to AlCl_3/AN have been tentatively explained on the basis that the first solvation sphere of the Al^{+3} ion contains both solvent (AN) molecules and ClO_4^- ions.

Mixed Complexes. A general conclusion which may be made for AlCl_3 , then, is that in strongly solvating (highly basic) solvents the preferred species is the solvated metal ion. In weakly solvating (low basicity) solvents strong complexing ions, such as Cl^- , make the complexed ion AlCl_4^- the preferred species. However, in the case where the solvating characteristics of the solvent and the complexing characteristics of the negative ion are comparable, the first solvation sphere of Al^{+3} may contain both solvent molecules and complexing ions.

The existence of such mixed complexes may possibly be the explanation for the minimum of the molar conductance observed in AlCl_3/PC at low concentrations. At extremely low concentrations of AlCl_3 in PC, the solvent may compete effectively with the Cl^- ions because of the relatively much higher solvent concentration than in concentrated, 0.1 to 1 molar, solutions. The change from a composition of $\text{Al}[\text{PC}]_6^{+3} + \text{Cl}^-$ at extremely low AlCl_3 concentration to $1/4 \text{ Al}[\text{PC}]_6^{+3} + 3/4 \text{ AlCl}_4^-$ at high concentration may occur over species such as $\text{Al}[\text{PC}]_{6-x} \text{Cl}_x^{+3-x}$ which could have lower overall molar conductance for AlCl_3 . These solutions were, however, not investigated in detail and these speculations were not confirmed.

Stability of AlCl_3/PC Solutions. One unfortunate characteristic of $\text{LiCl} + \text{AlCl}_3/\text{PC}$ electrolytes is a lack of stability. After preparation, these electrolytes darken in color and after some time a black tar-like substance forms. Adding LiCl to these electrolytes produces some stabilization, but the general features still exist. This suggests that the instability is due to the PC-Al^{+3} interaction inasmuch as the addition of LiCl decreases the concentration of $\text{Al}[\text{PC}]_6^{+3}$. The comparison of the relative strength of interaction of Cl^- and solvent molecules with Al^{+3} can be logically extended to conclude that DMF solvates Al^{+3} considerably more strongly than PC. This suggests a possible means of stabilizing AlCl_3/PC electrolytes, namely, addition of DMF to the electrolyte thus converting the $\text{Al}[\text{PC}]_6^{+3}$ to $\text{Al}[\text{DMF}]_6^{+3}$. To test this hypothesis, a solution of 1 M AlCl_3 in 80-percent PC + 20-percent DMF was prepared by adding DMF to 1.25 M AlCl_3/PC . Prior to addition of DMF the solution was dark. With the addition of DMF, the dark color of the solution disappeared and the solution became slightly yellow. After several months, the solution has remained unchanged to visual observation. During the same time period and under essentially identical storage conditions, a $\text{LiCl} + \text{AlCl}_3/\text{PC}$ solution has experienced the visual darkening and formation of the black tar-like substance. Within the limits of visual observation, the $\text{AlCl}_3/\text{PC} + \text{DMF}$ electrolyte is stable.

Anomalies in Methyl Formate Electrolytes

Some anomalies were observed in the LiAsF_6/MF and LiClO_4/MF electrolytes. The equivalent conductance displayed a minimum with decreasing concentration at about 0.1 to 0.2 molar (see Fig. 71). The minimum values, at 25 C, were approximately $12 \text{ ohm}^{-1} \text{ equ}^{-1} \text{ cm}^2$ for LiAsF_6 and $2 \text{ ohm}^{-1} \text{ equ}^{-1} \text{ cm}^2$ for LiClO_4 . Also, the dielectric constant of a 1 M LiAsF_6/MF solution was increased as compared to the value for the pure solvent, whereas the reverse was found for other solutions.

These anomalies have not been explained. They may be connected with the low dielectric constant of the solvent. Further experimental work should be designed to conclusively interpret the data.

COPPER HALIDE SOLUTIONS

Copper Species Formed

The structural studies by NMR and EPR indicate that, in general, cupric ions exist as blue solvent complexes with the exception of solutions containing appreciable amounts of chloride ion. Decisive evidence could not be obtained in all systems, however, because of the low solubility of the copper halides in many cases.

In a Hittorf experiment with 0.1 M CuF_2 + 1 M $\text{LiClO}_4/\text{DMF}$, the copper migrated overall towards the anode. It migrated only to a small extent, however; this seems to indicate the presence of more than one copper species, namely, some positive or neutral species besides a negatively charged one, the latter being a perchlorate complex.

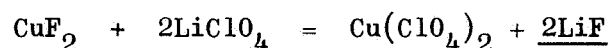
Anionic copper complexes, CuCl_4^{-2} , formed in the presence of chloride ions. If not enough chloride ion was present for a quantitative formation, new species containing less Cl appeared to form very slowly. Dimers such as

$\text{Cu}_2\text{Cl}_6^{-2}$ or $\text{Cu}_2[\text{DMF}]_2\text{Cl}_4$ were suspected to form in a reaction which occurred over a period of months and was accompanied by color changes. Possible effects of temperature and light on this process are not known, but their study could contribute significantly to the understanding of these systems.

The occurrence of negatively charged copper complexes may be of great significance during the battery discharge process. Such species migrate away from the cathode in the electric field. Reaction with the lithium at the anode would result in loss of utilization efficiency, and if dendritic growth would occur, it could lead to an internal short.

Solubility of Copper Halides

Copper fluoride displayed a low solubility in the pure solvents PC and DMF. This solubility was increased if lithium ions were available for the precipitation of lithium fluoride. The solubility of CuF_2 (whereby the fluoride was actually precipitated out of the solution) depended on the anion in the electrolyte. In cases where the resulting copper compound had ample solubility, as, e.g., in $\text{CuF}_2 + \text{LiClO}_4/\text{DMF}$, the reaction



proceeded stoichiometrically.

In the case of cupric chloride, the solubility depends largely on the availability of chloride ions. It was found to increase, e.g., from a value of 4.9×10^{-3} molar at 25 C in pure PC to 9.4×10^{-3} molar in a 0.7 M $\text{LiCl} + 1 \text{ M AlCl}_3/\text{PC}$, and to 0.54 molar in a $\text{LiCl} + 1 \text{ M AlCl}_3/\text{PC}$ solution in the presence of excess LiCl . Because chloride ions are produced as cathodic discharge product of a Li-CuCl_2 cell, the solubility of CuCl_2 will tend to increase during discharge of such a cell.

Slow equilibration processes which were followed in some instances in detail may introduce a time factor into solubility considerations. The solubility may be increased by dimerization, for instance. It was observed, furthermore, that the dissolution of CuF_2 in a 1 M $\text{LiClO}_4/\text{DMF}$ solution appeared to be rather slow. On the other hand, unidentified copper species were found to precipitate slowly from some propylene carbonate electrolytes leading to lower solubilities than previously found.

A means to control and tailor solubilities of electroactive materials may lie in the use of mixed solvent and mixed solute electrolytes.

ACTIVITY EFFECTS IN ELECTROLYTE SOLUTIONS

Molarity of Solvents

Solution concentrations are given in moles per liter throughout this report. This may be somewhat deceiving if comparison with aqueous solutions are made. It has to be kept in mind that these nonaqueous solvents have high molecular weights and their solutions have relatively high solute-solvent mole ratios. Table 49 lists the molecular weights of the solvents, their molarity in the pure state and in 1 molar LiClO_4 solutions.

TABLE 49
SOLVENT CONCENTRATIONS AT 25 C

Solvent	Molecular Weight	Density, gm/cm^3	Concentration of Solvent, moles/liter	Moles of Solvent Per Mole of Solute in 1 M LiClO_4 Solution
PC	102.09	1.203	11.78	11.24
DMF	73.10	0.944	12.91	12.48
AN	41.05	0.777	18.93	18.43
MF	60.05	0.968	16.12	15.6*
H_2O	18.02	0.997	55.33	53.7*

*Density data not available for LiClO_4 solution; values were estimated from density of 1.1 M LiAsF_6/MF , or 1 M $\text{LiNO}_3/\text{H}_2\text{O}$, respectively

Because of the high solute-solvent mole ratios, activity effects are pronounced in these nonaqueous solvents. Strong deviations from the ideal solution behavior due to solute-solute interactions occur at relatively low molar solute concentrations.

Solution Conductances

It has been found that ion mobilities at infinite dilution in the solutions studied were according to conventional predictions. A nearly constant Walden product was obtained; i.e., the ion mobilities at infinite dilution were determined by ion size and viscosity of the solvent only.

The well-known conductance maxima in aprotic electrolytes at solute concentrations of 1 to 2 molar are therefore due solely to activity effects. These maxima occur at low concentrations because relatively high solute-solvent mole ratios are already reached at those concentrations. This has the result that high specific solution conductances are not obtained. It appears that solvents with low molecular weights have better promise for relatively high solution conductances. Unfortunately, the selection of aprotic solvents with low molecular weights is limited.

DIELECTRIC CONSTANTS AND SOLUBILITIES

Because a higher dielectric constant means a decrease in the electrostatic forces between dissolved ions, it had been often assumed that a direct correlation between solubility of salts and dielectric constants exists. The present investigations indicate that other factors override, as discussed earlier for AlCl_3 systems. Solute solubilities in DMF were generally greater than in PC or AN due to the higher tendency to form complexes.

In the case of MF, it has been demonstrated that highly concentrated solutions can be obtained with a solvent having a small dielectric constant. The physical properties of such solutions displayed some irregular behavior which has not been explained, however, and a more detailed study of methyl formate solutions seems appropriate.

TRANSPORT PROPERTIES

Solubility of Discharge Products

Lithium fluoride will be the overall discharge product for a Li-CuF_2 cell, lithium chloride in the case of a Li-CuCl_2 cell. Extremely low solubilities were determined for LiF in the pure solvents as well as in some electrolytes. In a cell containing a lithium salt electrolyte, LiF will precipitate at a CuF_2 cathode during discharge. This may cause a blocking of the active cathode sites and a starvation of the electrolyte at the cathode.

In the case of Li-CuCl_2 , the LiCl may not precipitate because of the higher solubility of LiCl , and also because of copper chloride complex ion formation.

Diffusion Coefficients

Discharge rate limitations may in some cases be directly related to the diffusion coefficient of the electrolyte. In the case of a Li-CuF_2 cell with a LiClO_4 electrolyte, the electrolyte concentration at the cathode will essentially become zero at sufficiently high currents because perchlorate ions migrate away and LiF precipitates. The concentration gradient and the diffusion coefficient in connection with transference numbers determine then the diffusion limiting current.

The diffusion coefficients of 1 molar solutions appeared to be a function of solvent viscosity. Propylene carbonate may be an unfortunate choice if high discharge rates are of prime consideration; methyl formate electrolytes may be much better in such cases.

Transference Numbers

Transference numbers for the lithium ion were consistently low, between 0.2 and 0.3. This was found by Hittorf measurements of 1-molar solutions as well as by calculations from ion mobilities at infinite dilution. Low transference numbers for lithium ions, incidentally, also exist in aqueous systems.

The low transference number of Li^+ aggravates possible electrolyte starvation at the cathode. As ClO_4^- ions, for example, carry a large fraction of the discharge current, a large amount of Li^+ has to be supplied to the cathode by diffusion and convection.

IMPURITY EFFECTS

The effects of the addition of small amounts of water have been studied to a limited extent. It was shown that solubilities were generally increased for compounds having low solubilities, but they were not affected significantly in cases of high solubilities.

Present results, particularly conductance changes upon addition of water and observations made in chronopotentiometric studies, are consistent with a strong preferential solvation of the lithium ion by water in propylene carbonate as reported by other investigators (Ref. 70).

No indications that trace amounts of H_2O would alter physical property measurements of 1 molar electrolyte solutions were noticed.

CONCLUSIONS

Increased knowledge has been gained on nonaqueous aprotic electrolytes. Such solutions based on propylene carbonate (PC), dimethyl formamide (DMF), acetonitrile (AN), and methyl formate (MF) were studied in connection with the development of high-energy density lithium batteries.

The following summarizes the main conclusions of the investigation:

1. Structural studies by nuclear magnetic resonance (NMR) and conductance measurements showed that lithium perchlorate, lithium chloride, and tetramethylammonium hexafluorophosphate form univalent electrolyte solutions analogous to aqueous systems.
2. Aluminum has a tendency to form solvent complexes, $\text{Al}[\text{solvent}]_6^{+3}$. Chloride ions are stronger complexing agents, however, than PC or AN, and the ion AlCl_4^- forms in these cases (but not in DMF). When insufficient chloride is present for the quantitative formation of AlCl_4^- , the rest of the aluminum exists as the solvated trivalent ion, $\text{Al}[\text{PC}]_6^{+3}$ or $\text{Al}[\text{AN}]_6^{+3}$, respectively. This was shown by NMR studies which were complemented by Hittorf experiments and other physical property determinations.
3. The $\text{Al}[\text{PC}]_6^{+3}$ complex appears to cause instability of propylene carbonate solutions. Selection of appropriate mixed solvent or mixed solute systems should eliminate such instabilities.
4. Structural studies, dielectric constant measurements, and solubility determinations revealed that solvent complexing ability or basicity is generally more important than the dielectric constant in determining solubilities and the nature of the species formed in solution.
5. When copper halides dissolve in nonaqueous electrolytes, the copper forms various solvent and anion complexes, and has a strong tendency to form the CuCl_4^{2-} complex if chloride is present. This was established by structural studies by nuclear

magnetic resonance (NMR) and electron paramagnetic resonance (EPR); such investigations were complemented by Hittorf experiments and conductance data.

6. Very slow reactions were found to proceed in CuCl_2/DMF solutions over a period of months. New copper species such as dimers appear to form very slowly.
7. Solubility determinations confirm the low solubility of lithium fluoride in pure solvents as well as in electrolytes. Copper halide solubilities are determined to a large extent by the availability of complexing anions. A solubilization of CuF_2 can occur if lithium fluoride precipitates.
8. Conductance measurements gave no indication for an extraordinary behavior of nonaqueous solutions at low concentrations. At high concentrations, activity effects are more pronounced than in aqueous electrolytes, and specific conductance appears to be limited for these reasons.
9. An unusual behavior was found for methyl formate solutions in conductance and dielectric constant measurements. A minimum of the equivalent conductance was found at low concentrations for LiClO_4 and LiAsF_6 solutions, and the dielectric constant of such solutions was much greater than the one of the pure solvent, in contrast to the results obtained with the other solvents.
10. Measurement of diffusion coefficients and transference numbers were made. Such properties have to be considered to avoid discharge limitations due to mass transport. From such considerations, methyl formate electrolytes are to be preferred over propylene carbonate electrolytes.

REFERENCES

1. NASA CR-72106, Properties of Nonaqueous Electrolytes, First Quarterly Report, by R. Keller, J. N. Foster, and J. M. Sullivan, Rocketdyne, a division of North American Aviation, Inc., Canoga Park, California, October 1966.
2. NASA CR-72168, Properties of Nonaqueous Electrolytes, Second Quarterly Report, by R. Keller, J. N. Foster, J. D. Ray, and J. M. Sullivan, Rocketdyne, a division of North American Aviation, Inc., Canoga Park, California, January 1967.
3. NASA CR-72065, Properties of Nonaqueous Electrolytes, Third Quarterly Report, by R. Keller, J. N. Foster, J. F. Hon, and J. M. Sullivan, Rocketdyne, a division of North American Aviation, Inc., Canoga Park, California, April 1967.
4. NASA CR-72277, Properties of Nonaqueous Electrolytes, Fourth Quarterly Report, by R. Keller, J. N. Foster, J. F. Hon, O. F. Kalman, and J. M. Sullivan, Rocketdyne, a division of North American Aviation, Inc., Canoga Park, California, July 1967.
5. NASA CR-72324, Properties of Nonaqueous Electrolytes, Fifth Quarterly Report, by R. Keller, J. N. Foster, J. F. Hon, O. F. Kalman, and J. M. Sullivan, Rocketdyne, a division of North American Rockwell Corporation, Canoga Park, California, October 1967.
6. NASA CR-72407, Properties of Nonaqueous Electrolytes, Sixth Summary Report, by R. Keller, J. N. Foster, D. C. Hanson, J. F. Hon, O. F. Kalman, J. S. Muirhead, and J. M. Sullivan, Rocketdyne, a division of North American Rockwell Corporation, Canoga Park, California, April 1968.
7. Hollis, O. L.: Anal. Chem. **38**, 309 (1966).
8. Hollis, O. L. and W. V. Hayes: J. Gas Chromatography, **1**, 272 (1966).

9. Technical Bulletin on Propylene Carbonate, Jefferson Chemical Company, Inc., Houston, Texas.
10. DuPont Dimethyl Formamide, Product Information Bulletin, Industrial and Biochemicals Department, E. I. duPont de Nemours & Co., Inc., Wilmington, Delaware.
11. Handbook of Chemistry and Physics, 45th Edition, The Chemical Rubber Co., Cleveland, Ohio (1964).
12. Watanabe, M. and R. M. Fuoss; J. Am. Chem. Soc. **78**, 527 (1956).
13. Bass, S. J., W. I. Nathan, R. M. Meighan, and R. H. Cole: J. Phys. Chem. **68**, 509 (1964).
14. Maryott, A. A. and E. R. Smith: NBS Circular 514 (1951).
15. Mitchell, J. and O. Smith: Aquametry, Interscience, New York (1948).
16. Beilstein, Handbuch der Organischen Chemie, Vol. IV, 2nd Supplement, p 557, Springer-Verlag, Berlin (1942)
17. Contract NAS3-10613, Livingston Electronic Laboratory, Honeywell, Inc., Montgomeryville, Pennsylvania, Sixth Monthly Report (December 1967).
18. Fisher, H. D., W. J. Lehmann, and I. Shapiro: J. Phys. Chem. **65**, 1166 (1967).
19. Booth, H. S. and D. R. Martin: Boron Trifluoride and Its Derivations, P. Wiley & Sons, New York (1949).
20. Gutowski, H. S. and A. D. Liehr: J. Phys. Chem. **20**, 1652 (1952).
21. Pemsler, J. P. and W. G. Planet, Jr.: J. Chem. Phys. **24**, 920 (1956).
22. Selig, H. and H. H. Classen: J. Chem. Phys. **44**, 1404 (1966).
23. Fuoss, R. M., J. B. Berkowitz, E. Hirsch, and S. Petrucci: Nat. Acad. Sci. U.S., Proc., **44**, 27 (1958).
24. Gordon, W. E., F. E. Reed, and B. A. Lepper: Ind. Eng. Chem. **47**, 1794 (1955).

25. Fratiello, A., R. Schuster, and D. P. Miller: Mol. Phys. 11, 597 (1966).
26. Hon, J. F. and P. J. Bray: Phys. Rev. 110, 624 (1958).
27. Klamberg, F., J. P. Hunt, and H. W. Dodgen, Inorg. Chem. 2, 139 (1963).
28. Movius, W. G. and N. A. Matwiyoff: J. Phys. Chem. 72, 3063 (1968).
29. Hon, J. F.: Mol. Phys. 15, 57 (1968).
30. Supran, L. D. and N. Sheppard: Chem. Commun. 1967, 832.
31. Connick, R. E. and D. N. Fiat: J. Chem. Phys. 39, 1349 (1963).
32. Thomas, S. and W. L. Reynolds: J. Chem. Phys. 44, 3148 (1966).
33. Fratiello, A., D. P. Miller, and R. Schuster: Mol. Phys. 12, 111 (1967).
34. Masuda, Y.: J. Phys. Soc. Japan 11, 670 (1956).
35. Emsley, J. W., J. Feeney, and L. H. Sutcliffe: High Resolution Magnetic Resonance Spectroscopy, p 484, Pergamon Press, London.
36. Gersmann, H. R., and J. D. Swalen: J. Chem. Phys. 36, 3221 (1962).
37. Ballhausen, C. J.: Introduction to Liquid Field Theory, McGraw-Hill Book Company, Inc., New York, 1962, p 272.
38. Willett, R. D.: J. Chem. Phys. 41, 2243 (1964).
39. Kokoszka, G. K., H. C. Allen, Jr., and G. Gordon: J. Chem. Phys. 46, 3013 (1967).
40. Muettertides, E. L. and W. D. Phillips: J. Am. Chem. Soc. 81, 1084 (1959).
41. Muettertides, E. L., T. A. Bither, M. W. Farlow, and D. D. Coffman: J. Inorg. Nucl. Chem. 16, 52 (1960).
42. Ogg, R. A. and J. D. Ray: J. Chem. Phys. 26, 1515 (1957).
43. Laszlo, P., A. Speert, R. Ottinger, and J. Reisse: J. Chem. Phys. 48, 1732 (1968).
44. Packer, K. J. and E. L. Muettertides: Proc. Chem. Soc. 1964, 147.

45. R-7197, Electrochemically Controlled Ion-Exchange, Final Report, by S. Evans, M. A. Accomazzo, W. S. Hamilton, and J. E. Lewis, Rocketdyne, a division of North American Rockwell Corporation, Canoga Park, California, September 1967.
46. AFAP-TR-66-35, Lithium-Anode Limited Cycle Battery Investigation, by H. F. Bauman, J. E. Chilton, and R. Mauri, Lockheed Missiles and Space Company, April 1966.
47. NASA CR-54920, Development of High-Energy Density Primary Batteries, Second Quarterly Report, by S. G. Abens, T. X. Mahy, and W. C. Merz, Livingston Electronic Corporation, Montgomeryville, Pennsylvania, December 1965.
48. Wadso, I.: "Calculation Methods in Reaction Calorimetry," Science Tools, 13, 33 (1966).
49. NSRDS-NBS2, Thermal Properties of Aqueous Uni-univalent Electrolytes, National Bureau of Standards (1965).
50. Thomson, G. W.: Determination of Vapor Pressure, in A. Weissberger, Physical Methods of Organic Chemistry, Vol. 1, Part 1, 2nd Edition, Interscience Publishers, New York (1949).
51. Greenspan, M. and C. E. Tschiegg: "Tables of the Speed of Sound in Water," J. Acoust. Soc. Am., 31, 75 (1959).
52. Conway, B. E. and J. O'M. Bockris: Ionic Solvation, in Modern Aspects of Electrochemistry, Vol. 1, Butterworths Scientific Publications, London (1954).
53. Passynsky, A.: Acta Physicochimica U.R.S.S., 8, 385 (1938).
54. Kaurova, A. S. and G. P. Roshchina, Soviet Physics-Acoustics, 12, 276 (1967).
55. Mikhailov, I. G., V. A. Solov'ev, and Yu. P. Syrnikov: Fundamentals of Molecular Acoustics (in Russian), Izd. AN SSSR, Moscow-Leningrad (1945).

56. Fuoss, R. M. and E. Hirsch: J. Amer. Chem. Soc., 82, 1013 (1960).
57. Fowler, D. L. and C. A. Kraus: J. Amer. Chem. Soc., 62, 2237 (1940).
58. Prue, J. E. and P. J. Sherrington: Trans. Faraday Soc. 57, 1795 (1961).
59. Kortum, G.: Treatise on Electrochemistry, 2nd Edition, Elsevier Publishing Company, Amsterdam (1965).
60. Glasstone, S.: An Introduction to Electrochemistry, 5th Edition, D. Van Nostrand Company, New York (1951).
61. NASA CR-54153, The Development of High Energy Density Primary Batteries, 200 Watt Hours Per Pound of Total Battery Weight Minimum, by W. E. Elliott, S. Hsu, and W. L. Towle, Globe-Union Inc., Milwaukee, Wisconsin, January 1965.
62. Wall, F. T., G. S. Stent, and J. J. Ondrejcin: J. Phys. & Colloid. Chem. 54, 979 (1950); see also Weissberger, A., Physical Methods of Organic Chemistry, Part IV, 3rd Ed. (1960), p 3066.
63. Wall, F. T., P. F. Grieger, and C. W. Childer: J. Am. Chem. Soc. 74, 3562 (1952).
64. Wall, F. T. and C. W. Childer: J. Am. Chem. Soc. 75, 6340 (1953).
65. Taylor, G. B. and F. T. Wall: J. Am. Chem. Soc. 75, 3550 (1953).
66. Shoemaker, D. P. and C. W. Garland: Experiments in Physical Chemistry, McGraw-Hill, New York (1962), p 156.
67. Harris, F. E. and C. T. O'Konski: Rev. Sci. Instr. 26, 482 (1955).
68. Hasted, J. B., D. M. Titson, and C. H. Collie: J. Chem. Phys. 16, 1 (1948).
69. Cole, K. S. and R. H. Cole: J. Chem. Phys. 9, 341 (1941).
70. Jasinski, R., B. Burrows, and P. Malachuk: Research on Electrode Structures for High Energy Density Batteries, Second Quarterly Report, Tyco Laboratories, Inc., Waltham, Massachusetts, December 1967.

NATIONAL AERONAUTICS AND SPACE ADMINISTRATION
WASHINGTON, D. C. 20546
OFFICIAL BUSINESS

FIRST CLASS MAIL



POSTAGE AND FEES PAID
NATIONAL AERONAUTICS
SPACE ADMINISTRATION

POSTMASTER: If Undeliverable (Section
Postal Manual) Do Not

"The aeronautical and space activities of the United States shall be conducted so as to contribute . . . to the expansion of human knowledge of phenomena in the atmosphere and space. The Administration shall provide for the widest practicable and appropriate dissemination of information concerning its activities and the results thereof."

—NATIONAL AERONAUTICS AND SPACE ACT OF 1958

NASA SCIENTIFIC AND TECHNICAL PUBLICATIONS

TECHNICAL REPORTS: Scientific and technical information considered important, complete, and a lasting contribution to existing knowledge.

TECHNICAL NOTES: Information less broad in scope but nevertheless of importance as a contribution to existing knowledge.

TECHNICAL MEMORANDUMS: Information receiving limited distribution because of preliminary data, security classification, or other reasons.

CONTRACTOR REPORTS: Scientific and technical information generated under a NASA contract or grant and considered an important contribution to existing knowledge.

TECHNICAL TRANSLATIONS: Information published in a foreign language considered to merit NASA distribution in English.

SPECIAL PUBLICATIONS: Information derived from or of value to NASA activities. Publications include conference proceedings, monographs, data compilations, handbooks, sourcebooks, and special bibliographies.

TECHNOLOGY UTILIZATION PUBLICATIONS: Information on technology used by NASA that may be of particular interest in commercial and other non-aerospace applications. Publications include Tech Briefs, Technology Utilization Reports and Notes, and Technology Surveys.

Details on the availability of these publications may be obtained from:

SCIENTIFIC AND TECHNICAL INFORMATION DIVISION
NATIONAL AERONAUTICS AND SPACE ADMINISTRATION
Washington, D.C. 20546